May 2016

Intersections of Astrophysics, Cosmology and Particle Physics

Luiz Henrique Moraes da Silva
University of Wisconsin-Milwaukee

INTERSECTIONS OF ASTROPHYSICS, COSMOLOGY AND PARTICLE PHYSICS

by

Luiz Henrique Moraes da Silva

A Dissertation Submitted in

Partial Fulfillment of the

Requirements for the Degree of

Doctor of Philosophy

in Physics

at

University of Wisconsin-Milwaukee

May 2016

ABSTRACT
INTERSECTIONS OF ASTROPHYSICS, COSMOLOGY AND PARTICLE PHYSICS

by

Luiz Henrique Moraes da Silva

The University of Wisconsin-Milwaukee, 2016
Under the Supervision of Professor Anchordoqui and Professor Raicu

With the success of the Large Hadron Collider (LHC) at CERN, a new era of discovery has just begun. The $SU(3)_C \times SU(2)_L \times U(1)_Y$ Standard Model (SM) of electroweak and strong interactions has once again endured intensive scrutiny. Most spectacularly, the recent discovery of a particle which seems to be the SM Higgs has possibly plugged the final remaining experimental hole in the SM, cementing the theory further. Adding more to the story, the IceCube Collaboration recently reported the discovery of extraterrestrial neutrinos, heralding a new era in astroparticle physics. The collaboration was able to isolate 36 events in 3 years of data, with energies between 30 TeV $\lesssim \mathrm{E}_\nu \lesssim$ 2 PeV. These events are consistent with an isotropic distribution in the sky, and a purely atmospheric explanation of the data can be excluded at 5.7σ.

However, problems still exist. Cosmological observations concerning dark matter and the expansion rate of the Universe have shown us our picture of the basic constituents of the Universe and the interactions among them are not fully understood. In addition, the determination of the origin of high energy neutrinos has proven to be a quite formidable problem, with many possible candidates for sources. Motivated by these problems, we study and impose constraints on a dark matter model, and consider the idea of starburts and Galatic microquasars as possible astrophysical sources for the high energy neutrino events observed at IceCube. In addition, dark matter decay is considered as a way to explain high-energy neutrino events and reconcile the tension between measurements of the Hubble constant by different observation methods.

TABLE OF CONTENTS

LIST OF FIGURES

LIST OF TABLES

ACKNOWLEDGEMENTS

First of all, I would like to express my thanks to my advisor Professor Luis. A. Anchordoqui, for bringing me to the field of particle physics and for mentoring my research over these years. I would also like to thank all my committee members, and in particular Professor Valerica Raicu, and Professor Phillip Chang, for all the support even at hardship. I am also thankful to everybody I met here at UWM, all the professors from the Physics Department and graduate students, from whom I have learned so much.

This work is just one step in a journey that started a long time ago, in Brazil. I would like to thank the professors from Motivo, the place where it all started, and Prof. Daniel A.T. Vanzella, Prof. Hildebrando Munhoz Rodriguez and Prof. Márcio Gameiro from the University of São Paulo, for the guidance, support and friendship throughout my undergraduate years.

A special thanks to my friends, from Maceió and São Carlos, for staying by my side for all these years. I am extremely grateful for all the happy memories, support, and specially the patience you always had.

Finally, words cannot express how grateful I am to my family. All my achievements were only possible because you were always there for me, specially at the hardest of times, never letting me give up. It is to my mother, Vania, and my brother, Victor, that I dedicate this work.

1 Introduction

Recently, the IceCube Collaboration reported the discovery of extraterrestrial neutrinos [276]. By establishing a strict veto protocol, the collaboration was able to isolate 36 events in 3 years of data, with energies between 30 TeV $\lesssim E_\nu \lesssim$ 2 PeV. These events follow the expected spectral shape ($\propto E_\nu^{-2}$) of a Fermi engine, and are consistent with an isotropic distribution in the sky. A purely atmospheric explanation of the data can be excluded at 5.7σ.

At $E_\nu^{\rm res} \simeq 6.3$ PeV, one expects to observe a dramatic increase in the event rate for $\bar{\nu}_e$ in ice due to the "Glashow resonance" in which $\bar{\nu}_e e^- \to W^- \to$ shower greatly increases the interaction cross section [277]. The hypothesis of an unbroken power law $\propto E_\nu^{-\alpha}$ then requires $\alpha \gtrsim 2.45$ to be consistent with data at 1σ [280]. More recently, the IceCube search technique was refined to extend the neutrino sensitivity to lower energies $E_\nu \gtrsim 10$ TeV. A fit to the resulting data, assuming a single unbroken power law and equal neutrino fluxes of all flavors, finds a softer spectrum

$$\begin{aligned} \Phi_{\rm IceCube}^{\rm per\,flavor}(E_\nu) &= 2.06^{+0.4}_{-0.3} \times 10^{-18} \left(\frac{E_\nu}{10^5\ {\rm GeV}}\right)^{-2.46\pm0.12} \\ &\times \ {\rm GeV}^{-1}\,{\rm cm}^{-2}\,{\rm sr}^{-1}\,{\rm s}^{-1} \end{aligned} \tag{1}$$

and already mildly excludes the benchmark spectral index $\alpha = 2$. In this work, we will consider different candidates for the sources, from Galactic and extragalactic origin, and as we will see soon, this will not be enough.

Another piece of the puzzle comes when we consider the Standard Model of Particle Physics. First, some theoretical inconsistencies seem to exist. For example, the fact

that neutrinos oscillate and are massive as it was mentioned before is not completely understood yet. On the other hand, the success of the Large Hadron Collider (LHC) at CERN, seems to point on the other direction. The Standard Model (SM) of electroweak and strong interactions has once again endured intensive scrutiny, with a data set corresponding to an integrated luminosity of $\approx 20\text{fb}^{-1}$ of pp collisions at $\sqrt{s}$ =8 TeV. Most spectacularly, the recent discovery [105, 106] of a particle which seems to be the SM Higgs has possibly plugged the final remaining experimental hole in the SM, cementing the theory further. The LHC8 data have not yet turned up any evidence of physics beyond the SM [107]. Despite the resilience of the SM, it seems clear that there is more to the story, as in the moment this text is written, LHC is going through a new run, and apparently interesting (and unexpected!) physics seems may emerge in the near future [25], [26].

From the cosmological and astrophysical point of view, we have evidence that new physics, beyond the SM, might be necessary. The existence of dark matter (DM) has been solidified by multiple astrophysical observations [172]. Weakly interacting massive particles (WIMPs) are among the best motivated candidates [109]. If stable particles with mass and annihilation cross section set by the weak scale exist, they would be produced and annihilate in thermal equilibrium in the early Universe. As the Universe expands, these particles fall out of equilibrium and their number density is frozen in. A typical weak scale interaction rate yields a thermally averaged WIMP annihilation cross section, $\langle \sigma v_M \rangle \sim 10^{-9}\text{GeV}^{-2}$, which naturally produces a WIMP relic density $h^2\Omega_{WIMP} \sim 10^{-10}\text{GeV}^{-2}/\langle \sigma \text{v}_\text{M} \rangle$ ([166] - [170]) consistent with the measured DM abundance $h^2\Omega_{DM} = 0.111(6)$ [171], thus making WIMPs promising candidates of DM (throughout this work we adopt the usual convention of writing the Hubble constant at the present day as $100h\text{kms}^{-1}\text{Mpc}^{-1}$. For t = today, the various energy densities are expressed in units of the critical density ρ_c; e.g., the DM density $\Omega_{DM} \equiv \rho_{DM}/\rho_c$.

Since WIMPs are subject to the weak interaction, it is possible to search for them via direct detection experiments, γ-ray observatories, neutrino telescopes, and particle colliders. The first direct detection experiment to claim evidence for DM was DAMA/LIBRA [110], which has recorded an annual modulation in nuclear recoil event rate at the 8.9σ

level [111]. This modulation can be interpreted as a consequence of the change in the relative motion of the detector through the sea of DM as the Earth rotates around the Sun [112, 113]. Other direct detection experiments have provided supporting evidence for WIMP interactions, including CRESST [114], CoGeNT [115, 116, 117], and most recently the CDMS II [118] experiment. Interestingly, all of these observations favor a light WIMP, with mass ~ 10 GeV and an interaction with protons via spin-independent elastic scattering with a cross section $\sim 10^{41}\mathrm{cm}^2$. In contrast, the XENON-10 [119] and XENON-100 [120] DM experiments have reported limits which exclude the mass and cross-section regime favored by CoGeNT, CRESSTand CDMS II.

A variety of models were employed to reconcile hints of the signals mentioned above with the exclusion from XENON-10 and XENON-100. However, tension has increased even further after recent CDMS Low Ionization Threshold Experiment (CDMSlite) [121] and LUX [194] results. At this point only the xenophobic isospin violating dark matter [123, 124, 125, 126, 127], with a neutron to proton coupling ratio of -0.7 allows any overlap with the 68% favored contour of CDMS II [128, 129, 130]. Favored regions of all other experiments remain excluded.

Another, seemingly different, but perhaps closely related subject is the emerging tension between direct astronomical measurements at low redshift and cosmological parameters deduced from temperature fluctuations in the cosmic microwave background (CMB). As we already mentioned on the Cosmology chapter, the TT, TE, EE spectra recorded by the *Planck* spacecraft when combined with polarization maps (lowP) describe the standard spatially-flat 6-parameter ΛCDM model $\{\Omega_b h^2,\, \Omega_{\rm CDM} h^2,\, \Theta_s,\, \tau,\, n_s,\, A_s\}$ with high precision: *(i)* baryon density, $\Omega_b h^2 = 0.02225 \pm 0.00016$; *(ii)* CDM density, $\Omega_{\rm CDM} h^2 = 0.1198 \pm 0.0015$; *(iii)* angular size of the sound horizon at recombination, $\Theta_s = (1.04077 \pm 0.00032) \times 10^{-2}$; *(iv)* Thomson scattering optical depth due to reionization, $\tau = 0.079 \pm 0.017$; *(v)* scalar spectral index, $n_s = 0.9645 \pm 0.0049$; *(vi)* power spectrum amplitude of adiabatic scalar perturbations, $\ln(10^{10}\, A_s) = 3.094 \pm 0.034$ [231]. *Planck* data also constrain the Hubble constant $h = 0.6727 \pm 0.0066$, the dark energy density $\Omega_\Lambda = 0.6844 \pm 0.0091$, the amplitude of initial density perturbations $\sigma_8 = 0.831 \pm 0.013$, and

the mass density parameter $\Omega_m = 0.3156 \pm 0.0091$.[1] Unexpectedly, the H_0 inference from *Planck* observations deviates by more than 2.5σ from the previous interpretation of the Hubble Space Telescope (HST) data (based on over 600 cepheids in host galaxies and 8 samples of SNe Ia) which leads to $h = 0.738 \pm 0.024$, including both statistical and systematic uncertainties [93]. A separate study by the Carnegie Hubble program using mid-infrared calibration of the cepheid distance scale based on data from NASA's Spitzer Space Telescope yields $h = 0.743 \pm 0.021$ [94]. Besides, the interpretation of gravitational lensing time delay measurements of the system RXJ1131-1231 points to $h = 0.787^{+0.043}_{-0.045}$ [95].

In this dissertation, we outline will be as follows: we will present a brief overview of theoretical topics from chapters 1 to 5, which will be based on standard textbooks on the Standard Model, Quantum Field Theory and Cosmology, with focus on the electroweak interaction. On Chapter 6, we will present the first research results, concerning a model for dark matter. On chapters 7 and 8, we will talk in more detail about high energy neutrinos produced in astrophysical sources and their detection on the IceCube experiment. We finish the text on the later chapters discussing research results concerning the high energy neutrino flux from astrophysical sources and its possible connection to Cosmology through dark matter decay, which could be a way of reconciling the tension between the Hubble parameter measurements.

[1] Throughout we adopt the usual convention of writing the Hubble constant at the present day as $H_0 = 100\ h$ km s^{-1} Mpc^{-1}.

1.1 Natural Units

In particle physics and cosmology, it is common to adopt

$$\hbar = c = k_B = 1, \tag{2}$$

where the reduced Planck constant, the speed of light and the Boltzmann constant are equal to 1. Due to the fact that the speed of light equals 1, we use electronvolts (eV) to treat mass and energy. Distances become expressed as eV^{-1},

$$1\ m = 1\ \frac{m}{\hbar c} \approx 510\ \mathrm{eV}^{-1} \tag{3}$$

We will also adopt Einstein's summation convention for indices, unless stated otherwise. Quantities with an arrow, such as $\vec{v}$ are vectors with spatial components only, and the Minkowski metric has signatute (+ - - -).

2 $U(1)_Y \times SU(2)_L \times SU(3)_C$

2.1 Historical Introduction

The Standard Model is a physical theory that describes the Electromagnetic, Weak and Strong forces and the particles we know. In 1961, Sheldon Glashow found a way of combining the Electromagnetic and the Weak interactions [47]; a few years later, in 1967, Steven Weinberg and Abdus Salam combined Glashow's electroweak theory with the Higgs mechanism [48]. Weinberg, Glashow and Salam shared the Nobel Prize in Physics in 1979 for this theory, which was confirmed at CERN in 1973 via the detection of the Z boson exchange in neutral weak currents [46]. The Strong force was shaped into its modern form around 1974, with the experimental confirmation of the fact that hadrons are composed by quarks.

Quantum field theory differs from non-relativistic quantum mechanics in many ways. QFT is an attemp of formulating a covariant, fully relativistic theory of the fundamental interactions, something that traditional quantum mechanics does not attempt to do. In order to do so, time and space must have equal status on the theory; thus, we have two options: we can promote position and time to the status of operators, or we can demote all of them to the status of parameters.

It turns out that the second option (time and space as parameters) is much more viable. The real problem now is the following: we want to impose commutation relations (in order to do quantization), but we no longer have the position and momentum operators to do so. The answer is: the particles are the Hermitian operators now, and a particle operator will be parametrized by space an time coordinates. An electron, for example, is not described by a wavefunction in which operators act anymore; instead, the electron

is the operator. By acting on the vacuum, the "electron operator" creates an excited state, which we interpret physically as a single physical particle. Thus, particles are now excitations of the vacuum. Note that there is an analogy between this idea and ladder operators in harmonic oscillators; in fact, this idea is the essence of what is usually referred to as "Second Quantization".

After defining what a particle is, the next step is to treat the interactions and that's where gauge theories (or Yang Mills theories) become useful. In this framework, symmetries are interactions, and group theory becomes essential. The idea is to associate an interaction (strong force, weak force or electromagnetism) to a certain Lie group in a certain representation. The particles that couple to the interaction are the eigenvectors of the Cartan generators, the eigenvalues will be the physical charges, and there are as many charges as the dimension of the group under the fundamental representation. The Cartan generators will be the force carrying particles that transfer energy and momentum but don't affect the charge of the particles (such as the photon and the Z boson). The non-Cartan generators are associated with raising and lowering operators, therefore being able to change eigenvectors and, consequently, eigenvalues. This means that non-Cartan generators are associated with force carriers that transfer energy, momentum and affect the charge (gluons and W boson).

2.2 Canonical Quantization

2.2.1 The Harmonic Oscillator

In this section, we will recall some results from the quantum harmonic oscillator.

$$\hat{H} = \frac{\hat{P}^2}{2m} + \frac{1}{2}m\omega^2\hat{X}^2, \tag{4}$$

and we define the usual ladder operators (whch are not Hermitian)

$$a = \sqrt{\frac{m\omega}{2\hbar}}\left(\hat{X} + \frac{i}{m\omega}\hat{P}\right), \tag{5}$$

$$a^\dagger = \sqrt{\frac{m\omega}{2\hbar}}\left(\hat{X} - \frac{i}{m\omega}\hat{P}\right). \tag{6}$$

They act on the energy eigenstates,

$$H\left|n\right\rangle = E_n\left|n\right\rangle, \;\; E_n = \hbar\omega\left(n + \frac{1}{2}\right), \tag{7}$$

giving

$$a^\dagger\left|n\right\rangle = \sqrt{n+1}\left|n+1\right\rangle, \tag{8}$$

$$a\left|n\right\rangle = \sqrt{n}\left|n-1\right\rangle. \tag{9}$$

Recall that

$$a\left|0\right\rangle = 0, \tag{10}$$

and we can also define a number operator,

$$\hat{N} = a^\dagger a, \;\; N\left|n\right\rangle = n\left|n\right\rangle \Rightarrow \hat{H} = \left(N + \frac{1}{2}\right)\hbar\omega. \tag{11}$$

The ladder operator method is extremely useful in quantum mechanics. In our context, where particles are treated as excitations from a field, the idea of creation and anihillation operators seems to fit perfectly; thus, this approach will become the key stone in which we will try to build our theory upon.

2.2.2 Canonical quantization of scalar fields

This is the point when we begin to discuss the concept of a particle in our theory. Following [7], consider the Klein-Gordon lagrangian, in the absence of interactions,

$$\mathcal{L}_{KG} = \frac{1}{2}\partial^\mu\phi\,\partial_\mu\phi - \frac{1}{2}m^2\phi^2. \tag{12}$$

For convenience, we will add a constant term,

$$\mathcal{L}_{KG} = \frac{1}{2}\partial^\mu\phi\ \partial_\mu\phi - \frac{1}{2}m^2\phi^2 + \Phi, \tag{13}$$

which has no effect on the equations of motion but will be very useful in the mathematical manipulations we are about to perform. In order to say that a field is quantized, it has to satisfy the canonical commutation relations, which we are going to impose. Let's define the field momentum and the Hamiltonian density:

$$\Pi = \frac{\partial\mathcal{L}}{\partial\dot{\phi}} = \dot{\phi}, \tag{14}$$

$$\mathcal{H} = \Pi\dot{\phi} - \mathcal{L} = \frac{1}{2}\left(\Pi^2 + m^2\phi^2 + (\nabla\phi)^2\right) - \Phi, \tag{15}$$

and we impose

$$[\Pi(t, x^\mu), \phi(t, x^\nu)] = -i\delta^3(x^\mu - x^\nu), \tag{16}$$

$$[\phi(t, x^\mu), \phi(t', x'^\mu] = 0, \tag{17}$$

$$[\Pi(t, x^\mu), \Pi(t', x'^\mu] = 0, \tag{18}$$

the canonical commutation relations. The next step is to write the field in a more convenient form. Recalling the solution of the Klein-Gordon equation, the most general soultion for ϕ is a superposition of the following form:

$$\phi = \int \frac{d^3p}{f(p)}\left[a(p)e^{-iEt+i\vec{p}.\vec{x}} + b(p)e^{iEt-i\vec{p}.\vec{x}}\right], \tag{19}$$

where we decided to write the coefficients of the plane waves as a ratio of two functions for later convenience. If one imposes that the scalar field ϕ is real:

$$\phi^\dagger = \phi. \tag{20}$$

Taking the Hermitian conjugate has the following effect on one of the terms in the integral:

$$a(p)e^{-iEt+i\vec{p}.\vec{x}} \to a(p)^\dagger e^{iEt-i\vec{p}.\vec{x}}, \tag{21}$$

which implies (after imposing the reality condition):

$$b(p) = a(p)^\dagger, \tag{22}$$

and we get

$$\phi = \int \frac{d^3p}{f(p)} \left[a(p)e^{-iEt+i\vec{p}.\vec{x}} + a(p)^\dagger e^{iEt-i\vec{p}.\vec{x}}\right]. \tag{23}$$

Finally, we recall that the field ϕ must be Lorentz invariant. Well, in terms of four-vectors,

$$p^\mu.x_\mu = -Et + \vec{p}.\vec{x}, \tag{24}$$

and the exponentials can be written as a sum of such terms (if one thinks in terms of series). We need to make sure that the integration measure is also Lorentz invariant. It is, however, an integral over the spatial momentum and that does not satisfy Lorentz invariance. We will need the function $f(p)$ to enforce this symmetry. A general invariant measure we can write would look like

$$d^4(p)\delta(p^2 - m^2)\Theta(p^0), \tag{25}$$

where we have the Dirac delta and the Heaviside step function. The step function ensures causality, while the Dirac delta guarantees that

$$p^2 + m^2 = -E^2 + \vec{p}.\vec{p} + m^2 = -m^2 + m^2 = 0. \tag{26}$$

We have a problem here: the first one is that the integral we have for the solution has a measure proportional to d^3p, while the invariant one is proportional to d^4p, so one integral need to be performed over the measure. We need to choose $f(p)$ to solve both issues. The solution is to write (recall that $p^0 = E$)

$$\int d^4p = \int d^3p\, dp^0 \Rightarrow \int d^3p\, dp^0 \delta(p^2 + m^2)\Theta(p^0) = \int \frac{d^3p}{2E}, \tag{27}$$

and with this we use the auxiliary function $f(p)$ to define our measure (we introduce the $(2\pi)^3$ factor for convenience) as:

$$dP = \frac{d^3p}{(2\pi)^3 2E} \Rightarrow \phi = \int dP \left[a(p)e^{-iEt+i\vec{p}.\vec{x}} + a(p)^\dagger e^{iEt-i\vec{p}.\vec{x}}\right]. \tag{28}$$

By using this equation for ϕ and the canonical commutation relations, we get:

$$[a(p), a^\dagger(p')] = (2\pi)^3(2E)\delta^3(\vec{p} - \vec{p'}), \tag{29}$$

$$[a(p), a(p')] = 0, \tag{30}$$

$$[a^\dagger(p), a^\dagger(p')] = 0. \tag{31}$$

An interesting (but long) calculation is trying to obtain the Hamiltonian in terms of a and $a^\dagger$. From the definition of Hamiltonian density integrated over all space:

$$H = \int d^3x\, \mathcal{H} = \int d^3x \left[\frac{1}{2}\left(\Pi^2 + m^2\phi^2 + (\nabla\phi)^2\right) - \Phi\right], \tag{32}$$

and the definition of the dirac delta function from a plane wave,

$$\int d^3x\, e^{i\vec{x}.\vec{y}} = (2\pi)^3\delta^3(\vec{y}), \tag{33}$$

we get, after working out the algebra:

$$H = \frac{1}{2}\int dP\ E(a^\dagger a + aa^\dagger) - \frac{1}{2}\int d^3x\Phi, \tag{34}$$

with the use of the commutation relations, we obtain:

$$H = \frac{1}{2}\int dP\ E(a^\dagger a) + \frac{1}{2}\delta^3(0)\int d^3p - \frac{1}{2}\int d^3x\ \Phi \tag{35}$$

The second term is clearly divergent. However, the factor Φ has not be chosen yet; in fact, if we set

$$\Phi = \frac{1}{2}\frac{\delta^3(0)\int d^3p}{\int d^3x}, \tag{36}$$

the divergence is cancelled. This is an example of renormalization, a concept that we will approach later.

The whole point of this treatment was to see that we have reduced the scalar field to a problem very similar to a harmonic oscillator, a fact that can be seen by the commutation relations for the a and $a^\dagger$, which can be though as creation and annihilation operators now. We may write:

$$a^\dagger(\vec{p})\,|0\rangle = |\vec{p}\rangle\,, \tag{37}$$

$$a(\vec{p})\,|0\rangle = 0, \tag{38}$$

in addition,

$$\langle\vec{p}_2 \mid \vec{p}_1\rangle = \langle 0 \mid a(\vec{p}_2)a^\dagger(\vec{p}_1) \mid 0\rangle\,, \tag{39}$$

after using the commutation relation and the fact that $\langle 0 \mid 0\rangle = 1$,

$$\begin{aligned}\langle\vec{p}_2 \mid \vec{p}_1\rangle &= \langle 0 \mid (2\pi)^3 2E\delta^3(\vec{p}_1 - \vec{p}_2) + a^\dagger(\vec{p}_1)a(\vec{p}_2) \mid 0\rangle \\ &= (2\pi)^3 2E\delta^3(\vec{p}_1 - \vec{p}_2).\end{aligned} \tag{40}$$

An interesting thing happens when we consider complex scalar fields. Since it has two degrees of freedom, the expansion has two independent parameters. The reality condition we impose in the real field made the coefficients in the expansion be related by a Hermitian conjugation; this will not be exactly the case again:

$$\phi(x) = \int dP \left[a(p)e^{ip.x} + b^\dagger(p)e^{-ip.x}\right], \tag{41}$$

$$\phi^\dagger(x) = \int dP \left[a^\dagger(p)e^{-ip.x} + b(p)e^{ip.x}\right]. \tag{42}$$

Now we have two kinds of operators and particles, the kinds a and b. They are related for having a common mass but opposite charge, composing a particle and antiparticle pair.

2.2.3 The Pauli exclusion principle

This principle is a consequence of the spin-statistics theorem, a result from axiomatic quantum mechanics. Particles with integer spin (bosons) occupy symmetric quantum states, while particles with half-integer spin (fermions) occupy antisymmetric states.

From the point of view of usual quantum mechanics, it means that the wave function for two fermions is antisymmetric with respect to the operation of exchanging the particles, while the wave function for bosons is symmetric. In terms of commutation relations, we impose that the operators for spin-half fields satisfy

$$\{a_1^\dagger a_2^\dagger\} = a_1^\dagger a_2^\dagger + a_2^\dagger a_1^\dagger = 0, \tag{43}$$

which implies,

$$a_1^\dagger a_2^\dagger = -a_2^\dagger a_1^\dagger \Rightarrow a_1^\dagger a_1^\dagger |0\rangle = -a_1^\dagger a_1^\dagger |0\rangle \Rightarrow a_1^\dagger a_1^\dagger |0\rangle = 0. \tag{44}$$

This means that if we quantize with anticommutation relations, particles are not allowed to simultaneously occupy a given state.

2.2.4 Canonical quantization of spin-half fields

As we did in the scalar field case, our objective here is to express the free fermion field using the formalism of harmonic oscillators, through creation and destruction operators. We begin with the Dirac field, following a procedure analogous to that used when we were dealing with scalar fields.

By definition, a spin 1/2 particle has two states: spin up and spin down, so the field has to be summed over these possibilities. The most general solution is

$$\psi_D(x) = \sum_{j=1}^{2} \int \hat{dp} \left[a_j(\vec{p}) b_j(\vec{p}) e^{ipx} + c_j^\dagger(\vec{p}) d_j(\vec{p}) e^{-ipx} \right], \tag{45}$$

where we have a_j is the lowering operator for the particle and $c_j^\dagger$ as the raising operator for the antiparticle. The raising operator for the particle and the lowering for the antiparticle can be obtained if we take the charge conjugate of ψ_D we will obtain the raising operator for the particle and the lowering for the antiparticle. The terms b_j and d_j are contant spinors.

In order to implement Pauli's exclusion principle, we enforce anti-commutation relations.

$$\{\psi_\alpha(t, \vec{x}), \bar{\psi}_\beta(t, \vec{x})\} = \delta^3(\vec{x} - \vec{x'})(\gamma_0)_{\alpha\beta}. \tag{46}$$

Using our expression for ψ_D,

$$\{a_j^\dagger(\vec{p}), c_{j'}(\vec{p'})\} = 2\omega\delta_{ss'}(2\pi)^3\delta^3(\vec{p} - \vec{p'}), \tag{47}$$

$$\{c_j(\vec{p}), a_{j'}^\dagger(\vec{p'})\} = 2\omega\delta_{ss'}(2\pi)^3\delta^3(\vec{p} - \vec{p'}). \tag{48}$$

We have reduced the problem to that of a harmonic oscillator. Following the same steps for the scalar fields [7], we obtain

$$H = \sum_{j=1}^{2} \int d\hat{p}\ E[a_j^\dagger(\vec{p})a_j(\vec{p}) + c_j^\dagger(\vec{p})c_j(\vec{p})] - \lambda. \tag{49}$$

where λ is an infinite onstant that can be subtracted off through methods similar to those employed in the section for scalar fields. For Majorana fields we only have one kind of particle,

$$\psi_M = \sum_{j=1}^{2} \int d\hat{p}\ [a_j(\vec{p})d_j(\vec{p})e^{ikx} + a_j^\dagger(\vec{p})b_j(\vec{p})e^{-ikx}], \tag{50}$$

and,

$$H = \sum_{j=1}^{2} \int d\hat{p}\ Ea_j^\dagger(\vec{p})a_j(\vec{p}). \tag{51}$$

2.3 Symmetry breaking

Many features of the Standard Model and modern particle physics are based on symmetry breaking. For example, the Weak and the Electromagnetic forces emerge after the symmetry breaking of an Electroweak theory, while the gauge bosons become massive. It is clear why particles need mass, but in particular for the gauge bosons, who travel as virtual particles "carrying" the forces, their mass is crucial to determine the range of the interaction (by the uncertainty principle). In this section, we will explore this concept in detail. Our main references here will be [7] and [6].

2.3.1 The Abelian case and the Goldstone Theorem

W will look first at symmetries generated by Abelian groups, and then consider the non-Abelian case. As we know, the Klein-Gordon Lagrangian is invariant under global gauge transformations, so we start with it. Consider the complex boson case,

$$\mathcal{L} = -\frac{1}{2}\partial^\mu\phi^\dagger\partial_\mu\phi - \frac{1}{2}m^2\phi^\dagger\phi = -\frac{1}{2}\partial^\mu\phi^\dagger\partial_\mu\phi - V, \tag{52}$$

where we defined

$$V = \frac{1}{2}m^2\phi^\dagger\phi. \tag{53}$$

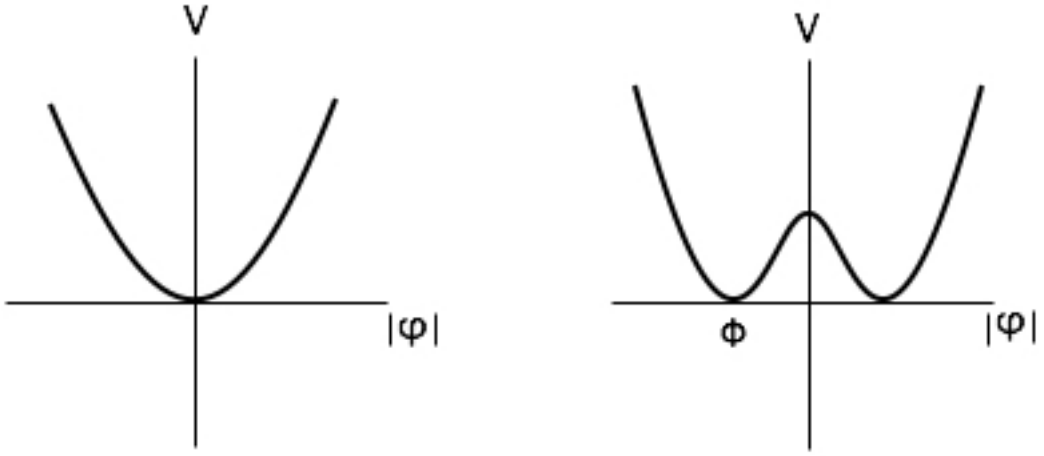

Figure 1: Potential before and after symmetry breaking

We have a minimum where $\phi^\dagger\phi = 0$, which corresponds to to the vacuum. Now consider the modified (by two real constants) potential:

$$V = \frac{1}{2}m^2\phi^\dagger\phi \rightarrow \frac{1}{2}\lambda m^2(\phi^\dagger\phi - \Phi)^2, \tag{54}$$

which still has the global U(1) symmetry. The minimum, however, is not the same anymore. It is not a point, but the set of points defined by $\mid \phi \mid = \Phi$. Note that the gauge transformation

$$\phi \rightarrow e^{i\alpha}\phi, \tag{55}$$

can be used to solve this problem. We choose a gauge (a value of α) that makes the vacuum real and equal to,

$$\phi = \Phi, \tag{56}$$

and define that as our vacuum state. The U(1) symmetry is not there anymore, and we have gauge fixed the symmetry. Now, we will expand around the new vacuum Φ,

$$\phi = \Phi + \alpha + i\beta, \tag{57}$$

and the reparametrized Lagrangian becomes

$$\mathcal{L} = -\frac{1}{2}\partial^\mu\alpha\partial_\mu\alpha - \frac{1}{2}\partial^\mu\beta\partial_\mu\beta - 2\lambda m^2\alpha^2\Phi^2 - \frac{1}{2}\lambda m^2\left(\alpha^4 + \alpha^2\beta^2 + \beta^4 + 4\Phi\alpha^3 + 4\Phi\alpha\beta^2\right). \tag{58}$$

Under these changes, we now have a theory that describes a number of fields:

I) Real massive scalar field α,

II) Real massless scalar field β,

III) Interaction terms combining α's and β's;

and doesn't have an explicit U(1) symmetry. This is why we say we are "breaking the symmetry"; by expanding around the new vacuum, a new massless field β was introduced. It can be shown that this happens whenever a global symmetry is broken, a massless boson is always introduced: they are called Goldstone bosons. This a general result, known as Goldstone Theorem (for proofs of the Theorem, see [23].

Let's now look at the case of a local U(1) symmetry for a complex scalar field by considering the following Lagrangian without an external source)

$$\mathcal{L} = \frac{1}{2}\left[(\partial^\mu - iqA^\mu)\phi^\dagger\right]\left[(\partial_\mu + iqA_\mu)\phi\right] - \frac{1}{4}F^{\mu\nu}F_{\mu\nu} - \frac{1}{2}\lambda m^2(\phi^\dagger\phi - \Phi)^2, \tag{59}$$

The vacuum state is degenerate, like before, and happens when $\mid \phi \mid = \Phi$. Since we can choose the phase $e^{i\alpha}$ to be different at every point, we can always set it to perform a rotation on the field ϕ at every point such that:

$$\phi \to e^{i\alpha(x)}\phi \in \mathbb{R}, \tag{60}$$

it belongs to the real numbers. Note that this is not restricted to the vacuum, like before.

Now that we have performed the gauge fixing, we expand around the new vacuum,

$$\phi = \Phi + h, \in \mathbb{R}, \tag{61}$$

and obtain the new Lagrangian,

$$\mathcal{L} = -\frac{1}{2}\partial^\mu h \partial_\mu h - \frac{1}{4}F^{\mu\nu}F_{\mu\nu} - 2\lambda(mh\Phi)^2 - \frac{1}{2}q^2\Phi^2 A^2 + (...), \tag{62}$$

where we omitted interaction terms. Before symmetry breaking, we had a massless field ϕ and a massless field A^μ (the photon). Now, the force-carrying field A_μ has aqcuired mass $q\Phi$ and we also have a real scalar field h with mass $\sqrt{4\lambda m^2\Phi^2}$. Therefore, mass was introduced through symmetry breaking. This is the Higgs mechanism, and h is the Higgs boson. Now, a local symmetry was broken, and the result is that the gauge field is now massive.

2.3.2 Symmetry breaking with a non-Abelian group

To make the result more general, consider now a collection of N fields ϕ, scalar or spinors. Following [7], let $\mathcal{L}$ denote the Lagrangian of the system, which is invariant under SO(N) or SU(N). Let's suppose that we are working in an certain representation R, spanned by the set of generators T^a of dimension $N \times N$. The gauge field can be expanded in terms of the generators, since A^μ is a matrix of order $D(R) \times D(R)$.

$$A^\mu = A^\mu_a T^a. \tag{63}$$

Each coefficient A^μ_a on the linear expansion can be thought of an independent scalar field. Since the gauge group has N generators, we have N such fields.

To illustrate this, let's consider a concrete example. Take the gauge group SU(N) in the fundamental representation, acting on a collection of N complex scalar fields,

$$\{\phi_j\} \in \mathbb{C}, \;\; j = 1...N. \tag{64}$$

As we did in the motivation example for the local U(1) case, we used the gauge group

to make the VEV (Vacuum Expectation Value) real. Now, we rotate everything to fall into a single component of the field, say ϕ_N

$$\langle 0 \mid \phi_j \mid \rangle = \langle 0 \mid \phi_N \mid 0 \rangle \, \delta_{j,N} = \Phi \, \delta_{j,N}, \tag{65}$$

where we introduced the Kronecker delta to say that all VEV's are zero except for the one of Φ_N. Expanding around the new vacuum:

$$\phi_j = \phi_j, \;\; j = 1...N-1; \tag{66}$$

$$\phi_N = \Phi + h. \tag{67}$$

so that in the vaccum state, we have for the VEV of the fields,

$$\begin{pmatrix} 0 \\ 0 \\ ... \\ \Phi \end{pmatrix},$$

Now take an element of SU(N) and act on the VEV,

$$\begin{pmatrix} a_{11} & a_{12} & ... & a_{1N} \\ a_{21} & a_{22} & ... & a_{2N} \\ ... & .... & ... & ... \\ a_{N1} & a_{N2} & ... & a_{NN} \end{pmatrix} \begin{pmatrix} 0 \\ 0 \\ ... \\ \Phi \end{pmatrix} = \begin{pmatrix} a_{1N}\Phi \\ a_{2N}\Phi \\ ... \\ a_{NN}\Phi \end{pmatrix},$$

Due to the fact that we have a VEV with all but one non-zero value, only the last collumn of the SU(N) group element is affected. The other N-1 rows and collumns are unnafected, and we have SU(N-1) left. Thus, we have broken

$$SU(N) \rightarrow SU(N-1). \tag{68}$$

2.4 The Standard Model of Particle Physics

In this section, we will provide an overview of the Standard Model. This is an extremely vast subject, and we will not explore all of its aspects in depth. Our main focus will mostly be on the Electroweak sector and the Higgs boson. We will follow [7] very closely, using also [6] when convenient.

Ou approach will be as follows: we will separate our analysis into the subgroups that act on each sector of our interest. We begin by looking at the Higgs fields and symmetry breaking. Once we understand the mechanism and how the gauge bosons for the Electroweak sector become massive, we move to the study of fermions, leptons and quarks, where we apply the results we obtained in the Higgs discussion. We will also comment quickly on the gluons, from the Strong force (the SU(3) portion).

2.4.1 The Electroweak sector

The gauge group here is $SU(2)_L \times U(1)_\gamma$. Our approach will start with the Higgs complex doublet ϕ in the representation $(\mathbf{2}, -1/2)$. Through the Higgs mechanism, the potential we will define for ϕ will (spontaneously) break the symmetry of the vacuum. The results will be:

I) A $U(1)$ symmetry that will describe a long ranged force: Electromagnetism.

II) Massive gauge bosons that describe the weak force, which is now a short ranged renormalizable gauge theory.

It is important to mention that the pattern assocaited with the masses of the gauge bososn provides an experimental test for the SM.

Let's construct the Lagrangian and all other important quantities of this sector; we begin by writing the covariant derivative. The generators of SU(2) on the representation **2** are given by

$$T_2^a = \frac{1}{2}\sigma^a, \tag{69}$$

which are the Pauli matrices, and we denote the gauge field by W_μ^a.

For the $U(1)_\gamma$ group, the generator is

$$Y = C \begin{pmatrix} 1 & 0 \\ 0 & 1 \end{pmatrix},$$

with C = -1/2 as the hypercherge and B_μ as the gauge field. The covariant derivative becomes

$$(D_\mu \phi)_i = \partial_\mu \phi_i - i[g_1 B_\mu Y + g_2 W_\mu^a T_2^a]_{ij} \phi_j, \tag{70}$$

where g_1 and g_2 are the coupling constants. If we write it expliciltly in matrix form,

$$\begin{pmatrix} D_\mu \phi_1 \\ D_\mu \phi_2 \end{pmatrix} = \begin{pmatrix} \partial_\mu \phi_1 + \frac{i}{2}(g_2 W_\mu^3 - g_1 B_\mu)\phi_1) + \frac{ig_2}{2}(W_\mu^1 - iW_\mu^2)\phi_2 \\ \partial_\mu \phi_2 + \frac{ig_2}{2}(W_\mu^1 + iW_\mu^2)\phi_1 + \frac{i}{2}(g_2 W_\mu^3 + g_1 B_\mu)\phi_2 \end{pmatrix}$$

.

Our Lagrangian has the form

$$\mathcal{L} = -\frac{1}{2} D_\mu \phi_i^\dagger D^\mu \phi_i - \frac{1}{4}\lambda \left(\phi^\dagger \phi - \frac{1}{2}\Phi^2 \right)^2. \tag{71}$$

All the 1/2 factors are a metter of convention and are simple rescalings of λ and Φ. For $\lambda > 0$, we have

$$\mid \phi \mid = \frac{\Phi}{\sqrt{2}}, \tag{72}$$

as the minimum. Now we will adress the symmetry breaking. As we did in the previous sections, we perfomr two gauge transformations: the first is a global SU(2) to put the VEV on the first component of ϕ, as in a rotation (that's why only the first component on the doublet is non-zero). With that fixed, we then perform a global U(1) transformation to make the field real,

$$\langle 0 \mid \phi \mid 0 \rangle = \frac{1}{\sqrt{2}} \begin{pmatrix} \Phi \\ 0 \end{pmatrix},$$

and now we may expand the field around this minimum,

$$\phi(x) = \frac{1}{\sqrt{2}} \begin{pmatrix} \Phi + h(x) \\ 0 \end{pmatrix},$$

from construction, $h(x)$ is a real scalar field. This is the Unitary Gauge for the Higgs field.

With these expresssions, we may go back to the Lagrangian and calculate is VEV. At the minimum,

$$\mathcal{L}_{\langle\phi\rangle} = -\frac{1}{8} \begin{pmatrix} \Phi & 0 \end{pmatrix} \begin{pmatrix} g_2 W_\mu^3 - g_1 B_\mu & g_2(W_\mu^1 - iW_\mu^2) \\ g_2(W_\mu^1 + iW_\mu^2) & -g_2 W_\mu^3 - g_1 B_\mu \end{pmatrix}^2 \begin{pmatrix} \Phi \\ 0 \end{pmatrix},$$

which is the kinetic term.

The next step is to find the masses of the four gauge bosons, W_μ^a (three of them) and B_μ. We rewrite the equation above (VEV for the Lagrangian) in a more convenient form,

$$\mathcal{L}_{\langle\phi\rangle} = -\frac{1}{8}\Phi^2 V_\mu^T \begin{pmatrix} g_2^2 & 0 & 0 & 0 \\ 0 & g_2^2 & 0 & 0 \\ 0 & 0 & g_2^2 & -g_1 g_2 \\ 0 & 0 & -g_1 g_2 & g_1^2 \end{pmatrix} V^\mu, \;\; V^\mu = \begin{pmatrix} W_\mu^1 \\ W_\mu^2 \\ W_\mu^3 \\ B_\mu \end{pmatrix}.$$

Looking at the mass matrix above, we see that two of the gauge bosons, W_μ^1 and W_μ^2 are diagonalized and have mass. We need to worry about the following block of the matrix,

$$M = \begin{pmatrix} g_2^2 & -g_1 g_2 \\ -g_1 g_2 & g_1^2 \end{pmatrix},$$

which mixes W_μ^3 and B_μ. Let's study it in more detail.

The first thing we notice is that its determinant is zero, so at least one of its eigenvalues has to be zero. In order to see this, recall that when diagonalized, all the eigenvalues of a matrix are on the diagonal; diagonalization, however, is a linear transformation and the determinant remains unchanged. So, at least on of the eigenvalues need to be null. The physical meaning of this is that there is still a massless gauge boson left. The eigenvalues for the block M are

$$\left\{0, -\frac{1}{8}\Phi^2(g_1^2 + g_2^2)\right\}, \tag{73}$$

which are associated to a massless state eigenvector and a massive one, repectively. Of course, the eigenvalues for the whole matrix are:

$$\left\{0, -\frac{1}{8}\Phi^2(g_1^2 + g_2^2), -\frac{1}{8}\Phi^2 g_1^2, -\frac{1}{8}\Phi^2 g_2^2\right\}. \tag{74}$$

Let's now look at the normalized eigenvectors that arise from the diagonalization process. They are:

$$A_\mu = \frac{1}{\sqrt{g_1^2 + g_2^2}} \begin{pmatrix} 0 \\ 0 \\ g_1 \\ g_2 \end{pmatrix}, \quad Z_\mu = \frac{1}{\sqrt{g_1^2 + g_2^2}} \begin{pmatrix} 0 \\ 0 \\ g_2 \\ -g_1 \end{pmatrix},$$

where Z_μ can be written as the following linear combination:

$$Z_\mu = g_2 W_\mu^3 - g_1 B_\mu. \tag{75}$$

If we look at the eigenvectors and their parameters, we may think of the mixing of states in a geometric way, and we define the Weak Mixing Angle by

$$\theta_W = \tan^{-1}\left(\frac{g_1}{g_2}\right). \tag{76}$$

and its trigonometric functions,

$$s_W = \sin(\theta_W) = \frac{g_1}{\sqrt{g_1^2 + g_2^2}}, \tag{77}$$

$$c_W = \cos(\theta_W) = \frac{g_2}{\sqrt{g_1^2 + g_2^2}}. \tag{78}$$

And now, we can also write four gauge fields are linear combinations of the original four we defined in the beginning,

$$W_\mu^+ = \frac{1}{\sqrt{2}}(W_\mu^1 - iW_\mu^2), \tag{79}$$

$$W_\mu^- = \frac{1}{\sqrt{2}}(W_\mu^1 + iW_\mu^2), \tag{80}$$

$$Z_\mu = c_W W_\mu^3 - s_W B_\mu, \tag{81}$$

$$A_\mu = s_W W_\mu^3 + c_W B_\mu, \tag{82}$$

where

$$\begin{pmatrix} Z_\mu \\ A_\mu \end{pmatrix} = \begin{pmatrix} W_\mu^3 cos\theta_W - B_\mu sin\theta_W \\ W_\mu^3 sin\theta_W + B_\mu cos\theta_W \end{pmatrix} \Rightarrow R(\theta_W) \begin{pmatrix} W_\mu^3 \\ B_\mu \end{pmatrix},$$

with $R(\theta_W)$ being a rotation. All of these equations may be inverted,

$$W_\mu^1 = \frac{1}{\sqrt{2}}(W_\mu^+ + W_\mu^-), \tag{83}$$

$$W_\mu^2 = \frac{i}{\sqrt{2}}(W_\mu^+ - W_\mu^-), \tag{84}$$

$$Z_\mu = c_W Z_\mu^3 + s_W A_\mu, \tag{85}$$

$$B_\mu = -s_W Z_\mu + c_W A_\mu. \tag{86}$$

It is important to mention that with this definiiton of the fields $W^\pm$, all terms in the lagrangian have an explicit $U(1)$ symmetry related to charge conservation. Note that Z_μ and A_μ are a massive and a massless linear combination of W^3_μ and B_μ, menaing that they are a combination of SU(2) and U(1). On the other hand, $W^\pm_\mu$ are massive linear combinations of W^1_μ and W^2_μ, meaning they are only from SU(2). Thus, $W^\pm_\mu$ are linear combinations of the fields associated with non-Cartan generators of SU(2), while Z_μ and A_μ are linear combinations of fields associated to Cartan generators of SU(2) and U(1). The consequence is that the fields $W^\pm_\mu$ will interact and change the charge, we see that they have the form of raising and lowering operators, while Z_μ, A_μ interact without changing charge.

In terms of the recently defined gauge fields, the kinetic term in the Lagrangian becomes

$$\mathcal{L}_\phi = -M_W^2 W^{+\mu} W^-_\mu - \frac{1}{2} M_Z^2 Z^\mu Z_\mu, \tag{87}$$

where

$$M_W = \frac{g_2 \Phi}{2}, \;\; M_Z = \frac{M_w}{c_w} = \frac{g_2 \Phi}{2 c_w} = \frac{\Phi}{2}\sqrt{g_1^2 + g_2^2}, \tag{88}$$

and the fields W^+_μ, W^-_μ, Z_μ are massive while A_μ remains massless through the symmetry breaking.

From this result, we draw some conclusions.

I) The W and Z bosons (masses $\approx$ 80.4 GeV and $\approx$ 91.2 GeV respectively) are the carries of the Weak Force, and their masses account for the short range of the force ($\approx 10^{-18}$ m)

II) A_μ is massless and is the carrier of the Electromagnetism, a result of the unbroken $U(1)$ symmetry.

Note that above the symmetry breaking scale we have a single theory: the Electroweak

Theory, with four massless bosons; when the symmetry is broken, we are left with the Weak and the Electromagnetic forces.

The neutrino event mentioned in the introduction is probe of the Weak interaction. Since it doesn't have electromagnetic charge, its interactions must be dictacted by the Weak force. There are essentially two processes involved this force: through neutral and charged currents. They will be explored in more detail in the Electroweak Physics chapter.

We are now ready to write the full Lagrangian for our effective theory of h(x). Our potential is (after using $\phi = \Phi + h(x)$)

$$V = \frac{1}{4}\lambda\left(\phi^\dagger\phi - \frac{\Phi^2}{2}\right)^2 \Rightarrow V = \frac{\lambda\Phi^2 h^2}{4} + \frac{\lambda\Phi h^3}{4} + \frac{\lambda h^4}{16}. \tag{89}$$

Note that the term

$$\sqrt{\frac{\lambda}{2}}\Phi, \tag{90}$$

gives the mass of the Higgs and the other terms account for interactions. The kinetic term is

$$-\frac{1}{2}\partial_\mu h \partial^\mu h. \tag{91}$$

We are still missing the gauge fields, and we need to get kinetic terms for them as well. We will do so by looking at the original fields before the symmetry is broken. We begin with B_μ. This is a U(1) gauge field, and we treat this case in Appendix B. Following the result presented in the appendix, we define

$$B_{\mu\nu} = \partial_\mu B_\nu - \partial_\nu B_\mu. \tag{92}$$

Now, we have the gauge fields $W^1_\mu,\ W^2_\mu,\ W^3_\mu$, and we need to do the same for them. Note that they are related to SU(2), a non-Abelian group. In Appendix B, we also considered the case of an arbitrary non-Abelian group; applying the results here:

$$F^1_{\mu\nu} = \partial_\mu W^1_\nu - \partial_\nu W^1_\mu + g_2(W^2_\mu W^3_\nu - W^2_\nu W^3_\mu), \tag{93}$$

$$F^2_{\mu\nu} = \partial_\mu W^2_\nu - \partial_\nu W^2_\mu + g_2(W^3_\mu W^1_\nu - W^3_\nu W^1_\mu), \tag{94}$$

$$F^3_{\mu\nu} = \partial_\mu W^3_\nu - \partial_\nu W^3_\mu + g_2(W^1_\mu W^2_\nu - W^1_\nu W^2_\mu), \tag{95}$$

which yelds

$$\mathcal{L}_{Kin} = -\frac{1}{4}F^{\mu\nu}_a F^a_{\mu\nu} - \frac{1}{4}B^{\mu\nu}B_{\mu\nu}. \tag{96}$$

We know how the old fields are related to the fields after symmetry breaking, so we can rewrite the kinetic Lagrangian to get:

$$\begin{aligned}
\mathcal{L}_{\rceil\{\{} = {} & \frac{1}{4}F^{\mu\nu}F_{\mu\nu} - \frac{1}{4}Z^{\mu\nu}Z_{\mu\nu} - D^{\dagger\mu}W^{-\mu}D_\mu W^+_\nu + D^{\dagger\mu}W^{-\nu}D_\nu W^+_\mu \\
& + ie(F^{\mu\nu} + \cot\theta_W Z^{\mu\nu})W^+_\mu W^-_\nu \\
& - \frac{1}{2}\left(\frac{e^2}{\sin^2\theta_W}\right)(W^{+\mu}W^-_\mu W^{+\nu}W^-_\nu - W^{+\mu}W^+_\mu W^{-\nu}W^-_\nu)\times \\
& \left(M^2_W W^{+\mu}W^-_\mu + \frac{1}{2}M^2_Z Z^\mu Z_\mu\right)\left(1 + \frac{h}{\nu}\right)^2 \\
& - \frac{1}{2}\partial^\mu h\partial_\mu h - \frac{1}{2}m_h h^2 - \frac{1}{2}\frac{m^2_h}{\nu}h^3 - \frac{1}{8}\frac{m^2_h}{\nu^2}h^4,
\end{aligned} \tag{97}$$

where

$$F_{\mu\nu} = \partial_\mu A_\nu - \partial_\nu A_\mu, \tag{98}$$

$$Z_{\mu\nu} = \partial_\mu Z_\nu - \partial_\nu Z_\mu, \tag{99}$$

$$D_\mu = \partial_\mu - ie(A_\mu + \cot\,\theta_W Z_\mu). \tag{100}$$

2.4.2 Leptons and Quarks

First, we define what we mean by a lepton: a lepton is a particle that interacts with the group $SU(2)_L \times U(1)_\gamma$ and possesses spin half. In total, we have six flavors of leptons, which belong to three generations (or families). Here, we list them.

I) First Generation: electron (e) and electron neutrino ν_e,

II) Second Generation: muon (μ) and muon neutrino ν_μ,

III) Third Generation: tau (τ) and tau neutrino ν_τ.

Each of the generations behave in the same way, so all we need to do is to derive the structure for one of the generations and then make three copies and then allow mixing between those copies.

The first problem we encounter is that we only need a left-handed neutrino (it only interacts through the Weak force and gravity), but the electron requires a left-handed and a right-handed state. To deal with this problem, we introduce the neutrino as part of a left-handed $SU(2)_L$ doublet together with the left handed electron,

$$L = \begin{pmatrix} \nu_e \\ e \end{pmatrix},$$

and we set the right-handed electron as a singlet under the $SU(2)_L$.

To make sense of the statements above, we now define two fields, L and $\bar{e}$, where L is the doublet we just defined (both are left-handed Weyl spinors). From our definition of L, it belongs to the (**2**,-1/2) representation, while $\bar{e}$ is in the (1,1) representation. Note that the neutrino is part of the doublet, and therefore does not possess a representation just for himself.

As we did in the beginning of the previous section, we can write the covariant derivative for these fields,

$$(D_\mu L)_i = \partial_\mu L_i - i g_2 W^a_\mu (T^a)_{ij} L_j - i g_1 B_\mu Y_L L_I, \tag{101}$$

$$D_\mu \bar{e} = \partial_\mu \bar{e} - i g_1 B_\mu Y_{\bar{e}} \bar{e}, \tag{102}$$

where

$$Y_L = -\frac{1}{2}\begin{pmatrix} 1 & 0 \\ 0 & 1 \end{pmatrix}, \;\; Y_{\bar{e}} = (1)\begin{pmatrix} 1 & 0 \\ 0 & 1 \end{pmatrix}.$$

Since $\bar{e}$ is in the trivial representation, it has no SU(2) term in its covariant derivative. If we follow the Lagrangian density for spin half fields (Dirac Lagrangian), we get

$$\mathcal{L}_{KIN} = i L^{\dagger i} \bar{\sigma}^\mu (D_\mu L)_i + i \bar{e}^\dagger \bar{\sigma}^\mu D_\mu \bar{e}. \tag{103}$$

The next step is to write the covariant derivative presented in this section in terms of the gauge fields after symmetry breaking. In order to do so, we will separate the analysis in two parts: the Cartan (A_μ and Z_μ) and the non-Cartan ($W^\pm_\mu$).

For the non-Cartan part:

$$g_2(W^1_\mu T^1 + W^2_\mu T^2) = \frac{1}{2} g_2 \left[W^1_\mu \begin{pmatrix} 0 & 1 \\ 1 & 0 \end{pmatrix} + W^2_\mu \begin{pmatrix} 0 & -i \\ i & 0 \end{pmatrix} \right] = \frac{g_2}{\sqrt{2}} \begin{pmatrix} 0 & W^+_\mu \\ W^-_\mu & 0 \end{pmatrix}, \tag{104}$$

since

$$W^\pm_\mu = W^1_\mu \mp i W^2_\mu. \tag{105}$$

For the Cartan part:

$$\begin{aligned} g_2 W^3_\mu T^3 + g_1 B_\mu Y &= \frac{e}{s_W}(s_W A_\mu + c_W Z_\mu) T^3 + \frac{e}{c_W}(c_W A_\mu - s_W Z_\mu) Y \\ &= e(A_\mu + \cot\theta_W Z_\mu) T^3 + e(A_\mu - \tan\theta_W Z_\mu) Y \\ &= e(T^3 + Y) A_\mu + e(\cot\theta_W T^3 - \tan\theta_W Y) Z_\mu. \end{aligned} \tag{106}$$

Since A_μ is the photon and e the elecric charge, we conclude that $T^3 + Y$, a linear combination of the generators of $SU(2) \times U(1)$, must be the generator of the electric charge. Let's look at this closely. First, T^3 is given by

$$T^3 = \frac{1}{2}\frac{1}{2}\sigma^3. \tag{107}$$

Note that

$$T^3 L = \frac{1}{2}\begin{pmatrix} 1 & 0 \\ 0 & 1 \end{pmatrix}\begin{pmatrix} \nu_e \\ e \end{pmatrix} = \frac{1}{2}\begin{pmatrix} \nu_e \\ -e \end{pmatrix}, \tag{108}$$

$$Y_L L = -\frac{1}{2}\begin{pmatrix} 1 & 0 \\ 0 & 1 \end{pmatrix}\begin{pmatrix} \nu_e \\ e \end{pmatrix} = -\frac{1}{2}\begin{pmatrix} \nu_e \\ e \end{pmatrix}, \tag{109}$$

$\bar{e}$ does not carry T^3 charge, giving an eigenvalue zero; for $Y_{\bar{e}}$, the eigenvalue is 1. Thus,

$$T^3 \nu_e = \frac{1}{2}\nu_e, \tag{110}$$

$$Y \nu_e = -\frac{1}{2}\nu_e, \tag{111}$$

$$T^3 e = -\frac{1}{3}e, \tag{112}$$

$$Y_e = -\frac{1}{2}e, \tag{113}$$

$$T^3 \bar{e} = 0, \tag{114}$$

$$Y \bar{e} = \bar{e}. \tag{115}$$

Define

$$Q = T^3 + Y \Rightarrow Q\nu_e = 0, \;\; Qe = -e, \;\; Q\bar{e} = \bar{e}. \tag{116}$$

Thus, the electron neutrino is massless, the electron has charge $-e$ and the positron has charge $+e$, as expected.

Now we need to incorporate mass in our theory, since we know that electrons and neutrinos are massive. The first option is clearly to try to directly write the mass in the Lagrangian, but that violates Lorentz invariance [7]. However, we can add a term of the form

$$\mathcal{L}_{Yukawa} = -y\epsilon^{ij}\phi_i(L_j\bar{e}) + h.c., \tag{117}$$

and use the Higgs mechanism. In the expression above, y is the Yukawa coupling, $(L\ e)$ is the Lorentz invariant combination of the supressed spinor indices for L and $\bar{e}$, ϵ^{ij} is the totally antisymmetric tensor which has the effect of combining the two SU(2) doublets into a singlet. In this term we only have singlets after performing all the contractions and the net hypercharge is zero.

Now, we go to the Unitary Gauge,

$$\phi_2 = 0, \;\; \phi_1 = \frac{1}{\sqrt{2}}(\nu + h(x)), \tag{118}$$

which gives

$$\begin{aligned}
\mathcal{L}_{Yukawa} &= -y\epsilon^{ij}\phi_i(L_j\bar{e}) + h.c. = -y(\phi_1 L_2 - \phi_2 L_1)\bar{e}) + h.c. \\
&- \frac{1}{\sqrt{2}}y(\nu + h)L_2\bar{e} + h.c. = -\frac{1}{\sqrt{2}}y(\nu + h)(e\bar{e}) - \frac{1}{\sqrt{2}}y(\nu + h)(\bar{e}^\dagger e^\dagger) \\
&= -\frac{1}{\sqrt{2}}y\nu\bar{\zeta}\zeta - \frac{1}{\sqrt{2}}y\nu h\bar{\zeta}\zeta, \;\; \zeta = \begin{pmatrix} e \\ i\sigma^2\bar{e}^\dagger \end{pmatrix}, \;\; \bar{\zeta} = \zeta^\dagger\gamma^0.
\end{aligned} \tag{119}$$

ζ is the Dirac field for the electron (the term e is the electron and the other the positron). The mass term for these particles is

$$m_e = \frac{y\nu}{\sqrt{2}}. \tag{120}$$

The problem of assigning mass to the neutrino is a non-trivial one, so we will not present it in detail here (see [6]).

Z_μ and A_μ interact without affecting the particles charges, since they are Cartan gauge particles. $W^\pm$ acts as raising oeprators for $SU(2)$. We can see its effect as follows: W^+ interacts with a left-handed electron rasing its charge and making it a neutrino, but it does not interact with a left-handed neutrino. W^- interacts with a neutrino, making it an electron. In Weak force terms, the exchange of a Z_μ is a neutral current and the exchange of $W^\pm$ is a charged current, as we will see in the Electroweak chapter.

We now turn our attention to quarks, and we will proceed in a way similar to what was done to leptons, working with one generation. We define the fields

$$\mathcal{Q}, \bar{u}, \bar{d}, \tag{121}$$

which are in the representation $(\mathbf{3}, \mathbf{2}, +1/6)$, $(\bar{\mathbf{3}}, 1, -2/3)$ and $(\mathbf{3}, 1, +1/2)$ of the Standard Model gauge group. Note that Q is a doublet under SU(2),

$$\mathcal{Q} = \begin{pmatrix} u \\ d \end{pmatrix}, \tag{122}$$

just as we defined L, and Q is the left handed part of u and d. The covariant derivatives are

$$(D_\mu \mathcal{Q})_{\alpha i} = \partial_\mu \mathcal{Q}_{\alpha i} - i g_3 A^a_\mu (T^a_3)^\beta_\alpha \mathcal{Q}_{\beta i} - i g_2 W^a_\mu (T^a_2)^j_i q_{\beta j} - i g_1 \left(\frac{1}{6}\right) b_\mu Q_{\alpha i}, \tag{123}$$

$$(D_\mu \bar{u})^\alpha = \partial_\mu \bar{u}^\alpha - g_3 A^a_\mu (T^a_{\bar{3}})^\alpha_\beta \bar{u}^\beta - i g_1 \left(-\frac{2}{3}\right) B_\mu \bar{u}^\alpha, \tag{124}$$

$$(D_\mu \bar{d})^\alpha = \partial_\mu \bar{d}^\alpha - i g_3 A^a_\mu (T^\alpha_{\bar{3}})^\alpha_\beta \bar{d}^\beta - i g_1 \left(\frac{1}{3}\right) B_\mu \bar{d}^\alpha. \tag{125}$$

In this notation, i is an $SU(2)_L$ index and α is an $SU(3)_C$ index, which is lowered for the **3** representation and raised for the $\bar{\mathbf{3}}$ representation. A^a_μ is the gluon field, and the 8 generators acting on the representation **3** are T^a_3, and for $\bar{\mathbf{3}}$ they are $T^a_{\bar{3}} = -(T^a_3)^\star$.

We need to apply symmetry breaking in order to give mass to quarks. We begin wuth the Yukawa Lagrangian,

$$\mathcal{L}_{Yukawa} = -y' \epsilon^{ij} \phi_i \mathcal{Q}_{\alpha j} \bar{d}^\alpha - y'' \phi^{\dagger i} \mathcal{Q}_{\alpha i} \bar{u}^\alpha + h.c, \tag{126}$$

and after symmetry breaking,

$$\mathcal{L}_{Yukawa} = -\frac{1}{\sqrt{2}} y'(\nu + h) \bar{\mathcal{D}}^\alpha \mathcal{D}_\alpha - \frac{1}{\sqrt{2}} y''(\nu + h) \bar{\mathcal{U}}^\alpha \mathcal{U}_\alpha, \tag{127}$$

where

$$\mathcal{D}_\alpha = \begin{pmatrix} d_\alpha \\ \bar{i}\sigma^2 d^\star_\alpha \end{pmatrix}, \ \mathcal{U}_\alpha = \begin{pmatrix} u_\alpha \\ \bar{i}\sigma^2 u^\star_\alpha \end{pmatrix}, \tag{128}$$

and the masses are given by

$$m_d = \frac{y'\nu}{\sqrt{2}}, \ \ m_u = \frac{y''\nu}{\sqrt{2}}. \tag{129}$$

The non-Cartan and Cartan parts of the covariant derivatives when written on terms of the low-energy gauge fields are

$$g_2 W^1_\mu T^1 + g_2 W^2_\mu T^2 = \frac{g_2}{\sqrt{2}} \begin{pmatrix} 0 & W^+_\mu \\ W^-_\mu & 0 \end{pmatrix} \tag{130}$$

$$g_2 W^3_\mu T^3 + g_1 B_\mu Y = eQA_\mu + \frac{e}{s_W c_W}(T^3 - s_W Q) Z_\mu, \tag{131}$$

where $Q = T^3 + Y$. The electric charges are

$$Qu = \frac{2}{3}u, \tag{132}$$

$$Qd = -\frac{1}{3}d, \tag{133}$$

$$Q\bar{u} = -\frac{2}{3}\bar{u}, \tag{134}$$

$$Q\bar{d} = \frac{1}{3}\bar{d}. \tag{135}$$

As mentioned before, the Standard Model has three generations of particles; each one of them possessing the structure described above. In order to allow couplings among generations, one must generalize the Yukawa couplings (see [7], [6]).

3 Elementary Topics in Quantum Field Theory

In this chapter, we present some results on Quantum Field Theory. Our goal is not to provide a deep explanation on this (extremely vast) topic, but to emphasize some fundamental concepts that will be useful later. The main references here will be [6], [11] and [10], but we will use others as necessary.

3.1 Non-relativistic perturbation theory

Let's discuss perturbation theory in the context of non-relativistic quantum mechanics, where all the dynamics is given by Schrodinger's equation. Within this framework, suppose that we have a Hamiltonian which can be written as a sum of two terms,

$$H = H_0 + V, \tag{136}$$

where H_0 is a time independent Hamiltonian (one that we know how to obtain the equations of motion from) and $V(t)$ is a time dependent potential, small compared to H_0, that can be treated as a perturbation. In our context, H_0 can be used to describe a free particle as our initial and final states for instance.

Now, we know that the eigenstates of H_0 satisfy

$$H_0 \left|n\right\rangle = E_n \left|n\right\rangle, \tag{137}$$

$$\left\langle m \mid n \right\rangle = \int_V d^3x \; \phi_m^\star \phi_n = \delta_{mn}, \quad \sum_n \left|n\right\rangle \left\langle n\right| = \mathbb{I}, \tag{138}$$

as they form a complete set of orthogonal states. A general solution of a problem defined by H_0 is given by

$$|\psi_n(t)\rangle = e^{-itH_0/\hbar}\,|n\rangle = e^{-itE_n/\hbar}\,|n\rangle\,. \tag{139}$$

At this point, we consider the effect of the perturbing potential, which is " "turned on" during a time interval, let's say, from 0 to T. The Schrodinger equation becomes

$$i\hbar\frac{d}{dt}\,|\psi(t)\rangle = (H_0 + V)\,|\psi(t)\rangle\,. \tag{140}$$

Since the eigenstates of H_0 form a complete set, we can expand the solution for the problem above as follows

$$|\psi\rangle = \sum_n c_n(t)e^{-iE_nt}\,|n\rangle\,. \tag{141}$$

This is the usual method for solving this problem. Instead, we will work with the interaction picture [19], because it makes the derivation less cumbersome and easier to generalize to higher orders of perturbation. Thus,

$$i\hbar\frac{d}{dt}\,|\psi\rangle_I = V_I(t)\,|\psi\rangle_I\,, \tag{142}$$

with

$$|\psi\rangle_I = e^{itH_0t}\,|\psi\rangle\,,\;\; V_I = e^{itH_0t}Ve^{-itH_0t}. \tag{143}$$

In this picture, the time evolution operator appears as

$$|\psi(t)\rangle_I = e^{itH_0t}U(t,t_i)\,|\psi(t_i)\rangle = e^{itH_0t}U(t,t_i)e^{-itH_0t}\,|\psi(t_i)\rangle_I = U_I\,|\psi(t_i)\rangle_I\,. \tag{144}$$

Using this result,

$$i\hbar\frac{d}{dt}U_I(t,t_i) = V_I U_I(t_{t_i}), \tag{145}$$

and the solution for this is the integral equation

$$U_I(t,t_i) = \mathbb{I} - \frac{i}{\hbar}\int_{t_i}^{t} dt' V_I(t') U_I(t',t_i), \tag{146}$$

where the initial condition chosen was

$$U_I(t_i,t_i) = \mathbb{I}. \tag{147}$$

The way time-dependent perturbation theory works is to provide approximate solutions to the expression above through iterations, under the assumption that the perturbing potential is small. To make the point clear, the first order solution is obtained when we set the evolution operator equal to the identity in the integral,

$$U_I^{(1)} = \mathbb{I} - \frac{i}{\hbar}\int_{t_i}^{t} dt' V_I(t'). \tag{148}$$

The second order solution is given by

$$\begin{aligned} U_I^{(2)} = \mathbb{I} - \frac{i}{\hbar}\int_{t_i}^{t} dt' V_I(t') U_I^{(1)} \Rightarrow U_I^{(2)} = \\ \mathbb{I} - \frac{i}{\hbar}\int_{t_i}^{t} dt' V_I(t') + \left(-\frac{i}{\hbar}\right)^2 \int_{t_i}^{t} dt'' V_I(t'') \int_{t_i}^{t''} dt''' V_I(t'''). \end{aligned} \tag{149}$$

If one keeps following this procedure the result obtained is known as the Dyson series, with U_I being

$$\begin{aligned} U_I(t_i,t_i) = \mathbb{I} - \frac{i}{\hbar}\int_{t_i}^{t} dt_1 V_I(t_1) + \left(-\frac{i}{\hbar}\right)^2 \int_{t_i}^{t} dt_2 V_I(t_2) \int_{t_i}^{t_2} dt_3 V_I(t_3) + ... \\ \left(-\frac{i}{\hbar}\right)^n \int_{t_i}^{t} dt_2 V_I(t_2) \int_{t_i}^{t_2} dt_3 V_I(t_3) \int_{t_i}^{t_4} dt_4 V_I(t_4) ... \int_{t_i}^{t_{n-1}} dt_n V_I(t_n) + ... \end{aligned} \tag{150}$$

The Dyson series can be used to define the S-matrix (S comes from scattering). The

whole idea remains the same; the difference is that now we will split a Hamiltonian density into a known portion and an interaction portion, so that we can write

$$S = \sum_{n=0}^{\infty} \frac{(-1)^n}{n!} \int_{-\infty}^{\infty} dx_1^4 ... \int_{-\infty}^{\infty} dx_n^4 T[H_I^1 H_I^2 ... H_I^n], \tag{151}$$

where T denotes time-ordering (we need to respect the order of the operators and integrals since each integral has limits of integration that depend on the previous integration). In addition, note that S is unitary operator.

We could try to define a transition probability now. Let $|i\rangle$ denote the initial unperturbed state, while $|f\rangle$ is the final one. We have:

$$T_{fi} = | \langle f | U_I(t, t_i) | i \rangle |^2 = | \langle f | i \rangle - \frac{i}{\hbar} \int_0^t dt' e^{i\omega_{fi} t'} \langle f | V(t') | i \rangle + ... |^2 . \tag{152}$$

Note that

$$\begin{gathered} \langle f | V_I(t') | i \rangle = \langle f | e^{iH_0 t'/\hbar} V(t') e^{iH_0 t^{-\prime}/\hbar} | i \rangle = e^{i\omega_{fi} t'} \langle f | V(t') | i \rangle , \\ \omega_{fi} = \frac{E_f - E_i}{\hbar} = E_f - E_i \ (\hbar = 1). \end{gathered} \tag{153}$$

Since $\langle f | i \rangle = \delta_{ij}$, the result at first order for $f \neq i$ is

$$T_{fi} = | -\frac{i}{\hbar} \int_0^t dt' e^{i\omega_{fi} t'} \langle f | V(t') | i \rangle |^2 . \tag{154}$$

In order to better understand this expression and check its consistency, we now look at the integral when our potential is time independent. This yelds

$$-iV_{fi} \int_{-\infty}^{\infty} dt e^{i\omega_{fi} t} = -\frac{2\pi i}{\hbar} V_{fi} \delta(E_f - E_i). \tag{155}$$

We can interpret the delta function as the statement that energy is conserved in the transition, but it poses a problem with the normalization of this expression. Instead, we should work with a transition probability per unit time, and define it as

$$W = \lim_{T\to\infty} \frac{T_{fi}}{T}, \tag{156}$$

which implies

$$\begin{aligned} W &= \lim_{T\to\infty} \frac{2\pi}{\hbar^2} \frac{|V_{fi}|^2}{T} \delta(E_f - E_i) \int_{-T/2}^{+T/2} dt\, e^{i(E_f - E_i)t/\hbar} \\ &= \lim_{T\to\infty} \frac{2\pi}{\hbar} \frac{|V_{fi}|^2}{T} \delta(E_f - E_i) \int_{-T/2}^{+T/2} dt \\ &= \frac{2\pi}{\hbar} |V_{fi}|^2 \delta(E_f - E_i)\ . \end{aligned} \tag{157}$$

This expression needs to be integrated to have physical meaning. If we denote by $\rho(E_f)$ the density of final states, with $\rho(E_f)dE_f$ being the number of states in the energy interval $(E_f, E_f + dE_f)$, the result is

$$W_{fi} = \frac{2\pi}{\hbar^2} \int dE_f \rho(E_f) \mid V_{fi} \mid^2 \delta(E_f - E_i) = \frac{2\pi}{\hbar^2} \mid V_{fi} \mid^2 \rho(E_i). \tag{158}$$

Under those assumptions, we can look at higher order terms through the Dyson series. Consider, for example, the second order term, which is proportional to the factor

$$\sum_n V_{fn} V_{ni} \int_{-\infty}^{\infty} dt_2 e^{i(E_f - E_i)t_2\hbar} \int_{-\infty}^{t_2} dt_3 e^{i(E_f - E_i)t_3/\hbar}. \tag{159}$$

In order to regularize the integral ofer t_3, we introduce a parameter ϵ, such that the original expression is recovered in the limit $\epsilon \to 0$.

$$\int_{-\infty}^{t_2} dt_3 e^{i(E_f - E_i)t_3\hbar} \to \int_{-\infty}^{t_2} dt_3 e^{i(E_f - E_i - \epsilon)t_3/\hbar} = i \frac{e^{i(E_f - E_i - \epsilon)t_2/\hbar}}{E_f - E_i + i\epsilon}, \tag{160}$$

and the second order correction is given by

$$T_{fi}^{(2)} = -\frac{2\pi i}{\hbar} \sum_n \frac{V_{fn} V_{ni}}{E_i - E_n + i\epsilon} \delta(E_f - E_i), \tag{161}$$

and we see that the effect of considering the higher order is

$$V_{fi} \to V_{fi} + \sum_n \frac{V_{fn}V_{ni}}{E_i - E_n + i\epsilon}. \tag{162}$$

3.2 Invariant amplitude

Particle physics has essentially three ways of probing theories: by looking at bound states, scattering and decays. In particular, scattering and decays are crucial to the study of quantum field theory. As it was mentioned in the Standard Model chapter, particle interactions are mediated by the exchange of virtual particles, which are associated with the Cartan generators of the group that defines the interaction. Those particles can not travel indefinetely, as they are subject to the uncertainty principle, and that explains the range of the different forces. When we calculate cross sections, the interaction between particles can be descrided by free fields in the initial and the final state, while the exchange of virtual particles (the interaction) happens in between.

The invariant amplitude $\mathfrak{M}$ for scattering is the sum of each possible interaction history over all possible intermediate states. This notion fits nicely with the idea of path integrals and perturbation theory, where the order of perturbation is given by the number of times the interaction Hamiltonian acts. The way that we calculate the invariant amplitude $\mathfrak{M}$, summing the terms of this perturbative approach, is through the use of Feynman diagrams.

For the discussion that follows, we will assume for that $\mathfrak{M}$ is given. A detailed prescription on how to find through perturbative methods will be explained when we present the Feynman rules. In the next section, we will study the role the invariant amplitude plays when we consider decays and scatterings.

3.3 Decay rates and cross-sections

As it was mentioned, bound states, decays and scatterings are the probes of particle physics. For decays, a quantity of great interest is the lifetime of the particle we are studying, but there are a few caveats we need to be aware of when we try to understand a decay process. The first is with respect to the inertial frame we are using: due to

special relativity, the lifetime depends if we look at the process from the rest frame or a lab frame. The second observation is known from our studies of radioacive material: there is an inherently randomness in decays, which, in simpler terms, is equivalent to saying that particles have no memory; the chances of a muon decaying at a given instant of time is independent of the moment of time when the muon was created. Thus, what we can truly measure and understand is the mean lifetime of particles in a large sample.

We define the notion of decay rate Γ, the probability per unit time that any given particle will decay. Thus, the number of particles (before decaying) in a certain sample is a function of time, and this number changes as:

$$dN = -\Gamma N dt \Rightarrow N(t) = N(t_0)e^{t\Gamma}, \tag{163}$$

which motivates the definition for the mean lifetime,

$$\tau = \frac{1}{\Gamma}. \tag{164}$$

Another important fact (which has been observed on experiments) is that a given particle can have multiple decay paths. Later, we will consider charged pions, which are of great interest for us, as their decay produce neutrinos. A charged pion can decay through many routes,

$$\pi^- \to e^- + \nu_e, \;\; \mu^- + \nu_\mu, \tag{165}$$

and so on. Quantum field theory allows us to predict those different routes and calculate the chance that a certain particle decays choosing a certain route, as we will see later in this chapter. Thus, it is of interest to us to define the notion of branching ratios. Let Γ_i be the deay rate through a certain mode for a given particle. We define the branching ration fot the $i-th$ mode as

$$B = \frac{\Gamma_i}{\Gamma_{total}}, \tag{166}$$

where

$$\Gamma_{total} = \sum_i \Gamma_i. \tag{167}$$

We also define the lifetime of a particle as

$$\tau = \frac{1}{\Gamma_{total}}. \tag{168}$$

For scattering, the quantity of interest is the cross-section. Note, however, that we a re not talking about billiard balls, but quantum particles. In classical mechanics, you either hit or miss the target, but in our context a test particle can be deflected by getting close enough to its target and being subject through interaction with the target.

Collisions can be elastic,

$$e + p \rightarrow e + p, \tag{169}$$

or inelastic,

$$e + p \rightarrow e + p + \gamma. \tag{170}$$

The energy of the incident particle (as well as many other properties like helicity) plays a crucial in the outcome of a scattering reaction. In particular, resonances can occur. When this is the case, we can calculate the cross-section and see that there is a certain energy that greatly increases it, and the particles, incident and target, form a short lived semibound state before breaking apart. These resonant peaks in the cross-sections are one of the main methods we have that allow the detection of short-lived particles.

Recalling the definition of the S-matrix in terms of the Dyson series,

$$S = \sum_{n=0}^{\infty} \frac{(-1)^n}{n!} \int_{-\infty}^{\infty} dx_1^4 ... \int_{-\infty}^{\infty} dx_n^4 T[H_I^1 H_I^2 ... H_I^n], \tag{171}$$

Now, we know that the 3-momentum can be used in quantum mechanics to form a complete set of states. Now, we extended this notion for the 4-momentum in the following

expressions (completeness and orthogonality)

$$1 = \int \frac{d^4p}{(2\pi)^4} 2\pi\delta(p^2 - m^2)\Theta(p_0) \left|p\right\rangle \left\langle p\right| , \tag{172}$$

$$\left\langle p \mid p'\right\rangle (2\pi)^4 \delta^4(p^\mu - p^{\mu'}) \tag{173}$$

The first expression is the completeness relation. The integral is a combination of over the usual integral over spatial components together with an integral over the zero-th component of the 4-momentum (the energy), where the Heaviside function $\Theta(x)$ is introduced to ensure energy positivity, while the delta function is the conservation of energy, which constrains the components of the 4-momentum. The other numerical factors on the expression are there for normalization purposes. Finally, the second expression is the orthogonality relation.

Now, if we look at the Dyson series and keep terms up to first order while using the definitions above, we obtain for the transition

$$\left\langle f \mid S \mid i\right\rangle = \delta_{fi} - i(2\pi)^4 \delta^4(p_f^\mu - p_i^\mu)\mathfrak{M}_{fi} \tag{174}$$

Recall from the canonical quantization discussed before that we can create particles by acting on the vacuum with a creation operator,

$$\left|p\right\rangle = a^\dagger \left|p\right\rangle , \tag{175}$$

and if we want to create an arbitrary number of particles,

$$\left|p_1, p_2, ..., p_n\right\rangle = a^\dagger(p_1)... = a^\dagger(p_n) \left|0\right\rangle . \tag{176}$$

On the perturbation theory section, we introduced the result usually known as Fermi's Golden rule:

$$T_{fi} = \frac{2\pi}{\hbar} \mid V_{if} \mid^2 \delta(E_f - E_i). \tag{177}$$

When the transtion we are talking about is related to scatterings and decays, the invariant amplitude is what plays the role of V, since it is what describes the interaction. Thus, in our context, we can see this result as:

$$(\text{transition rate}) = 2\pi \mid \mathfrak{M} \mid^2 (\text{phase space}). \tag{178}$$

Note that by "phase space" we are referring to energy, momentum and masses, which will be subject to constraints, such as conservation laws, in those reactions. Using these results, one can obtain general expressions for the decay rate and the cross section. According to [11], we have:

I) Particle decays

Consider the following reaction:

$$1 \to 2 + 3 + 4 + ... + n, \tag{179}$$

which has a decay rate given by

$$d\Gamma = \mid \mathfrak{M} \mid^2 \frac{C}{2m_1}(2\pi)^4 \delta^4(p_1^\mu - p_2^\mu - ... - p_n^\mu) \prod_{i=2}^{n} \frac{d^3\vec{p}_i}{2(2\pi)^3 E_i}, \tag{180}$$

where C is a product of factors of the form

$$\frac{1}{j!}, \tag{181}$$

to account for groups of j identical particles in the final state.

II) Particle scattering

Consider the reaction

$$1 + 2 \to 3 + 4 + ... + n, \tag{182}$$

which has a cross section given by (the definition of C remains the same here)

$$d\sigma = \mid \mathfrak{M} \mid^2 \frac{C}{4\sqrt{(p_1^\mu p_{2\,\mu})^2 - (m_1 m_2 c^2)^2}} (2\pi)^4 \delta^4(p_1^\mu - p_2^\mu - ... - p_n^\mu) \prod_{i=3}^{n} \frac{d^3\vec{p}_i}{2(2\pi)^3 E_i}, \quad (183)$$

Just to have a better intuition on how we operate with these equations, consider the decay of a neutral pion, which we will try to describe using this framework. Suppose that we know the value of $\mathfrak{M}$,

$$\pi^0 \to \gamma + \gamma, \quad (184)$$

and we choose to work in the rest frame of the pion. The pion is the particle 1, while the photons are 2 and 3. Note that:

$$E_1 = mc^2, \;\; \vec{p}_1 = 0, \quad (185)$$

and

$$m_2 = m_3 = 0, \;\; E_2 = \mid \vec{p}_2 \mid c, \;\; E_3 = \mid \vec{p}_3 \mid c. \quad (186)$$

In addition,

$$\delta^4(p_1^\mu - p_2^\mu - p_3^\mu) = \delta\left(mc - \frac{E_2}{c} - \frac{E_3}{c}\right) \delta^3(-\vec{p}_2 - \vec{p}_3). \quad (187)$$

Integrating over $\vec{p}_3$ first,

$$\begin{aligned} \Gamma &= \frac{1}{2} \frac{1}{(4\pi)^2} \frac{C}{m\hbar} \int d^3\vec{p}_2 d^3\vec{p}_3 \frac{\mid \mathfrak{M} \mid^2}{p_2 p_3} \delta\left(mc - \frac{E_2}{c} - \frac{E_3}{c}\right) \delta^3(-\vec{p}_2 - \vec{p}_3) \\ &= \frac{1}{2} \frac{1}{(4\pi)^2} \frac{C}{m\hbar} \int d^3\vec{p}_2 \frac{\mid \mathfrak{M} \mid^2}{(p_2)^2} \delta(mc - 2p_2), \end{aligned} \quad (188)$$

where p_2 and p_3 are the magnitudes of the 3-momentum. Making

$$d^3\vec{p}_2 = p_2^2 \sin\theta \; dp_2 \; d\theta \; d\phi, \quad (189)$$

nd integrtting over the angles to get 4π, we obtain

$$\Gamma = \frac{C}{8\pi\hbar m}\int_0^\infty dp_2 \mid \mathfrak{M} \mid^2 \delta(mc - 2p_2) \Rightarrow \Gamma = \frac{C}{16\pi\hbar m} \mid \mathfrak{M} \mid^2 . \tag{190}$$

Note that in this case C =1/2.

When we are dealing with particles that have spin, this fact will obviously be reflected on the invariant amplitude. Thus, we introduce the idea of an unpolarized cross section. Most of the time, an experiment starts with a beam of particle (such as in a collider) with spins randomly oriented, and all that we care about is spatial distribution of scattered particles, for example. In this kind of situation, the cross section of interest is the average of all initial spin configurations and the sum over all final spin configurations.

$$\begin{aligned} \mid \mathfrak{M} \mid^2 \rightarrow \overline{\mid \mathfrak{M} \mid^2} &\equiv \frac{1}{(2s_A+1)(2s_B+1)} \sum_{spins} \mid \mathfrak{M} \mid^2 \\ &= \frac{1}{(2s_A+1)(2s_B+1)} \left(\sum_{spins} \mathfrak{M} \right) (\mathfrak{M}^\star) , \end{aligned} \tag{191}$$

where $\overline{\mid \mathfrak{M} \mid^2}$ is the unpolarized cross section and s_A and s_B are the spin of the particles (in the definition above we considered inly two particles).

We now need to understand how to evaluate expressions like the definition above. We will be dealing with terms of the form

$$G = [\bar{u}_a M_1 u_b][\bar{u}_a M_2 u_b]^\star, \tag{192}$$

where a and b label the spinors that describe different particles, each one of them with their own value for spin and momentum, and the M's are 4x4 matrices. This is common when one works in Quantum Electrodynamics, when we have reactions involving electrons (or positrons) and photons, with gamma matrices appearing everywhere. An example of a QED process of interest to us is the Compton scattering, of great importance on stablishing bounds on multi-messenger searches of other observables.

First, evaluate the complex conjugate, which is the same as an Hermitian conjugate

since the quantity inside the brackets is a 1x1 matrix,

$$\begin{aligned}[\bar{u}_a M_2 u_b]^\star &= [u_a^\dagger \gamma^0 M_2 u_b]^\dagger = u_b^\dagger M_2^\dagger \gamma^{0\dagger} u_a \\ &= u_b^\dagger \gamma^0 \gamma^0 M_2^\dagger \gamma^0 u_a = \bar{u}_b (\gamma^0 M_2 \gamma^0) u_a,\end{aligned} \tag{193}$$

and we define

$$\bar{M}_2 = \gamma^0 M_2 \gamma^0 \Rightarrow G = [\bar{u}_a M_1 u_b][\bar{u}_b \bar{M}_2 u_a]. \tag{194}$$

In order to continue, we will need one result: the completeness relation for spinors. Let u be a spinor that represents a particle, and v a spinor that represents the correponding antiparticle; we have:

$$\sum_{s=1,\ 2} u_p^{(s)} \bar{u}_p^{(s)} = \gamma^\mu p_\mu + m = \not{p} + m, \tag{195}$$

$$\sum_{s=1,\ 2} v_p^{(s)} \bar{v}_p^{(s)} = \gamma^\mu p_\mu - m = \not{p} - m, \tag{196}$$

where we introduced Feynman's slash notation: whenever we have a contraction of the form shown above, we use the "slash". Now we perform the sum over the spins of particle b,

$$\sum_{b\ \text{spins}} G = u_a M_1 \left(\sum_{s_b=1,\ 2} u_b^{(s_b)} \bar{u}_b^{(s_b)} \right) \bar{M}_2 u_a = \bar{u}_a M_1 (\not{p}_b + m_b) M_2 u_a, \tag{197}$$

and doing the same for particle a,

$$\sum_{a\ \text{spins}} \sum_{b\ \text{spins}} G = \sum_{s_a=1,\ 2} \bar{u}_a^{(s_a)} M_1 (\not{p}_b + m_b) M_2 u_a^{(s_a)}. \tag{198}$$

This is a bit trickier. To simplify the notation, define

$$M_3 = M_1 (\not{p}_b + m_b) \bar{M}_2, \tag{199}$$

and we will use index notation to do the following matrix multiplication (note that i and j range from 1 to 4):

$$\sum_{s_a=1,\ 2} (\bar{u}_a^{(s_a)})_i (M_3)_{ij} (u_a^{(s_a)})_j = (M_3)_{ij} \left[\sum_{s_a=1,\ 2} u_a^{(s_a)} \bar{u}_a^{(s_a)} \right]_{ji} \tag{200}$$
$$= (M_3)_{ij} (\not{p}_a + m_a)_{ji} = Tr[M_1(\not{p}_b + m_b)\bar{M}_2(\not{p}_a + m_a)],$$

Thus,

$$\sum_{\text{all spins}} G = Tr[M_1(\not{p}_b + m_b)\bar{M}_2(\not{p}_a + m_a)], \tag{201}$$

and all we need to do is matrix multiplication and take a trace, since there are no spinors anymore. The relation above is known as the "Casimir trick". Note that if we have antiparticles spinors, the corresponding mass changes sign and becomes negative. There are a number of theorems and results on traces, and we list them on Appendix D.

Let's consider an example in order to use the result presented above. We will consider a muon decay; we will not show how to obtain the amplitude since it is a Weak interaction process, and we will see it in the next chapter. We are only interested in summing over the spins, and according to [6],

$$\mathfrak{M} = \frac{G_F}{\sqrt{2}} [\bar{u}(k)\gamma^\mu(\mathbb{I} - \gamma^5)u(p)][\bar{u}(p')\gamma^\mu(\mathbb{I} - \gamma^5)v(k')], \tag{202}$$

Now, we need to perform the sum,

$$\overline{|\ \mathfrak{M}\ |^2} = \frac{1}{2} \sum_{spins} |\ \mathfrak{M}\ |^2 = \frac{1}{2} \left(\frac{G_F}{\sqrt{2}} \right)^2 \sum_{spin} [\bar{u}(k)\gamma^\mu(\mathbb{I} - \gamma^5)u(p)\bar{u}(p)\gamma^\nu(\mathbb{I} - \gamma^5)u(k)] \times \tag{203}$$
$$\sum_{spin} [\bar{u}(p')\gamma_\mu(\mathbb{I} - \gamma^5)v(k')\bar{v}(k')\gamma_\nu(\mathbb{I} - \gamma^5)u(p')],$$

using Casimir's trick, we turn the sums into traces

$$\begin{aligned}\overline{|\,\mathfrak{M}\,|^2} &= \frac{1}{2}\frac{G_F^2}{2}\mathrm{Tr}[\not{k}\gamma^\mu(\mathbb{I}-\gamma^5)(\not{p}-\mathrm{m}_\mu)\gamma^\nu(\mathbb{I}-\gamma^5)]\times\mathrm{Tr}[\not{p}'\gamma^\mu(\mathbb{I}-\gamma^5)(\not{k}'-\mathrm{m}_\mu)\gamma^\nu(\mathbb{I}-\gamma^5)] \\ &= \frac{G_F^2}{4}\mathrm{Tr}[\not{k}\gamma^\mu(\mathbb{I}-\gamma^5)\not{p}\gamma^\nu(\mathbb{I}-\gamma^5)]\times\mathrm{Tr}[\not{p}'\gamma^\mu(\mathbb{I}-\gamma^5)\not{k}'\gamma^\nu(\mathbb{I}-\gamma^5)] \\ &- m_\mu\mathrm{Tr}[\not{k}\gamma^\mu(\mathbb{I}-\gamma^5)\gamma^\nu(\mathbb{I}-\gamma^5)]\times\mathrm{Tr}[\not{p}'\gamma^\mu(\mathbb{I}-\gamma^5)\not{k}'\gamma^\nu(\mathbb{I}-\gamma^5)],\end{aligned} \tag{204}$$

Finally, it is worth mentioning that we can apply the definition of Mandelstam variables (Appendix A) on all the expressions we used in here, in particular to the invariant amplitude.

3.4 VEV's, path integrals and matrix elements

One of the most famous quantum mechanics experiments is, without a doubt, the double slit experiment. There, we have a source emitting electrons, a screen with two small slits and a wall afterwards, which serves as a detector. As we know, when a electron goes though the screen with slits, it actually goes through both slits at the same time (as long as we don't try to measure by which slit it travelled). There is a superposition of the paths, and we see an interference pattern on the detection wall.

We can think of it in the following way: when travelling (without being observed) from point A to point B in space, a particle actually travels through all posiblle paths at the same time. Once we observe it, there is a probablility associated with each path. In the double slit case, there is a probabiblity associated with the path that goes through the first slit, a probability associated with the path that goes through the second slit, a non-zero (extremely small) probablity that the electron travelled all the way around Earth and landed on the wall, and so on. Until the moment of observation, there is a superposition of all possible paths; this is the idea behind the path integral formalism.

Consider a particle that goes from the position x_A at t_A to x_B at t_B. The transition amplitude is given by:

$$\langle x_B, t_B \mid x_A, t_A \rangle = \langle x_B | \, e^{iH(t_B - t_A)} \, | x_A \rangle \, . \tag{205}$$

Assume that $|x\rangle$ forms a complete set of states,

$$\int dx \, |x\rangle \, \langle x| = 1, \tag{206}$$

and break the interval $\tau = t_B - t_A$ into N+1 intervals of equal length. We use the completeness of states to write:

$$\langle x_B, t_B \mid x_A, t_A \rangle = \int_{-\infty}^{\infty} \prod_{i=1}^{N} dx_i \, \langle x_B | \, e^{-iH\delta t} \, | x_N \rangle \, \langle x_N | \, e^{-iH\delta t} \, | x_{N-1} \rangle \, ... \, \langle x_1 | \, e^{-iH\delta t} \, | x_A \rangle \, . \tag{207}$$

with $\delta t = T/(N+1)$. Take one of the factors $\langle x_{j+1}| \, e^{-iH\delta t} \, |x_j\rangle$:

$$\langle x_{j+1}| \, e^{-iH\delta t} \, |x_j\rangle = \langle x_{j+1}| \, e^{-i\left(\frac{K^2}{2m}\right)\delta t} \, |x_j\rangle \, . \tag{208}$$

For simplicity, we will consider a Hamiltonian composed of only a kinetic part. We could include a potential but it would make the expressions a bit more cumbersome and it doens't make any difference in our treatment, so we will do the calculations for the simplest case. We will use the completeness relation again, but now for the momentum states:

$$\langle x_{j+1}| \, e^{-iH\delta t} \, |x_j\rangle = \langle x_{j+1}| \, e^{-i\frac{K^2}{2m}\delta t} \, |x_j\rangle = \int dk \, \langle x_{j+1}| \, e^{-i\frac{K^2}{2m}\delta t} \, |k\rangle \, \langle k| \, |x_j\rangle \, . \tag{209}$$

Recall that the expression for a plane wave (in one dimension) is given by:

$$\langle x \mid k \rangle = \frac{1}{\sqrt{2\pi}} e^{ikx}, \tag{210}$$

and we have:

$$\langle x_{j+1}|\, e^{-iH\delta t}\, |x_j\rangle = \int dk\; e^{-i\frac{k^2}{2m}\delta t}\, \langle x_{j+1}\mid k\rangle\, \langle k\mid x_j\rangle = \int dk\; \frac{1}{2\pi} e^{ik(x_{j+1}-x_j)} e^{-iH(k,x_j)\delta t}$$
$$= \int dk\; \frac{1}{2\pi} e^{\frac{ik(x_{j+1}-x_j)}{\delta t}\delta t}\, e^{-i\frac{k^2}{2m}\delta t} \tag{211}$$

Note that the integral bove can be performed, it is a Gaussian integral. In addition, if we have included a term for the potential in the Hamiltonian we would have a factor of $e^{iV(x)}$ in the integrand, and the integral could still be done.

$$\begin{aligned}\langle x_{j+1}|\, e^{-iH\delta t}\, |x_j\rangle &= \int dk\; \frac{1}{2\pi} e^{\frac{ik(x_{j+1}-x_j)}{\delta t}\delta t}\, e^{-i\frac{k^2}{2m}\delta t} \\ &= \sqrt{-\frac{2\pi m i}{\delta t}}\, exp\left[\frac{i\; m\delta t}{2}\left(\frac{x_{j+1}-x_j}{\delta t}\right)^2\right].\end{aligned} \tag{212}$$

With this result, we go back to the initial expression

$$\langle x_B, t_B\mid x_A, t_A\rangle = \int_{-\infty}^{\infty}\prod_{j=1}^{N} dx_i \left(-\frac{2\pi m i}{\delta t}\right)^{N/2} exp\left(\frac{i\; m\delta t}{2}\right)\left[\sum_{j=0}^{N}\left(\frac{x_{j+1}-x_j}{\delta t}\right)^2\right], \tag{213}$$

and take the limit when $\delta t \to 0$ (note that's equivalent ot make infinitesimal intervals with $N \to \infty$), which makes

$$\frac{x_{j+1}-x_j}{\delta t} \to \dot{x}, \tag{214}$$

and the sum $\sum_{j=1}^{N}\delta t$ becomes an integral over time. This yelds

$$\langle x_B, t_B\mid x_A, t_A\rangle = \int \mathcal{D}x\; exp\left(i\int_0^T dt\; \frac{1}{2}m\dot{x}^2\right), \tag{215}$$

where we defined,

$$\int \mathcal{D}x = \lim_{N\to\infty}\lim_{\delta t\to 0}\left(-\frac{2\pi m i}{\delta t}\right)^{N/2}\prod_{j=1}^{N}\int dx_j. \tag{216}$$

If we had a spatially dependent potential, we would have

$$\langle x_B, t_B \mid x_A, t_A\rangle = \int \mathcal{D}x\; exp\left(i\int_0^T dt\;\frac{1}{2}m\dot{x}^2 - V(x)\right), \tag{217}$$

and we recognize the Lagrangian, and its integral, the action:

$$\langle x_B, t_B \mid x_A, t_A\rangle = \int \mathcal{D}x\; exp\left(i\int_0^T dtL\right) = \int \mathcal{D}x\; e^{iS}. \tag{218}$$

The equation above clearly states that given an initial and a final configuration, any path that connects them is allowed and must be taken into account; that's the $\mathcal{D}x$ term. Now, the weight of each path is given by the exponential of the action along that path. Our next step is to see how different paths contribute to the end result of the calculation. The standard way of doing this is by performing a Wick's rotation in time:

$$t \to it \Rightarrow dt \to idt, \tag{219}$$

and this affects the action,

$$S = \int dtL \to i\int dtL = iS. \tag{220}$$

Therefore, our exponential becomes

$$\langle x_B, t_B \mid x_A, t_A\rangle = \int \mathcal{D}x\; e^{-S}. \tag{221}$$

Now suppose that we have a path that deviates from x_0 in the following way:

$$x' = x_0 + \delta x, \tag{222}$$

which has a statistical weight

$$e^{S'} = e^{-S(x_0) - \frac{\delta S}{\delta x_0}\delta x} \tag{223}$$

the path is favored if $\frac{\delta S}{\delta x_0}$ is small. The minimum happens at:

$$\frac{\delta S}{\delta x_0} = 0, \tag{224}$$

which is just the path of least action. This has a curious consequence: the classical result is the nothing but the most probable quantum paths.

For a single particle system, quantum mechanics rules. However, as we start adding particles to form a macroscopic object, in order to see a quantum mechanical effect, we would need 10^{23} particles far from the least action possibility, and the chance that this happens is extremely small. In that sense, that's macroscopic phenomena are dominated by classical mechanics.

The natural extension to what we just did is to consider the expectation values of operators acting on states. In order to do that, we introduce a few new concepts. The functional derivative of $f(x)$ is defined as

$$\frac{\delta}{\delta f(y)} f(x) = \delta(x - y). \tag{225}$$

Now, suppose that we want to calculate the expectation value of the operator X(t). To do so, we will use the functional derivative and a modified Lagrangian by the addition of an auxiliary function,

$$\mathcal{L} \to \mathcal{L} + f(t)X(t), \tag{226}$$

which gives

$$\langle x_B, t_B \mid x_A, t_A \rangle_f = \int \mathcal{D}x \; exp\left(i \int dt \mathcal{L} + fX \right). \tag{227}$$

The "trick" here is to take a functional derivative and evaluate it at $f = 0$:

$$\begin{aligned}\langle x_B, t_B \mid X \mid x_A, t_A\rangle &= \frac{1}{i}\frac{\delta}{\delta f}\langle x_B, t_B \mid x_A, t_A\rangle_f\Big|_{f=0} \\ &= \int \mathcal{D}x\; X \exp\left(i\int dt\mathcal{L} + fX\right)\Big|_{f=0} = \int \mathcal{D}x\; X\; e^{iS}.\end{aligned} \tag{228}$$

As mentioned before, the idea of Quantum Field Theory is to build particles by defining particle operators that act on the vacuum. Therefore, we are particularly interested in the vacuum to vacuum expectation value (VEV), $\langle 0 \mid 0\rangle$ and the VEV for field operators, such as $\langle 0 \mid \phi \mid 0\rangle$, for instance.

To start, let $\mathcal{L}$ be a given Lagrangian. Then we can write

$$\langle 0 \mid 0\rangle = \int \mathcal{D}\phi \exp\left[i\int d^4x\mathcal{L}\right] \equiv Z_0. \tag{229}$$

In order to calculate VEV's, we introduce an auxiliary field J,

$$\langle 0 \mid 0\rangle_J = \int \mathcal{D}\phi \exp\left[i\int d^4x\mathcal{L} + J\phi\right] \equiv Z(J). \tag{230}$$

Let's say we are interested in calculating $\langle 0 \mid \phi \mid 0\rangle$. We can make use of $\langle 0 \mid 0\rangle_J$ and the definition of functional derivative. Note that:

$$\begin{aligned}\langle 0 \mid \phi \mid 0\rangle = \langle 0 \mid \phi \mid 0\rangle_J\Big|_{J=0} &= \left(\int \mathcal{D}\phi\; \phi\; e^{i\int d^4x\mathcal{L}+J\phi}\right)\Big|_{J=0} \\ &= \frac{\delta}{\delta J}\left(\int \mathcal{D}\phi\; e^{i\int d^4x\mathcal{L}+J\phi}\right)\Big|_{J=0} = \frac{\delta}{\delta J}Z(J)\Big|_{J=0}\end{aligned} \tag{231}$$

So the expectation values can be obtained by taking functional derivatives of a known VEV. If we have multiple fields in the Lagrangian, we just add as many auxiliary terms (J, Q, R and so on) and take the necessary functional derivatives.

3.5 Quantum Electrodynamics

In this section we will present a quick, heuristic derivation of the Feynman rules for Quantum Electrodynamics, as a generalization of the ideas presented before. We will

mostly follow [6] in addition to [11] here. [10] has a very comprehensive explanation on this.

If we look at the perturbative calculation of the transition amplitude through the use of the Dyson series, we have

$$T_{fi} = -2\pi i\delta(E_f - E_i)\left(V_{fi} + \sum_{n\neq i}\frac{V_{fn}V_{ni}}{E_i - E_n}\right) + ... \ , \tag{232}$$

which looks like

$$T_{fi} = -2\pi i\delta(E_f - E_i)\left(\langle f \mid V \mid i\rangle + \sum_{n\neq i}\langle f \mid V \mid n\rangle \frac{1}{E_i - E_n}\langle n \mid V \mid i\rangle\right) + ... \ . \tag{233}$$

Now let's take a look on the structure of this equation. We are calculating an amplitude, a transition amplitude between two given states. Since the potential contains all the information about the interaction, we can think of its matrix elements as a vertex for the inetraction between two states, and note that the first order term only contains one vertex. When we look at the second order term we have two vertexes, and there is a term,

$$\frac{1}{E_i - E_n}, \tag{234}$$

which can be thought as the internal line connecting the two vertexes, the propagators. In addition, the sum takes into account all possible configurations that contribute to the amplitude. Thus, we can make an association between this perturbative expression and the Feynamn rules we presented on the previous seection; all thatwe need is to make the necessary generalizations to apply these rules for Quantum Electrodynamics. Let's look at the propagator in more detail. Following [6],

$$T_{fi} = 2\pi i\delta(E_f - E_i)\langle f \mid (-iV) + (-iV)\frac{i}{E_i - H_0}(-iV) + ... \mid i\rangle \, , \tag{235}$$

where the completeness relation for the states was used. From the equation above, we

can take $(-iV)$ to be the parameter used in the perturbation expansion. This will be our vertex, for the reasons discussed on the paragraph above. Also, the propagator will be the inverse of the Schrodinger operator,

$$-i(E_i - H_0)\psi = -iV\psi. \tag{236}$$

Now that we have unravelled the structure, we can make the generalizations. For a system that obeys the Klein-Gordon equation, the propagator is the inverse of

$$i(\Box^2 + m^2)\phi = -iV\phi \Rightarrow \frac{1}{i(-p^2 + m^2)} = \frac{i}{p^2 + m^2}, \tag{237}$$

is the propagator, where p is the momentum of the intermediate state.

For an electron moving in an electric field, we have the Dirac equation and a term that depends on the vector potential of the electric field,

$$(\not{p} - m_e)\psi = e\gamma^\mu A_\mu \psi, \tag{238}$$

where we have introduced Feynman's slash notation:

$$\gamma^\mu a_\mu = \not{a}. \tag{239}$$

Multiplying bi $(-i)$,

$$-i(\not{p} - m_e)\psi = e\gamma^\mu A_\mu \psi = -ie\gamma^\mu A_\mu \psi, \tag{240}$$

and we take $-ie\gamma^\mu$ to be the vertex. Following the same ideas, the propagator of the elctron is

$$\frac{1}{-i(\not{p} - m_e)} = \frac{i}{\not{p} - m_e}. \tag{241}$$

Using the fact that $\not{p}\not{p} = p^2$,

$$\frac{i}{\not{p} - m_e} = \frac{i(\not{p} + m_e)}{p^2 - m_e^2}, \tag{242}$$

and inserting the completeness relation obtained from summing over all the spins of the virtual electron.

$$\frac{i(\not{p} + m_e)}{p^2 - m_e^2} = \frac{i}{p^2 - m_e^2} \sum_{spins} u\bar{u}. \tag{243}$$

Thus, for a virtual massive particle,

$$\frac{i}{p^2 - m^2} \sum_{spins} . \tag{244}$$

For the photon propagator, the situation is more complicated due to the gauge freedom of A_μ. It can be shown [6] that if one works in the Lorentz gauge,

$$\frac{-ig_{\mu\nu}}{q^2}, \tag{245}$$

where

$$g_{\alpha\nu} g^{\nu\beta} = \delta^\beta_\alpha, \tag{246}$$

δ^β_α is the Kronecker delta, and q^μ is the photon's 4-momentum, $q_\mu \epsilon^\mu = 0$(scalar product with the polarization). For a photon propagating on the z-axis,

$$\epsilon_1 = (1, 0, 0), \;\; \epsilon_2 = (0, 1, 0). \tag{247}$$

Finally, for a massive spin-1 particle with wavefunction ψ_λ, one obtains

$$[g^{\alpha\beta}(\Box^2 + M^2) - \partial^\alpha \partial^\beta]\psi_\beta = 0 \Rightarrow \frac{-ig^{\mu\nu} + ip^\mu p^\nu / M^2}{p^2 - M^2}. \tag{248}$$

Our next step is to present the rules. We write them as tables with the particle types and their contributions to the amplitude.

I) Multiplicative factors

Vertexes

Vertex type	Factor
Photon - spin 0 (charge e)	$-ie(p+p')^\mu$
Photon - spin 1/2 (charge e)	$-ie\gamma^\mu$

External lines

Particle type	Ingoing	Outgoing
Spin 0 boson/antiboson	1	1
Spin 1/2 fermion	u	$\bar{u}$
Spin 1/2 antifermion	$\bar{v}$	v
Spin 1 photon	ϵ_μ	$\epsilon^\star_\mu$

Internal lines (propagators)

Particle type	Factor
Spin 0 boson	$\dfrac{i}{p^2-m^2}$
Spin 1/2 fermion	$\dfrac{i(\not{p}+m)}{p^2-m^2}$
Massive spin 1 boson	$\dfrac{-i(g_{\mu\nu}-p_\mu p_\nu/M^2)}{p^2-M^2}$
Massless spin 1 boson on the Feynman gauge	$\dfrac{-ig_{\mu\nu}}{p^2}$

II) For each vertex, write a delta function

$$(2\pi)^4\delta^4(k_1 + k_2 - k_3), \tag{249}$$

where the k_i's are the 4-momenta for the particles lines that connect at the vertex. Lines going into the vertex (in our example, k_1 and k_2) get a positive sign, while particles going out get a negative sign (k_3). The purpose of this term is to ensure conservation of energy and moementum at the vertex.

III) Perform an integral over all the internal momenta (the ones that appear into the propagator)

$$\int \frac{d^4q}{(2\pi)^4}. \tag{250}$$

IV) At this point, we should have a delta function of the form

$$(2\pi)^4\delta^4(p_1 + p_2 + ... - p_n), \tag{251}$$

eliminate this factor and what is left in the expression is the inavriant amplitude $-i\mathfrak{M}$.

V) Repeat these steps for very possible diagram, performing antisymmetrization when necessary: whenever two diagrams differ only by the interchange of two incoming (or outgoing) electrons (or positrons) or if they differ by the interchange of an incoming electron with an outgoing positron (or vice versa) we include a minus sign between the dagrams.

Those rules apply to the first oder, or "tree level".

In order to apply these rules, we will consider the Compton scattering, which involves an electron and a photon. For astrophysics, the inverse Compton scattering is of particular importance (we will mention this in later chapters). Note that the only difference between the Compton and the inverse Compton scattering is the energy of the electron: in the

inverse process the energy of the electron is comparable to the energy of the photon, and unlike the usual Compton scattering, energy can be transferred to the photon. Thus, the diagrams are the same for both situations [10].

At tree level, we have two diagrams for the Compton scattering,

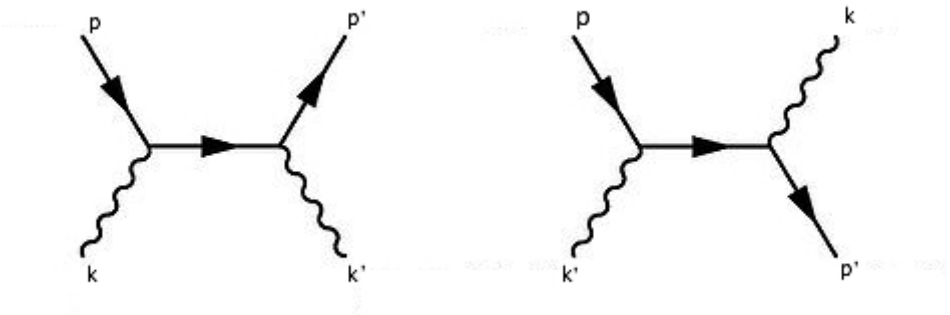

Figure 2: Feynman diagrams at tree level for the Compton scattering.

where p is used for the electron and k is used for the photon.

Let's apply the rules for the diagrams. First the multiplicatives factors for the first diagram, together with the delta functions for each vertex,

$$[\bar{u}(p')(-ie\gamma^{\mu})\epsilon^{\star}_{\mu}(k')]\left[\frac{i(\not{q}+m)}{q^2-m^2}\right][(-ie\gamma^{\nu})\epsilon_{\nu}(k)u(p)](2\pi)^8\delta^4(k^{\mu}+p^{\mu}-(p+k)^{\mu})\delta^4(k'^{\mu}+(p+k)^{\mu}-p'^{\mu}), \tag{252}$$

Now, we need to inetgrate pver the internal momenta, and eliminate the delta function that will be left. Doing this for the other diagram as well, we get (for the two diagrams)

$$\begin{aligned} i\mathfrak{M} &= [\bar{u}(p')(-ie\gamma^{\mu})\epsilon^{\star}_{\mu}(k')]\left[\frac{i(\not{p}+\not{k}+m)}{(p+k)^2-m^2}\right][(-ie\gamma^{\nu})\epsilon_{\nu}(k)u(p)] \\ &+ \bar{u}(p')(-ie\gamma^{\nu})\left[\epsilon_{\nu}(k)\frac{i(\not{p}-\not{k}+m)}{(p-k')^2-m^2}\right](-ie\gamma^{\mu}\epsilon^{\star}_{\mu}(k')u(p)) \\ &= -ie^2\epsilon^{\star}_{\mu}(k')\epsilon(k')\epsilon_{\nu}(k)\bar{u}(p')\left[\frac{\gamma^{\mu}(\not{p}+\not{k}+m)\gamma^{\nu}}{(p+k)^2-m^2}+\frac{\gamma^{\nu}(\not{p}-\not{k}+m)\gamma^{\mu}}{(p-k')-m^2)}\right]u(p). \end{aligned} \tag{253}$$

Note that we don't need to apply antisymmetrization, and the amplitudes will add.

Finally, to compute the amplitude, one needs to calculate

$$| \mathfrak{M}_1 + \mathfrak{M}_2 |^2 = | \mathfrak{M}_1 |^2 + | \mathfrak{M}_2 |^2 + \mathfrak{M}_1 \mathfrak{M}_2^\star + \mathfrak{M}_2 \mathfrak{M}_1^\star. \tag{254}$$

3.6 A comment on renormalization

Historically speaking, the first use of renormalization was done by Hans bethe, in 1947. In that time, there was a problem known as the Lamb shift, the energy gap between the $2s$ and $2p$ levels of the Hydrogen atom. The experimental value was well known and measured but all calculations (even including Dirac's theory) lead to divergencies. In [43], Bethe was able to obtain a finite result.

Renormalization was initially employed in a perturbative way. However, it was with Wilson's work on continuous phase transitions [74] that the renormalization group formalism was presented, and a better understanding of renormalization was obtained; it is a problem not only restricted to particle physics. Put simply, during phase transitions the correlation length of a physical system becomes infinite, since the system becomes invariant under rescaling. Thus, the system loses its typical length scale. It turns out that the renormalization group becomes the ideal formalism to treat these scenarios.

In particle physics, the "running of the coupling" and the β-function are the terms usually employed. The idea is that if one assumes a certain scale R for the theory, any other scale can be acessed, thus defining a group action. Let R be a dimensionless observable [6]:

$$R = R\left(\alpha, \frac{s}{\Lambda^2}\right), \tag{255}$$

with s being a scale, and with α as the elctromagnetic coupling,

$$\alpha = \frac{e^2}{4\pi}, \tag{256}$$

m is mass and Λ is cutoff we introduce to regularize a divergence (for example, instead of integrating from zero to infinity and getting a divergence, one integrates from 0 to Λ).

We have the renormalization group equation,

$$\Lambda^2 \frac{dR}{d\Lambda^2} \Rightarrow \Lambda^2 \frac{\partial R}{\partial \Lambda^2} + \Lambda^2 \frac{\partial \alpha}{\partial \Lambda^2} \frac{\partial R}{\partial \alpha} = 0. \tag{257}$$

As we can see, R can depend on Λ directly or through the coupling parameter α. We can define a new variable,

$$t = \ln(\mathrm{s}/\Lambda^2), \tag{258}$$

$$\left(-\frac{\partial}{\partial t} + \beta \frac{\partial}{\partial \alpha} \right) R\left(\alpha(s), \frac{s}{\Lambda^2} \right) = 0, \;\; \beta = \Lambda^2 \frac{\partial \alpha}{\partial \Lambda^2} = \frac{\partial \alpha}{\partial t}. \tag{259}$$

If we make the identification $\Lambda^2 = s$, the equation becomes

$$R(\alpha(s), 1). \tag{260}$$

The "running of the coupling" is described by the β function, which can be calculated pertutbatively. We will apply these results directly when we discuss physics beyond the Standard Model.

4 Electroweak Physics

4.1 Super selection rules, CPT and violations

4.1.1 Super selection rules

Suppose that, in a given theory, the states that describe a physical system belong to a Hilbert space. One can ask the follwoing question: if every state lies in a Hilbert space, does every element of the Hilbert space corresponde to a physical state? No, this statement does not necessarily hold true.

In order to make the point of the last paragraph clear, look for example at electric charge. There is no physical system we know that is defined by a superposition of states with different charges. This is not the same situation as usual conservation laws, like energy or selection rules from angular momentum conservation. One can find states which are not eigenstates of a certain component of angular momentum J, say J_x, but are eigenstates of J_z. On the other hand, it seems that every physical system must be an eigenstate of a charge operator, which we shall name Q.

This notion can be also extended to the baryon number, B, and $(-1)^F$ where F is an even integer when the state has an integer spin and an odd integer when the state has an odd integer spin. These operators are conserved in time. Any rule that sets some states as physically unrealizable is called a super selection rule.

The consequence of this in a theory with super selection rules is that not every Hermitian operator is an observable, and that the superposition principle only holds within a subspace of a Hilbert space, the one allowed by these operators. They are called the charge, baryon and univalence superselection rules.

4.1.2 The CPT theorem

However, as we know, a theory can contain many other symmetries in addition to the super selection rules. The ones taht are of particular interest to quantum field theory (and us) are usually called "CPT". We will begin our discussion of them, starting with the charge conjugation operator, $\hat{C}$.

Consider the transformation

$$\psi \to C\bar{\psi}^T, \;\; \bar{\psi} = \psi^\dagger \gamma^0, \tag{261}$$

where C is the matrix given by

$$C = \begin{pmatrix} 0 & -1 & 0 & 0 \\ 1 & 0 & 0 & 0 \\ 0 & 0 & 0 & 1 \\ 0 & 0 & -1 & 0 \end{pmatrix} = \begin{pmatrix} -(i\sigma^2) & 0 \\ 0 & i\sigma^2 \end{pmatrix}$$

.

It can be shown by direct inspection that if ψ is a solution to the Dirac equation for a particle with charge q, $C\bar{\psi}^T$ is a solution for the Dirac equation for a particle with charge $-q$. The terms $\pm i\sigma^2$ stablish a connection between left-handed and right-handed spinors. In the context of the Lorentz group, the $(1/2, 0)$ is the left-handed spinor representation, and the $(0, 1/2)$ is the right-handed spinor representation. We write those spinors as ψ_L and ψ_R respectively.

Now, if we use the following mapping,

$$\psi_L \to \psi'_L = i\sigma^2 \psi_L^\star, \tag{262}$$

one can check how ψ'_L transforms under rotations and boots. Under rotations, ψ_L and ψ'_L transform in the same, but under boosts:

$$\psi'_L \to \psi'_L = i\sigma^2 (e^{i\theta.\sigma/2}\psi_L)^\star = i\sigma^2 (e^{-i\theta.\sigma/2}\mathbb{I})\psi_L^\star, \tag{263}$$

use

$$\mathbb{I} = (-i\sigma^2)(-i\sigma^2), \tag{264}$$

$$\psi'_L = i\sigma^2(e^{-i\theta.\sigma/2}(-i\sigma^2)(-i\sigma^2))\psi^\star_L, \tag{265}$$

now apply

$$(i\sigma^2)\sigma^\star(-i\sigma^2), \tag{266}$$

to get

$$\psi'_L = e^{i\theta.\sigma/2}(i\sigma^2)\psi^\star_L = e^{i\theta.\sigma/2}\psi'_L, \tag{267}$$

which is the transformation law for the right-handed spinor. Therefore, the mapping that we defined via the use of $i\sigma^2$ together with the complex conjugation maps left-handed spinors into right-handed ones. One can define an inverse mapping as well,

$$\psi_L = -i\sigma^2\psi^\star_R, \tag{268}$$

transforms as a left-handed spinor.

Let α and β denote two left handed fields. In the chiral representation, we can write a spinor as

$$\psi = \begin{pmatrix} \psi_L \\ \psi_R \end{pmatrix} = \begin{pmatrix} \alpha \\ (i\sigma^2)\beta^\star \end{pmatrix},$$

showing all components explicitly,

$$\alpha = \begin{pmatrix} \alpha_1 \\ \alpha_2 \end{pmatrix}, \ \beta = \begin{pmatrix} \beta_1 \\ \beta_2 \end{pmatrix} \Rightarrow \psi = \begin{pmatrix} \alpha_1 \\ \alpha_2 \\ \begin{pmatrix} 0 & 1 \\ -1 & 0 \end{pmatrix} \begin{pmatrix} \beta_1^\star \\ \beta_2^\star \end{pmatrix} \end{pmatrix} = \begin{pmatrix} \alpha_1 \\ \alpha_2 \\ \beta_2^\star \\ -\beta_1^\star \end{pmatrix}$$

where we used the fact that we write a right handed field in terms of a left handed field through the use of the mapping

$$\lambda \to \lambda' = (i\sigma^2)\lambda^\star, \tag{269}$$

where we have the Pauli matrix σ^2, λ' is a right handed field and λ is a left handed one. Writing $\bar{\psi}$,

$$\bar{\psi} = \psi^\dagger\gamma^0 = (\alpha_1^\star \ \alpha_2 \ \beta_2 \ -\beta_1) \begin{pmatrix} 0 & 0 & 0 & 1 \\ 0 & 0 & 0 & 1 \\ 1 & 0 & 0 & 0 \\ 0 & 1 & 0 & 0 \end{pmatrix} = (\beta_2 \ -\beta_1 \ \alpha_1^\star \ \alpha_2^\star).$$

Note that after this operation, we are left with a row spinor. In order to make it a collumn spinor, after we take the transpose,

$$\bar{\psi}^T = \begin{pmatrix} \beta_2 \\ \beta_1 \\ \alpha_1^\star \\ \alpha_2^\star \end{pmatrix} = \begin{pmatrix} (i\sigma^2)\beta \\ \alpha^\star \end{pmatrix}.$$

This is not a spinor yet; notice that we a missing a factor of $i\sigma^2$ between the top and bottom components, and to fix it we use the matrix C,

$$C\bar{\psi}^T = \begin{pmatrix} -(i\sigma^2) & 0 \\ 0 & i\sigma^2 \end{pmatrix} \bar{\psi}^T = \begin{pmatrix} -(i\sigma^2) & 0 \\ 0 & i\sigma^2 \end{pmatrix} \begin{pmatrix} (i\sigma^2)\beta \\ \alpha^\star \end{pmatrix} = \begin{pmatrix} \beta \\ (i\sigma^2)\alpha^\star \end{pmatrix}$$

. This is now a spinor with a left handed Weyl field on top and a right Weyl field on the bottom, as desired.

We now turn our attention to the parity transformation. By definition, the parity operator is responsible for performing a spatial inversion. Consider, for instance, a quantum mechanical wave function,

$$\psi(\vec{x}, t) \to \psi'(\vec{x}, t) = \hat{P}\, \psi(\vec{x}, t) = \psi(-\vec{x}, t), \tag{270}$$

If we apply the operator twice, the wave function returns to its original state, which implies

$$\hat{P}\hat{P} = \mathbb{I} \Rightarrow \hat{P} = \hat{P}^{-1}. \tag{271}$$

We also have a constraint from the normalization of the wavefunction,

$$\langle \psi \mid \psi \rangle = \langle \psi' \mid \psi' \rangle = \langle \psi \mid P^\dagger P \mid \psi \rangle \Rightarrow P^\dagger P = \mathbb{I}. \tag{272}$$

This condition, together with the fact that $\hat{P}$ is its own inverse, implies that the Parity operator is Hermitian. Note that it also agrees with the super selection rules, therefore, it is an observable.

Let's now see look closer at the relation of parity operators and bosons and fermions. First, if the parity operator commutes with the Hamiltonian, it is an observable conserved quantity. Secondly, we can find the eigenvalues of the parity operator.

$$\psi = \hat{P}\hat{P}\psi = \hat{P}\lambda\psi = \lambda^2\psi \Rightarrow \lambda^2 = 1 \Rightarrow \lambda = \pm 1. \tag{273}$$

From Gauge Theory, it can be shown that the gauge bosons have parity eigenvalue equal

to -1. For spin half fermions, the particles have opposie parity to their correpondent antiparticles. The convention we adopt is the usual one, where particles have parity $+1$. In particular, for spinors that satisfy Dirac's equation,

$$\hat{P} = \gamma^0 = \begin{pmatrix} 1 & 0 & 0 & 0 \\ 0 & 1 & 0 & 0 \\ 0 & 0 & -1 & 0 \\ 0 & 0 & 0 & -1 \end{pmatrix},$$

Finally, T is related to the time reversal symmetry. We are now ready to briefly introduce the CPT theorem, a very famous result of axiomatic field theory. We will not try to be very rigorous or give a proof of it (for a great detailed explanation, see [18]), and we will focus on its physical interpretations.

Theorem

If the following conditions are satisfied,

I) The theory is local, characterized by Lagrangian which is Hermitian and invariant under proper Lorentz transformations,

II) The quantization scheme uses commutators for integer spin (bosons) and anticommutators for half-integer,

then the Hamiltonian for the Theory is invariant under CPT:

$$(CPT)\ H\ (CPT)^{-1} = H(x'). \tag{274}$$

as stated on [22].

We can interpret this theorem as a statement that it is possible to construct a mirror image of our Universe. The charge conjugation takes matter into antimatter (C), parity reflects the positions (P) and the momenta of the particles is reversed through time reversal (T). It is important to mention that there is a close connection between the CPT

theorem and the Spin-Statistics theorem; in fact, CPT can be used in the proof of the theorem that clearly states the fundamental difference between bosons and fermions.

4.1.3 Violations

CPT can be regarded as a fundamental symmetry of Nature. However, it does not mean that violations of, for example, parity are not allowed; there exist physical phenomena that violate P and CP (but not CPT).

The weak interaction does not conserve parity, and this has been experimentally verified (in 1957 C. S. Wu, E. Ambler, R. W. Hayward, D. D. Hoppes, and R. P. Hudson found a clear violation of parity conservation in the beta decay of cobalt-60 [49]). The Standard Model takes that into account by describing the weak interaction as a chiral gauge interaction, where only the left-handed portion of particle spinors and right handed portion of antiparticle spinors take part into the interactions. We will not get into further detail here, as this topic will be discussed in the next section, when we discuss electroweak physics.

The weak interaction also violates the product of charge conjugation and parity, CP, in some weak decays. But CP violation is described and implemented in a more subtle way than parity violation. It appears in the form of a complex phases in matrices that describe flaour mixing in quarks an leptons (this will be directly adressed in the elctroweak section as well). Examples are the PMNS matrix for neutrino mixing and the CKM matrix for quark mixing. (CP violation has also been experimentally observed [50]).

4.2 Weak currents

Historically, the motivation for the study of weak currents come from some very famous particle reactions. To name a few, we have the β decay of nuclei in atoms, the neutron decay and muonless neutrino induced events. We will mainly follow [6] here, with additional details added as necessary.

We start by writing the parity violating process known as the charge raising weak current [51]:

$$J^{\mu} = \bar{u}_{\nu}\gamma^{\mu}\frac{1}{2}\left(\mathbb{I} - \gamma^{5}\right)u_{e}, \tag{275}$$

where the combination of the terms γ^{μ} and $\gamma^{5}\gamma^{\mu}$ ensures the parity violation, and u denotes a usual spinor,

$$u = \begin{pmatrix} u_L \\ u_R \end{pmatrix},$$

with the subscript being used to label the particle described by the spinor.

We can also obtain the charge lowering weak current by taking the Hermitian conjugate of the expression above,

$$J^{\mu\dagger} = \left[\bar{u}_{\nu}\gamma^{\mu}\frac{1}{2}\left(\mathbb{I} - \gamma^{5}\right)u_{e}\right]^{\dagger}. \tag{276}$$

Recall that

$$(AB)^{\dagger} = B^{\dagger}A^{\dagger}, \tag{277}$$

and we get

$$\begin{aligned} J^{\mu\dagger} &= \left[u_{\nu}^{\dagger}\gamma^{0}\gamma^{\mu}\frac{1}{2}(\mathbb{I} - \gamma^{5})u_{e}\right]^{\dagger} = u_{e}^{\dagger}\gamma^{0}\gamma^{0}\frac{1}{2}(\mathbb{I} - \gamma^{5})\gamma^{\mu\dagger}\gamma^{0}u_{\nu} \\ &= \bar{u}_{e}\gamma^{0}\frac{1}{2}(\mathbb{I} - \gamma^{5})\gamma^{0}\gamma^{\mu}u_{\nu} = \bar{u}_{e}\gamma^{\mu}\frac{1}{2}(\mathbb{I} - \gamma^{5})\gamma^{0}\gamma^{\mu}u_{\nu}. \end{aligned} \tag{278}$$

Finally,

$$J^{\mu\dagger} = \bar{u}_{e}\gamma^{\mu}\frac{1}{2}(\mathbb{I} - \gamma^{5})u_{\nu}. \tag{279}$$

Our next goal is to find an expression for the interaction amplitude. Clearly, we need to conserve charge; therefore, the charge-raising and the charge-lowering operations must appear as a combination. The simplest guess would be a dependence of the form

$$\mathfrak{M} \ \alpha \ J^{\mu} J^{\dagger}_{\mu}, \tag{280}$$

and we introduce a proportionality constant

$$\mathfrak{M} = \frac{4G_F}{\sqrt{2}} J^{\mu} J^{\dagger}_{\mu}. \tag{281}$$

The number 4 comes from the normalization with respect to $(\mathbb{I} - \gamma^5)/2$, while the $\sqrt{2}$ is matter of convenienece and historical purposes, as we want to keep the constant G_F in the same way Fermi originally did when he first studied these physical processess.

Now we list the lepton pairs coupled by the charge-raising weak current (following the notation of [6] the first particle of the pair is an ingoing particle and the second an outgoing one):

I) (e^-_L, ν_L),

II) $(\bar{\nu}_R, e^+_R)$,

III) $(0, \nu_L e^+_R)$,

IV) $(e^-_L \bar{\nu}_R, 0)$,

where e^+_R denotes a right-handed positron and $\bar{\nu}_R$ a right-handed antineutrino. In addition, we have a few comments to make here. First of all, we mention the particle/antiparticle relation: the spinor component of a right-handed antiparticle and the spinor component of a left-handed particle with negative energy are related to each other, with the projection operator of the right-handed particle being $(\mathbb{I} - \gamma^5)/2$.

Secondly, we look at C, P and CP transformations. Experimentally (as far as we have seen), we do not detect the states $\bar{\nu}_L$ and ν_R which is a violation of parity invariance. In addition, there is violation of the charge conjugation C, which takes ν_L into $\bar{\nu}_L$. However, the CP invariance exists, and we will discuss this topic more in the next topic.

Finally, we present the experimental value for G_F,

$$G_F = 1.1 \times 10^{-5} \text{GeV}^{-2}. \tag{282}$$

It is important to mention that there is a small change, of a few percent, when G_F is measured in different physical events, such as the β decay and the muon decay, and we adress this later.

Now we turn ourselves into the problem of studying quark weak currents. The practical importance of this for neutrino astronomony is that we will then be able to calculate and predict neutrino-quark cross sections, which are crucial interactions for the IceCube detector and will be adressed on chapter 9. In the spirit of the lepton weak charge-raising current, we write

$$J_q^\mu = \bar{u}_u \gamma^\mu \frac{1}{2}(\mathbb{I} - \gamma^5) u_d, \tag{283}$$

with the charge-lowering current being given by the Hermitian conjugate of the expression above.

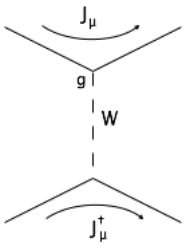

Figure 3: Charged Current (CC)

From the diagram,

$$\left(\frac{g}{\sqrt{2}} J_\mu\right) \frac{1}{m_W} \left(\frac{g}{\sqrt{2}} J^{\mu\dagger}\right) = \frac{4G_F}{\sqrt{2}} J_\mu J^{\mu\dagger}. \tag{284}$$

The invariant amplitude is given by

$$\mathfrak{M} = \frac{4G_F}{\sqrt{2}} J_\mu J^{\mu\dagger}, \tag{285}$$

as well. The short range of the interaction exists due to exchange of a heavy gauge boson, of mass m_W. The expression above is the invariant amplitude for charged current neutrino-quark cattering, usually refered to as CC interaction. Note that this holds true for free u and d quarks, but they are bound (as in the pion) and therefore corrections

will be necessary when one studies reactions such as pion decay.

A remarkable discovery changed particle physics: neutrino induced muonless events [53]. The reason why they are so important is taht they are not explained by CC interactions, but by Neutral Charge interactions (NC). Those events can be interpreted as

$$\nu_\mu(\bar{\nu}) + \text{Nucleus} \rightarrow \nu_\mu(\bar{\nu}) + \text{Hadrons}, \tag{286}$$

with

$$J_\mu^{NC}(\nu) = \frac{1}{2}\left(\bar{u}_\mu \gamma^\mu \frac{1}{2}(\mathbb{I} - \gamma^5) u_\nu\right), \tag{287}$$

$$J_\mu^{NC}(q) = \left(\bar{u}_q \gamma^\mu \frac{1}{2}(c_V^q \mathbb{I} - c_A^q \gamma^5) u_q\right), \tag{288}$$

where

$$c_V^f = T_f^3 - 2sin^2\theta_w Q_f, \;\; c_A^f = T_f^3. \tag{289}$$

T_f^3 and Q_f are available in the table from the Standard Model section. This is not a pure V-A current, since $c_V \neq c_A$. Note that the neutral current interaction has a coupling $g/cos\theta_w$.

4.3 Neutrino flavor mixing

One can now try to extend the idea of "rotation of states" to other problems. A very famous one in the recent years was related to neutrino oscillations, which resulted The Nobel Prize in Physics of 2015 being awarded jointly to Takaaki Kajita and Arthur B. McDonald "for the discovery of neutrino oscillations, which shows that neutrinos have mass". Experiments provided evidence that (time dependent) oscillatory transitions of the form

$$\nu_\alpha \rightleftharpoons \nu_\beta, \tag{290}$$

between the different neutrino flavors exist. The data from all the experiments conducted in this area suggest that the neutrino eigenstates that travel through space are the mass eigenstates, and not the weak force flavor eigenstates.

The flavor and mass eigenstates are related by a unitary matrix. We will label the flabor eigenstates woth latin letters ($i = 1, 2, 3$), and the flavor eigenstates with greek letters ($\alpha = e, \mu, \tau$)

$$|\nu_\alpha\rangle = \sum_i U_{\alpha n} |\nu_n\rangle , \tag{291}$$

which has the inverse

$$|\nu_n\rangle = \sum_\alpha (U^\dagger)_{n\alpha} |\nu_\alpha\rangle = \sum_\alpha U^\star_{\alpha n} |\nu_\alpha\rangle . \tag{292}$$

For antineutrinos, it is necessary to make the replacement

$$|\bar{\nu}_\alpha\rangle = \sum_n U^\star_{\alpha n} |\bar{\nu}_n\rangle . \tag{293}$$

Note that

$$U^\dagger U = \mathbb{I}, \tag{294}$$

which means in terms of matrix elements

$$\sum_n U_{\alpha n} U^\star_{\beta n} = \delta_{\alpha\beta}, \quad \sum_\alpha U_{\alpha m} U^\star_{\alpha n} = \delta_{mn}. \tag{295}$$

Now let's see what's the relation between those two sets of eigenstates as time evolves. For the mass eigenstates we can write

$$|\nu_n(t)\rangle = e^{-iE_n t} |\nu_n\rangle . \tag{296}$$

Thus, for a given time t, a flavor eigenstate is given in terms of a mass eigenstate by

$$|\nu_\alpha(t)\rangle = \sum_n U_{\alpha n} e^{-iE_n t} |\nu_n\rangle = \sum_n U_{\alpha n} e^{-iE_n t} |\nu_n\rangle = \sum_n \sum_\beta U_{\alpha n} U^\star_{\beta n} e^{-iE_n t} |\nu_\beta\rangle . \quad (297)$$

Calculating the scalar product to get the transition amplitude,

$$\langle \nu_\beta \mid \nu_\alpha(t)\rangle = \sum_n = U_{\alpha n} U^\star_{\beta n} e^{-iE_n t}, \quad (298)$$

At this point, we will try to manipulate the equatioon above a bit, by using the fact that the neutrino is nearly massless.

$$p >> m \rightarrow E_n = \sqrt{p^2 + M_n^2} = p\sqrt{1 + \left(\frac{M_n}{p}\right)^2} \approx p + \frac{M_n^2}{2p}. \quad (299)$$

Using $E \approx p$,

$$E_n \approx E + \frac{M_n^2}{2E}, \quad (300)$$

where M is the neutino mass. We now have the following expression for the amplitude

$$\langle \nu_\beta \mid \nu_\alpha(t)\rangle = e^{-iEt} \sum_n = U_{\alpha n} U^\star_{\beta n} e^{-\frac{iM_n^2 t}{2E}} \rightarrow \langle \nu_\beta \mid \nu_\alpha(t)\rangle = \sum_n = U_{\alpha n} U^\star_{\beta n} e^{-\frac{iM_n^2 t}{2E}}, \quad (301)$$

where we eliminate the global phase factor since it does not contribute to the transition probability. Replace

$$t = \frac{L}{c} \Rightarrow t = L \ \ (c = 1) \Rightarrow \langle \nu_\beta \mid \nu_\alpha(t)\rangle = \sum_n U_{\alpha n} U^\star_{\beta n} e^{-\frac{iM_n^2 L}{2E}}, \quad (302)$$

where L is the distance travelled by the neutrino from its origin to its detection. Finally, for an arbitrary chosen fixed m, we get

$$e^{iE_m t}\,\langle \nu_\beta \mid \nu_\alpha(t)\rangle = \sum_n U_{\alpha n} U^{\star}_{\beta n} e^{-i(E_n - E_m)t} \Rightarrow \delta_{\alpha\beta} + \sum_{n\neq m} U_{\alpha n} U^{\star}_{\beta n}[e^{-i\Delta_{nm}} - 1], \tag{303}$$

$$\Delta_{nm} = (E_n - E_m) = 1.27\frac{\delta M^2_{nm} L}{E}. \tag{304}$$

The units used here are eV^2 for the mass difference squared and km for L. Given experimental evidence, there is strong evidence that $\mid U_{e3} \mid^2 << 1$ [54] , and we can make an approximation by neglecting its contribution as follows. We can can define a mass basis as

$$|\nu_1\rangle = sin\theta_\odot\,|\nu^\star\rangle + cos\theta_\odot\,|\nu_e\rangle\,, \tag{305}$$

$$|\nu_2\rangle = -sin\theta_\odot\,|\nu_e\rangle + cos\theta_\odot\,|\nu^\star\rangle\,, \tag{306}$$

$$|\nu_3\rangle = \frac{1}{\sqrt{2}}(|\nu_\mu\rangle + |\nu_\tau\rangle), \tag{307}$$

$$|\nu^\star\rangle = \frac{1}{\sqrt{2}}(|\nu_\mu\rangle - |\nu_\tau\rangle), \tag{308}$$

with $\theta_\odot$ being the solar mixing angle. The analysis of KamLAND and solar neutrino data show agreement up to 3σ CL [55],

$$tan^2\theta_\odot = 0.39^{+0.05}_{-0.04}. \tag{309}$$

The idea is that the mass eigenstates and the flavor eigenstates are connected by a mixing matrix, which describes an unitary operator.

$$|\nu_\alpha\rangle = \sum_i U_{\alpha i}\,|\nu_i\rangle\,, \tag{310}$$

where the greek letter indicates a flavor eigenstate and the latin letter a mass eigenstate.

Since U is unitary,

$$|\nu_i\rangle = \sum_\alpha (U^\dagger)_{i\alpha} |\nu_\alpha\rangle = \sum_\alpha U^\star_{\alpha i} |\nu_\alpha\rangle \,. \tag{311}$$

For antineutrinos,

$$|\bar{\nu}_\alpha\rangle = \sum_i U^\star_{\alpha i} |\bar{\nu}_i\rangle \,. \tag{312}$$

4.4 Parity violation and helicity

We will mostly flollow the approach presented on [6], [56] in this topic. Consider, for example, a current of the following form (apart from constants)

$$j^\mu_V = \bar{u}_f \gamma^\mu u_i, \tag{313}$$

which commonly appears in QED for two states, initial and final. The reason for the subscript V will be explained soon. Now, if we apply a parity transformation,

$$u_i \to u'_i = \hat{P} u_i = \gamma^0 u_i, \tag{314}$$

$$\bar{u}_f = u^\dagger_f \gamma^0 \to \bar{u}'_f = (\hat{P} u_f)^\dagger \gamma^0 = u^\dagger_f \gamma^{0\dagger} \gamma^0 = u^\dagger_f \gamma^0 \gamma^0 = \bar{u}_f \gamma^0. \tag{315}$$

Therefore, the current transforms as

$$j^\mu_V = \bar{u}_f \gamma^\mu u_i \to j'^\mu = \bar{u}'_f \gamma^\mu u'_i = \bar{u}_f \gamma^0 \gamma^\mu \gamma^0 u_i. \tag{316}$$

Now, we use some properties of the gamma matrices. For $\mu = 0$,

$$\gamma^0 \gamma^0 = \mathbb{I} \Rightarrow j'^0_V = \bar{u}_f \gamma^0 \gamma^0 \gamma^0 u_i = j^0, \tag{317}$$

and for $\mu \neq 0$, $\mu = m = 1, 2, 3$,

$$\begin{aligned}\gamma^0\gamma^m = -\gamma^m\gamma^0,\ \ m = 1,2,3 \rightarrow j'^m &= \bar{u}_f\gamma^0\gamma^m\gamma^0 u_i \\ &= -\bar{u}_f\gamma^m\gamma^0\gamma^0 u_i = -\bar{u}_f\gamma^m u_i = -j^m.\end{aligned} \tag{318}$$

The time component does not change sign, but the spatial part does. If one considers the scalar product of the current (recall that matrix elements are proportional to this scalar product),

$$\eta_{\mu\nu}j^\mu j^\nu = j^0 j^0 - j^m j^m, \tag{319}$$

under a parity transformation,

$$\eta_{\mu\nu}j'^\mu j'^\nu = j^0 j^0 - (-j^m)(-j^m) = \eta_{\mu\nu}j^\mu j^\nu, \tag{320}$$

it remains unchanged. Thus, QED is parity invariant. QCD has similar vertex structure, and is parity invariant as well.

Now, we look at Weak currents. They have the form (ignoring constants)

$$J^\mu = \bar{u}_f\gamma^\mu(\mathbb{I} - \gamma^5)u_i, \tag{321}$$

which is referred to as a V-A structure. The reason for this term lies in the fact that the equation above is a combination of a vector current and an axial vector current, the most general expression for the exchange of a spin-1 particle. In addition, a vector changes sign under a parity transformation, while an axial vector does not.

From the example we just showed above, we saw that QED and QCD are vector interactions, from the way their current change. What we will do now is study the behavior of the extra term that contais γ^5,

$$j^\mu_A = \bar{u}_f\gamma^\mu\gamma^5 u_i. \tag{322}$$

Let's see how this term transforms under parity.

$$\gamma^5 = i\gamma^0\gamma^1\gamma^2\gamma^3, \;\; \gamma^5\gamma^0 = -\gamma^0\gamma^5 \Rightarrow j_A^\mu \to j_A'^\mu = \bar{u}_f\gamma^0\gamma^\mu\gamma^5\gamma^0 u_i = -\bar{u}_f\gamma^0\gamma^\mu\gamma^0\gamma^5 u_i. \quad (323)$$

Our next step is the same as when studied vector currents, we look at the components of the current. For the zeroth component,

$$j_A'^0 = -\bar{u}_f\gamma^0\gamma^0\gamma^0\gamma^5 u_i = -\bar{u}_f\gamma^0\gamma^5 u_i = -j_A^0, \quad (324)$$

For $\mu \neq 0, \;\; m = 1, 2, 3$:

$$j_A^m = -\bar{u}_f\gamma^0\gamma^m\gamma^0\gamma^5 u_i = \bar{u}_f\gamma^m\gamma^5 u_i = j_A^m, \quad (325)$$

This is the opposite of the vector current; the time component changes sign, but the spatial part does not. If we look at the scalar product,

$$\eta_{\mu\nu} j_A'^\mu j_A'^\nu = \eta_{\mu\nu} j_A^\mu j_A^\nu, \quad (326)$$

it remains unchanged as well. The conclusion is: pure vector and pure axial currents preserve parity. Now, let's see what happens when we have a linear combination of them,

$$J^\mu = g_V j_V^\mu + g_A j_A^\mu, \quad (327)$$

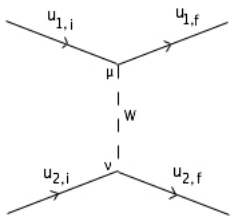

Figure 4: Weak interaction

$$J_1^\mu = \bar{u}_{1,f}(g_V\gamma^\mu + g_A\gamma^\mu\gamma^5)u_{1,i} \equiv g_V j_{1,V}^\mu + g_A j_{1,A}^\mu, \quad (328)$$

$$J_2^\mu = \bar{u}_{2,f}(g_V\gamma^\mu + g_A\gamma^\mu\gamma^5)u_{2,i} \equiv g_V j_{2,V}^\mu + g_A j_{2,A}^\mu, \tag{329}$$

$$\frac{g_{\mu\nu}}{q^2 - m^2}, \tag{330}$$

and this gives

$$J_1^\mu J_{2\mu} = g_A^2\left(j_{1,A}^\mu j_{\mu_{2,A}}\right) + g_V^2\left(j_{1,V}^\mu j_{\mu_{2,V}}\right) + g_V g_A\left(j_{1,V}^\mu j_{\mu_{2,A}} + j_{1,A}^\mu j_{\mu_{2,V}}\right). \tag{331}$$

Under a parity transformation, the pure vector and axial terms remain unchanged, but the cross term

$$g_V g_A\left(j_{1,V}^\mu j_{\mu_{2,A}} + j_{1,A}^\mu j_{\mu_{2,V}}\right) \to -g_V g_A\left(j_{1,V}^\mu j_{\mu_{2,A}} + j_{1,A}^\mu j_{\mu_{2,V}}\right), \tag{332}$$

changes sign. The scalar product of this current does not remain unchanged, and therefore, parity is not conserved. The cross term only vanishes if

$$g_V g_A = 0 \Rightarrow g_V = 0 \text{ or } \mathrm{g_A} = 0, \tag{333}$$

which is a restatament that parity is conserved by pure vector or pure axial currents. Note that the ratio

$$f = \frac{g_V g_A}{g_A^2 + g_V^2}, \tag{334}$$

is an indicative of the relative strength of the parity violating term and the parity preserving portion.

With that said, we turn to the helicity analysis of the Weak interaction, which plays a crucial role in pion decay, for instance, which is a process of great interest to us due to astrophysical neutrino production. If we use projection operators in the Chiral representation, the operator defined by $(1-\gamma^5)/2$ gives a left-handed projection, while $(1+\gamma^5)/2$

a right-handed projection) we can decompose the spinor as a sum of a right handed and a left handed spinor. In addition, from the study of the solutions of the Dirac equation, chiral states are associated to helicity states. If we apply this for a spinor in a QED vertex,

$$u = u_L + u_R \Rightarrow \bar{u}_f \gamma^\mu u_i = \bar{u}_{L,f}\gamma^\mu u_{L,i} + \bar{u}_{R,f}\gamma^\mu u_{R,i} + \bar{u}_{L,f}\gamma^\mu u_{R,i} + \bar{u}_{R,f}\gamma^\mu u_{L,i}, \tag{335}$$

and looking at cross terms,

$$\begin{aligned} \bar{u}_{L,f}\gamma^\mu u_{R,i} &= \frac{1}{2}u_f^\dagger(1-\gamma^5)\gamma^0\gamma^\mu\frac{1}{2}(1+\gamma^5)u_i = \frac{1}{4}u_f^\dagger(\gamma^0-\gamma^5\gamma^0)\gamma^\mu(1+\gamma^5)u_i \\ &= \frac{1}{4}u_f^\dagger(\gamma^0+\gamma^0\gamma^5)\gamma^\mu(1+\gamma^5)u_i = \frac{1}{4}u_f^\dagger\gamma^0(1+\gamma^5)\gamma^\mu(1+\gamma^5)u_i \\ &= \frac{1}{4}u_f^\dagger\gamma^0(\gamma^\mu+\gamma^5\gamma^\mu)(1+\gamma^5)u_i, \end{aligned} \tag{336}$$

we will use

$$\{\gamma^5, \gamma^0\} = \gamma^5\gamma^0 + \gamma^0\gamma^5 = 0, \tag{337}$$

and that gives

$$\begin{aligned} \bar{u}_{L,f}\gamma^\mu u_{R,i} &= \frac{1}{4}u_f^\dagger\gamma^0(\gamma^\mu-\gamma^\mu\gamma^5)(1+\gamma^5)u_i \\ &= \frac{1}{4}u_f^\dagger\gamma^0\gamma^\mu(1-\gamma^5)(1+\gamma^5)u_i = \frac{1}{4}u_f^\dagger\gamma^0\gamma^\mu(1-1)u_i = 0, \end{aligned} \tag{338}$$

since $(\gamma^5)^2 = 1$. The cross terms both vanish, and only two terms remain, ones with one left-handed and right-handed portions.

We can try to do the same for a Weak vertex. The vertex for the CC interaction is

$$\frac{-ig_W}{2\sqrt{2}}\gamma^\mu(1-\gamma^5) = \frac{-ig_W}{\sqrt{2}}\gamma^\mu P_-, \tag{339}$$

where P_- is a left-handed projection operator. Thus,

$$\bar{u}_f \frac{-ig_W}{\sqrt{2}} \gamma^\mu P_- u_i = \bar{u}_f \frac{-ig_W}{\sqrt{2}} u_{L,i} = (\bar{u}_{L,f} + \bar{u}_{R,f}) \frac{-ig_W}{\sqrt{2}} \gamma^\mu u_{L,i} = \left(\frac{-ig_W}{\sqrt{2}} \right) \bar{u}_{L,f} \gamma^\mu u_{L,i}. \tag{340}$$

As we see, since the vertex depends on the left-handed chiral projection operator, the interaction vertex ends up selecting a portion of the spinor. For particles, only the left-handed chiral components of particle spinors (and the right-handed for antiparticles) take part in CC interactions.

It is important o check some energy regimes. From our studies of solutions of the Dirac equations, when we look at the high energy limit, where the energy of the paricle is much bigger then its mass, the helicity eigenstates are the left-handed chiral components. Helicity $+1$ is associated with left-handed particles, and -1 with right-handed antiparticles, and only these elements participate in CC interactions in this energy limit.

4.5 The Glashow resonance

Consider the following process:

$$\bar{\nu}_e + e^- \to W^-, \tag{341}$$

which is usually referred to as the Glashow resonance [24]. There are other similar reactions for each neutrino and antineutrino flavor

$$\nu_l + l^+ \to W^+, \tag{342}$$

$$\bar{\nu}_l + l^- \to W^-, \tag{343}$$

but they are not relevant for our purposes, because positrons, muons, taus and their antiparticles are not available in usual matter at our detector. Thus, only the interaction between $\bar{\nu}_e$ and e^- is likely to happen.

Once created, the W^- can decay into leptons or hadrons, originating cascades at the

detector. We will briefly describe them, as done in [57]. The branching fractions of the W^- are about 10 to 11% to each of the leptons (and other products), and around 68% for a hadronic decay [171]. In the leptonic decay possibility, we expect to see cascades (see the chapter on the IceCube experiment). In the case of hadronic decays, boson dominantly decays producing two jets leading to many pions and kaons, which also decay producing neutrinos.

5 Cosmology

5.1 The Homogeneous, Isotropic Universe

Cosmological solutions of Einstein's equation are generally charaterized by their high degree of symmetry. The reason for this is due to some of the defining cosmological postulates: the notions of isotropy and homogeneity. Loosely speaking, isoptropy means that there is no privileged direction in the Universe; it looks the same given a sufficiently large scale no matter what direction we are looking at. The second assumption is that there is no privileged point in the Universe, meaning that for any given point our surroundings would essentially look the same on a certain (cosmological) scale. This second condition is what we refer to as homogeneity.

Over the course of history, we have faced many problems as we try to undertand the large scale Universe, and one of the main difficulties we have (and always will) face is the extremely small amount of observation time mankind has accumulated when compared to the age of the Universe. However, there are many "windows" through which we can look at the past of the Universe and predict its future, all motivated by observations of the present. With that in mind, the outline of this section will be as follows: first, we show the set of equations and observational data that constitute the current mostly accepted model of the Universe. Then, we will explore the history of the Universe, which has an evolution constrained by what we see today. Finally, we expose what is still unknown and how this affects our predictions about the fate of the Universe.

The solution for the Einstein's equations that satisfy the homogeneity and isotropy postulates is called the Friedmann - Robertson - Walker solution (a precise derivation can be found in many traditional texts, such as [9]; we ommit it here for brevity but it can be

obtained by symmetry arguments without directly solving Einstein's Equations). Those solutions account for three possibilities in terms of spatial curvature: the geometry of a sphere, hyperboloid or flat Euclidian space. The metric is given by

$$ds^2 = dt^2 - a^2(t)\left[\frac{dr^2}{1-kr^2} + r^2(d\theta^2 + sin^2(\theta)d\phi^2)\right], \tag{344}$$

where $a(t)$ is called the scale factor and $k = 0$ for a flat Universe. Note that $k = 1$ for the sphere (the positive curvature, called closed universe) and $k = -1$ for the hyperboloid (negative curvature, called open universe). The metric above is written in comoving coordinates, which are independent of the expansion. Physical distances are related to the comving coordinates through the use of the scale factor, thus the origin of its name. If one wants to calculate the physical distance, we need the following definition.

Definition

The proper distance (the physical distance) is given by

$$d_p(t) = R(t)\int_0^r \frac{dr'}{\sqrt{1-kr'^2}}. \tag{345}$$

Even though the proper distance seems to be most natural definition in order to measure distancesit is not practical because its definition requires synchronized local distance measurements along the line between two points. Astronomers normally use other definitions of distances, such as the angular diameter distance and the luminosity distance.

Probably, the most puzzling part of the observations refers to the components of the Universe, which seems to be 70% dark energy, responsible for the accelerating expansion, and 30% non-relativistic matter. However, only about 4% of the components seem to be baryonic matter, and the rest, dark matter. Dark matter does not interact through electromagnetism, but does interact gravitationally. One of the greatest open problems in this field is to elucidate the nature of dark matter, and to detect it; this topic was actually part of the research presented in later chapters. We will address it in more

detail on the section where we discuss Λ-CDM model and, of course, when we present the research results.

With the metric, it is possible to find the Christoffel symbols and the components of the Ricci tensor. We define

$$\dot{a} \equiv \frac{da}{dt}, \tag{346}$$

and we also obtain (the non-zero Γ's)

$$\Gamma^0_{11} = \frac{a\dot{a}}{1-kr^2}, \tag{347}$$

$$\Gamma^0_{22} = a\dot{a}r^2, \tag{348}$$

$$\Gamma^0_{33} = a\dot{a}r^2 sin^2(\theta), \tag{349}$$

$$\Gamma^1_{01} = \Gamma^1_{10} = \Gamma^2_{02} = \Gamma^2_{20} = \Gamma^3_{03} = \Gamma^3_{30} = \frac{\dot{a}}{a}, \tag{350}$$

$$\Gamma^1_{22} = -r(1-kr^2), \tag{351}$$

$$\Gamma^1_{33} = -r(1-kr^2)sin^2(\theta), \tag{352}$$

$$\Gamma^2_{12} = \Gamma^2_{21} = \Gamma^3_{13} = \Gamma^3_{31} = \frac{1}{r}, \tag{353}$$

$$\Gamma^2_{33} = -sin(\theta)cos(\theta), \tag{354}$$

$$\Gamma^3_{23} = \Gamma^3_{32} = cot(\theta). \tag{355}$$

Also, the components of the Ricci tensor and the curvature scalar are given by

$$R_{00} = -3\frac{\ddot{a}}{a}, \tag{356}$$

$$R_{11} = \frac{a\ddot{a} + 2\dot{a}^2 + 2k}{1 - kr^2}, \tag{357}$$

$$R_{22} = r^2(a\ddot{a} + 2\dot{a}^2 + 2k), \tag{358}$$

$$R_{33} = r^2(a\ddot{a} + 2\dot{a}^2 + 2k)sin^2(\theta), \tag{359}$$

$$R = \frac{6}{a^2}(a\ddot{a} + \dot{a}^2 + k). \tag{360}$$

A very good approxiamtion to many systems is that of a perfect fluid, in which the components interact weakly and in the rest frame of the fluid, an observer sees it as isotropic. This is the case when the free mean path between the collisions is small as compared by the length scale used by the observer. The stress-energy-momentum tensor for a perfect fluid is

$$T^{\mu\nu} = (P + \rho)u^\mu u^\nu - Pg^{\mu\nu} \tag{361}$$

where ρ is the energy density of the fluid in its rest frame, P denotes pressure and $u^{\mu\nu}$ is the 4-velocity of the fluid. In the rest frame of the fluid,

$$u^\mu = (1, 0, 0, 0), \tag{362}$$

and the tensor becomes

$$T^\mu_\nu = diag(-\rho, P, P, P). \tag{363}$$

Note that we are not working on a Minkowski spacetime; thus, we write the conservation law for T^μ_ν as

$$\nabla_\mu T^\mu_\nu = 0 \Rightarrow \frac{\partial T^\mu_\nu}{\partial x^\mu} + \Gamma^\mu_{\sigma\mu} T^\sigma_\nu - \Gamma^\sigma_{\nu\mu} T^\mu_\sigma, \tag{364}$$

and we look at each component separetely.

$$\frac{\partial T^\mu_0}{\partial x^\mu} + \Gamma^\mu_{\sigma\mu} T^\sigma_0 - \Gamma^\sigma_{0\mu} T^\mu_\sigma = 0. \tag{365}$$

Note that the only non-vanishing partial derivative is:

$$\frac{\partial T^\mu_0}{\partial x^\mu} = \frac{\partial T^0_0}{\partial x^0} = -\frac{\partial \rho}{\partial t}, \tag{366}$$

using this result and the Christoffel symbols for the FRW metric, we get:

$$\frac{\partial \rho}{\partial t} + 3\frac{\dot{a}}{a}(\rho + P) = 0 \Rightarrow \frac{1}{a^3}\frac{\partial \left[\rho a^3\right]}{\partial t} = -3\frac{\dot{a}}{a}P. \tag{367}$$

The equation above is particularly useful because it tells us how the different contents of the Universe relate to the scale parameter a. In order to do so, it is necessary to define a relationship between ρ and P, namely an equation of state. For an equation of the form

$$p = w\rho, \tag{368}$$

gives

$$\frac{\dot{\rho}}{\rho} + 3(1+w)\frac{\dot{a}}{a} \Rightarrow \rho \; \alpha \; a^{-3(1+w)}. \tag{369}$$

Perfect cosmological fluids obey the equation above. For example, if one considers colisionless nonrelativistic matter (usually reffered to as dust), we have $w = 0$

$$\frac{\partial \left[\rho_m a^3\right]}{\partial t} = 0 \Rightarrow \rho_m \; \alpha \; a^{-3}. \tag{370}$$

If most of the energy density of the Universe is in the form of dust, we say the Universe is matter-dominated.

Now we consider the radiation case. For a relativistic quantum gas in thermal equi-

librium (either bosons or fermions), we have:

$$P = \frac{\rho}{3}, \tag{371}$$

which gives

$$\frac{\partial \rho_r}{\partial t} + 3\frac{\dot{a}}{a}\left(\rho_r + P\right) = \frac{\partial \rho_r}{\partial t} + 3\frac{\dot{a}}{a}\left(\rho_r + \frac{\rho_r}{3}\right) = a^{-4}\frac{\partial\left[\rho_r a^4\right]}{\partial t} = 0. \tag{372}$$

This implies that the energy density of radiation scales as a^{-4}. The physical reason for this dependence of the density with the scale factor can be seen that the matter density decreases as the volume of the Universe increases (thus the factor a^{-3}), while for radiation we also have an extra factor: the redshift, which adds to the exponent giving a^{-4}.

The other form of energy we consider comes from the energy of the vacuum, which comes in the form of a cosmological constant,

$$G_{\mu\nu} = 8\pi G T_{\mu\nu} - \Lambda g_{\mu\nu}, \tag{373}$$

and we can define

$$T^{(vac)}_{\mu\nu} = -\frac{\Lambda}{8\pi G} g_{\mu\nu}. \tag{374}$$

This looks like a perfect fluid with

$$\rho = -P = \frac{\Lambda}{8\pi G} \rightarrow w = -1. \tag{375}$$

Note that the result is independent of a, the scale factor, unlike the previous cases. If we include all the contributions (matter, radiation and dark energy), we can define an energy-momentum tensor as

$$T^{\mu\nu} = T^{\mu\nu}_{\Lambda} + T^{\mu\nu}_{Matter} + T^{\mu\nu}_{Radiation}, \tag{376}$$

and we can write the values for the w of the equation of state,

I) $w = 0$, matter

II) $w = 1/3$, radiation

III) $w = -1$, vacuum energy

If one has the metric and puts it into Einstein's equations, after some algebra, one obtains

$$\left(\frac{\dot{a}}{a}\right)^2 = \frac{\Lambda}{3} + \frac{8\pi G}{3}\rho - \frac{Kc^2}{a^2}, \tag{377}$$

$$\frac{\ddot{a}}{a} = \frac{\Lambda}{3} - \frac{4\pi G}{3}\left(\rho + \frac{3P}{c^2}\right), \tag{378}$$

which are called Friedmann's equations. If we combine the equations from the last definition, we obtain

$$\frac{d}{dt}\left(\rho a^3 c^2\right) + P\frac{d}{dt}(a^3) = 0, \tag{379}$$

the relativistic analogue of

$$TdS = dE + PdV = 0, \tag{380}$$

an adiabatic condition.

At this point, it is useful to formally introduce the famous Hubble constant. It is important to mention again that Hubble originally obtained this by observation, while we are introducing it after having a developed theory. The Hubble constant is defined by

$$H = \frac{\dot{a}}{a}. \tag{381}$$

Note that this is not really a constant, because it can change with time. We also refer to it as the Hubble parameter often. Also, we introduce the scalled Hubble parameter h,

$$H = 100h \text{ km s}^{-1}\text{Mpc}^{-1} \tag{382}$$

One can rewrite the first Friedmann equation with this definition, and also define some other variables:

$$H^2 = \frac{8\pi G}{3}(\rho + \rho_\Lambda) - \frac{kc^2}{a^2}, \tag{383}$$

with

$$\rho_\Lambda \equiv \frac{\Lambda}{8\pi G}, \;\; \rho = \rho_m + \rho_r. \tag{384}$$

Note that ρ is a sum of the matter and radiation components. The matter content is a combination of baryonic and dark matter, while the radiation part can be written as a combination of photons and neutrinos.

$$\rho = \rho_{bar} + \rho_{CDM} + \rho_\gamma + \rho_\nu. \tag{385}$$

Definition

We define

$$\rho_{crit} = \frac{3H^2}{8\pi G} = 1.05 \times 10^{-5} h^2 \text{GeVcm}^{-3}, \tag{386}$$

as the critical density. Also, we have the density parameter

$$\Omega \equiv \frac{\rho}{\rho_c} = \frac{8\pi G\rho}{3H^2}. \tag{387}$$

If one puts $\rho + \rho_\Lambda = \rho_{crit}$, we see that $k = 0$. That's the condition for a flat Universe. The combination of the results and definitions so far, namely the first Friedmann equation, the densities and the way different components depend on the scale factor allow us to write

$$\frac{H^2}{H_0^2} = \Omega_R a^{-4} + \Omega_M a^{-3} + \Omega_k a^{-2} + \Omega_\Lambda. \tag{388}$$

The parameters Ω_M, Ω_R and Ω_Λ are, respectively, the density parameters of matter, radiation and cosmological constant today, when $a = 1$ (H_0 is also the present value of the Hubble constant). The term Ω_k depends on the critical density,

$$\Omega_k = 1 - \Omega. \tag{389}$$

It is usually called the spatial density parameter, as a relation to the curvature can be seen from its definition. For instance, suppose that $\Omega = 1$ and we have a flat Universe; that would imply $\Omega_k = 1$.

Before we move on to the last topic, we will briefly talk about the effect light undergoes as it propagates in an expanding Universe: the cosmological redshift. There is a very elegant exposure on [9]; here, we quote the final result, where the redshift factor z is given by

$$z \equiv \frac{\lambda_{observed} - \lambda_{emitted}}{\lambda_{emitted}} = \frac{f_{emitted}}{f_{observed}} - 1 = \frac{1}{a} - 1, \tag{390}$$

where λ is the wavelength and f the frequency.

5.2 An overview of the physics in the Early Universe

In the late 1920's, Edwin Hubble found that the Universe was expanding. He not only measured the distance between the other galaxies and the Milky Way, but also the their velocities relative to us. To measure the distance, he used Cepheid variable stars with known mean luminosity; a measurement of the luminosity received here allows us to tell the distance. To measure the velocity, he looked at the spectral lines of the galaxies, and noticed a red shift in the light of the vast majority of the sources.

One the most interesting results of the measurement is that the recessional velocities displayed an almost linear dependence with the distance between the galaxies. In other words, the farthest a galaxy is from us, the faster it is moving away.

Another piece of evidence is the relative abundance of the light elements like Hydrogen and Helium. They are sensitive functions of the baryon-to-photon ratio η and the current

cosmological model agrees very well with observtions.

Finally, and probably the most famous, is the Cosmic Microwave Background. In 1965, Penzias and Wilson observed a strange kind of noise, which seemed to be a uniform background (and thus motivated the name). Measurements showed that it had a blackbody temperature of about 3 K, and the radiation was identified as one of the "fingerprints" of the Big Bang. Later measurements provided much more accurate data, such as a better value for the temperature, $T = 2.725 \pm 0.002$ K, (small) anisotropies and so on.

5.2.1 The first moments

In the first 10^{-43}s of the existence of the Universe (as predicted by General Relativity), the Universe was extremely hot and dense. The spacetime curvature was greater than the scale of the Planck length,

$$\left(\frac{G\hbar}{c^3}\right)^{1/2} \approx 10^{-33} cm, \tag{391}$$

and we had a density $\rho \approx 10^{42} g/cm^3$. All of our current theories, including General Relativity, break at such extreme conditions. Quantum Gravity should be dominant at this timescale, but at the present we do not have a theory that sucessfully adresses those matters.

When observing the sky, two properties of the Universe immediately draw our attention. The first is the called the horizon problem, and is related to finding out why the cosmological principle (apparently) holds true; i.e, why the Universe seems to be statistically homgeneous and isoptropic in large scales. The second is the flatness problem, and as the name suggests, why the Universe is so flat. The most accepted explanation, even though it is not completely understood yet, is that the Universe went through a phase of great expansion, on a time of the order of 10^{-36} s after the Big Bang.

Today, when we observe the different portions of the sky, more precisely, causally disconnected ones, they seem to be remarkably similar. It is very unlikely that regions which were separated for so long would look so much alike, if they were not causally

connected in the past. One way to fix this is to propose that the Universe would be very hot and small in the beginning, and then underwent a phase of huge expansion. This would explain the homogeneities, since the Universe would have been causally connected, and also would account for the size we observe today.

Another effect of inflation is that it can be used to "flatten" the Universe. This topic is a bit more technical, so we won't get into much detail here, but the central idea is that as the Universe expands, any "wrinkles" would be washed away. This would help to explain why the Universe seems to be so flat.

The inflationary model is not perfect, however. Problems exist, like determining precisely why and when inflation stopped, the question of the topological defects like monopoles and cosmic strings, which arise when one enforces inflation, and so on. Nevertheless, the inflationary idea is the best we have so far.

Now, we will try to show how inflation is implemented mathematically, in the most simple case. According to [58], we start by introducing the inflaton, a scalar field ϕ. The dynamics of a scalar field minimally coupled to gravity is given by

$$S = \int d^4x\sqrt{-g}\left[\frac{1}{2}R + \frac{1}{2}g^{\mu\nu}\partial_\mu\phi\partial_\nu\phi - V(\phi)\right], \tag{392}$$

where g is the determinant of the metric. The energy-momentum tensor and the field equation of motion obtained upon variation of this action are,

$$T_{\mu\nu} \equiv -\frac{2}{\sqrt{-g}}\frac{\delta S_\phi}{\delta g^{\mu\nu}}, \tag{393}$$

which yelds

$$T_{\mu\nu} = \partial_\mu\phi\partial_\nu\phi - g_{\mu\nu}\left(\frac{1}{2}\partial^\alpha\,\phi\partial_\alpha\phi + V(\phi)\right), \tag{394}$$

$$\frac{\delta S_\phi}{\delta\phi} = \frac{1}{\sqrt{-g}}\partial_\mu(\sqrt{-g}\,\partial^\mu\phi) + \frac{\partial V}{\partial\phi} = 0. \tag{395}$$

For the FRW metric and a homogeneous field (only time dependent), one obtainst the following equations for the terms in the energy-momentum tensor (which looks like

a perfect fluid),

$$\rho_\phi = \frac{1}{2}\dot{\phi}^2 + V(\phi), \tag{396}$$

$$p_\phi = \frac{1}{2}\dot{\phi}^2 - V(\phi). \tag{397}$$

where $\rho_\phi$and p_ϕ are the density and pressure, respectively. Also, from the equations of motion,

$$\ddot{\phi} + 3H\dot{\phi} + \frac{\partial V}{\partial \phi} = 0, \tag{398}$$

$$H^2 = \frac{1}{3}\left(\frac{1}{2}\dot{\phi}^2 + V(\phi)\right). \tag{399}$$

We now have the equations that describe how the inflaton field evolves with time, and also how it will couple to the evolution of the scale parameter, through ρ_ϕ and p_ϕ. If the inflaton field dominates, the accelration equation becomes

$$\frac{\ddot{a}}{a} = -\frac{1}{6}(\rho_\phi + 3p_\rho) = H^2(1-\epsilon), \tag{400}$$

with

$$\epsilon = \frac{1}{2}\frac{\dot{\phi}^2}{H^2}. \tag{401}$$

Note that if the slow roll parameter $\epsilon < 1$, then we have accelerated expansion. This regime will be sustained for a long amount of time if $\ddot{\phi}$ is not very big,

$$\mid \ddot{\phi} \mid \ll \mid 3H\dot{\phi} \mid, \quad \mid \frac{\partial V}{\partial \phi} \mid, \tag{402}$$

which can be achieved by making $\mid \eta \mid < 1$, where

$$\eta = -\frac{\ddot{\phi}}{H\dot{\phi}}. \tag{403}$$

Under the slow roll conditions, one can show that

$$a(t) \sim e^{Ht}. \tag{404}$$

which accounts for an exponentially expanding Universe.

There is strong evidence that the Universe does not have matter-anti-matter symmetry. There are two possible explanations for this: one is that the Universe was created with a certain baryonic number, which would have to be strictly conserved. The other one is what is called baryogenesis; a mechanism that would allow the symmetry breaking and the production of outnumbering baryons. It is worth mentioning that this process has not been completely elucidated yet.

If one tries to find a mechanism for baryogenesis, his theory should satisfy the Sakarov conditions:

I) Baryon number B violation

II) Charge conjugation, C, and composition of charge conjugation and parity, CP, violation

III) Interactions happening out of thermal equilibrium

The first condition is straightfoward. The second one is related to the fact that if one produces more of a certain particle then its antiparticle, there is no balance in charge and parity (if parity is broken, the number of right handed baryons and left handed antibaryons doesn't need to be the same, and vice-versa). Finally, in order for these two conditions to be satisfied, the whole process must happen out of thermal equilibrium, and that is condition 3, otherwise PCT compensation would balance the processes that affect the baryon number [18].

5.2.2 An overview of Thermodynamics

We will begin by listing some important thermodynamics and statistical mechanics results. Then, we will apply those ideas when we discuss decoupling and freeze-out, the

Boltzmann equation, cross sections and dark matter. With that said, Thermodynamical quantities can be written in terms of phase space distributions,

$$n = \frac{g}{(2\pi)^3} \int d^3p \; f(\vec{p}), \tag{405}$$

$$\rho = \frac{g}{(2\pi)^3} \int d^3p \; f(\vec{p}) E(p), \tag{406}$$

$$P = \frac{g}{(2\pi)^3} \int d^3p \; \frac{p^2}{3E} f(\vec{p}), \tag{407}$$

where g represents the number of internal degrees of freedom that the species has. For weakly interacting quantum particles, we have

$$f = \frac{1}{e^{(E_i - \mu_i)/T_i} \pm 1}, \tag{408}$$

where the + and − signs representing Fermi-Dirac and Bose-Einstein statistics respectively. The f denotes the occupancy of a given state in phase state.

Note that the distributions are a function of temperature and μ, the chemical potential. For a system in chemical equilibrium, governed by a reaction of the type

$$A + B \leftrightarrow C + D, \tag{409}$$

we have

$$\mu_A + \mu_B = \mu_C + \mu_D. \tag{410}$$

Consider the FD and BE dustributions once again. Note that in the limit $m >> T$ (keep in mind that mass and energy are related) the exponential dominates the denominator and is much bigger then the unit. We then have:

$$f(\vec{p_i}) = e^{-[(E_i - \mu_i)/T_i]}, \tag{411}$$

and that is the Maxwell-Boltzmann distribution. In this regime, we don't distinguish between fermions and bosons.

With the distribution functions defined, for a system in equilibrium with $E^2 = p^2 + m^2$

$$n_i = \frac{g_i}{2\pi^2}\int_{m_i}^{\infty}(E_i^2 - m_i^2)^{\frac{1}{2}}\ f\ E_i dE_i = \frac{g_i}{2\pi^2}\int_{m_i}^{\infty}\frac{(E_i^2 - m_i^2)^{\frac{1}{2}}}{e^{(E_i-\mu_i)/T_i} \pm 1}E_i dE_i, \tag{412}$$

$$\rho_i = \frac{g_i}{2\pi^2}\int_{m_i}^{\infty}(E_i^2 - m_i^2)^{\frac{1}{2}}\ f\ E_i^2 dE_i = \frac{g_i}{2\pi^2}\int_{m_i}^{\infty}\frac{(E_i^2 - m_i^2)^{\frac{1}{2}}}{e^{(E_i-\mu_i)/T_i} \pm 1}E_i^2 dE_i, \tag{413}$$

$$P_i = \frac{g_i}{6\pi^2}\int_{m_i}^{\infty}(E_i^2 - m_i^2)^{\frac{1}{2}}\ f\ dE_i = \frac{g_i}{6\pi^2}\int_{m_i}^{\infty}\frac{(E_i^2 - m_i^2)^{\frac{3}{2}}}{e^{(E_i-\mu_i)/T_i} \pm 1}dE_i, \tag{414}$$

It is safe to assume

$$\mu << T, \tag{415}$$

for almost all times for nearly all particles through the history of the Universe. With this in mind the distribution functions we mentioned earlier can be regarded as functions of the ratio E/T. Now, look at the definition of pressure for a given distribution:

$$P = \frac{g}{(2\pi)^3}\int d^3p\frac{p^2}{3E}f, \tag{416}$$

and take the derivative with respect to T:

$$\frac{\partial P}{\partial T} = \frac{g}{(2\pi)^3}\int d^3p\frac{p^2}{3E(p)}\frac{\partial f}{\partial T}. \tag{417}$$

Using the chain rule, we write:

$$\frac{\partial f}{\partial T} = \frac{\partial f}{\partial E}\frac{\partial E}{\partial (E/T)}\frac{\partial (E/T)}{\partial T} = -\frac{E}{T}\frac{\partial f}{\partial E} \tag{418}$$

Note that this result is obtained for a chemical potential equal to zero for simplicity (the derivation is exactly the same if we don't do it, the only difference is an extra term that leads to a bit more algebra so we ommit it here) and because of teh fact that it is mostly

used in cosmology in this form. Putting this result on the equation for the pressure,

$$\frac{\partial P}{\partial T} = -\frac{g}{(2\pi)^3}\int d^3p \frac{p^2}{3E(p)}\frac{E}{T}\frac{\partial f}{\partial E} = -\frac{1}{T}\left(\frac{g}{(2\pi)^3}\int d^3p \frac{p^2}{3}\frac{\partial f}{\partial E}\right). \tag{419}$$

Note that

$$E^2 = p^2 + m^2 \Rightarrow 2EdE = 2pdp \Rightarrow dp = \frac{E}{p}dE = \frac{E}{\sqrt{E^2 - m^2}}dE, \tag{420}$$

where p is the magnitude of the momentum. Furthermore,

$$d^3\vec{p} = 4\pi p^2 dp, \tag{421}$$

if one assumes isotropy. Thus,

$$\begin{aligned} -\frac{\partial P}{\partial T} &= \frac{1}{T}\left(\frac{g}{(2\pi)^3}\int d^3p \frac{p^2}{3}\frac{\partial f}{\partial E}\right) = \frac{1}{T}\frac{g}{(2\pi)^3}\left(\int_0^\infty dp\ \frac{4\pi p^4}{3}\frac{\partial f}{\partial E}\right) \\ &= \frac{1}{T}\frac{g}{(2\pi)^3}\left(\int_0^\infty dE \frac{E}{\sqrt{E^2 - m^2}}\ \frac{4\pi}{3}(E^2 - m^2)^2\frac{\partial f}{\partial E}\right) \\ &= \frac{1}{T}\frac{g}{6\pi^2}\left(\int_0^\infty dE\ E(E^2 - m^2)^{3/2}\frac{\partial f}{\partial E}\right), \end{aligned} \tag{422}$$

and using integration by parts,

$$\begin{aligned} -\frac{\partial P}{\partial T} &= \frac{1}{T}\frac{g}{6\pi^2}\left(\int_0^\infty dE\ E(E^2 - m^2)^{3/2}\frac{\partial f}{\partial E}\right) \\ &= \frac{1}{T}\frac{g}{6\pi^2}\left[E(E^2 - m^2)^{3/2}f\Big|_0^\infty - \int_0^\infty dE\ \frac{\partial}{\partial E}\left(E(E^2 - m^2)^{3/2}\right)f\right] \\ &= -\frac{1}{T}\frac{g}{6\pi^2}\left[\int_0^\infty dE\ (E^2 - m^2)^{3/2}f + 3E^2(E^2 - m^2)^{1/2}f\right] = -\frac{1}{T}(P + \rho), \end{aligned} \tag{423}$$

$$\frac{\partial P}{\partial T} = \frac{1}{T}(P + \rho) \Rightarrow s_i = \frac{P_i + \rho_i}{T_i} \tag{424}$$

If one wants to include the chemical potential, the expression for the entropy becomes

$$s_i = \frac{P_i + \rho_i - \mu_i n_i}{T_i}. \tag{425}$$

An important remark: in the SM, the net baryon density relative to the photon density is very small (on the order of 10^{-10}), the chemical potential associated with the baryon number can be safely neglected. It scales as a^{-3}, even if two different species have different temperatures.

Following [12], [6] and [14], we will now present some results for the quantities n_i, P_i and ρ_i. This is done by directly applying the expressions we just presented for different particles. Note that

$$\zeta(s) = \frac{1}{\Gamma(s)} \int_0^\infty \frac{x^{s-1}}{e^x - 1} dx, \tag{426}$$

which is the definition of the Riemann zeta function ($\Gamma(s)$ is the usual Gamma function). With that in mind, if we consider a nondegenerate relativistic species (this means $T_i >> \mu_i$ and $T_i >> m_i$ respectively) we obtain for bosons

$$n_i = \frac{1}{\pi^2} \zeta(3) g_i T_i^3, \tag{427}$$

$$\rho_i = \frac{\pi^2}{30} g_i T_i^4, \tag{428}$$

$$P_i = \frac{\rho_i}{3}, \tag{429}$$

and for fermions

$$n_i = \frac{3}{4\pi^2} \zeta(3) g_i T_i^3, \tag{430}$$

$$\rho_i = \frac{7\pi^2}{240} g_i T_i^4, \tag{431}$$

$$P_i = \frac{\rho_i}{3}, \tag{432}$$

where $\zeta(3) = 1.20206....$ If we have a nonrelativistic particle species $T_i << m_i$, the

distribution is Maxwell- Boltzmann and we obtain for both bosons and fermions,

$$n_i = g_i \left(\frac{m_i T_i}{2\pi}\right)^{3/2} e^{-m_i/T_i}, \;\; \rho_i = m_i n_i, \;\; P_i = n_i T_i \tag{433}$$

Due to our assumptions for this case, we see that $\rho_i >> P_i$. One can also calculate the average energy per particle (by dividing ρ/n) which is given by

$$\langle E_i \rangle \approx 2.701 T_i \;\; \text{(bosons)}, \tag{434}$$

$$\langle E_i \rangle \approx 3.151 T_i \;\; \text{(fermions)}, \tag{435}$$

$$\langle E_i \rangle = m_i + \frac{3T_i}{2} \;\; \text{(nonrelativistic)}. \tag{436}$$

For photons,

$$n_\gamma = \frac{2\zeta(3)}{\pi 2} T_\gamma^3, \tag{437}$$

$$\rho_\gamma = \frac{\pi}{15} T_\gamma^4, \tag{438}$$

$$P_\gamma = \frac{1}{3}\rho_\gamma, \tag{439}$$

$$s_\gamma = \frac{4\rho_\gamma}{3T_\gamma}. \tag{440}$$

These relations hold true when we have particles in thermal equilibrium. However, as the Universe expands the mean free paths of the interactions increase, and consequently the interaction rate decreases. There is a point when the particles decouple, as they fall out of thermal equilibrium and are left to evolve independently. An example of this is the cosmic microwave background, which decoupled from the background. Mathematically, we implement decoupling as

Table 1: Effective numbers of degrees of freedom in the standard model

Temperature	**New particles**	$4\boldsymbol{N(T)}$
$T < m_e$	γ's + ν's	29
$m_e < T < m_\mu$	$e^\pm$	43
$m_\mu < T < m_\pi$	$\mu^\pm$	57
$m_\pi < T < T_c^*$	π's	69
$T_c < T < m_{\text{charm}}$	- π's + $u, \bar{u}, d, \bar{d}, s, \bar{s}$ + gluons	247
$m_c < T < m_\tau$	$c, \bar{c}$	289
$m_\tau < T < m_{\text{bottom}}$	$\tau^\pm$	303
$m_b < T < m_{W,Z}$	$b, \bar{b}$	345
$m_{W,Z} < T < m_{\text{Higgs}}$	$W^\pm, Z$	381
$m_H < T < m_{\text{top}}$	H^0	385
$m_t < T$	$t, \bar{t}$	427

*T_c corresponds to the confinement–deconfinement transition between quarks and hadrons.

$$\Gamma \sim H, \tag{441}$$

where the expansion rate is given by H and Γ is the interaction rate.

5.2.3 Degrees of freedom

We can start by trying to write the total radiation energy density as a funtion of the photons from the CMB,

$$\rho_R = \frac{g_{eff}}{2}\rho_\gamma. \tag{442}$$

where g denotes the effective number of relativistic degrees of freedom. Photons are vector bosons and have two degrees of freedom (due to their helicity). For them, we have

$$\langle E_\gamma \rangle = \frac{\rho_\gamma}{n_\gamma} = 2.7\ KT_\gamma. \tag{443}$$

If we look at other bosons, we can compare them to photons. Note that scalar bososns have 1 degree of freedom, vector bosons have 2 and so on. If the boson species we are talking about have already decouples from the photons, then their temperature might note be the same, since they are not interacting anymore. Therefore, we denote the

bososns temperature by T_B.

$$\frac{n_B}{n_\gamma} = \frac{g_B}{2}\left(\frac{T_B}{T_\gamma}\right)^3, \tag{444}$$

$$\frac{\rho_B}{\rho_\gamma} = \frac{g_B}{2}\left(\frac{T_B}{T_\gamma}\right)^4. \tag{445}$$

One can also relate relativistic fermions (for example, electrons and neutrinos) to photons. Due to the difference between Bose and Fermi integrals, we have some extra numerical factors [12].

$$\frac{n_F}{n_\gamma} = \frac{3}{4}\frac{g_F}{2}\left(\frac{T_F}{T_\gamma}\right)^3, \tag{446}$$

$$\frac{\rho_F}{\rho_\gamma} = \frac{7}{8}\frac{g_F}{2}\left(\frac{T_F}{T_\gamma}\right)^4. \tag{447}$$

For example, for electrons we have 4 degrees of freedom (electron, positron, spin up/down). In the table from [6], we have a list of the degrees of freedom for the Standard Model.

If we consider the limit $T_i >> m_i$,

$$g_{eff} = \sum_B g_B\left(\frac{T_B}{T_\gamma}\right)^4 + \sum_F g_F\left(\frac{T_F}{T_\gamma}\right)^4. \tag{448}$$

Note that as the temperature raises, more particle degrees of freedom must be taken into account on this calculation.

When the Universe was very young (age on the order of $t < 10^5$ years) it is believed that it was dominated by radiation. Recall that the equation of state for this situation has $\omega = 1/3$, and for such small times we can neglect the contribution from other cosmological terms (like matter and Λ) to find

$$a \sim t^{1/2}, \;\; \rho_R \sim a^{-4}, \tag{449}$$

which yelds

$$H = 1.66\sqrt{g_{eff}}\frac{T^2}{M_{Pl}}, \tag{450}$$

$$t = 0.301\frac{1}{\sqrt{g_{eff}}}\frac{M_{Pl}}{T} \sim \left(\frac{T}{MeV}\right)^{-3} \text{ seconds}, \tag{451}$$

with M_{Pl} as the Planck mass. As we can see, there is a relation between the expansion of the Universe, the relativistic degrees of freedom and temperature.

Another useful quantity is the effective number of neutrino species, which can be used to write the energy density of relativitic species in an alternative way,

$$N_\nu^{\text{eff}} \equiv \left(\frac{\rho_R - \rho_\gamma}{\rho_\nu}\right) \approx \frac{8}{7}\sum_B \frac{g_B}{2}\left(\frac{T_B}{T_\gamma}\right)^4 + \sum_F \frac{g_F}{2}\left(\frac{T_F}{T_\gamma}\right)^4, \tag{452}$$

$$\rho_R = \left[1 + \frac{7}{8}\left(\frac{4}{11}\right)^{4/3} N_\nu^{\text{eff}}\right]. \tag{453}$$

Finally, we point out that it is possible to use the relation

$$\dot{\rho} = -3H(\rho + P), \tag{454}$$

to find an equation for the conservation of energy per comoving volume when we have a thermodynamic system in equilibrium. Since

$$\dot{P} = s\dot{T} \tag{455}$$

from thermodynamics, we obtain

$$\frac{d}{dt}(sa^3) = 0. \tag{456}$$

5.2.4 The Boltzmann equation

Suppose that we have a statistical distribution of particles $f(p; x)$, with 3-momentum between $(p, p + dp)$, energy between $(E, E + dE)$, and space-time coordinates between $(x, x+dx)$ in an expanding isotropic Universe, and we are interested in finding an equation

on how those particles evolve with time. The expression that describes this is called Boltzmann equation, we will present a brief derivation of it for the colliisonless case. An extension of this result can be extended to take into account scattering and annihilations, and it can be found on [14], [12],

The Boltzmann equation is defined as:

$$L(f) = C(f) \tag{457}$$

where L is the Liouville operator, C is the collision operator, and $f = f(x^\mu, p^\nu)$ is the distribution function of the particle in phase space. We are not considering collisions, so we will only worry about the Liouville operator. Consider the total time derivative of f:

$$\frac{df}{dt} = \frac{\partial f}{\partial t} + \frac{\partial f}{\partial x^i}\frac{dx^i}{dt} + \frac{\partial f}{\partial p}\frac{dp}{dt}. \tag{458}$$

Since we are working in a cosmological context, the background metric is not flat (FRW metric), so we need to take that into account. Recall the geodesic equation for a vector v^μ defined in an arbitrary spacetime:

$$\frac{dv^\mu}{dt} + \Gamma^\mu_{\alpha\beta} v^\alpha v^\beta = 0, \tag{459}$$

where $\Gamma^\mu_{\alpha\beta}$ is the Christoffel symbol. Applying this to the total derivative of the momentum:

$$\frac{df}{dt} = \frac{\partial f}{\partial t} + \frac{\partial f}{\partial x^\nu} p^\nu - \frac{\partial f}{\partial p^\mu}\Gamma^\mu_{\alpha\beta} p^\alpha p^\beta, \tag{460}$$

and we define:

$$L = \frac{\partial}{\partial t} + \frac{\partial}{\partial x^\nu} p^\nu - \frac{\partial}{\partial p^\mu}\Gamma^\mu_{\alpha\beta} p^\alpha p^\beta. \tag{461}$$

For a FRW metric, and assuming that $E = p$ (we take $c = 1$) for the neutrinos,

$$L = E\frac{\partial f}{\partial t} - HE^2\frac{\partial f}{\partial E}. \tag{462}$$

For the collisionless case, $L(f) = 0$.

$$\frac{\partial f}{\partial t} - HE\frac{\partial f}{\partial E} = 0. \tag{463}$$

The number density is defined as:

$$n_\nu = \frac{g}{(2\pi)^3}\int d^3p\ f, \tag{464}$$

so we multiply the equation by $\frac{g}{(2\pi)^3}$ and integrate. Since the integration is over the momentum, the first term (time derivative) is simple, and becomes just $\frac{\partial n_\nu}{\partial t}$. The other one is a bit more subtle. Let's take a closer look:

$$\frac{g}{(2\pi)^3}\int d^3p\ HE\frac{\partial f}{\partial E} = \frac{g}{(2\pi)^3}\int 4\pi p^2 dp\ HE\frac{\partial f}{\partial E}, \tag{465}$$

where isotropy over the momentum space is assumed. But energy and momentum are interchangable (we are still using c=1), so we use integration by parts:

$$\frac{g}{(2\pi)^3}\int 4\pi p^3 dp\ H\frac{\partial f}{\partial p} = 3\frac{g}{(2\pi)^3}\int 4\pi p^2 dp\ Hf = 3H\frac{g}{(2\pi)^3}\int d^3p\ f = 3Hn_\nu. \tag{466}$$

Finally, the Boltzmann equation becomes:

$$\frac{\partial n_\nu}{\partial t} + 3Hn_\nu = 0 \Rightarrow \frac{\partial[n_\nu/(1+z)^3]}{\partial t} = 0. \tag{467}$$

We can modify this equation by introducing two terms: a source term and a term to account for continuous redshift loss. They will appear on the right hand side of the equation.

$$\frac{\partial[n_\nu/(1+z)^3]}{\partial t} = \frac{\partial(HEn_\nu/(1+z)^3)}{\partial E} + Q_\nu. \tag{468}$$

We will need the equation in this form later in Part III, when we study the neutrinos produced by heavy dark matter decay.

5.3 Dark matter, dark energy and the ΛCDM model

5.3.1 Observational evidence

The first and still most powerful evidende for the existence of dark matter comes from the observation of the motion of astrophysical objects, such as stars [60]. By looking at objects on the sky and measureing their speeds, one sees that they move faster than they should if only the gravitational attraction of visible matter is taken into account.

The most famous case is the measurement of galactic rotation curves. If we have a body moving on a stable Keplerian orbit aroud a galaxy,

$$v(r)\alpha \sqrt{\frac{M(r)}{r}}, \tag{469}$$

with $M(r)$ the mass inside the orbit of radius r. However, when we measure the velocity distribution this is not what we observe; instead we see that the velocity becomes essentially constant for large r. For the Milky Way, this velocity is $v \approx 220\ m/s$. Other observations, such as galactic clusters also provide evidence for dark matter.

In 2011 the Nobel Prize in Physics was awarded to Saul Perlmutter, Brian P. Schmidt and Adam G. Riess "for the discovery of the accelerating expansion of the Universe through observations of distant supernovae". By observing type Ia supernova, the Saul Perlmutter's team and another team headed by Brian P. Schmidt and Adam G. Riess they concluded that the Universe was expanding at an accelerated rate ([62], [63], [64]. The general belief is that this expansion is driven by dark energy.

The most accurate measurements we have are made indirectly, and come from fits of cosmological data. The WMAP mission is one of those experiments, which collected data from seven years of observations. According to the results [65], we have the matter density

$$\Omega_m = 0.266 \pm 0.26, \tag{470}$$

and the vacuum energy density

$$\Omega_\Lambda = 0.734 \pm 0.029. \tag{471}$$

The matter budget has tree free parameters, h_0, $\Omega_m h_0^2$ and $\Omega_b h_0^2$,

$$h_0 = 0.710 \pm 0.025, \tag{472}$$

$$\Omega_m h_0^2 = 0.1334^{+0.0056}_{0.0055}, \tag{473}$$

$$\Omega_b h_0^2 = 0.02258^{+0.00057}_{0.00056}, \tag{474}$$

which are the Hubble expansion rate, the matter density and the baryon density all measured in the present. By looking at this and the diference between the matter and baryon density we conclude that there exists a cold dark matter density, but we are not sure about its nature.

We can, however, infer some general properties that dark matter must satisfy. Essentially we now that dark matter can not affect the other observed cosmological processess, such as the nucleossynthesis, and a very plausible candidate is made of weakly interacting massive particles (WIMPs) which only interacts thorugh the weak force and gravity. Most of the dark matter must be stable or decays in such a way that does not affect other physical processess, the gravitational interaction explains structure formation and rotation curves (agreeing with individual and galxy cluster observations) and the weak interaction accounts for the fact that it is dark (not visible) and cold. in addition, WIMPs are naturally produced with the required cosmological densities [66].

5.3.2 The *Planck* spacecraft and cosmological parameters

The Cosmic Microwave Background has been extensively used over the years as a source of data to mesure cosmological parameters and test theories. The CMB radiation, and in particular the study of its anisotropies, provides information about the matter

content, geometry and evolution of the Universe on late times. The *Planck* spacecraft is a third-generation space mission following the ground breaking work of COBE and WMAP that is dedicated to the study of those anisotropies, and so far has provided us excellent cosmological measurments [40].

The results of the observations are consistent with a certain cosmological model. According to that model, we live a spatially flat Universe, with dark energy, cold dark matter, baryons and radition following the description we provided along this chapter. Due to its sucess, it is usully referred to as the standard model of Big Bang cosmology, and is called ΛCDM. It assumes General Relativity as the fundamental theory, and makes accurate predictions concerning the CMB, nucleosysthesis and much more.

Strictly speaking, the TT, TE, EE spectra recorded by the *Planck* spacecraft when combined with polarization maps (lowP) describe the standard spatially-flat 6-parameter ΛCDM model

$$\{\Omega_b h^2,\, \Omega_{\rm CDM} h^2,\, \Theta_s,\, \tau,\, n_s,\, A_s\}, \tag{475}$$

with high precision: *(i)* baryon density, $\Omega_b h^2 = 0.02225 \pm 0.00016$; *(ii)* CDM density, $\Omega_{\rm CDM} h^2 = 0.1198 \pm 0.0015$; *(iii)* angular size of the sound horizon at recombination, $\Theta_s = (1.04077 \pm 0.00032) \times 10^{-2}$; *(iv)* Thomson scattering optical depth due to reionization, $\tau = 0.079 \pm 0.017$; *(v)* scalar spectral index, $n_s = 0.9645 \pm 0.0049$; *(vi)* power spectrum amplitude of adiabatic scalar perturbations, $\ln(10^{10}\, A_s) = 3.094 \pm 0.034$ [231]. *Planck* data also constrain the Hubble constant $h = 0.6727 \pm 0.0066$, the dark energy density $\Omega_\Lambda = 0.6844 \pm 0.0091$, the amplitude of initial density perturbations $\sigma_8 = 0.831 \pm 0.013$, and the mass density parameter $\Omega_m = 0.3156 \pm 0.0091$

However, this is not the end of the story. Other experiments and collaborations also provide information about cosmological parameters; the problem is that the results do not entirely agree. This was a motivation for part of the research presented in this dissertation.

6 Beyond the Standard Model

6.1 Introduction

The conspicuously well-known accomplishments of the $SU(3)_C \times SU(2)_L \times U(1)_Y$ standard model (SM) of strong and electroweak forces can be considered as the apotheosis of the gauge symmetry principle to describe particle interactions. Most spectacularly, the recent discovery [131, 132] of a new boson with scalar quantum numbers and couplings compatible with those of a SM Higgs has possibly plugged the final remaining experimental hole in the SM, cementing the theory further.

Arguably, the most challenging puzzle in high energy physics today is to find out what is the underlying theory that completes the SM. The overly conservative approach to this dilemma has been to assess the consistency of the SM assuming a vast desert between the electroweak scale $M_{\rm EW} \sim 10^3$ GeV and the Planck mass $M_{\rm Pl} \sim 10^{19}$ GeV. The relevant physics of the desert hypothesis is determined by running couplings into the ultraviolet (UV) using renormalization group (RG) equations. The behavior of the running couplings depends sensitively on the weak scale boundary conditions, among which the mass of the Higgs boson is perhaps the most critical. The measured Higgs mass $m_H = 125.5 \pm 0.5$ GeV [133, 134, 135, 136] corresponds to a Higgs quartic coupling λ close to zero when renormalized at energies above $\Lambda \sim 10^{11}$ GeV.

Strictly speaking, next-to-leading order (NLO) constraints on SM vacuum stability based on two-loop RG equations, one-loop threshold corrections at the electroweak scale (possibly improved with two-loop terms in the case of pure QCD corrections), and one-loop effective potential seem to indicate m_H saturates the minimum value that ensures a vanishing Higgs quartic coupling around $M_{\rm Pl}$, see *e.g.* [137, 138, 139, 140, 141, 142, 143,

144, 145, 146, 147]. However, the devil is in the details. More recent NNLO analyses [148, 149, 150] yield a very restrictive condition of absolute stability up to the Planck scale

$$\begin{aligned} m_H &> \left[129.4 + 1.4\left(\frac{m_t/\mathrm{GeV} - 173.1}{0.7}\right)\right. \\ &- \left. 0.5\left(\frac{\alpha_s(m_Z) - 0.1184}{0.0007}\right) \pm 1.0_{\mathrm{th}}\right] \ \mathrm{GeV}\,. \end{aligned} \tag{476}$$

On combining in quadrature the theoretical uncertainty with experimental errors on the mass of the top (m_t) and the strong coupling constant (α_s), one obtains $m_H > 129 \pm 1.8$ GeV. The vacuum stability of the SM up to the Planck scale is excluded at 2σ (98% C.L. one sided) for $m_H < 126$ GeV [148, 149, 150].

The instability of the SM vacuum does not contradict any experimental observation, provided its lifetime τ is longer than the age of the universe T_{U}. Since the stability condition of the electroweak vacuum is strongly sensitive to new physics, from the phenomenological point of view it is clear that beyond SM physics models have to pass a sort of "stability test" [151, 152, 153]. Indeed, only new physics models that reinforce the requirement of a stable or metastable (but with $\tau > T_{\mathrm{U}}$) electroweak vacuum can be accepted as a viable UV completion of the SM [154, 155, 156, 157, 158, 159, 160, 161, 162, 163, 164, 165].

From a theoretical perspective some modification of the Higgs sector has long been expected, as the major motivation for physics beyond the SM is aimed at resolving the huge disparity between the strength of gravity and of the SM forces. Even if one abandons this hierarchy motivation, which does not conflict with any experimental measurement, the SM has many other (perhaps more basic) shortcomings. Roughly speaking, the SM is incapable of explaining some well established observational results. Among the most notable of these are neutrino masses, the QCD theta parameter, and the presence of a large non-baryonic dark matter (DM) component of the energy density in the universe. Interestingly, if the new dynamics couples directly to the Higgs sector, this may induce deviations from the usual vacuum stability and perturbativity bounds of the SM. However, beyond SM physics models are usually driven by rather high scale dynamics (*e.g.*, the

neutrino seesaw and the QCD axion), in which case there will be a negligible effect on the running of the couplings. A notable exception to this is the weakly interacting massive particle (WIMP) DM, whose mass scale is constrained to be low if produced by thermal freeze-out [172].

The scalar Higgs portal is a compelling model of WIMP DM in which a renormalizable coupling with the Higgs boson provides the connection between our visible world and a dark sector consisting of $SU(3)_C \times SU(2)_L \times U(1)_Y$ singlet fields [173, 174, 175, 176]. This is possible because the Higgs bilinear $\Phi^\dagger\Phi$ is the only dimension-2 operator of the SM that is gauge and Lorentz invariant, allowing for an interaction term with a complex singlet scalar S of the form

$$\Delta V = \lambda_3 \Phi^\dagger \Phi S^\dagger S \,. \tag{477}$$

Given that S develops a vacuum expectation value (VEV), the Higgs mixes with the singlet leading to the existence of two mass eigenstates (h_1 and h_2), which in turn open the portal into a weak scale hidden sector. Despite its simplicity, in fact, this model offers a rich phenomenology, and it provides a simple and motivated paradigm of DM.

In this chapter we carry out a general analysis of vacuum stability and perturbativity in the SM augmented by a Higgs portal with a minimal weak scale hidden sector. The layout is as follows. In Sec. 6.2 we outline the basic setting of the scalar Higgs portal model and discuss general aspects of the effective low energy theory resulting from a minimal hidden sector. In Sec. 6.3 we confront the model with a variety of experimental data, including direct DM searches, heavy meson decays with missing energy, the invisible Higgs width, as well as astrophysical and cosmological observations. In Sec. 6.4 we derive the RG equations and in Sec. 6.5 we present the analysis of vacuum stability. Our conclusions are collected in Sec. 6.6.

6.2 Minimal Higgs Portal Model

A viable DM candidate must be stable, or nearly so. Stability results from either an unbroken or mildly broken symmetry in the Lagrangian. A discrete Z_2 symmetry is the

simplest available symmetry to guarantee absolute stability of the DM particle. Under Z_2 the SM particles are even while the DM particle is odd [177]. The required symmetry may be simply introduced by hand into the SM, or, more naturally, may remain after breaking of some global continuous symmetry. For example, a concrete realization of such a hidden sector could emerge when a global $U(1)$ symmetry is spontaneously broken by a scalar field with charge 2 under that symmetry, and so a discrete Z_2 symmetry arises automatically in the Lagrangian. After spontaneous symmetry breaking, fields with an even (odd) charge under the global $U(1)$ symmetry will acquire an even (odd) discrete charge under Z_2. Consequently the lightest particle with odd charge will be absolutely stable, and thus a plausible dark matter candidate. The simplest approach to realize this scenario is to introduce one new complex scalar field S and one Dirac fermion field ψ into the SM. These new fields are singlets under the SM gauge group, and charged under $U(1)_W$ symmetry, such that $U(1)_W(\psi) = 1$ and $U(1)_W(S) = 2$. Spontaneous breaking of a global continuous symmetry generates a massless Goldstone boson and a CP-even scalar, and splits the Dirac fermion into two new mass-eigenstates, corresponding to Majorana fermions.

The renormalizable scalar Lagrangian density of the set up described above is found to be

$$\mathscr{L}_s = (\mathcal{D}^\mu \Phi)^\dagger \mathcal{D}_\mu \Phi + (\mathcal{D}^\mu S)^\dagger \mathcal{D}_\mu S - V \,, \tag{478}$$

where

$$V = \mu_1^2 \Phi^\dagger \Phi + {\mu_2}^2 S^\dagger S + \lambda_1 (\Phi^\dagger \Phi)^2 + \lambda_2 (S^\dagger S)^2 + \Delta V \tag{479}$$

is the potential and

$$\mathcal{D}_\mu = \partial_\mu - i g_2 \tau^a W_\mu^a - i g_Y Y B_\mu \tag{480}$$

is (in a self-explanatory notation) the covariant derivative. In the spirit of [178], we write S in terms of two real fields (its massive radial component and a massless Goldstone

boson). The radial field develops a VEV $\langle r \rangle$ about which the field S is expanded

$$S = \frac{1}{\sqrt{2}} \left(\langle r \rangle + r(x) \right) \; e^{i\, 2\alpha(x)} \,. \tag{481}$$

The phase of S is adjusted to make $\langle \alpha(x) \rangle = 0$. Next, we impose the positivity conditions [176]

$$\lambda_1 > 0, \qquad \lambda_2 > 0, \qquad \lambda_1 \lambda_2 > \frac{1}{4} \lambda_3^2 \,. \tag{482}$$

If the conditions (482) are satisfied, we can proceed to the minimization of (479) as a function of constant VEVs for the two scalar fields. In the unitary gauge the Higgs doublet is expanded around the VEV as

$$\Phi(x) = \frac{1}{\sqrt{2}} \begin{pmatrix} 0 \\ \\ \langle \phi \rangle + \phi(x) \end{pmatrix} , \tag{483}$$

where $\langle \phi \rangle = 246$ GeV.

The physically most interesting solutions to the minimization of (479) are obtained for $\langle \phi \rangle$ and $\langle r \rangle$ both non-vanishing

$$\langle \phi \rangle^2 = \frac{-\lambda_2 \mu_1^2 + \frac{1}{2} \lambda_3 {\mu_2}^2}{\lambda_1 \lambda_2 - \frac{1}{4} \lambda_3^2} \tag{484}$$

and

$$\langle r \rangle^2 = \frac{-\lambda_1 \mu_2^2 + \frac{1}{2} \lambda_3 \mu_1^2}{\lambda_1 \lambda_2 - \frac{1}{4} \lambda_3^2} \,. \tag{485}$$

To compute the scalar masses, we must expand the potential (479) around the minima (484) and (485). We denote by h_1 and h_2 the scalar fields of definite masses, m_{h_1} and m_{h_2} respectively. After a bit of algebra, the explicit expressions for the scalar mass eigenvalues and eigenvectors read

$$m_{h_1}^2 = \lambda_1 \langle \phi \rangle^2 + \lambda_2 \langle r \rangle^2 - \zeta \,, \tag{486}$$

and

$$m_{h_2}^2 = \lambda_1 \langle\phi\rangle^2 + \lambda_2 \langle r\rangle^2 + \zeta \,, \tag{487}$$

with

$$\zeta = \left| \sqrt{(\lambda_1 \langle\phi\rangle^2 - \lambda_2 \langle r\rangle^2)^2 + (\lambda_3 \langle\phi\rangle\langle r\rangle)^2} \right| \tag{488}$$

and

$$\begin{pmatrix} h_1 \\ h_2 \end{pmatrix} = \begin{pmatrix} cos\theta & -sin\theta \\ sin\theta & cos\theta \end{pmatrix} \begin{pmatrix} r \\ \phi \end{pmatrix} . \tag{489}$$

Here, $\theta \in [-\pi/2, \pi/2]$ also fullfils

$$sin2\theta = \frac{\lambda_3 \langle\phi\rangle\langle r\rangle}{\sqrt{(\lambda_1 \langle\phi\rangle^2 - \lambda_2 \langle r\rangle^2)^2 + (\lambda_3 \langle\phi\rangle\langle r\rangle)^2}} \,. \tag{490}$$

Now, it is convenient to invert (486), (487) and (490), to extract the parameters in the Lagrangian in terms of measurable quantities: m_{h_1}, m_{h_2} and $sin2\theta$. We obtain

$$\begin{aligned} \lambda_1 &= \frac{m_{h_{2,1}}^2}{4\langle\phi\rangle^2}(1 - \cos 2\theta) + \frac{m_{h_{1,2}}^2}{4\langle\phi\rangle^2}(1 + \cos 2\theta), \\ \lambda_2 &= \frac{m_{h_{1,2}}^2}{4\langle r\rangle^2}(1 - \cos 2\theta) + \frac{m_{h_{2,1}}^2}{4\langle r\rangle^2}(1 + \cos 2\theta), \\ \lambda_3 &= sin2\theta \left(\frac{m_{h_{2,1}}^2 - m_{h_{1,2}}^2}{2\langle\phi\rangle\langle r\rangle} \right) . \end{aligned} \tag{491}$$

Note that there are two distinct regions of the parameter space: one in which the hidden scalar singlet is heavier than the Higgs doublet and one in which is lighter. The small θ limit leads to the usual SM phenomenology with an isolated hidden sector.

For the DM sector we assume at least one Dirac field

$$\mathscr{L}_\psi = i\bar{\psi}\gamma \cdot \partial\psi - m_\psi \bar{\psi}\psi - \frac{f}{\sqrt{2}}\bar{\psi^c}\psi \, S^\dagger - \frac{f^*}{\sqrt{2}}\bar{\psi}\psi^c \, S \,. \tag{492}$$

As advanced above, we assign to the hidden fermion a charge $U(1)_W(\psi) = 1$, so that the Lagrangian is invariant under the global transformation $e^{iW\alpha}$. Assuming the transformation is local we express ψ as

$$\psi(x) = \psi'(x)e^{i\alpha(x)}. \tag{493}$$

Now, after r achieves a VEV we expand the DM sector to obtain

$$\begin{aligned}\mathscr{L}_\psi = &\frac{i}{2}\left(\bar{\psi}'\gamma.\partial\psi' + \bar{\psi}'^c\gamma.\partial\psi'^c\right) - \frac{m_\psi}{2}\left(\bar{\psi}'\psi'^c + \bar{\psi}'^c\psi'^c\right)\\ &- \frac{f\langle r\rangle}{2}\bar{\psi}^c\psi' - \frac{\langle f\rangle}{2}\bar{\psi}'\psi'^c - \frac{1}{2}\left(\bar{\psi}'\gamma\psi' - \bar{\psi}'^c\gamma\psi'^c\right).\partial\alpha - \frac{f}{2}\left(\bar{\psi}^2\psi' + \bar{\psi}'\psi'^c\right).\end{aligned} \tag{494}$$

The diagonalization of the ψ' mass matrix generates the mass eigenvalues,

$$m_\pm = m_\psi \pm f\langle r\rangle, \tag{495}$$

for the two mass eigenstates

$$\psi_- = \frac{i}{\sqrt{2}}\left(\psi'^c - \psi'\right) \quad \text{and} \quad \psi_+ = \frac{1}{\sqrt{2}}\left(\psi'^c + \psi'\right). \tag{496}$$

In the new basis, the act of charge conjugation on $\psi_\pm$ yields

$$\psi_\pm^c = \psi_\pm\,, \tag{497}$$

which implies that the fields $\psi_\pm$ are Majorana fermions. The Lagrangian is found to be

$$\begin{aligned}\mathscr{L}_\psi = &\frac{i}{2}\bar{\psi_+}\gamma.\partial\psi_+ + \frac{i}{2}\bar{\psi_-}\gamma.\partial\psi_-\\ &- \frac{1}{2}m_+\bar{\psi}_+\psi_+ - \frac{1}{2}m_-\bar{\psi}_-\psi_-,\\ &\frac{i}{4\langle r\rangle}(\bar{\psi}_+\gamma\psi_- + \bar{\psi}_-\gamma\psi_+).\partial\alpha',\\ &\frac{f}{2}r(\bar{\psi}_+\psi_+ + \bar{\psi}_-\psi_-)\,,\end{aligned} \tag{498}$$

Table 2: Definition of most common variables.

Φ	Higgs doublet
S	Complex scalar field
ϕ	Neutral component of Φ
r	Massive CP-even scalar
α'	Goldstone boson
H	SM Higgs boson
$h_{1,2}$	Scalar mass eigenstates
λ_3	Quartic coupling between SM and hidden sector
θ	Mixing angle between h_1 and h_2
w	Lightest Majorana fermion (WIMP)
f	$w-r$ coupling constant – see Eq. (498) –

where $\alpha' \equiv 2\alpha \langle r \rangle$ is the canonically normalized Goldstone boson [178]. We must now put r into its massive field representation, for which the interactions of interest are

$$\begin{aligned} \mathscr{L} &= -\frac{f sin\theta}{2} h_{1,2}(\bar{\psi}_+\psi_+ + \bar{\psi}_-\psi_-) - \frac{f\cos\theta}{2} h_{2,1} \\ &\times \quad (\bar{\psi}_+\psi_+ + \bar{\psi}_-\psi_-). \end{aligned} \tag{499}$$

This leads to 3-point interactions between the Majorana fermions and the Higgs doublet.

All in all, the Dirac fermion of the hidden sector splits into two Majorana mass-eigenstates. The heavier state will decay into the lighter one by emitting a Goldstone boson. The lighter one, however, is kept stable by the unbroken reflection symmetry. Hence, we can predict that today the universe will contain only one species of Majorana WIMP, the lighter one w, with mass m_w equal to the smaller of $m_\pm$. Therefore, the dark sector contains five unknown parameters: m_w, $m_{h_{1,2}}$, λ_2, θ, and f. To facilitate the calculation of the WIMP relic density, throughout we impose a supplementary constraint relating some of these free parameters: $\Delta m/m_w \ll 1$, where $\Delta m = |m_+ - m_-| = 2|f\langle r \rangle|$. (The most common variables used in this article are summarized in Table 2.)

A cautionary note is worth taking on board at this juncture. It is well known that the spontaneous breaking of a global $U(1)$ symmetry have several disconnected and degenerate vacua (the phase of the vacuum expectation value $\langle 0|S|0\rangle$ can be different in different regions of space, and actually we expect it to be different in casually discon-

nected regions), yielding dangerous domain-wall structure in the early universe [179, 180]. In the spirit of [179], it may be possible to explicitly break the symmetry introducing (possibly small) terms in V, such that the domain walls disappear before dominating the matter density of the universe, while leaving (pseudo-)Goldstone bosons and the same dark matter phenomenology [156].[2] For simplicity, we restrict our considerations to the potential in (479), but generalizations are straightforward.

6.3 Constraints from experiment

The mixing of r with the Higgs doublet ϕ can be analyzed in a two-parameter space characterized by the mass of hidden scalar m_{h_i} and the mixing angle θ, where $i = 1$ for a light scalar singlet (*i.e.* $m_{h_2} = m_H$) and $i = 2$ for a heavy one (*i.e.* $m_{h_1} = m_H$). We begin to constrain this parameter space by using data from DM searches at direct detection experiments.

6.3.1 Constraints from direct DM searches

The wN cross section for elastic scattering is found to be

$$\sigma_{wN} = \frac{4}{\pi}\frac{m_w^2 m_N^2}{(m_w + m_N)^2}\,\frac{f_p^2 + f_n^2}{2}\,, \tag{500}$$

where $N \equiv \frac{1}{2}(n+p)$ is an isoscalar nucleon in the renormalization group-improved parton model [184, 185]. The effective couplings to protons f_p and neutrons f_n are given by

$$\begin{aligned} f_{p,n} &= \sum_{q=u,d,s} \frac{G_q}{\sqrt{2}} f_{Sq}^{(p,n)} \frac{m_{p,n}}{m_q} + \frac{2}{27} f_{SG}^{(p,n)} \\ &\times \sum_{q=c,b,t} \frac{G_q}{\sqrt{2}} \frac{m_{p,n}}{m_q}, \end{aligned} \tag{501}$$

[2] Other approaches, if exceedingly fine-tuned, may offer alternative solutions [181, 182, 183].

where G_q is the WIMP's effective Fermi coupling for a given quark species,

$$\mathscr{L} = \frac{G_q}{\sqrt{2}} \bar{\psi}_- \psi_- \bar{\psi}_q \psi_q \,, \tag{502}$$

with ψ_q the SM quark field of flavor q. The first term in (501) reflects scattering with light quarks, whereas the second term accounts for interaction with gluons through a heavy quark loop. The scalar spin-independent form factors, $f_{Sq}^{(p,n)}$, are proportional to the matrix element, $\langle \bar{q} q \rangle$, of quarks in a nucleon. Herein we take [186]

$$\begin{aligned} f_{Su}^{p} &= 0.016(5)(3)(1), \qquad & f_{Su}^{n} &= 0.014(5)(^{+2}_{-3})(1), \\ f_{Sd}^{p} &= 0.029(9)(3)(2), \qquad & f_{Sd}^{n} &= 0.034(9)(^{+3}_{-2})(2), \\ f_{Ss}^{p} &= 0.043(21), \qquad & f_{Ss}^{n} &= 0.043(21) \,, \end{aligned} \tag{503}$$

in good agreement with the scalar strange content of the nucleon from lattice QCD calculations [187]. The gluon scalar form factor is given by $f_{SG}^{(p,n)} = 1 - \sum_{u,d,s} f_{Sq}^{(p,n)}$. For the case at hand,

$$\frac{f_p^2 + f_n^2}{2 m_N^2} \simeq \left(0.29 \frac{G_q}{\sqrt{2} m_q} \right)^2 , \tag{504}$$

with

$$\frac{G_q}{m_q} = \frac{\sqrt{2} f \lambda_3 \langle r \rangle}{2 m_{h_1}^2 m_{h_2}^2}, \tag{505}$$

yielding [188]

$$\sigma_{wN} = \frac{1}{\pi} \frac{m_w^2 m_N^4}{(m_w + m_N)^2} \left(\frac{0.29 \, \lambda_3 \, \langle r \rangle \, f}{m_{h_1}^2 m_{h_2}^2} \right)^2 \,; \tag{506}$$

see Appendix D for details. We may re-express this result in terms of the mixing angle,

$$\sigma_{wN} = (0.29)^2 \frac{1}{4\pi} \frac{m_w^2 m_N^4}{(m_w + m_N)^2} \left(\frac{1}{m_{h_1}^2} - \frac{1}{m_{h_2}^2} \right)^2 \times \left(\frac{f}{\langle \phi \rangle} \right)^2 sin^2 2\theta \ . \quad (507)$$

For $\theta \ll 1$, the upper limits on the nucleon-wimp cross sections derived by the various experiments translate into upper limits on the mixing angle

$$|\theta| < \frac{(m_w + m_N)}{m_N^2 m_w} \frac{\langle \phi \rangle}{f} \left| \frac{1}{m_{h_1}^2} - \frac{1}{m_{h_2}^2} \right|^{-1} \times \frac{\sqrt{\pi}}{0.29} \sqrt{\sigma_{wN}(m_w)} \ . \quad (508)$$

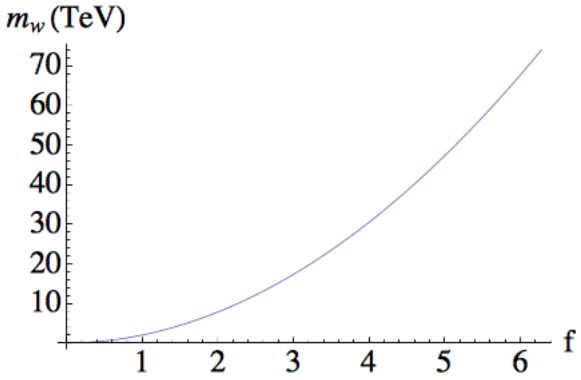

Figure 5: The relation in Eq. (510).

To determine f we require the w relic density to be consistent with $h^2\Omega_{\rm DM} \simeq 0.111(6)$ [189]. In our study we consider the interesting case in which $m_{h_i} < m_w$ and hence the instantaneous freeze-out approximation is valid [190]. In this region of the parameter space, the w's predominantly annihilate into a pair of h_i's or co-annihilate with the next-to-lightest Majorana fermion, producing a scalar h_i and a Goldstone boson. All of the final state h_i subsequently decays into α'. We note, however, that for $m_w \approx m_H/2$ one expects dominant annihilation into fermions. We have found that for the considerations in the

present work, the effective thermal cross section can be safely approximated by [190]

$$\lim_{\Delta m/m_w \to 0} \langle \sigma_{ww} v_M \rangle \approx \frac{f^4}{32\pi m_w^2}, \tag{509}$$

yielding

$$f \approx \left(\frac{1.04 \times 10^{11}\ \text{GeV}^{-1}\, x_f}{\sqrt{g(x_f)}\ M_{\text{Pl}}\, \Omega_{\text{DM}} h^2} \right)^{1/4} \sqrt{m_w}\ , \tag{510}$$

where $x_f = m_w/T_f$, $g(x_f)$ is is the number of relativistic degrees of freedom at the freeze-out temperature T_f, and $m_{h_i}/m_w \lesssim 0.8$ [190]. In general for WIMP DM $x_f \approx 20 - 25$ [191]. The precise relation between the WIMP mass and the required Yukawa coupling to attain the relic density condition is shown in Fig. 5. We note that the mass upper limit, $m_w < 74$ TeV, is in agreement with the unitarity limit $\Omega_{\text{DM}} h^2 \geq 1.7 \times 10^{-6} \sqrt{x_f}\, [m_w/(1\ \text{TeV})]^2$ [192], which implies $m_w \leq 110$ TeV [193].

Using (508) we can now translate the 90% confidence limit on the spin independent elastic WIMP-nucleon cross section as obtained by direct detection experiments into an upper limit of $|\theta|$. In Fig. 6 we show constraints on this parameter space from direct dark matter searches. For $m_w \gtrsim 8$ GeV, the most restrictive constraint comes from the LUX experiment [194], whereas for $m_w \lesssim 8$ GeV, the most restrictive upper limit is from the SuperCDMS low threshold experiment [195]. It should be noted that indirect DM searches (*e.g.* by detecting neutrinos from annihilation of captured low-mass WIMPs in the Sun) also constrain the WIMP-nucleon elastic scattering cross section. However, these searches are in general model dependent. For example, for 100% annihilation into $\tau^+\tau^-$ pairs, the Super-Kamiokande Collaboration [196] has set the current best upper limit on σ_{wN} for WIMP masses below 8 GeV. Because of the assumed dominant decay into SM fields, this limit cannot be used to further constrain the (θ, m_h) parameter space.

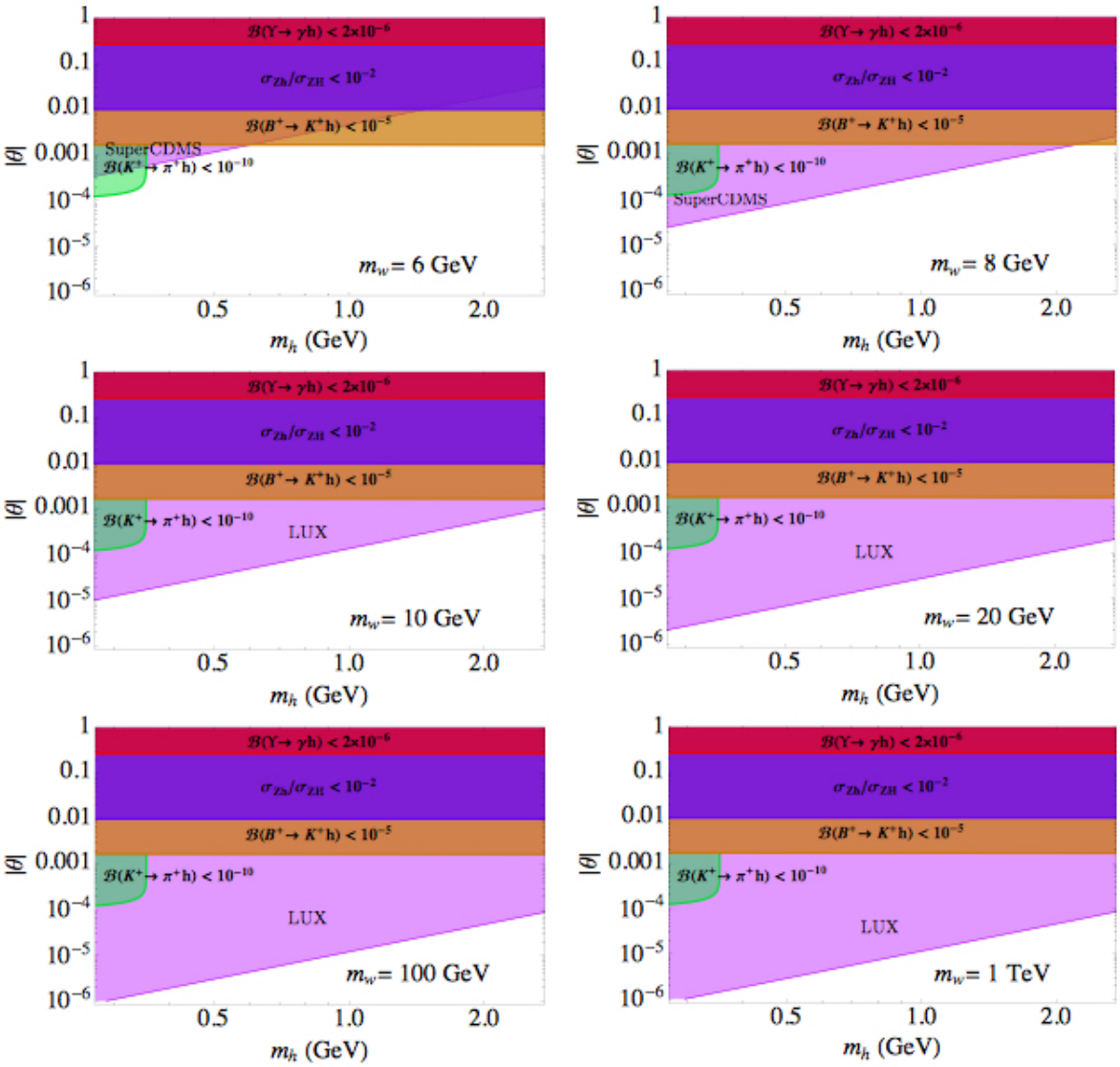

Figure 6: Excluded regions of the $(|\,\theta\,|, m_h)$ parameter space from interactions involving SM particles in the initial state and the CP-even scalar in the final state, as well from DM direct detection experiments. The horizontal bands indicate bounds are from heavy meson decays with missing energy (no significant excess of such decays over background has been observed yielding bounds on the processes $\Upsilon \to \gamma h,\ B^+ \to K^+ h,\ K^+ \to \pi^+ h$) as well as from LEP limits on the production of invisibly-decaying Higgs bosons σ_{Zh}/σ_{ZH}. The diagonal bands represent bounds from DM direct detection experiments (Super-CDMS and LUX), for different values of the WIMP mass. Note that all bounds other than the LEP bound can be smoothly extrapolated to the smallest $m_h \sim 35$MeV stipulated by cosmology.

6.3.2 Constraints from heavy meson decay

For $m_w \lesssim 10$ GeV, searches for heavy meson decays with missing energy provide comparable bounds [197, 198, 199]. In particular, the upper limit reported by the BaBar

Collaboration $\mathcal{B}(\Upsilon(1S) \to \gamma + \not{E}_T) < 2 \times 10^{-6}$ [200] yields an upper bound for the mixing angle, $\theta < 0.27$ [201].[3] A stronger constraint follows from LEP limits on the production of invisibly-decaying Higgs bosons $\sigma_{Zh}/\sigma_{ZH} < 10^{-4}$ [204, 205, 206, 207, 208], which implies $\theta < 10^{-2}$ [209]. More restrictive constraints come from searches for the rare flavor-changing neutral-current decay $B^+ \to K^+ + \not{E}_T$ reported by the BaBar [211, 212, 210], CLEO [213], and BELLE [214] collaborations, as well as limits on $K^+ \to \pi^+ + \not{E}_T$ from the E787 [215] and E949 experiments [216, 217, 218]. The resulting excluded regions of the $(|\theta|, m_h)$ plane from all these experiments are compared in Fig. 6 with those from direct DM searches.

6.3.3 Constraints from LHC and SN1987A

Before proceeding we note that additional constraints on the $(|\theta|, m_h)$ parameter space can be obtained from limits on Higgs decay into invisible particles and from emission of α'-particle pairs in a post-collapse supernova core. However, these are not direct constraints as they depend also on the quartic coupling of the hidden scalar. In particular, since invisible decays reduce the branching fraction to the (visible) SM final states, it is to be expected that $\mathcal{B}(H \to \text{invisible})$ is strongly constrained. Indeed $\mathcal{B}(H \to \text{invisible})$ is known to be less than about 19% at 95%CL [219, 220, 221, 222, 223]. This implies exclusion contours in the $(|\theta|, m_h)$ plane as a function of the free parameter λ_2 given by [199]

$$|\theta(\lambda_2)| < 1.27 \times 10^{-2} \left[\lambda_2 \frac{m_H^2}{m_h^2} + f^2 \sqrt{1 - \frac{4m_w^2}{m_H^2}} \right]^{-\frac{1}{2}} .$$

In addition, the emissivity of α' due to nucleon bremsstrahlung ($NN \to NN\alpha'\alpha'$) cannot exceed the limits imposed by SN1987A observations: $\epsilon_{\alpha'} \leq 7.324 \times 10^{-27}$ GeV [224]. For typical supernova core conditions ($T = 30$ MeV and $\rho = 3 \times 10^{14}$ g/cm^3) it is easily seen that $|\lambda_3| \leq 0.011 \left(\frac{m_h}{500 \text{ MeV}}\right)^2$ [225]. For $\theta \ll 1$ we can translate this limit into a bound on the mixing angle via

[3] Comparable bounds are obtained from searches for $\mathcal{B}(\Upsilon(3S) \to \gamma + \not{E}_T)$ [202] and $\mathcal{B}(J/\psi \to \gamma + \not{E}_T)$ [203].

$$\theta \approx \frac{\lambda_3 \ \langle r \rangle \, \langle \phi \rangle}{m_H^2 - m_h^2} \ . \tag{511}$$

By use of $m_h \approx \sqrt{2\lambda_2}\, \langle r \rangle$ we can express this bound as

$$|\theta| \leq \frac{7.65 \ m_h^3}{\sqrt{\lambda_2}|m_H^2 - m_h^2|} \ \text{GeV}^{-1} \ . \tag{512}$$

In Fig. 7 we show the exclusion contours for the $\lambda_2 = 1$ and $\lambda_2 = 0.05$. For smaller values of λ_2, the excluded regions of the $(|\theta|, m_h)$ plane are dominated by upper limits on B-meson decay into invisibles. All in all, for $m_{h_2} = m_H$, we can conclude from Figs. 6 and 7 that 2×10^{-3} is a conservative 90% CL upper limit on the mixing angle.

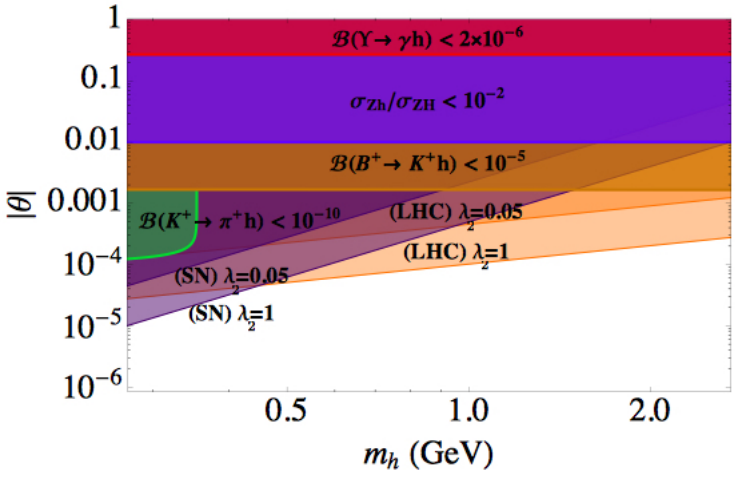

Figure 7: Bounds on the $(|\theta|, m_h)$ including invisible Higgs decays and α' emission in a post-collapse supernova core for different assumptions about the value of the quartic coupling λ_2.

For $m_{h_2} \gg m_H$, (508) can be rewritten as

$$\begin{aligned} f \ |\theta| \ &< \ \frac{1}{m_N^2} \ \langle \phi \rangle \ m_H^2 \ \frac{\sqrt{\pi}}{0.29} \ \sqrt{\sigma_{wN}(m_w)} \\ &\simeq \ 2.7 \times 10^7 \ \sqrt{\sigma_w N(m_w)} \ \text{GeV} \, . \end{aligned} \tag{513}$$

Dedicated searches for DM candidates serve as an essential component of the LHC physics programme. The typical experimental signature of DM production at the LHC

consists of an excess of events with a single final-state partilce X recoiling against large amounts of missing transverse momentum or energy. In Run I, the ATLAS and CMS collaborations have examined a variety of such "mono-X" topologies involving jets of hadrons, gauge bosons, top and bottom quarks as well as the Higgs boson in the final state. In particular, the CMS Collaboration has reported very restrictive bounds on the DM-nucleon scattering cross section from searches in events containing a jet and an imbalanced transverse momentum [226]. However, it is important to stress that the contact operator approximation adopted in [226] only holds if the mediator is heavy and can be integrated out [227]. If the mediator is light and contributes to resonant DM production (as in the minimal Higgs portal model discussed herein), the contact approximation fails and the mono-jet bounds do not apply. Future LHC14 mono-X searches will also probe vertex operators for which the mediator between dark matter and quarks is heavy [228, 229], and therefore cannot constrain the Higgs portal model discussed here.

6.3.4 Constraints from cosmology

Cosmological observations further constrain the model. The earliest observationally verified landmarks – big bang nucleosynthesis (BBN) and the cosmic microwave background (CMB) decoupling epoch – have become the de facto worldwide standard for probing theoretical scenarios beyond the SM containing new light species. It is advantageous to normalize the extra contribution to the SM energy density to that of an "equivalent" neutrino species. The number of "equivalent" light neutrino species,

$$N_{\rm eff} = \frac{\rho_{\rm R} - \rho_\gamma}{\rho_{\nu_L}}\,, \tag{514}$$

quantifies the total "dark" relativistic energy density (including the three left-handed SM neutrinos) in units of the density of a single Weyl neutrino

$$\rho_{\nu_L} = \frac{7\pi^2}{120}\,\left(\frac{4}{11}\right)^{4/3} T_\gamma^4, \tag{515}$$

where ρ_γ is the energy density of photons (which by today have redshifted to become the CMB photons at a temperature of about $T_\gamma^{\rm today} \simeq 2.7$ K) [230].

Recent results reported by the Planck Collaboration [231] have strongly constrained the the presence of an excess $\Delta N_{\rm eff}$ above SM expectation: $N_{\rm eff}^{\rm SM} = 3.046$ [232]. Specifically, the 68% C.L. constraints on $N_{\rm eff}$ from Planck TT, TE, and EE spectra, when combined with polarization maps (lowP) and baryon acoustic oscillation (BAO) measurements are [231]:

$$N_{\rm eff} = \begin{cases} 3.13 \pm 0.32 & \text{PlanckTT} + \text{lowP}, \\ 3.15 \pm 0.23 & \text{PlanckTT} + \text{lowP} + \text{BAO}, \\ 2.99 \pm 0.20 & \text{PlanckTT, TE, EE} + \text{lowP}, \\ 3.04 \pm 0.18 & \text{PlanckTT, TE, EE} + \text{lowP} + \text{BAO}. \end{cases}$$

The joint CMB+BBN predictions on $N_{\rm eff}$ provide comparable constraints. The 95% C.L. preferred range on $N_{\rm eff}$ when combining Planck data (TT, TE, EE+lowP) with the helium abundance estimated in [233] is $N_{\rm eff} = 2.99 \pm 0.39$, whereas the combination of Planck data with the deuterium abundance measured in [234] yields $N_{\rm eff} = 2.91 \pm 0.37$ [231]. (See also [235].) In summary, one fully thermalize neutrino, $\Delta N_{\rm eff} \simeq 1$, is excluded at over 3σ. Models predicting fractional changes of $\Delta N_{\rm eff} \approx 0.39$ are marginally consistent with data, saturating the 1σ upper limit. Models predicting, $\Delta N_{\rm eff} \approx 0.57$, are ruled out at about 2σ.

As noted in [178] the Goldstone boson α' is a natural candidate for an imposter equivalent neutrino. The contribution of α' to $N_{\rm eff}$ is $\Delta N_{\rm eff} = \rho_{\alpha'}/\rho_\nu$. Thus, taking into account the isentropic heating of the rest of the plasma between the decoupling temperatures, $T_{\alpha'}^{\rm dec}$ and $T_\nu^{\rm dec}$, we obtain

$$\Delta N_{\rm eff} = \frac{4}{7}\left(\frac{g(T_\nu^{\rm dec})}{g(T_{\alpha'}^{\rm dec})}\right)^{4/3}, \tag{516}$$

where $g(T)$ is the effective number of interacting (thermally coupled) relativistic degrees of freedom at temperature T; for example, $g(T_\nu^{\rm dec}) = 43/4$.[4] For the particle content of

[4] If relativistic particles are present that have decoupled from the photons, it is necessary to distinguish

the SM, there is a maximum of $g(T^{\rm dec}_{\alpha'}) = 427/4$ (with $T^{\rm dec}_{\alpha'} > m_t$). This corresponds to a minimum value of $\Delta N_{\rm eff} = 0.027$, which is consistent with cosmological observations. However, a fully thermalized α', *i.e.* $T^{\rm dec}_{\nu} = T^{\rm dec}_{\alpha'}$ is excluded at 90% C.L.. Note that if α' goes out of thermal equilibrium while the temperature is just above the muon mass

$$\Delta N_{\rm eff} = (4/7)(43/57)^{4/3} = 0.39\,. \tag{517}$$

This corresponds to a number of equivalent light neutrino species that is consistent at the 1σ level with current data.

The α' decouples from the plasma when its mean free path becomes greater than the Hubble radius at that time. The α' collision rate with any fermion species of mass m_f at or below T is of order [178]

$$\Gamma(T) \sim \frac{\lambda_3^2 m_f^2 T^7}{m_{h_1}^4 m_{h_2}^4}\,, \tag{518}$$

whereas the expansion rate of the universe is of order

$$H(T) \approx \frac{T^2}{M_{\rm Pl}}\,. \tag{519}$$

We equate these two rates to obtain

$$T^{\rm dec}_{\alpha'} \approx \left(\frac{m_{h_1}^2\, m_{h_2}^2}{\lambda_3\; m_f\; M_{\rm Pl}}\right)^{1/5}\,. \tag{520}$$

Now, taking $m_f = T = m_\mu$ we obtain

$$m_h \approx \frac{\left(\lambda_3^2\, m_\mu^7\, M_{\rm Pl}\right)^{1/4}}{m_H^4}\,. \tag{521}$$

Substituting the conservative value $\lambda_3 = 5 \times 10^{-3}$ in (521) we have $m_h \approx 500$ MeV. Note that if the α' goes out of equilibrium when the only massive SM particles left are e^+e^- pairs, $\Delta N_{\rm eff} = 0.57$. In such a case the value of m_h would have to be less than given by (521) by a factor between $(m_e/m_\mu)^{1/2}$ and $(m_e/m_\mu)^{7/4}$ [178]. This sets a lower limit on

between two kinds of g: g_ρ, which is associated with the total energy density, and g_s, which is associated with the total entropy density. For our calculations we use $g = g_\rho = g_s$.

the mass of the hidden scalar: $m_h \approx 35$ MeV.

6.4 RG Evolution Equations

One-loop corrections to (479) can be implemented by making λ_1, λ_2, and λ_3 energy dependent quantities. The positivity conditions of (482) then must be satisfied at all energies.

A straightforward calculation leads to the RG equations for the five parameters in the scalar potential

$$\begin{aligned}
\frac{d\mu_1^2}{dt} &= \frac{\mu_1^2}{16\pi^2}\left(12\lambda_1 + 6Y_t^2 + 2\frac{\mu_2^2}{\mu_1^2}\lambda_3 - \frac{9}{2}g_2^2 - \frac{3}{2}g_Y^2\right), \\
\frac{d\mu_2^2}{dt} &= \frac{\mu_2^2}{16\pi^2}\left(8\lambda_2 + 4\frac{\mu_1^2}{\mu_2^2}\lambda_3 + 4f^2\right), \\
\frac{d\lambda_1}{dt} &= \frac{1}{16\pi^2}\left(24\lambda_1^2 + \lambda_3^2 - 6Y_t^4 + \frac{9}{8}g_2^4 + \frac{3}{8}g_Y^4\right. \\
&+ \left.\frac{3}{4}g_2^2 g_Y^2 + 12\lambda_1 Y_t^2 - 9\lambda_1 g_2^2 - 3\lambda_1 g_Y^2\right), \\
\frac{d\lambda_2}{dt} &= \frac{1}{8\pi^2}\left(10\lambda_2^2 + \lambda_3^2 - \frac{1}{4}f^4 + 4\lambda_2 f^2\right), \\
\frac{d\lambda_3}{dt} &= \frac{\lambda_3}{8\pi^2}\left(6\lambda_1 + 4\lambda_2 + 2\lambda_3 + 3Y_t^2 - \frac{9}{4}g_2^2\right. \\
&- \left.\frac{3}{4}g_Y^2 + 2f^2\right),
\end{aligned} \tag{522}$$

where $t = \ln Q$ and Y_t is the top Yukawa coupling, with

$$\frac{dY_t}{dt} = \frac{Y_t}{16\pi^2}\left(\frac{9}{2}Y_t^2 - 8g_3^2 - \frac{9}{4}g_2^2 - \frac{17}{12}g_Y^2\right), \tag{523}$$

and $Y_t^{(0)} = \sqrt{2}\, m_t/\langle\phi\rangle$ (see Appendix E for details). The RG running of the gauge couplings follow the standard form

$$\begin{aligned}
\frac{dg_3}{dt} &= \frac{g_3^3}{16\pi^2}\left[-11+\frac{4}{3}n_g\right] = -\frac{7}{16}\,\frac{g_3^3}{\pi^2}\,,\\
\frac{dg_2}{dt} &= \frac{g_2^3}{16\pi^2}\left[-\frac{22}{3}+\frac{4}{3}n_g+\frac{1}{6}\right] = -\frac{19}{96}\,\frac{g_2^3}{\pi^2}\,,\\
\frac{dg_Y}{dt} &= \frac{1}{16\pi^2}\left[\frac{41}{6}\;g_Y^3\right]\,,
\end{aligned} \tag{524}$$

where $n_g = 3$ is the number of generations [236]. Finally, the running of f is driven by [237]

$$\frac{df}{dt} = \frac{f^3}{4\pi^2}\,. \tag{525}$$

6.5 Vacuum Stability Constraints

We now proceed to study the vacuum stability of the model through numerical integration of the equation we just obtained. To ensure perturbativity of f between the TeV scale and the Planck scale we find from (526),

$$f = \left(\frac{1}{f_0^2} - \frac{(t-t_0)}{2\pi^2}\right)^{-1/2}\,, \tag{526}$$

yielding $f_0 < 0.7$. For normalization, we set $t = \ln(Q/125\text{ GeV})$ and $t_{\max} = \ln(\Lambda/125\text{ GeV})$. Now, using the SM relation $m_H^2 = -2\mu^2$, with $m_H \simeq 125$ GeV, and setting $\langle\phi\rangle^2 = 246$ GeV at the same energy scale $Q = 125$ GeV we fix the initial conditions for the parameters μ and λ. Throughout we take the top Yukawa coupling renormalized at the top pole mass [238].

6.5.1 Light scalar singlet

We integrate the RG equations from $m_{h_2} = m_H$ and impose the initial conditions for $\lambda_{1,2,3}$ by putting the observed values into their equations,

$$\langle\phi_{\rm SM}\rangle^2\big|_{Q=m_{h_2}} = \langle\phi\rangle^2\big|_{Q=m_{h_2}} \ , \quad m_{h_2} = m_H \ . \tag{527}$$

The other quantities in the equations for the λ's $m_{h_1} = m_h, \theta$ and $\langle r\rangle$ remain free parameters. It is easily seen through numerical integration of the λ's, Y_t and g's and the running of f, that there are stable vacua up to the Planck scale. However, for those stable vacua, the required values of θ and m_h are excluded at 90% C.L.

As an illustration, we note that there is a stable solution for $\langle r\rangle = 2.8$ GeV and $m_h = 0.3$ GeV, which corresponds $\theta = 0.01$. As can be seen in Fig. 6, this region of the parameter space is excluded at 90% C.L. Actually, for $m_h = 0.3$ GeV, it can be shown that the mixing angle is bounded from below: $\theta > 0.004$. The argument is as follows. The Yukawa coupling f of the Majorana fermion does not suppress the growth of λ_2, but does exactly the opposite. This is due to the smallness of f and therefore $f^4 < 16\lambda_2^2 f^2$ in $d\lambda_2/dt$. As a result, we can simply set $f = 0$. The RG equation of λ_2 then implies a constraint on its boundary value: $\lambda_2\,|_{Q=m_H} < 0.2$ or it blows up before reaching the Planck scale. For $\lambda_2\,|_{Q=m_H} = 0.2$, we need $\lambda_3\,|_{Q=m_H} < -0.28$ to have λ_1 always positive. We note that a positive λ_3 only makes λ_1 grows slower and does not help the situation. A smaller $\lambda_2\,|_{Q=m_H}$ only slows down the growth of λ_3 and does not improve the stability. In other words, the maximum of $\lambda_3\,|_{Q=m_H}$ is -0.28. Moreover, from (491) we see that the mixing angle decreases monotonically when either $\lambda_3\,|_{Q=m_H}$ (when it is negative) or $\lambda_2\,|_{Q=m_H}$ increases. So we reach a minimum angle when $\lambda_2\,|_{Q=m_H} = 0.2$ and $\lambda_3\,|_{Q=m_H} = -0.28$, which gives $\theta = 0.004$. Such a value is excluded at the 90% C.L.

Next, we show that for $m_h > 0.3$ GeV, the required mixing angle for a stable vacuum up to the Planck scale is $\theta > 0.004$. To this end, we rewrite (491) as

$$\lambda_2 = \frac{m_H^2}{4y^2}2x^2 + \frac{m_h^2}{4y^2}(2-2x^2)\,, \tag{528}$$

$$\lambda_3 = 2x\frac{m_h^2 - m_H^2}{2\langle\phi\rangle y}\,, \tag{529}$$

where we have taken $x = sin\theta$ and $y = \langle r\rangle$. Now, since $m_h < m_H$ by increasing m_h we

decrease $|m_h^2 - m_H^2|$ and therefore from (529) we see that x/y increases. Consequently, the term

$$\frac{m_H^2}{4y^2}2x^2 - \frac{m_h^2}{4y^2}2x^2 \tag{530}$$

in (528) increases (because it is proportional to x^2/y^2) and therefore the other term $\propto 1/y^2$ decreases. In other words, we have both x/y and y rising and therefore $x(\theta)$ increases with increasing m_h.

It should be noted that a theoretical lower limit on the mass of the hidden scalar can be obtained by generalizing the Weinberg-Linde [239, 240] bound (see also [241]). Herein instead we have used experimental data to determine such a lower limit. For $m_h < 0.3$ GeV, the previously derived lower bound on θ can be relaxed. However, for $m_h = 35$ MeV, we cannot reduce the mixing angle to a level consistent with searches for the rare flavor-changing neutral-current decay $K^+ \to \pi^+ + \not{E}_T$ without sacrificing vacuum stability, *i.e.* $\lambda_3 \sim 1$ is required to obtain $\theta \lesssim 10^{-4}$. Moreover, the upper limit set by SN1987A observations excludes values of $m_h < 35$ MeV, for $\lambda_2 \lesssim 0.2$. As an illustration, in Fig. 8 we show a comparison between the θ behavior imposed by vacuum stability and the upper limit on the mixing angle derived from (512), fixing the quartic coupling of the hidden scalar to the fiducial value that saturates the condition of vacuum stability, *i.e.* $\lambda_2 = 0.2$.

We conclude that, for $m_{h_2} = m_H$, there are no stable solutions up to the Planck scale in the allowed region of the parameter space.

6.5.2 Heavy scalar singlet

For energies below the mass of the heavier Higgs h_2, the effective theory is (of course) the SM. In the low energy regime the Higgs sector is given by

$$\mathscr{L}_{\rm SM} \supset (\mathcal{D}_\mu \Phi)^\dagger \, (\mathcal{D}^\mu \Phi) - \mu^2 \Phi^\dagger \Phi - \lambda (\Phi^\dagger \Phi)^2 \,, \tag{531}$$

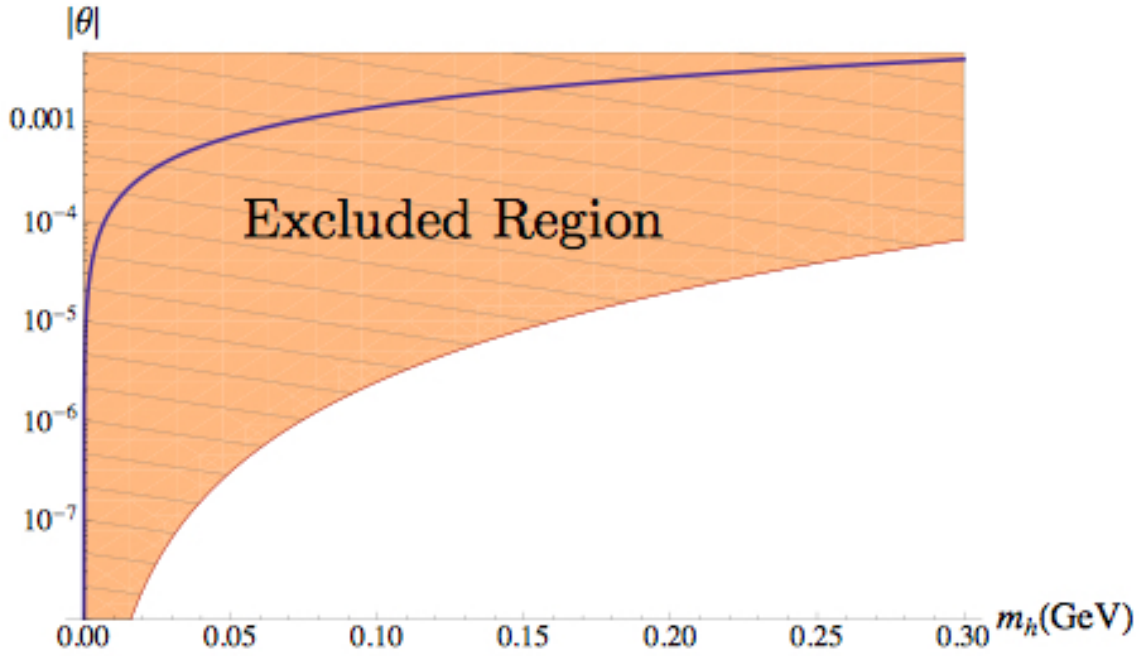

Figure 8: Comparison of vacuum stability requirements in the (θ, m_h) plane (blue curve) with the upper limit set by SN1987A observations.

and the RG equations are those of SM. To obtain the matching conditions connecting the two theories, following [156] we integrate out the field S to obtain a Lagrangian of the form (531). Identifying the quadratic and quartic terms in the potential yields

$$\mu^2 = \mu_1^2 - \mu_2^2 \, \frac{\lambda_3}{2\lambda_2} \tag{532}$$

and

$$\lambda = \lambda_1 \, \left(1 - \frac{\lambda_3^2}{4\lambda_1\lambda_2}\right) , \tag{533}$$

respectively. This is consistent with the continuity of $\langle\phi_{\rm SM}\rangle \leftrightharpoons \langle\phi\rangle$; namely

$$\langle\phi_{\rm SM}\rangle^2 = -\left.\frac{\mu^2}{\lambda}\right|_{Q=m_{h''}} = -\left.\frac{\mu_1^2 - \frac{\mu_2^2\,\lambda_3}{2\lambda_2}}{\lambda_1\,\left(1-\frac{\lambda_3^2}{4\lambda_1\lambda_2}\right)}\right|_{Q=m_{h_2}} ,$$

or equivalently

$$\langle\phi_{\rm SM}\rangle^2\big|_{Q=m_{h_2}} = \langle\phi\rangle^2\big|_{Q=m_{h_2}} , \tag{534}$$

with $\langle\phi\rangle$ given by (484). The quartic interaction between the heavy scalar singlet and the Higgs doublet provides an essential contribution for the stabilization the scalar field potential [156].

When we refer to the stability of (479) at some energy Q (with the use of the couplings at that scale), we are assuming that the field values are at the scale Q. Note that the field values are the only functional arguments when talking about a potential like (479), and therefore the appropriate renormalization scale must also be at that scale. For $\lambda_3 > 0$, the third condition in (482) could potentially be violated only for field values $\langle\phi\rangle$ around m_{h_2}, regardless of the renormalization scale Q [156]. Consequently, the region of instability is found to be:

$$\begin{aligned} \langle r\rangle &< m_{h_2}/\sqrt{2\lambda_2}, \\ Q_- &< \langle\phi\rangle < Q_+, \\ Q_\pm^2 &= \frac{m_{h_2}^2\lambda_3}{8\lambda_1\lambda_2}\left(1 \pm \sqrt{1-\frac{4\lambda_1\lambda_2}{\lambda_3^2}}\right)\Bigg|_{Q_*}, \end{aligned} \tag{535}$$

where Q_* is some energy scale where the extra positivity condition is violated; see Appendix **??**.[5] Therefore, $Q_\pm \sim m_{h_2}$ when the extra positivity condition is saturated, that is $\lambda_1\lambda_2 = \lambda_3/4$. From (535) it follows that $Q_\pm \sim m_{h_2}$ when all the λ_i are roughly at the same scale. If one of the $\lambda_{1,2}$ is near zero, then Q_+ can be $\gg m_{h_2}$, but this region of the parameter space is constrained by the condition $\lambda_{1,2} > 0$. The stability for field values at m_{h_2} is then determined by the potential with coupling at scale m_{h_2} (instead of Q). Therefore, for $\lambda_3 > 0$, we impose the extra positivity condition in the vicinity of m_{h_2}. Even though the potential seems unstable at $Q \gg m_{h_2}$, it is actually stable when all the field values are at the scale Q. Note that the potential with $\lambda_i(Q)$ can only be used when the functional arguments (field values $\langle\phi\rangle$, $\langle r\rangle$) are at the scale Q. On the other hand,

[5] Note that (535) is where the potential can become negative. If the third condition in (482) is satisfied, $Q_\pm$ will be imaginary, which implies that the potential is always positive. So we need to make sure the third condition is satisfied $Q_\pm \sim m_{h_2}$ so that the potential can never be negative. On the other hand, we only need to consider the third condition in this range as for other $\langle\phi\rangle$, the potential is positive regardless of the value of $\frac{1}{4}\lambda_3^2 - \lambda_1\lambda_2$.

the instability region for $\lambda_3 < 0$ is given by

$$\begin{aligned} \langle r \rangle &> \frac{m_{h_2}}{\sqrt{2\lambda_2}}, \\ c_- &< \frac{\langle \phi \rangle}{\langle r \rangle} < c_+, \\ c_\pm^2 &= -\frac{\lambda_3}{2\lambda_1}\left(1 \pm \sqrt{1 - \frac{4\lambda_1\lambda_2}{\lambda_3^2}}\right)\Bigg|_{Q_*}, \end{aligned} \tag{536}$$

and hence is given by the ratio of $\langle \phi \rangle$ and $\langle r \rangle$, which can be reached even with both $\langle \phi \rangle$ and $\langle r \rangle$ being $\gg m_{h_2}$; see Appendix F. Therefore, for $\lambda_3 < 0$, we impose the extra positivity condition at all energy scales. Note that the asymmetry in λ_3 will carry over into an asymmetry in θ.

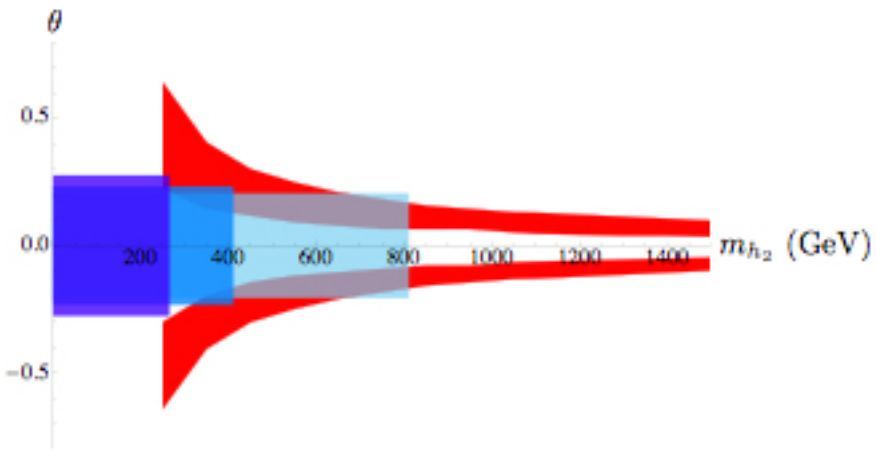

Figure 9: The red area shows the allowed parameter space in the m_{h_2} *vs.* θ plane under the vacuum stability constraint of Eq. (482), with $\Lambda = 10^{19}$ GeV. The blue areas indicate the regions of the parameter space that are not excluded by direct DM searches for $f_0 = 0.4, 0.5, 0.7$, from light to dark shading. The perturbative upper bound is defined by $\lambda_i < 2\pi$.

To solve the system we run the SM couplings from 125 GeV up to the mass scale m_{h_2} and use the matching conditions to determine $\langle \phi_{\rm SM} \rangle$, which in turns allows one to solve algebraically for m_{h_1}. In Fig. 9 we compare the region of the parameter space which contains stable vacua up to the Planck scale (red area) with the allowed (blue) bands

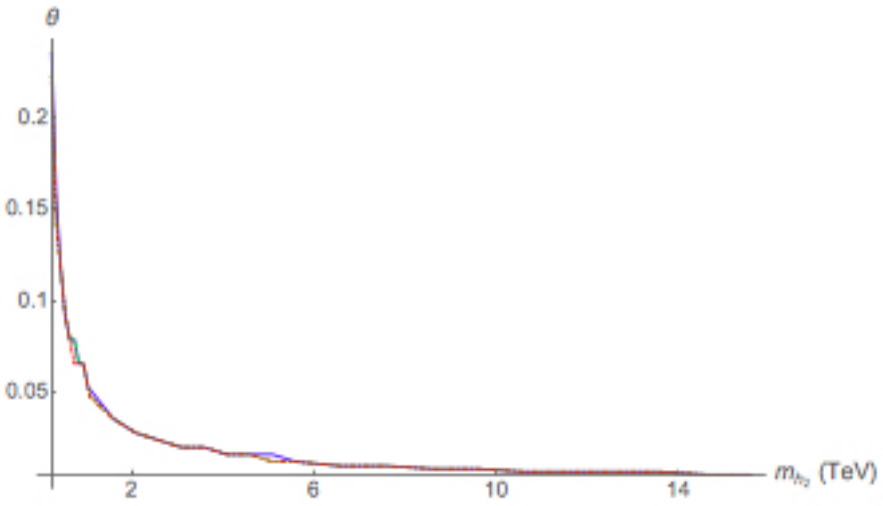

Figure 10: Comparison of three solutions of stable vacua, with identical initial conditions except for $f_0 = 0.4$ (red dashed line), $f_0 = 0.5$ (green dot-dashed line), and $f_0 = 0.7$ (blue solid line).

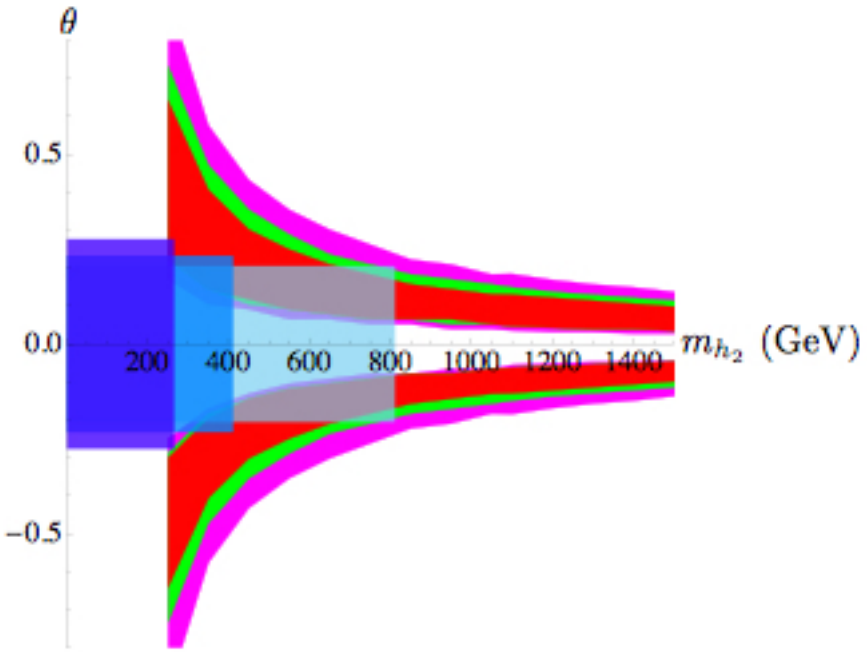

Figure 11: The allowed parameter space in the m_{h_2} *vs.* θ plane under the vacuum stability constraint of Eq. (482), with $\Lambda = 10^{11}$ GeV (magenta), $\Lambda = 10^{15}$ GeV (green), and $\Lambda = 10^{19}$ GeV (red). The blue areas indicate the regions of the parameter space that are not excluded by direct DM searches for $f_0 = 0.4, 0.5, 0.7$, from light to dark shading. The perturbative upper bound is defined by $\lambda_i < 2\pi$.

from direct DM searches. From (510) it is straightforward to see that the heaviest WIMP satisfying the relic density constraint, $m_w = 70$ TeV, is near the unitarity limit [192]. However, one can immediately recognize in Fig. 5 that such a WIMP mass exceeds the

perturbativity limit, $f_0 \leq 0.7$. The maximum WIMP mass that simultaneously satisfies the relic density constraint in (510) and the f_0 perturbativity limit in (526) is $m_w = 1$ TeV. This maximum mass then determines the range of the darker blue band in the horizontal axis (m_{h_2}) of Fig. 9. The LUX upper bound on the WIMP-nucleon cross section for elastic scattering [194] via (513) sets an upper limit on the mixing angle. The allowed values of θ determine the range of the (blue) bands in the vertical axis of Fig. 9. The different blue bands correspond to three fiducial values of the Majorana coupling $f_0 = 0.4,\ 0.5,\ 0.7$. It is important to stress that the f_0 dependence of the RG running can be safely neglected; see Fig. 10. It is also important to stress that new physics thresholds, which may appear near the Planck mass, does not significantly modify the region of the parameter space with stable vacua, see Fig. 11. In summary, the superposition of the blue and red areas in Fig. 9 indicates the region of the parameter space which develops a stable vacuum, satisfies the relic density condition, and is in agreement with direct DM searches. The interesting region of the parameter space comprises WIMP masses 350 GeV $\lesssim m_w \lesssim$ 1 TeV.[6] The region of interest is within reach of second generation DM direct detection experiments, such as DEAP3600, DarkSide G2, XENONnT, and DARWIN [244, 245].

6.6 Conclusions

We have studied the vacuum stability of a minimal Higgs portal model in which the SM particle spectrum is extended to include one complex scalar field S and one Dirac fermion field ψ. These new fields are singlets under the SM gauge group and are charged under a global $U(1)$ symmetry: $U(1)_W(\psi) = 1$ and $U(1)_W(S) = 2$. The spontaneous breaking of this $U(1)$ symmetry results in a massless Goldstone boson, a massive CP-even scalar, and splits the Dirac fermion into two new mass-eigenstates $\psi_\pm$, corresponding to Majorana fermions. The symmetry breaking yields naturally a WIMP candidate. Fields with an even (odd) charge under the global $U(1)$ symmetry will acquire, after symmetry breaking, an even (odd) discrete charge under a Z_2 discrete symmetry. While the SM particles are all even under Z_2, the Majorana fermions $\psi_\pm$ are odd. In such a set up the

[6] Curiously, the ATLAS Collaboration has reported a 3σ excess of Higgs pair production $HH \to \gamma\gamma b\bar{b}$ for $m_{h_2} \sim 300$ GeV [242]. See also [243].

lightest particle with odd charge, ψ_-, will be absolutely stable, and hence a plausible WIMP candidate.

We have shown that interactions between the extended Higgs sector and the lightest Majorana fermion which are strong enough to yield a thermal relic abundance consistent with observation can easily destabilize the electroweak vacuum or drive the theory into a non-perturbative regime at an energy scale well below the Planck mass. However, we have also unmasked a small region of the parameter space which develops a stable vacuum (up to the Planck scale), satisfies the relic abundance, and is in agreement with direct DM searches. This region comprises WIMP masses 350 GeV $\lesssim m_w \lesssim$ 1 TeV. The region of interest is within reach of second generation DM direct detection experiments.

Needless to say, here we have considered a minimal model to ensure that bounding the parameter space remains tractable. However, our extension of the dark sector enlarges the parameter space sufficiently to contain stable vacua up to the Planck scale.

7 Astrophysical Neutrino Production and multi-messenger search

The key idea behind multi-messenger searches is very simple: a physical process, such as particle physics reactions taking places in astrophysical sources, can produce multiple observables. A simple example of this would be a cosmic ray entering the atmosphere; as it moves and interacts multiple different particles are produced and different can be detected at the ground. A GRB can produce high neutrinos neutrinos, cosmic rays and gamma rays, all which can be observed by different experiments even though it is just a single source. The main consequences of this is that by looking at astrophysical phenomena from multiple angles we make our conclusions much more precise, since each observable is connected to each other, imposing mutual bounds and making theories easier to check. Cosmic rays will also play a crucial role, as they will be used to impose many bounds and constraints in our results. For a detailed discussion on many astrophysical sources and multi-messenger search in general, see [67]

7.1 Astrophysical accelerators

Particles can increase their energy gradually, through what is called statistical acceleration. This can be accomplished in astrophysical sites where the particles are subject to numerous encounters with shock waves and regions of changing magnetic fields. These different prossesses are usually treated as variations of the famous "Fermi engine", and we will present the basic version of it here. Following [17], suppose that we have a test particle confined in a certain region, where it can interact through shocks and energy can be transfered from the shocks to the particle. In addition, there is a chance that the

particle might escape the region. Physically speaking, it makes sense to think that the more energetic a particle becomes, the harder it is to confine it to a certain region and provide even more energy.

Suppose that in every interaction, the energy of the particle is increased by the factor

$$\delta E = kE, \tag{537}$$

Thus, after an encounter:

$$E_1 = E_0 + kE_0 = E_0(1+k), \tag{538}$$

after two encounters:

$$E_2 = E_1 + kE_1 = E_1(1+k) = E_0(1+k)^2. \tag{539}$$

This leads to the law

$$E_n = E_0(1+k)^n, \tag{540}$$

where E_0 is the initial (injection) energy of the particle. In addition, suppose that the particle has a certain probability of escapingi each encounter is p, so the probability P of remaining after n encounters is

$$P = (1-p)^n. \tag{541}$$

To reach a certain energy E, we need the following number of encounters

$$E = E_0(1+k)^n \Rightarrow (1+k)^n = \frac{E}{E_0}, \tag{542}$$

$$n = \frac{\ln\left(\frac{E}{E_0}\right)}{\ln(1+k)}. \tag{543}$$

If one is interested in the fraction of particles which reaches energies higher than E,

$$N\ \alpha\ \sum_{m=n}^{\infty}(1-p)^m = \frac{(1-p)^n}{p}, \tag{544}$$

which can be rewritten as

$$\frac{(1-p)^n}{p} = p^{-1}(1-p)^{\frac{\ln\left(\frac{E}{E_0}\right)}{\ln(1+k)}} \Rightarrow N\ \alpha\ p^{-1}\left(\frac{E}{E_0}\right)^{-\gamma}, \tag{545}$$

Following our main reference [17], we define the coefficient γ by

$$\gamma = \ln\left(\frac{1}{1-p}\right)/\ln(1+k). \tag{546}$$

Recall that

$$\ln(1+x) \approx x, \tag{547}$$

and we write

$$\gamma \approx \frac{p}{k}. \tag{548}$$

Finally, we introduce one more parameter: the characteristic time. It is plausible to assume that the probability of escaping is given by

$$\gamma \approx \frac{p}{k} = \frac{1}{k}\frac{T_{cycle}}{T_{esc}}, \tag{549}$$

where we have T_{cycle} as the characteristic time for a cycle and T_{esc} the characteristic time it takes for a particle to escape. As we can see, the Fermi engine leads to a power law spectrum of energies. There are other cases and generalizations of this model, and they can be found at [17]. The main disadvantages are the amount of time it takes to reach higher energies, and when such energies are reached, it can be hard to account for energy losses.

Another general argument is known as the Hillas condition, of great interest for cosmic ray physics. Suppose that we have a particle of charge q is moving in a magnetic field,

in a relativistic regime. The Larmor radius is given by

$$r_l = 1.08E/qB_\perp, \tag{550}$$

where $B_\perp$ denotes the component of the field perpendicular to the velocity in microgauss. The size L of the acellerating reagion must be greater than [68].

$$L > 2r_L \sim 2E_{15}/B_{\mu G}, \tag{551}$$

with the energy given in 10^{15} eV.

Particles can also be accelerated in more sudden ways, such as in phenomena like GRB's. These kind of sources can accelerate particles to extremely high energies, but there are a few problems. Since this is a high energy density environment, energy losses can occur, and it's hard to obtain a power law spectrum due to the complexity of the events.

7.2 Proton-proton, proton-photon interactions

The main production mechanisms of neutrinos in astrophysical sources come from proton-proton collisions and proton-photon interactions. Fermi engine and accretion are (very likely) to be the main mechanisms of producing high energy protons, as the gas moves and heats driven by the source. On the other hand, in events like gamma ray bursts are the best to produce the high energy photons necessary for proton-photon interactions.

First, we consider inelastic collisions between protons which have been accelerated, which are usually referred to as *pp* interactions. For an inelastic *pp* collision, we have:

$$p + p \to \pi^0, \pi^\pm. \tag{552}$$

and the decay of those particles generate γ's and ν's. In these reactions, charged and neutral pions are produced in similar numbers. The decay of these pions produce neutrinos and gamma rays (this will be explored in detail in the next section), and this connection leads naturally to the multi messenger approach.

According to [69], the pion emissivity per unit volume (the units are $\mathrm{GeV}^{-1}\mathrm{s}^{-1}\mathrm{cm}^{-3}$) [70],

$$q_{pp}^{\pi} = \int dE\; n f_p c N_\pi \frac{d\sigma_{pp}(E_\pi, E)}{dE}, \tag{553}$$

where n is the density of protons in the target, f_p is the proton spectrum,

$$f_p = \frac{dN_p}{dE}\mathrm{GeV}^{-1}\mathrm{cm}^{-3}, \tag{554}$$

N_π is the pion multiplicity. We also have the differential cross section in the integral. If we make the approximation

$$d\sigma_{pp} \approx \sigma_{pp}\delta(E_\pi - K_p E/N_\pi), \tag{555}$$

with

$$\sigma_{pp} \approx 30\mathrm{mb}, \tag{556}$$

for the proton-proton inelastic cross section on TeV energies on the laboratory frame,

$$K_p \approx 0.4, \tag{557}$$

for the inelasticity and

$$N_\pi \approx 15. \tag{558}$$

This gives

$$q_{pp}^{\pi} \approx nc\;\sigma_{pp}\frac{N_\pi^2}{K_p} f_p\left(\frac{N_\pi E_\pi}{K_p}\right). \tag{559}$$

About 1/3 of the energy of the protons goes into each of the charged and neutral pions. If the source is not too dense, the pions are allowed to decay without interacting with other particles. Each of the neutrinos that come from the decay gets 1/4 of the

parent pion (we will detail the energetics analysis soon), and this gives

$$q_{pp}^{\nu} \approx \frac{1}{4} \times \frac{2}{3} \times 3 q_{pp}^{\pi}(4E_{\nu}) = \frac{1}{2} q_{pp}^{\pi}(4E_{\nu}). \tag{560}$$

Finally,

$$\frac{d\Phi}{dE_{\nu}} = \int dL \; q_{pp}^{\nu} \mathrm{GeV}^{-1} \mathrm{s}^{-} \mathrm{cm}^{-2}. \tag{561}$$

Note that the integral above is calculated over the source spatial extension.

It is important to mention that the interaction between a proton and a high energy photon can also lead to the production of charged and neutral pions, which will decay into neutrinos. The cross section analysis is similar to the one presented above, with a few adjustments. First, we need to specify the photon spectrum (blackbody, power law from emission and so on). It is also necessary to make $\sigma_{p\gamma} \approx 120 \; \mu\mathrm{b}$, $K_p \approx 0.3$, $N_{\pi} \approx 3$ [70].

7.3 Particle decays

In this section, we will provide and overall discussion about decays of particles commonly produced by proton-proton and proton-photon interaction. Due to large number of reactions we will look at, we will not provide a very detailed derivation (such as a precise calculation of lifetimes, branching ratios and so on), which can be found in standard textbooks, such as [8].

We begin with the decay of charged pions, the most common process tho produce muon neutrinos and antineutrinos. The charged pions are hadrons composed by the following combination of quarks and antiquarks:

$$\pi^{+} = u\bar{d}, \;\; \pi^{-} = d\bar{u}. \tag{562}$$

and they have a mass of 139.6 MeV and a mean lifetime of 2.6×10^{-8}s. The decay of $\pi^{\pm}$ is mediated by the boson $W^{\pm}$, a weak interaction process.

The main decay mode of the charged pion is into muons and muon neutrinos,

$$\pi^+ = \mu^+ + \nu_\mu, \tag{563}$$

$$\pi^- \to \mu^- + \bar{\nu}_\mu, \tag{564}$$

with a branching fraction of 0.999877. The pions can also decay into electrons,

$$\pi^+ \to e^+ + \nu_e, \tag{565}$$

$$\pi^- \to e^- + \bar{\nu}_e, \tag{566}$$

with a branching fraction of 0.000123. The reason for such a difference in the branching ratios is due to helicity supression. Note that the tau mass is 1776.82 MeV (and the lifetime is 2.9×10^{-13}s), while the muon has mass 105.7 MeV and the electron 0.511 MeV. That's why the decay of the pion does not goes to tau.

To understand the statement of the paragraph above, let's take a look at the decay on the pion rest frame, for π^-. The pion has spin zero, what implies that the spins of the products must be opposite. In addition, one of the products of the decay is a antineutrino and recall the V-A structure of the Weak interaction, which only couples right-handed chiral antiparticles. So, there is consistency here. The problem is that the neutrino is nearly massless and therefore relativistic, and therefore is in a righ-handed helicity state. In order to conserve angular momentum, the muon must be a right-handed helicity state.

However, the Weak interaction only couples to left-handed chiral particles. Thus, we need to study the relationship between a right-handed helicity state and a left-handed chiral one. We will do so by using a projection. The right-handed helicity solution to the Dirac equation is given by

$$\psi_{\uparrow} = N \begin{pmatrix} cos(\theta/2) \\ e^{i\phi} sin(\theta/2) \\ \frac{\mid \vec{p} \mid}{E+m} cos(\theta/2) \\ \frac{\mid \vec{p} \mid}{E+m} e^{i\phi} sin(\theta/2) \end{pmatrix},$$

and we project this into right and left handed chiral solutions.

$$\psi^{\uparrow} = P_L \psi^{\uparrow} + P_R \psi^{\uparrow}, \tag{567}$$

with

$$P_L = \frac{1}{2}(1-\gamma^5), \;\; P_R = \frac{1}{2}(1+\gamma^5), \tag{568}$$

what gives

$$P_L u_{\uparrow} = \frac{1}{2} N \left(1 - \frac{\mid \vec{p} \mid}{E+m}\right) \begin{pmatrix} cos(\theta/2) \\ e^{i\phi} sin(\theta/2) \\ -cos(\theta/2) \\ -e^{i\phi} sin(\theta/2) \end{pmatrix} = \frac{1}{2} N \left(1 - \frac{\mid \vec{p} \mid}{E+m}\right) \psi_L,$$

$$P_R u_{\uparrow} = \frac{1}{2} N \left(1 + \frac{\mid \vec{p} \mid}{E+m}\right) \begin{pmatrix} cos(\theta/2) \\ e^{i\phi} sin(\theta/2) \\ cos(\theta/2) \\ e^{i\phi} sin(\theta/2) \end{pmatrix} = \frac{1}{2} N \left(1 - \frac{\mid \vec{p} \mid}{E+m}\right) \psi_R.$$

Note that in the relativistic limit when the energy is much greater than the mass and $E \approx \mid \vec{p} \mid$, we have

$$\frac{\vec{p}}{E+m} \rightarrow 1 \Rightarrow \psi_{\uparrow} = \psi_R. \tag{569}$$

Now, we see that the right-handed helicity state has a left handed chiral component proportional to

$$\frac{1}{2}\left(1-\frac{\vec{p}}{E+m}\right)=\frac{m}{m_\pi+m}, \tag{570}$$

where the equality above comes from the study of the pion decay on its rest frame, and m is the mass of the product. Now, when we look at the possibilities we have, the mass of the muon and the electron, we see that the mass of the electron is much smaaller than the mass of the pion (the muon has mass 105.7 MeV and the electron 0.511 MeV), so the term

$$\frac{m}{m_\pi+m}, \tag{571}$$

is very small, and the decay into the electron is very suppressed.

If we have a charged particle that decays into a muon, we still have another reaction to consider: the decay of the muon itself,

$$\mu^- = e^- + \bar{\nu}_e + \nu_\mu, \tag{572}$$

$$\mu^+ = e^+ + \nu_e + \bar{\nu}_\mu, \tag{573}$$

which has a lifetime of 2.1969811 ± 0.0000022 μs. Other decays are forbidden by lepton flavour conservation.

Now, we turn to the energetics of the pion decays [71]. Consider, for instance, π^- and define

$$f=\left(\frac{m_\mu}{m_{pi}}\right)^2, \tag{574}$$

and the average energy for the muon neutrino that comes straight from the decay is

$$\langle E^\pi_{\nu_\mu}\rangle = \frac{(1-f)E_\pi}{2} \approx 0.22E_\pi, \tag{575}$$

and for the muon,

$$\langle E_\mu^\pi \rangle = \frac{(1+f)E_\pi}{2} \approx 0.78 E_\pi. \tag{576}$$

When the muon decays, the ν_μ takes 1/3 of the energy of the muon,

$$\langle E_{\nu_\mu}^\mu \rangle = \frac{\langle E_\mu^\pi \rangle}{3} = \frac{(1+f)E_\pi}{6} = 0.26 E_\pi, \tag{577}$$

and we say that each neutrino that comes out of the decay gets 1/4 fo the energy of the parent pion.

In the neutral pion decay,

$$\pi^0 \to \gamma + \gamma, \tag{578}$$

each photon carries half of the energy of the parent neutral pion.

We can also consider the results of photon-proton interactions. In those interactions, if the energies are geat enough, one can excite a Δ^+ resonance. From those resonances, the one which has the largest cross section and is of greater importance to us is the Δ^+, composed of two up quarks and one down (just like the proton). Its mass is 1232 MeV, and it has the decay modes

$$\Delta^+ \to \pi^+ + n^0, \pi^0 + p^+, \tag{579}$$

and the pions contribute to the neutrino production. Note that this reaction can occur in an astrophysical source, such as a GRB, or in space through the interaction between a cosmic ray and the Cosmic Microwave Background.

7.4 On the astrophysical flavor ratio

As we have already discussed, neutrinos oscillate as they travel away from their source. From what we have discussed in this chapter, we expect the flavor ratio at the source to be

$$(\nu_e : \nu_\mu : \nu_\tau) \approx (1 : 2 : 0). \tag{580}$$

We know that δm^2 is somewhere on the range 10^{-3} to 10^{-5}eV^2 . Also, we are talking about distances on the order of kiloparsecs ($1\text{kpc} \approx 3.1 \times 10^{19}\text{m}$), so the argument on the sine functions that describe the transition probability take huge values, on the order of 10^9 to 10^{11}.

If we look at the results from the neutrino oscillations in the Electroweak Physics chapter, we can see that the probability of detecting the flavor α is given by

$$P_{\nu_\alpha} = \sum_j U_{\alpha j}^2 \sum_\beta r_\beta U_{\beta j}^2, \tag{581}$$

where r denotes a flavor ratio,

$$r_e : r_\mu : r_\tau, \quad \sum_\alpha r_\alpha = 1, \tag{582}$$

It can be shown that any initial flavor ratios that contains one third of the initial neutrinos as electron neutrinos will arrive on Earth with an equipartition of the three flavors. Thus, the observation of tau neutrinos and such flavor ratios is a strong indicator of astrophysical neutrino production.

7.5 Solar and atmospheric neutrinos

In this section, we will make some comments on neutrinos that do not come from astrophysical sources, beginning with solar neutrinos and then moving to neutrinos produced at the atmosphere from cosmic rays. We will mainly follow [8] here.

The thermonuclear reactions that take place in the solar core are an extraordinary source for the production of neutrinos of energies on the order 1 MeV. Those neutrinos travel and reach Earth, with a flux of $6 \times 10^{10}\text{cm}^{-2}\text{s}^{-1}$ and they possess a very small cross section, making detection difficult. Many experiments have dedicated themselves to the study of such neutrinos, from Homestake (first detection of solar neutrinos, experiment started in 1970) to the Super-Kamiokande and SNO experiments, which provided high

precision measurements (and actually led to the Nobel Prize of 2015 for the neutrino oscillations).

Neutrinos can also be produced on the atmosphere by interactions of cosmic rays. as those high energy particles come, they interact with molecules on the atmosphere; this create showers and the decays of those secondary particles, such as muons, generate neutrinos. It is important to mention that this flux come from all directions in space, and is mainly used in the IceCube Collaboration for callibration (see the The IceCube experiment chapter for mored details). In addition, it is important to mention that atmospheric neutrinos play a crucial role in the study of flavor oscillations, since muon neutrino oscillation is the simplest explanation to many features observed in atmospheric neutrino data [72]

7.6 Neutrinos and Cosmic Rays

In this section we present some topics that help to stablish the connection between neutrinos and other observables. The actual use of this result and how those different pieces of the puzzle look when put together will be presented in Part V.

7.6.1 The Waxman - Baccal bound

In their work [41], Eli Waxman and John Bahcall showed that a model independent upper bound to the high energy neutrinos based on cosmic ray observations, which applies in particular for Active Galactic Nuclei (AGN) and Gamma Ray Bursts (GRB's). It is an upper bound to neutrino fluxes from $p\gamma$ interactions for sources that are optically thin to those reactions .According to the authors, we have a model independent upper bound of $E^2\Phi_\nu < 2 \times 10^{-8}\text{GeV/cm}^2\text{ssr}$ to the intensity of the high energy neutrinos in the type of sources we mentioned. Probably the most striking feature of their results is its ridigity, in the sense that the bound is immune to the consideration of evolutionary effects of the sources or magnetic field scenarios.

7.6.2 γ-rays and Fermi - LAT

As it was already seen in this chapter, there is an intrinsic connection between gamma rays and high energy neutrinos produced by pion decays. Therefore, it is of great importance to us to better understand gamma ray production and how they are detected. First, note that gamma rays can be produced in essentially two ways: hadronic origin (the decays and reactions we already mentioned) and leptonic origin, which is by pure leptonic phenomena such as inverse Compton scattering. We will begin by exploring the hadronic origin of gamma rays, then look at the leptonic processess and comment on detection and measurement.

Decay of π^0 occur at sites where such particles are produced, where the astrophysical sources provide acceleration mechanisms to produce not only proton collisions but also baryonic cosmic rays. Since such cosmic rays are observed (in experiments like the Pierre Auger Observatory), we can assume that some gamma ray sources operate through hadronic means (for a more detailed analysis, see [67].

In addition, as cosmic rays propagate, they can interact with the CMB background photon through inverse Compton scattering. This is not just an energy loss mechanism for the cosmic rays, but it also leads to production of secondary particles, such as gamma rays and pions, which ultimately lead to neutrino production in a process called GZK effect [42]. The secondary particles produced decay to produce neutrinos, known as Berezinsky-Zatspein neutrinos (the BZ flux). The accumulation of such neutrinos over cosmological time is known as the BZ or often the cosmogenic neutrino flux. Thus, it is natural to ask if high energy cosmic rays (around 10^{18} eV) can produce neutrinos with a spectrum that agrees with obeservational data [44], but this is not the case [45].

When it comes to detection, this dissertation is mostly based on the data from the Fermi Large Area Telescope. It is a high energy gamma ray telescope that detects photons with energies ranging from a few MeV to about 300 GeV. It is the main scientific instrument of the Fermi Gamma-ray Telescope. Its measurements will be of great importance to impose bounds and constrain our models.

8 The IceCube experiment

8.1 An overview of the experiment

IceCube is a neutrino detector located at the South Pole, composed of an array of photosensors buried in the ice of Antartica. As the high energy neutrinos come to Earth, they interact with the water molecules of the ice as we discussed in the previous sections, and the resulting Cherenkov light emitted by secondary charged particles is observed.

The basic detection unit of IceCube is the DOM, the Digital Optical Module.This technology was developed when the AMANDA collaboration was going on, which had as one of its goals to test the concept behind this kind of experiment. They are glass spheres which contain a photomultiplier and auxiliary electronics. The spheres are connected to each other in strings, and deployed in vertical holes that are drilled in the ice. Each string has 60 DOM's, and each sphere is 17 meters apart in the string. The DeepCore array is made up of a more densely spaced array of strings that are below 2100 m where the ice is the cleanest and also contains better photomultipliers. In addition to that, IceCube has a detection system at the surface, called IceTop, which is made of frozen water tanks for the purpose of detecting cosmic rays and showers originated by them. They also work detecting Cherenkov light.

8.1.1 Next generations and upgrades

Due to the sucess of IceCube, there are already plans about upgrades on the experiment [269]. The next generation of the IceCube detector would be an extended array of detection modules covering an area of $10km^3$. It would allow unprecedent sensitivity and angular resolution on the PeV scale and above. The increased event rate would greatly

increase the potential for point source detection and new discoveries.

Recently, IceCube and ANTARES, another neutrino observatory performed a follow-up search of neutrinos [39] for the event detected by the LIGO collaboration recently, the gravitational waves emitted by the merging of two black holes[38]. Upgraded detectors and refined techniques would definetely lead to a new era of multi-messenger searching.

8.2 Cherenkov radiation

Cherenkov light is the electromagnetic analogue of a sonic boom, which occurs when an object travels faster than the speed of sound in a certain medium (also known as "breaking the sound barrier"). In our situation, when a charged particle travels faster than the speed of light in a certain medium, radiation is emmited, with the wavefront of the emmited light having the format of a cone.

The cone opening angle θ is given by

$$cos\theta = \frac{1}{n\beta} < 1 \Rightarrow \beta = \frac{v}{c} > \frac{1}{n}, \tag{583}$$

where n is the refraction index of the medium. For ice, $n \approx 1.33$. There is a lower limit for the momentum of the particle; it it moves slower than it, the radiation is not emmited. This limit is dictated by the constraint of the equation above; on the lab frame, the magnitude of the 3-momentum of the particle is

$$p = \gamma mc = mc\frac{1}{\sqrt{1-\beta^2}} = mc\frac{1}{\sqrt{1-(1/n)^2}}. \tag{584}$$

The spectrum of the Cherenkov radiation is given by the Frank-Tamn formula [37]. Nuclear reactors, which exhibit a blue glow, are examples of systems that emmit Cherenkov radiation.

8.3 Cross sections for interactions at the detector

In this section we will present and discuss the cross sections for the neutrino interactions that occur at the IceCube detector for different energy ranges. Due to number

of different reactions and subtleties in the analysis, we will not provide a very detailed explanation or calculation for each one of them, but references will be given for the interested reader. Our focus will be on the energy dependence of the cross sections, and what reactions tend to occur at certain energy ranges.

Elastic and quasielastic scattering[7] are the relevant processess for the energy range of solar neutrinos ($\lesssim 100$ MeV). The reaction

$$\bar{\nu}_e + p \to e^+ + n, \tag{585}$$

which is called the inverse beta decay is particularly famous. This is how Reines and Cowan detected neutrinos for the first time [36], it was the elementary reaction for KamLAND and will remain the key process for upcoming oscillation neutrino experiments. Other reactions are also possible (and in fact were used in studies of the solar neutrinos [8]), even though the inverse beta decay has the dominating cross section.

When we increase the energy leaving the MeV and reach the GeV scale, we still have quasielastic reactions of the form [8]

$$\nu_l + n \to l^- + p, \tag{586}$$

$$\bar{\nu}_l + p \to l^+ + n, \tag{587}$$

but some resonances also become acessible,such as the $\Delta(1232)$ resonance we already discussed, and charged and neutral pions can be produced,

$$\nu_l + N \to \pi + N'. \tag{588}$$

In this energy range, the total cross section satisfy [52].

$$\sigma(\nu N) = 0.677 \times 10^{-38} \frac{\mathrm{cm}^2 \mathrm{E}_\nu}{\mathrm{GeV}}, \tag{589}$$

[7]Quasielastic scattering is the name of a particular case of inelastic scattering where energy transfers are small compared to the incident energy of the scattered particles

$$\sigma(\bar{\nu}N) = 0.334 \times 10^{-38} \frac{\mathrm{cm}^2 \mathrm{E}_\nu}{\mathrm{GeV}}. \tag{590}$$

Finally, when we go beyond 100 GeV we enter at the high energy scale, the one of greatest interest for IceCube. At high energies the neutrino scatters from the quarks themselves, and this breaks the nucleon creating a hadronic shower. This is called the deep inelastic scattering regime,

$$\nu_l + N \to l + N', \tag{591}$$

and the CC deep inelastic cross section for an isoscalar target is given by

$$\frac{d\sigma}{dx\ dy} = \frac{2G_F^2 M E_\nu}{\pi} \left(\frac{1}{1 + \frac{G^2}{m_W^2}} \right)^2 [xq(x, Q^2) + x\bar{q}(x, Q^2)(1 - y^2)], \tag{592}$$

where

$$Q^2 \approx 4E_\nu E_l sin^2 \frac{\theta_l}{2}, \tag{593}$$

$$x = \frac{Q^2}{2M_N(E_\nu - E_l)},\ \ \frac{Q^2}{(s - M_N^2)x},\ \ s \approx 4E_\nu E_l sin^2 \frac{\theta_l}{2}, \tag{594}$$

and $q(x, Q^2)$, $\bar{q}(x, Q^2)$ are quark distribution functions [35]. For the NC cross section,

$$\frac{d\sigma}{dx\ dy} = \frac{2G_F^2 M E_\nu}{\pi} \left(\frac{1}{1 + \frac{G^2}{m_Z^2}} \right)^2 [xq'(x, Q^2) + x\bar{q}'(x, Q^2)(1 - y^2)] \tag{595}$$

note that the distributions must be changed [34] [33].

8.4 Neutrino tracks

The most common neutrinos that IceCube detects are atmospheric neutrinos, and they came from all directions. As cosmic rays come towards Earth and interact with the

atmosphere, showers occur and muons and neutrinos are produced, travelling across the atmosphere and Earth itself being detected at IceCube from all angles. They are both the background and the source for calibration of the equipment. The energy spectrum goes as E^{-3}, becoming steeper, $E^{-3.7}$ for $E >> 1\text{TeV}$; thus, it can be used for calibration up to TeV and beyond.

The astrophysical neutrinos are the ones of interest to us. Their energy, close and on the PeV scale is fortunately well above the atmospheric background, and they have very characeristic event signatures on the detector. However, as the energy of the neutrinos gets in this range, the Earth becomes more opaque to them and it becomes necessary to use events from neutrinos that come from horizontal or downgoing directions. Due to the planet's opacity, there is a supression on upgoing neutrinos.

Neutrinos of different flavor possess different event signatures of the detector, and we will discuss them now. Recall that the DIS produces a lepton related to the incident neutrino. The propagation of this lepton (and other compoents of the shower) produce Cherenkov light as well as the products of the decay of the lepton in question, in the case it is a muon or a tau lepton. There are many different possible topologies and subtleties concerning them [31], [30], [29], so we will focus on more general properties of these events and signatures.

We begin by looking at the electron neutrino, ν_e. When a high energy electron neutrino comes and interacts with the ice through DIS, an electron is created. As this electron propagates, it will emmit a high energy photon through bremsstrahlung, and the photon can become an electron-positron pair, which in turn will also propagate and emmits new photons and so on. The result of this is a cascade of high energy photons, electrons and positrons. Note that the recoilling nuclei after the DIS interaction will produce a jet of particles, which will also turn into a shower. However, this kind of cascade does not produce as much Cherenkov light as the electromagnetic cascade described above, mainly because of the nature of the particles in the jet. They are heavier than electrons, with a fraction of the energy in the form of binding, and the possible presence of neutral particles like neutrons which do not emmit Cherenkov light. This kind of event

has a good energy measurement but poor angular resolution (10^o to 15^o).

The next kind of event is the one related to muon neutrinos. The main difference between this kind of event and the previous one is that once a muon is produced from the first interaction it travels for a certain length losing energy in form of radiation. The result of this is a track with good angular resolution (about 1^o) but bad energy measurement.

Finally, we talk about tau neutrinos.This kind of neutrino can be detected in several ways [30]. The main idea is that a tau neutrino interacts, and a tau lepton is produced. Due to its huge mass (1776.82 MeV), it does not lose too much energy in the form of radiation. The tau then decays, and the products of this decay create a cascade. Depending on where the initial inetraction (the first DIS scattering) happens, one can see a "lollipop" or a "double bang" shape on the detector. this happens for energies above a few hundred TeV, when it becomes possibles to distiguish the two cascades.

Differently from muon and electron neutrinos, tau neutrinos can not be produced on the atmosphere. Therefore, their detection is a smoking gun for astrophysical origin, but the direct detection of tau neutrinoshasn't occured yet, but it doesn't seem to contradict the hypothesis of democratic flavor ratio at the Earth [28].

Before we end this section, it is important to make a brief comment on antineutrinos. From the way that IceCube makes the detection (based on the light emmited from secondary particles), it can't essentially tell the difference between neutrinos and antineutrinos, and that's the reason we have been referring to only "neutrinos" in this section. The main signature for an antineutrino detection would be a Glashow resonance.

8.5 Event maps

The IceCube has observed a diffuse flux of neutrinos with energies on the order of TeV and above with 5.7σ significance, and an atmospheric origin for these high energy events has practically been discarded, with three events possessing energy above 1 PeV (they were called Bert, Ernie and Big Bird, and their energies are 1.0, 1.1 and 2.2 PeV respectively). Topics such as energy spectrum, correlation with sources and others will be extensively studied in the last chapters.

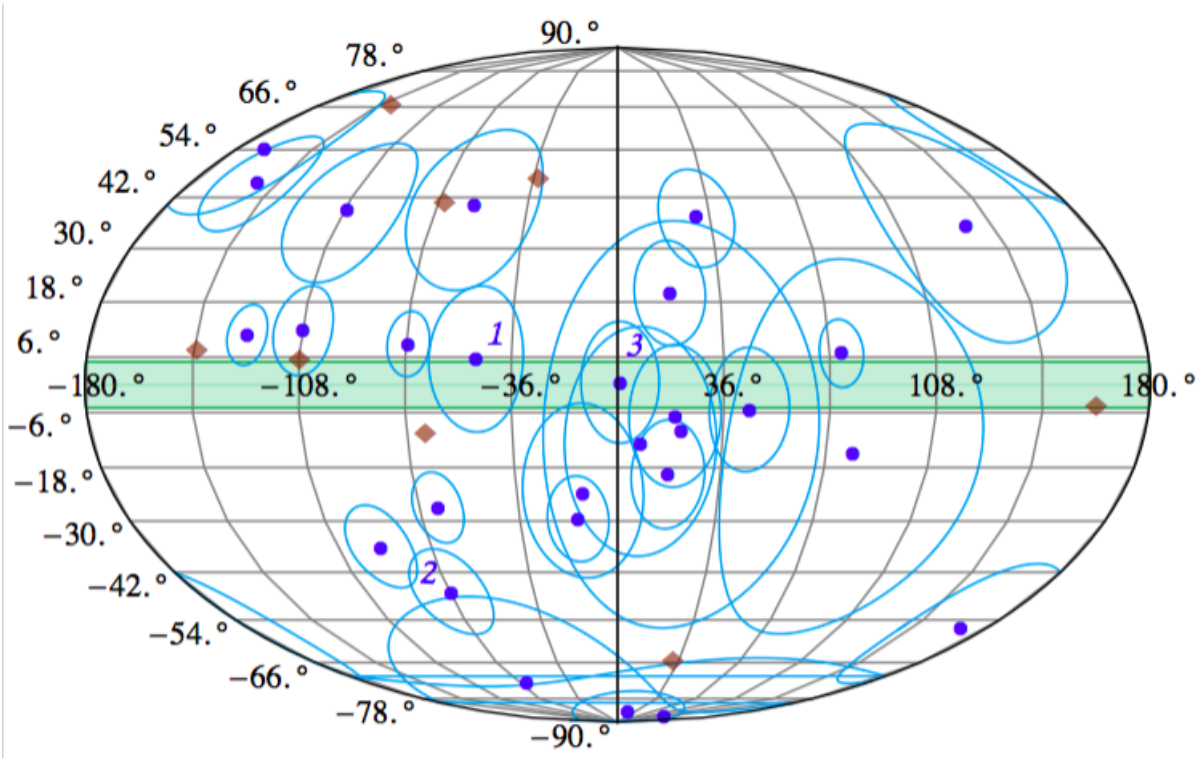

Figure 12: IceCube event locations [27]. The contains 27 shower events (circles) and 8 track events (diamonds) reported by the IceCube Collaboration. The three events with highest energy are labelled as 1, 2 and 3. The surrounding circles denote the angular resolution of the events, while the shaded band delimits the Galactic plane.

9 Looking for high energy neutrino sources

Several explanations have been proposed to explain the origin of IceCube's events [285]. Interestingly, a priori predictions for the diffuse ν flux from FRI radiogalaxies [286] and starbursts [287] provide a suitable α and normalization for the ν flux while simultaneously retaining consistency with a cutoff at $E_\nu \sim 3$ PeV [288]. Other potential sources that can partially accommodate IceCube data include gamma-ray bursts [289], clusters of galaxies [290] (see however [291]), and active galactic nuclei [292]. However, the identification of extragalactic neutrino point-sources from a quasi-diffuse flux is challenging due to the (large) atmospheric neutrino background [293].

9.1 Astrophysical sources: Galactic microquasars

On the basis of existing data a significant contribution from Galactic sources cannot yet be excluded [294, 295]. Searches for multiple correlations with the Galactic plane have been recently reported by the IceCube Collaboration [276]. When letting the width of the plane float freely, the best fit corresponds to $\pm 7.5^\circ$ with a post-trial chance probability of 2.8%, while a fixed width of $\pm 2.5^\circ$ yields a p-value of 24%. In particular, some of the events seem to cluster near the Galactic center [296], which has been whimsically described as a neutrino lighthouse [297]. Indeed, a particularly compelling source of some of these neutrinos could be LS 5039 [276]. Figure **??** contains a display of the shower and track events reported by the IceCube Collaboration [276]. Using these data, the Collaboration conducted a point source search using an un-binned maximum likelihood method described in [298]. For both the clustering and point source search, the number of estimated signal events, x_s, is left as a free parameter and the maximum of the likelihood is found at each location. For the point source search, the most significant source is the

binary system LS 5039, with a value of $x_s = 4.9$, and a corresponding p-value of 0.002. Of course there are many sources in the sky; whether this one turns out to be a good candidate, time will tell.

In summary, though the clustering is not statistically significant one cannot rule out a Galactic origin for some of these events. Motivated by this fact we perform a generalized calculation of the flux expected from various source distributions, taking account of the location of the Earth in the Galaxy. In particular, we reduce the problem to two specific parameters, the distance to the nearest source and the overall population density. LS 5039 has been discussed in the literature as potential high energy neutrino emitter [299]. We consider this source as specific example and assume it typifies the population of Galactic microquasars (μQSOs).[8] We generalized the argument such that it can be applied to various source populations. First we bracket the realm of plausibility and consider a uniform distribution and an exponential distribution peaked at the Galactic center. For illustrative purposes, we consider several conceivable different distances to the nearest source. After that we turn our attention to the interesting possibility of μQSOs for which the overall distribution of surface density in the Galaxy has a peak at galactocentric radii $5 - 8$ kpc [302, 303].

The layout of this discussion is as follows. First, we revisit the model presented in [299] in order to better estimate the expected neutrino flux, especially in the PeV region, and then we compare the properties of LS 5039 with other Galactic microquasars, showing that LS 5039 provides a reasonable lower bound on the power of this type of source. In The next step is to estimate the contribution of Galactic sources to the overall diffuse neutrino flux on the assumption that LS 5039 typifies the population. By comparing this estimate with IceCube data we find the minimum neutrino production efficiency required to dominate the spectrum. Finally, we employ constraints from γ-ray observations to bolster our hypothesis. We also address the relevance of our previous finding [295] that a spectral index of 2.3 is consistent with the most recent IceCube spectral shape as well

[8] μQSOs are a sub-class of X-ray binary systems that produce collimated outflows observed as non-thermal radio structures [300]. This particular morphology probably originates in relativistic jets launched from the inner parts of accretion disks around stellar mass black holes or neutron stars [301].

as current bounds on cosmic ray anisotropy.

9.1.1 IceCube neutrinos as the smoking ice of LS 5039 engine

LS 5039 is a high-mass X-ray binary (HMXB) system that displays non-thermal persistent and variable emission from radio frequencies to high-energy (HE), $E_\gamma > 100$ MeV, and very-high-energy (VHE), $E_\gamma > 100$ GeV, gamma rays. The system contains a bright ON6.5 V((f)) star [304, 305] and a compact object of unknown nature. This degenerate companion has a mass between 1.4 and 5 $M_\odot$ [306]. The orbit of the system has a period of 3.9 days and an eccentricity around 0.35 [306, 307, 308]. The distance to the source has recently been updated to 2.9 ± 0.8 kpc [309]. At the apastron the orbital separation of the binary system is 2.9×10^{12} cm and becomes 1.4×10^{12} cm at periastron [306]. Variability consistent with the orbital period in the energy range 100 MeV $\lesssim E_\gamma \lesssim$ 300 GeV was detected by Fermi [310]. The system is also a TeV emitter, with persistent, variable, and periodic emission, as detected by H.E.S.S. [311, 312]. The overall luminosity in the frequency band keV $\lesssim E_\gamma \lesssim$ GeV is $L \sim 10^{35}$ erg s^{-1} [313].

Whether the HE/VHE gamma rays are a of hadronic or leptonic origin is a key issue related to the origin of Galactic cosmic rays. In all gamma-ray binaries, the nature of the compact object is fundamental for understanding the physical processes involved in the particle acceleration that is responsible for the multi-wavelength emission. If the compact object is a black hole, the accelerated particles would be powered by accretion, and produced in the jets of a μQSO. On the other hand, if the compact object is a young non-accreting pulsar, the particle acceleration would be produced in the shock between the relativistic wind of the pulsar and the stellar wind of the massive companion star. The detection of elongated asymmetric emission in high-resolution radio images was interpreted as mildly relativistic ejections from a μQSO jet and prompted its identification with an EGRET gamma-ray source [313, 314]. However, recent Very Long Baseline Array observations [315] show morphological changes on short timescales that might be consistent with a pulsar binary scenario [316, 317, 318]. On the other hand, no short-period pulsations were observed either in radio [319] or X-rays [320] definitively demonstrating

the compact object to be a pulsar. New IceCube data will clarify this situation, as the only plausible high energy neutrino emission mechanism requires a compact object powering jets.

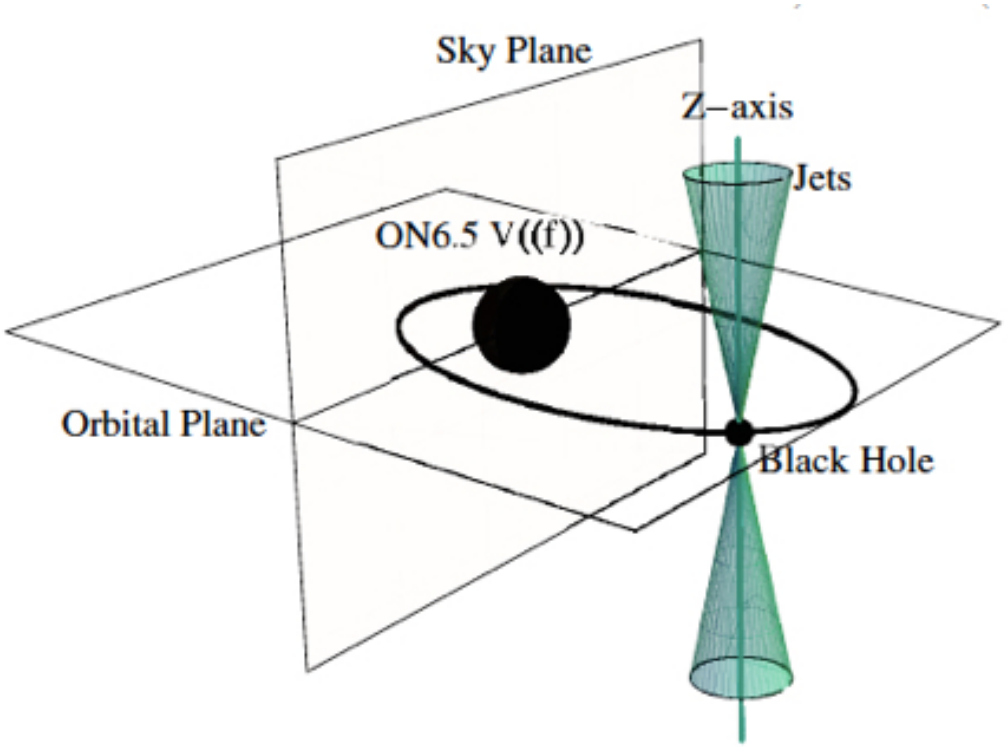

Figure 13: A sketch of the binary system LS 5039.

Simultaneous production of γ's and ν's generally requires two components: *(i)* an effective proton accelerator, up to $E \approx 16\, E_\nu^{\rm max}$ and beyond; *(ii)* an effective target (converter). The maximum observed neutrino energies then require proton acceleration up to at least $E \gtrsim 20$ PeV. The most likely site for particle acceleration in LS 5039 is the jet, which with a speed $v = 0.2c$ and a half-opening angle $\theta \lesssim 6^\circ$ extends out to 300 milliarcsecond (mas), that is about 10^{16} cm [314]. Within the inner parts of the jet, with a radius $R_{\rm jet} \sim 10^9$ cm, a magnetic field $B \gtrsim 10^5$ G could be sufficient to boost protons up to very high energies. The maximum proton energy is determined by the Hillas condition $r_L \leq R_{\rm jet}$, which gives

$$E_{\rm max} \lesssim 30 \left(\frac{R_{\rm jet}}{10^9\ {\rm cm}}\right) \left(\frac{B}{10^5\ {\rm G}}\right)\ {\rm PeV}\,, \tag{596}$$

where r_L is the Larmor radius. A value compatible with this maximum energy has been obtained in an independent calculation [321]. The accelerated protons can interact efficiently with the ambient cold plasma throughout the entire jet. In what follows we assume that the base of the jet is located close to the inner parts of the accretion disk, that is, the jet axis z is taken normal to the orbital plane, as shown in Fig. **??**. Here, $z_0 \sim 30 R_{\rm S}$, where

$$R_{\rm S} \simeq 3 \times 10^5 \left(\frac{M_{\rm BH}}{M_\odot} \right) \ {\rm cm} \tag{597}$$

is the Schwarzschild radius. If the magnetic field drops as $B \propto z^{-1}$, the condition of the confinement of protons in the jet, $r_{\rm L} \leq R$ implies $E_{\rm max} \propto Bz$=constant, where $R = \theta z$ is the radius of the jet at a distance z. Thus, one may expect acceleration of protons to the same maximum energy $E_{\rm max}$ over the entire jet region. However, if there is a faster drop of B with z, the protons at some distance z_t from the compact object will start escaping the jet. If this happens within the binary system, i.e. $z_t \leq 10^{12}$cm, protons interacting with the dense wind of the optical star will result in additional γ-ray and neutrino production outside the jet.

If the jet power is dominated by the kinetic energy of bulk motion of cold plasma, the baryon density of the jet $n_{\rm jet}$ can be estimated from the jet power,

$$L_{\rm jet} = \frac{\pi}{2} R_{\rm jet}^2(z)\, n_{\rm jet}(z)\, m_p v^3 \,. \tag{598}$$

The efficiency of γ-ray production in the jet is

$$\rho_\gamma = \frac{L_\gamma}{L_p} = \sigma_{pp} f_\pi \int_{z_0}^{z_t} n_{\rm jet}(z) dz \leq 1 \,, \tag{599}$$

where L_γ is the luminosity of VHE γ-rays and L_p is the power of accelerated protons. Here, $\sigma_{pp} \approx 40$ mb is the cross-section of inelastic pp interactions, and $f_\pi \approx 0.15$ is the fraction of the energy of the parent proton transfered to a high energy γ-ray [322]. Given the recent estimate of the black hole mass in LS 5039 $M = 3.7^{+1.3}_{-1.0}\, M_\odot$ [306], we set $z_0 \simeq 3 \times 10^7$ cm. For the profile of the number density, we adopt a power law form

$n_{\rm jet} = n_0(z_0/z)^{-s}$, where $s = 0$ for a cylindrical geometry, $s = 2$ for a conical jet, and $s = 1$ for the intermediate case. Expressing the acceleration power of protons in terms of the total jet power, $L_p = \kappa L_{\rm jet}$, one finds the following requirement for the jet power,

$$L_{\rm jet} \approx 2 \times 10^{37} \frac{L_{\gamma,34}^{1/2}(v/0.2c)^{3/2}}{\sqrt{\mathcal{C}(s)\kappa/0.1}} \ {\rm erg\ s^{-1}}\ , \tag{600}$$

where $L_{\gamma,34} = L_\gamma/10^{34}$ erg s^{-1} and κ is the acceleration efficiency. The parameter $\mathcal{C}(s)$ characterizes the geometry/density profile of the jet: for $s = 0,\ 1,\ 2$, we find $\mathcal{C}(s) = z_t/z_0$, $\ln(z_t/z_0)$, and 1, respectively. The cylindrical geometry provides the highest efficiency of γ-ray production. However, since $L_\gamma \lesssim 1/30 L_{\rm jet}$ (assuming $\approx 10\%$ efficiency of proton acceleration, and taking into account that the fraction of energy of protons converted to γ-rays cannot exceed 30%) the γ-ray production cannot be extended beyond $z_t \sim 10^4 z_0 \sim 3 \times 10^{11}$cm. The conical geometry corresponds to the minimum efficiency of γ-ray production, and thus the largest kinetic power of the jet. In this case the bulk of γ-rays are produced not far from the base. For $s = 1$, γ-rays are produced in equal amounts per decade of length of the jet, until the jet terminates.

If γ-rays are indeed produced in *pp* interactions, one would expect production of high energy neutrinos at a rate close to the γ-ray production rate. However, since γ-rays are subject to energy-dependent absorption, both the energy spectrum and the absolute flux of neutrinos,

$$\phi_\nu(E_\nu) \simeq 2\ \phi_\gamma(E_\gamma)\ \exp[\tau(E_\gamma)], \tag{601}$$

could be quite different from that of the detected γ-rays, where $E_\nu \simeq E_\gamma/2$. The optical depth $\tau(E)$ depends significantly on the location of the γ-ray production region, and therefore varies with time if this region occupies a small volume of the binary system. This may lead to time modulation of the energy spectrum and the absolute flux of TeV radiation with the orbital period [323]. Moreover, the $\gamma\gamma$ interactions generally cannot be reduced to a simple effect of absorption. In fact, these interactions initiate high energy electron-photon cascades, driven by inverse Compton scattering and $\gamma\gamma$ pair production.

The cascades significantly increase the transparency of the source. The spectra of γ-rays formed during the cascade development significantly differ from the spectrum of γ-rays that suffer only absorption.

To model the electromagnetic cascade developed in the plasma we adopt the method described in [324]. In our calculations we include the three dominant processes driving the cooling of the electromagnetic cascade: photon-photon pair production, inverse Compton scattering, and synchrotron radiation from electrons. Because of the orbital motion, both the absolute density and the angular distribution of the thermal radiation of the star relative to the position of the compact object vary with time. We take into account the effect induced by the anisotropic (time-dependent) distribution of the target photons on the Compton scattering and pair-production processes [325]. We normalize the cascade spectrum of photons to the flux reported by the H.E.S.S. Collaboration in the TeV energy range [311, 312]. Interestingly, if pion production is mostly dominated by collisions close to the base of the jet (i.e. $z \lesssim 10^8$ cm) then the resulting flux of γ-rays can marginally accommodate observations in the GeV-range [310, 326]. However, if pion production takes place well above the base of the jet ($z = 10^{13}$ cm) the flux of GeV-photons becomes about an order of magnitude smaller. These two extreme situations, which are shown in Fig. 25, provide an upper and a lower bound on the resulting neutrino flux

$$\phi_\nu(E_\nu) = \zeta \;\; E_\nu^{-2} \; \mathrm{GeV}^{-1} \; \mathrm{cm}^{-2} \; \mathrm{s}^{-1} \, , \tag{602}$$

where $1.8 \times 10^{-9} < \zeta < 1.6 \times 10^{-8}$. The lower value of ζ is in good agreement with the results of Ref. [328].[9] It is notable that while our results are ultimately derived from demanding consistency between neutrino and photon data, the results in Ref. [328] are derived from assumption on source parameters. For a source distance $d \simeq 3$ kpc, the flux range given in (602) corresponds to an integrated luminosity per decade of energy,

[9]The two analyses assume the same fiducial value for κ. Good agreement is achieved by taking the fiducial value for the fraction of the jet kinetic energy which is converted to internal energy of electrons and magnetic fields.

$$L_\nu^{LS\,5039} = 4\pi d^2 \int_{E_1}^{E_2} E_\nu\, \phi(E_\nu)\, dE_\nu$$
$$= 4\pi \left(\frac{d}{\rm cm}\right)^2 \zeta\, \ln 10\ {\rm GeV\ s^{-1}}, \qquad (603)$$

in the range $7.0 \times 10^{33}\ {\rm erg\,s^{-1}} \lesssim L_\nu^{LS\,5039} \lesssim 6.4 \times 10^{34}\ {\rm erg\,s^{-1}}$.

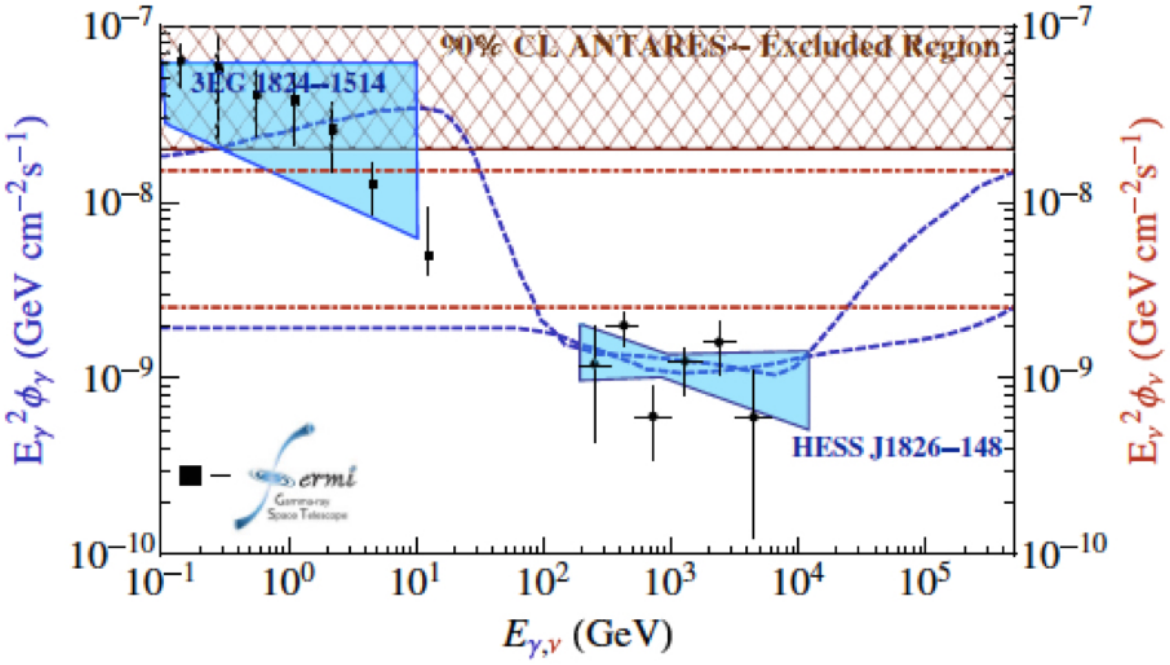

Figure 14: The dashed curves represent the time averaged γ-ray spectra of LS 5039 after cascading in the anisotropic radiation field of the normal companion star. The curves are normalized to reproduce the observed γ-ray flux by H.E.S.S. in the TeV range [311, 312]. If pions are produced near the base of the jet, the γ's produced through π^0 decay can trigger cascades in the plasma, yielding a photon flux which can marginally accommodate EGRET [326] and Fermi [310] data. The dot-dashed horizontal lines indicate the accompanying neutrino flux. All curves are averaged over the orbital period taking into account data on the geometry of the binary system [306]. The cross-hatched area indicates the 90% upper limit on the flux from LS 5039 reported by the ANTARES Collaboration [327].

Herein we have assumed the usual Fermi injection spectral index of $\alpha = 2$. The spectral index of γ-radiation measured by H.E.S.S. varies depending upon the orbital configuration, reaching a maximum value of 2.53 [311, 312]. In the next two sections we will assume the "traditional" spectral index. In Sec. **??** we comment on the effect of a steeper spectrum.

Determining whether this analysis can be straightforwardly generalized to all sources in the Galaxy depends on whether neutrino emission from LS 5039 can typify the population of μQSOs. It is this that we now turn to study.

9.1.2 Generalities of the microquasar population in the Galaxy

The most recent catalogues show 114 HMXBs [329] and about 130 low-mass X-ray binaries (LMXBs) [330]. The INTEGRAL/IBIS nine-year Galactic plane survey, limited to $|b| < 17^\circ$, contains 82 high-mass and 108 low-mass sources [331]. The sensitivity of this survey is about 10^{-11} erg s^{-1} cm^{-2} in the 17-60 keV energy band, which ensures detection of sources with luminosities $\lesssim 10^{35}$ erg s^{-1} within half of the Galaxy ($\lesssim 9$ kpc from the Sun) and $\lesssim 5 \times 10^{35}$ erg s^{-1} over the entire Galaxy ($\lesssim 20$ kpc from the Sun); see Fig. **??** . The number of X-ray binaries in the Galaxy brighter than 2×10^{34} erg s^{-1} is thought to comprise 325 HMXBs and 380 LMXBs [303]. These estimates may be uncertain by a factor of approximately two due to our limited knowledge of the source spatial distribution, rendering them consistent with the observations from the surveys reported above. Taken together this suggests an upper limit of μQSOs in the Galaxy of $\mathcal{O}(100)$ [332].

About twenty μQSOs have been discovered so far. An illustrative sample can be found in Table 3. Note that the estimated jet luminosity of LS 5039 is relatively low, implying that we can in principle use this source to estimate a lower bound on the neutrino production efficiency required to be consistent with observation. Note also that the only source with $L_{\rm jet}$ less than that for LS 5039 has been observed in bursting and quiescent states. In Table 3 we quote the quiescent value which is about a factor of two lower than for the case of bursting state [337].

A comparison among all IceCube events and the Galactic μQSO population is shown in Fig. **??**. Not surprisingly given the size of the localization error, the two PeV neutrino events with arrival direction consistent with the Galactic plane can be associated with μQSOs within 1σ uncertainties.

It appears that the impulse from supernovae explosions can eject a system from its

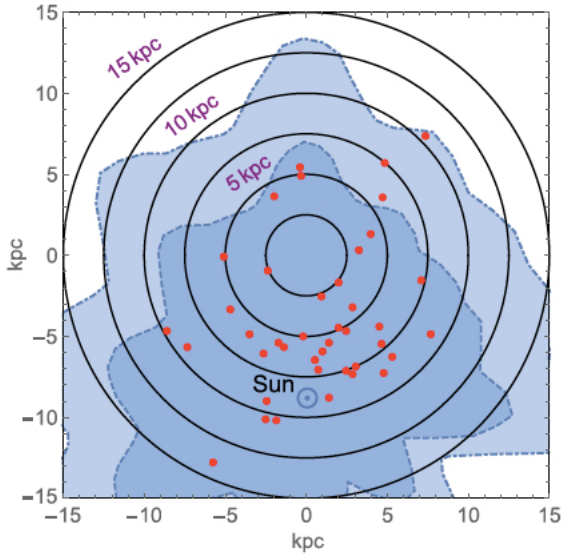

Figure 15: Illustrative view of the surface density of HMXBs in the Galaxy. The red points indicate positions of HMXBs. The dot-dashed and dashed curves show the regions of the Galaxy, within which the INTEGRAL Galactic survey detects all sources with luminosities $> 10^{35.5}$ ergs^{-1} and $> 10^{35}$ erg s^{-1}.

original position in the disk into the halo. In fact a number of μQSOs have been observed with very high velocities. For instance, XTE J1118-480 moves at 200 km s^{-1} in an eccentric orbit around the Galactic Center [338]. Additionally, the position and velocity of Scorpius X-1 suggest it is a halo object [339]. Such speedy objects are called runaway μQSOs. LS 5039 qualifies as a such runaway μQSO with a velocity of 150 km s^{-1}. Its computed trajectory suggest it could reach a galactic latitude of $\sim 12°$. The IceCube analysis search for multiple correlation in the Galactic plane favors latitudes less than about $\pm 7.5°$, which is not inconsistent with the latitude reached by runaway μQSOs.

The next to highest energy neutrino event is not in the Galactic plane. It is also interesting to note that the position of this PeV event is within 10 degrees in the hottest spot of IceCube search [340] for PeV γ-ray sources [341]. If it turns out that PeV photons and neutrinos are generated at the same sites, then observation of coincidences implies these sites must be within the Galaxy, given the short mean free path of PeV photons, which is less than 10 kpc. Conceivably, this could be associated with an as-yet undiscovered μQSO.

At about 2 kpc from Earth, there is another HMXB system with similar characteris-

Table 3: Properties of μQSOs in the Galaxy.

Classification	Name	position (J2000.0)	distance [kpc]	$L_{\rm jet}$ [erg/s]	Reference
HMXB	LS I +61 303	$(02^{\rm h}40^{\rm m}31.70^{\rm s}, +61°13'45.6'')$	2	5.69×10^{36}	[328]
HMXB	CI Cam	$(04^{\rm h}19^{\rm m}42.20^{\rm s}, +55°59'58.0'')$	1	5.66×10^{37}	[328]
LMXB	GRO J0422+32	$(04^{\rm h}21^{\rm m}42.70^{\rm s}, +32°54'27.0'')$	3	4.35×10^{37}	[328]
LMXB	XTE J1118+480	$(11^{\rm h}18^{\rm m}10.79^{\rm s}, +48°02'12.3'')$	1.9	3.49×10^{37}	[328]
LMXB	GS 1354-64	$(13^{\rm h}58^{\rm m}09.70^{\rm s}, -64°44'05.0'')$	10	3.62×10^{37}	[328]
LMXB	Circinus X-1	$(15^{\rm h}20^{\rm m}40.84^{\rm s}, -57°10'00.5'')$	10	7.61×10^{38}	[328]
LMXB	XTE J1550-564	$(15^{\rm h}50^{\rm m}58.67^{\rm s}, -56°28'35.3'')$	2.5	2.01×10^{38}	[328]
LMXB	Scorpius X-1	$(16^{\rm h}19^{\rm m}55.09^{\rm s}, -15°38'24.9'')$	2.8	1.04×10^{38}	[328]
LMXB	GRO J1655-40	$(16^{\rm h}54^{\rm m}00.16^{\rm s}, -39°50'44.7'')$	3.1	1.6×10^{40}	[328]
LMXB	GX 339-4	$(17^{\rm h}02^{\rm m}49.40^{\rm s}, -48°47'23.3'')$	8	3.86×10^{38}	[328, 333]
LMXB	1E 1740.7-2942	$(17^{\rm h}43^{\rm m}54.82^{\rm s}, -29°44'42.8'')$	8.5	$10^{36} - 10^{37}$	[334]
LMXB	XTE J1748-288	$(17^{\rm h}48^{\rm m}05.06^{\rm s}, -28°28'25.8'')$	8	1.84×10^{39}	[328]
LMXB	GRS 1758-258	$(18^{\rm h}01^{\rm m}12.40^{\rm s}, -25°44'36.1'')$	8.5	$10^{36} - 10^{37}$	[335]
HMXB	V4641 Sgr	$(18^{\rm h}19^{\rm m}21.63^{\rm s}, -25°24'25.9'')$	9.6	1.17×10^{40}	[328]
HMXB	LS 5039	$(18^{\rm h}26^{\rm m}15.06^{\rm s}, -14°50'54.3'')$	2.9	8.73×10^{36}	[328]
HMXB	SS 433	$(19^{\rm h}11^{\rm m}49.57^{\rm s}, +04°58'57.8'')$	4.8	1.00×10^{39}	[328]
LMXB	GRS 1915+105	$(19^{\rm h}15^{\rm m}11.55^{\rm s}, +10°56'44.8'')$	12.5	2.45×10^{40}	[328]
HMXB	Cygnus X-1	$(19^{\rm h}58^{\rm m}21.68^{\rm s}, +35°12'05.8'')$	2.1	$10^{36} - 10^{37}$	[336]
HMXB	Cygnus X-3	$(20^{\rm h}32^{\rm m}25.77^{\rm s}, +40°57'28.0'')$	10	1.17×10^{39}	[328]

tics to LS 5039. LS I +61 303 has been detected at all frequencies, including TeV and GeV energies [342]. Observations of persistent jet-like features in the radio domain at ~ 100 mas scales prompted a classification of the source as a μQSO [343], but subsequent observations at $\sim 1 - 10$ mas scales, covering a whole orbital period, revealed a rotating elongated feature that was interpreted as the interaction between a pulsar wind and the stellar wind [316]. More recently, evidence favoring LS I +61 303 as the source of a very short X-ray burst led to the analysis of a third alternative: a magnetar binary [344]. This binary system has also been suspected to be a high energy neutrino emitter [345]. The source has been periodically monitored by the AMANDA and IceCube collaborations [346]. The most recent analysis leads to a 90% CL upper limit on the neutrino flux at the level $E_\nu^2 \Phi_{90}(E_\nu) = 1.95 \times 10^{-9}$ GeV cm^{-2} s^{-1} [347]. This implies that if we were to consider LS 5039 as a standard neutrino source of the μQSO population then γ's and ν's should be produced well above the base of the jet, without γ-ray absorption. For such a case, the predicted neutrino flux is compatible with an independent analysis presented in [296], which assumes the neutrino cluster arrives from the direction of the Galactic center. Such a flux is also compatible with studies described in [285], which also postulate a Galactic center origin, but with steeper spectral indices. Finally, we stress that the predicted high energy neutrino flux that can typify the μQSO population is about an order of magnitude below the 90% upper limit reported by the ANTARES

Collaboration [327].

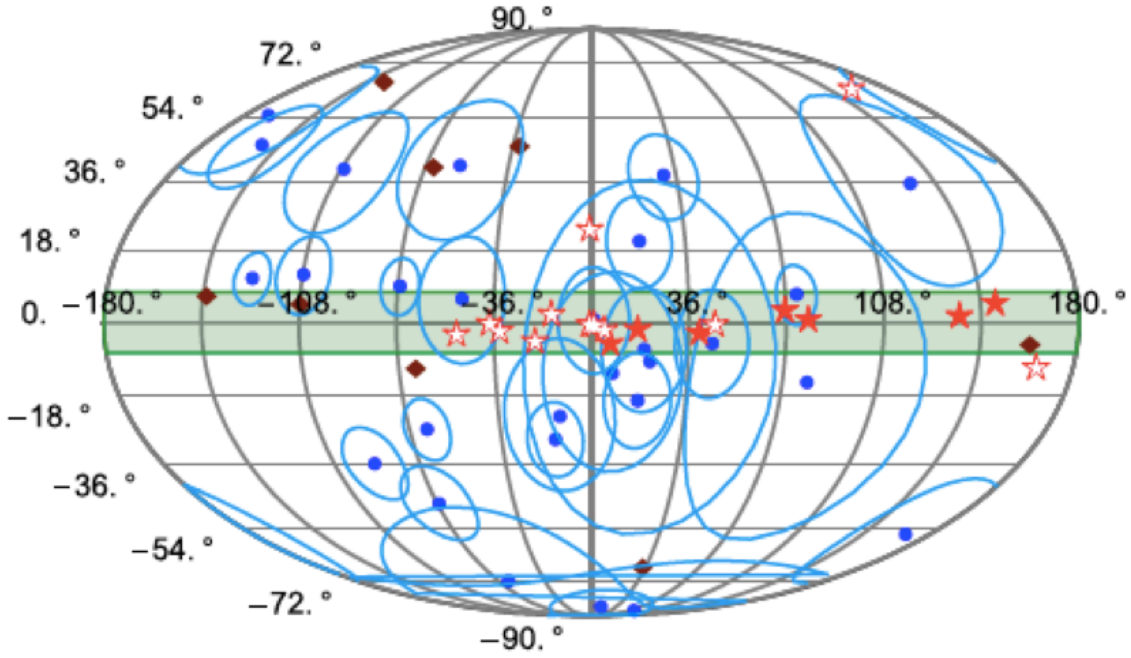

Figure 16: Comparison of IceCube event locations [276] with Galactic μQSOs in a Mollweide projection. The 27 shower events are indicated by circles and the 8 track events by diamonds. The solid stars indicate the 7 μQSOs classified as HMXB and the outlined stars the 12 μQSOs classified as LMXB. The shaded band delimits the Galactic plane.

In summary, if we assume the luminosity of LS 5039 truly typifies the power of a μQSO then we should adopt as fiducial $L_\nu^{LS\,5039} \approx 10^{33}$ erg s^{-1}, otherwise we will be inconsistent with the IceCube limit on LS I +61 303. However, it is important to stress that the value of $L_\nu^{LS\,5039}$ we will adopt to typify the population is very conservative for far away sources, as one can observe in Table 4. In closing, we note that though the IceCube bounds are currently the most stringent, ANTARES has the potential to discover exceptionally bright bursting sources in the Southern sky [348].

9.1.3 High energy Neutrinos from Galactic microquasars

Galactic μQSOs have long been suspected to be sources of high energy neutrinos [321]. In this section, we consider the overall contribution of these candidate sources to the diffuse neutrino flux, assuming LS 5039 is the nearest source and typifies the μQSO

Table 4: 90% C.L. upper limits on the squared energy weighted flux of $\nu_\mu + \nu_{\bar{\mu}}$ in units of 10^{-9} GeV cm^{-2} s^{-1}.

Name	$E_\nu^2 \Phi^{\text{IceCube}}_{90\%\text{C.L.}}$	$E_\nu^2 \Phi^{\text{ANTARES}}_{90\%\text{C.L.}}$	Reference
LS I 63 303	1.95	–	[347]
Circinus X-1	–	16.2	[327]
GX 339-4	–	15.0	[327]
LS 5039	–	19.6	[327]
SS 433	0.65	23.2	[347, 327]
Cygnus X-3	1.70	–	[347]
Cygnus X-1	2.33	–	[347]

population. We improve the procedure sketched elsewhere [285], in which the Earth was assumed to be at the edge of the Galactic disk. In our current approach we place the Earth in its actual position (about 8 kpc from the Galactic center) and perform the requisite integrations numerically. We further enhanced our previous analysis by considering several source distributions. Firstly, we assume the sources are uniformly distributed. Secondly, we assume the source density decreases exponentially with distance from the Galactic center. These extremes are likely to bound the true source distribution. Finally, we consider a more realistic distribution to describe the particular case of μQSOs.

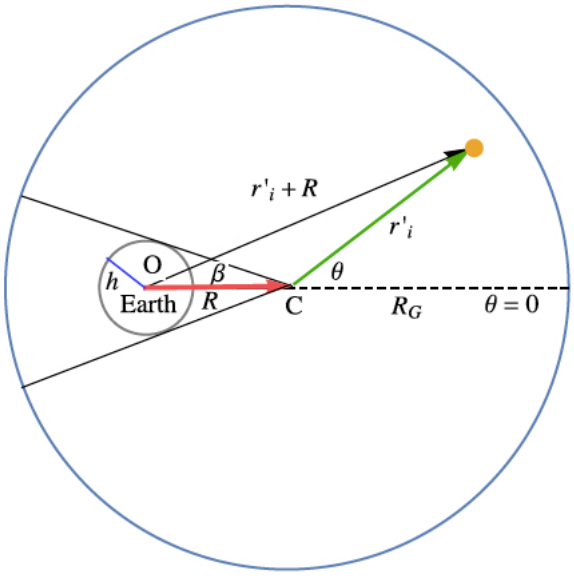

Figure 17: Sketch used to calculate the flux. Notice that we take account of the approximate location of the Earth in the Galactic disk. h is a void placed around the Earth to regularize the integration.

The ensuing discussion will be framed in the context of the thin disk approximation.

We model the Milky Way as a cylinder of radius $R_G = 15$ kpc and thickness $\delta = 1$ kpc. Consider the situation displayed in Fig. **??** in which the observer O is at the Earth, located at a distance $R = 8.3$ kpc from the center of the Galaxy C. Denote the vector from O to C by $\vec{R}$, from C to the source S_i by $\vec{r}_i'$ and from O to S_i by $\vec{r}_i$; then $\vec{r}_i = \vec{R} + \vec{r}_i'$ and so $r_i^2 = R^2 + r_i'^2 + 2Rr_i' \cos\theta$. The integrated energy weighted total neutrino flux from the *isotropic* Galactic source distribution with normal incidence at O is

$$\begin{aligned} 4\pi \int_{E_1}^{E_2} E_\nu \Phi(E_\nu) dE_\nu &= \frac{1}{4\pi} \sum_i \frac{L_{\nu,i}}{r_i^2} \\ &= \frac{1}{4\pi} \sum_i \frac{L_{\nu,i}}{R^2 + 2Rr' \cos\theta + r'^2}, \end{aligned} \tag{604}$$

where $L_{\nu,i}$ is the power output of source i and θ is the angle subtended by $\vec{r}_i'$ and $\vec{R}$. Assuming equal power for all sources, $L_{\nu,i} = L_\nu^{\text{LS 5039}}$, we convert the sum to an integral

$$\begin{aligned} 4\pi \int_{E_1}^{E_2} E_\nu \Phi(E_\nu) dE_\nu &= \frac{L_\nu^{\text{LS 5039}}}{4\pi} \\ &\times \iint \frac{\sigma(r')\, r' dr' d\theta}{R^2 + r'^2 + 2Rr' \cos\theta}, \end{aligned} \tag{605}$$

where $\sigma(r')$ is the source number density. Any infrared divergence in (605) is avoided by cutting off the integral within the void of radius h as shown in Fig. **??**. For the sector of the circle *(i)* containing the observer, the integral in (605) can be written as

$$\begin{aligned} \mathcal{I}_1 &= \int_{\pi+\phi}^{\pi-\phi} d\theta \int_0^{r_1} \frac{\sigma(r')\ r' dr'}{R^2 + r'^2 + 2Rr' \cos\theta} \\ &+ \int_{\pi+\phi}^{\pi-\phi} d\theta \int_{r_2}^{R_G} \frac{\sigma(r')\ r' dr'}{R^2 + r'^2 + 2Rr' cos\theta}, \end{aligned} \tag{606}$$

where $sin\phi = h/R$. To determine r_1 we use the cosine law, $h^2 = r_1^2 + R^2 - 2Rr_1 \cos\beta$,

$$r_1 = R\cos\beta \pm \sqrt{h^2 - R^2 sin^2\beta}, \tag{607}$$

where $\beta = \pi - \theta$. For $\beta = 0$, we must recover $r_1 = R - h$ and so we take the minus sign in (607). The geometry of the problem then allows identification of r_2 as the solution with the positive sign in (607). For the sector of the circle *(ii)* outside the observer, the integral in (605) becomes

$$\mathcal{I}_2 = \int_0^{R_G} \int_{-\pi+\phi}^{\pi-\phi} \frac{\sigma(r')\ r' dr' d\theta}{R^2 + r'^2 + 2Rr'\cos\theta}\,. \tag{608}$$

Putting all this together, for $E_1 \sim 100$ TeV and $E_2 \sim 1$ PeV, the diffuse neutrino flux on Earth is given by

$$\begin{aligned} E_\nu^2\ \Phi(E_\nu) &= \frac{d^2 E_\nu^2 \phi_\nu(E_\nu)}{4\pi}\ (\mathcal{I}_1 + \mathcal{I}_2) \\ &= \frac{d^2\zeta}{4\pi}\ (\mathcal{I}_1 + \mathcal{I}_2) \\ &= \frac{L_\nu^{\text{LS 5039}}}{16\pi^2 \ln 10}\ (\mathcal{I}_1 + \mathcal{I}_2)\ . \end{aligned} \tag{609}$$

For 100 TeV $\lesssim E_\nu \lesssim$ 3 PeV, the IceCube Collaboration reports a flux

$$\Phi(E_\nu) = 1.5 \times 10^{-8} \left(\frac{E_\nu}{100\ \text{TeV}}\right)^{-2.15\pm0.15} (\text{GeV cm}^2\ \text{s sr})^{-1}\,,$$

assuming an isotropic source distribution and democratic flavor ratios [276]. For direct comparison with IceCube data, (609) can be rewritten in standard units using the fiducial value of the source luminosity derived in the previous section,

$$E_\nu^2\ \Phi(E_\nu) \approx 1.27 \times 10^{-9}\ \text{GeV cm}^{-2}\ \text{s}^{-1}\ \text{sr}^{-1} \frac{\mathcal{I}_1 + \mathcal{I}_2}{\text{kpc}^2}\ . \tag{610}$$

The integrals $\mathcal{I}_1$ and $\mathcal{I}_2$ have been computed numerically for various void configurations assuming equal power density per unit area of the disk, that is $\sigma_\Theta(r') = N/\pi R_G^2$, where N is the total number of sources. The results are given in Table 5. The number of sources required to provide a dominant contribution to IceCube data depends somewhat

on the size of the void h. For $h \approx 3$ kpc, about 900 sources are needed to match IceCube observations. This corresponds to a total power in neutrinos of about 6×10^{36} erg s^{-1}. If we assume that these accelerators also produce a hard spectrum of protons with equal energy per logarithmic interval, then the estimate of the total power needed to maintain the steady observed cosmic ray flux is more than two orders of magnitude larger [295, 349].

Table 5: Results for numerical integration of (606) and (608), assuming various source distributions, and equivalent point source number N. The values listed in the table are in units of kpc^{-2}.

h [kpc]	$(\mathcal{I}_1 + \mathcal{I}_2)_\Theta$	$(\mathcal{I}_1 + \mathcal{I}_2)_{\rm exp}$	$(\mathcal{I}_1 + \mathcal{I}_2)_{\mu{\rm QSO}}$
1	0.0224 N	0.0211 N	0.0273 N
2	0.0163 N	0.0178 N	0.0193 N
3	0.0127 N	0.0163 N	0.0146 N
4	0.0101 N	0.0154 N	0.0113 N
5	0.0081 N	0.0148 N	0.0088 N

In this note we have advocated a scenario in which a nearby source contributes significantly to the overall flux, rendering it anisotropic. Should this be the case, *the isotropic contribution to the overall flux must be smaller than that derived based on the assumption that all IceCube events contribute to the isotropic flux.* To model the isotropic background of the nearby source scenario we duplicate the procedure substituting in (605) an exponential distribution of sources which is peaked at the Galactic center, $\sigma_{\rm exp}(r') = n_0\, e^{-r'/r_0}$. We normalize the distribution to the total number of sources in the Galaxy, $N = \int_0^{2\pi} d\theta \int_0^{R_G} \sigma_{\rm exp}(r') r' dr'$. Because we have two parameters we need an additional constraint. We choose to restrict the percentage of the total number of sources beyond the distance $R - h$ to the galactic edge R_G,

Table 6: Number of sources required for each distribution to dominate the neutrino flux reported by the IceCube Collaboration.

h [kpc]	N_Θ	$N_{\rm exp}$	$N_{\mu{\rm QSO}}$
1	527	560	433
2	724	663	612
3	930	725	809
4	1169	767	1045
5	1458	798	1342

Table 7: Best fit parameters of the HMXB spatial density distribution.

r' [kpc]	$N(L > 10^{35}\ \mathrm{erg\,s^{-1}})\ \mathrm{kpc}^{-2}$
0-2	0.0 ± 0.05(syst.)
2-5	$0.11^{+0.05}_{-0.04}$(stat.)$\pm$0.02(syst.)
5-8	$0.13^{+0.04}_{-0.03}$(stat.)$\pm$0.01(syst.)
8-11	$(3.8^{+2.1}_{-1.2}) \times 10^{-2}$(stat.)$\pm 6.5 \times 10^{-3}$(syst.)
11-14	$(6.2^{+7.2}_{-4.3}) \times 10^{-3}$(stat.)$\pm 4.8 \times 10^{-3}$(syst.)

$$P_{R-h} = 2\pi \int_{R-h}^{R_G} n_0 e^{-r'/r_0}\ r' dr'\ , \tag{611}$$

We choose to take $P_{R-h} = 10\%$. The number of sources required to produce a diffuse neutrino flux at the level reported by the IceCube Collaboration is given in Table 6, for different values of h.

Recent studies [302, 303] of persistent HMXBs in the Milky Way, obtained from the deep INTEGRAL Galactic plane survey [331], provide us a new insight into the population of μQSOs. The HMXB surface densities (averaged over corresponding annuli) are given in Table 7. It can be seen that the overall distribution of surface density in the Galaxy has a peak at galactocentric radii of $5 - 8$ kpc and that HMXBs tend to avoid the inner $2 - 4$ kpc of the Galaxy [303]. Therefore, it is clear that a simple exponential disk component is not a good description for the radial distribution. In the spirit of [350], we assumed a source density distribution in the form

$$\sigma_{\mu\mathrm{QSO}}(r') = N_0 \exp\left[-\frac{R_0}{r'} - \frac{r'}{R_0}\right]\ , \tag{612}$$

where the first term in the exponential allows for the central density depression. To describe the observed central depression for high-mass X-ray binaries we take $R_0 = 4$ kpc [303]. This is also supported by a fit to the data in Table 7. The number of sources required to produce a diffuse neutrino flux at the level reported by the IceCube Collaboration is given in Table 6, for different values of h. For a void of 1 kpc, which is the distance to the nearest source in Table 3 (CI Cam), about 500 sources are needed to reproduce IceCube observations.

It is worth commenting on an aspect of this analysis which may seem discrepant at first blush. We find that some 500 μQSOs are required to satisfy energetics requirements, while current catalogs/estimates describe about 100 such known objects. This is not so worrying for the following reasons. First, we have considered only the lower bound on μQSO jet luminosity, which may vary by up to three orders of magnitude in the catalog listings (see Table 3). In this sense our estimated required number of μQSOs that can plausibly explain the IceCube data is a conservative one. Secondly, when considering the nearby source scenario we did not re-evaluate the background conditions, which would yield a smaller isotropic flux.[10] Again, this is a conservative path. Thus, the analysis presented herein adheres to a "cautious" approach throughout, lessening (or eliminating) concerns about the discrepancy between our estimates of the required number of μQSOs versus the cataloged quantities.

We could however, use different assumptions in the calculation; for instance, instead of using the luminosity for LS 5039, one could use the average luminosity for the sources given in Table 3. If we assume a proportionality factor between the luminosity of the jet and the neutrino luminosity similar to the one for LS 5039, one can check that the number of necesary microquasars to match the flux is reduced; this leads us to conclude that μQSOs could provide the dominant contribution to the diffuse neutrino flux recently observed by IceCube.

9.1.4 Constraints from gamma rays and baryonic cosmic rays

Very recently the IceCube Collaboration has extended their neutrino sensitivity to lower energies [351]. One intriguing result of this new analysis is that the spectral index which best fits the data has steepened from 2.15 ± 0.15 to 2.46 ± 0.12. If one assumes the neutrino spectrum follows a single power law up to about 10 GeV, then the latest data from the Fermi telescope [352] can be used to constrain the spectral index assuming the γ-rays produced by the π^0's accompanying the $\pi^{\pm}$'s escape the source. In such a scenario, Fig. **??** shows that only a relatively hard extragalactic spectrum is consistent with the

[10] Evaluating the background, of course, require detailed knowledge of detector properties and properly belongs to the territory of the IceCube Collaboration.

data. On the other hand, the Galactic photon flux in the 10 GeV region is about an order of magnitude larger than than the extragalactic flux; this allows easier accommodation of a softer single power law spectrum. For the Galactic hypothesis, however, one must consider an important caveat, namely that the expected photon flux in the PeV range has been elusive [353]. However, a recent refined analysis of archival data from the EAS-MSU experiment [354] has confirmed previous claims of photons in the 10 PeV region. This analysis also results in a larger systematic uncertainty at all energies, relaxing previously reported bounds in the PeV range. While previous bounds were marginally consistent with non-observation of PeV photons expected to accompany the IceCube neutrinos [295], this new less stringent bound is more comfortably consistent.

There is an additional interesting consequence of the new IceCube data. The neutrino spectral index should follow the source spectrum of the parent cosmic rays. We have shown elsewhere [295, 355] that a spectral index of ~ 2.4 is required for consistency with current bounds on cosmic ray anisotropy. Further credence regarding our best-fit spectral index has been recently developed via numerical simulations [356]. It is worth stressing that our discussion regarding source energetics assumes the canonical Fermi index of $\alpha = 2$. Given the current level of uncertainties on the atmospheric neutrino background, the spatial distribution and total number of microquasars, as well as the large variation in microquasar jet luminosities (see Table 3), shifting our assumed spectral index from $\alpha = 2$ to $\alpha = 2.4$ will have little impact on the arguments concerning energetics explored herein. In the future, improved measurements all-round will require a considerably more elaborate analysis, including detailed numerical simulations.

9.1.5 Final remarks

Motivated by recent IceCube observations we have re-examined the idea that μQSOs are high energy neutrino emitters. We considered the particular case of LS 5039, which as of today represents the source with lowest p-value in the IceCube sample of selected targets [276]. We have shown that if LS 5039 has a compact object powering jets, it could accelerate protons up to above about 30 PeV. These highly relativistic protons

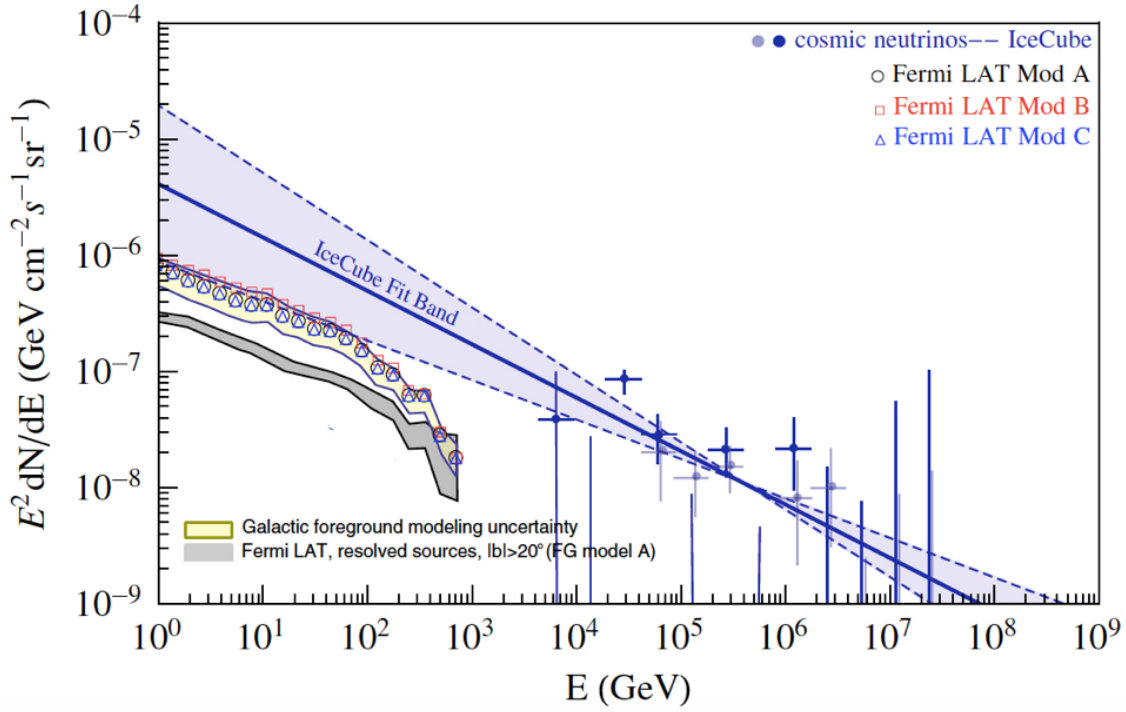

Figure 18: The open symbols represent the total extragalactic γ-ray background for different foreground (FG) models as reported by the Fermi Collaboration [352]. For details on the modeling of the diffuse Galactic foreground emission in the benchmark FG models A, B and C, see [352]. The cumulative intensity from resolved Fermi LAT sources at latitudes $|b| > 20^\circ$ is indicated by a (grey) band. The solid symbols indicate the neutrino flux reported by the IceCube Collaboration. The best fit to the data (extrapolated down to lower energies) is also shown for comparison.

could subsequently interact with the plasma producing a neutrino beam that could reach the maximum observed energies, $E_\nu \gtrsim$ PeV. There are two extreme possibilities for neutrino production: *(i)* close to the base of the jet and *(ii)* at the termination point of the jet. By normalizing the accompanying photon flux to H.E.S.S. observations in the TeV energy range [311, 312] we have shown that, for the first scenario, photon absorption on the radiation field leads to a neutrino flux $\mathcal{O}(10^{-8} E_\nu^{-2}\ \mathrm{GeV}^{-1}\,\mathrm{cm}^{-2}\,\mathrm{s}^{-1})$. Should this be the case, the neutrino flux almost saturates the current upper limit reported by the ANTARES Collaboration [327]. The second possibility yields a flux of neutrinos which is about an order of magnitude smaller. *A priori* these two extreme flux predictions are partially consistent with existing data. However, one can ask why a source with similar characteristics (LS I +61 303) which is in the peak of the field of view of IceCube has not been already discovered. The current 90% CL upper limit on LS I +61 303 reported by

the IceCube Collaboration is $\mathcal{O}(10^{-9} E_\nu^{-2}\ \mathrm{GeV}^{-1}\,\mathrm{cm}^{-2}\,\mathrm{s}^{-1})$, favoring neutrino production near the end of LS 5039 jets.

We have also generalized our discussion to the population of μQSOs in the Galaxy. Using the spatial density distribution of high-mass X-ray binaries obtained from the deep INTEGRAL Galactic plane survey and assuming LS 5039 typifies the μQSO population we have demonstrated that these powerful compact sources could provide the dominant contribution to the diffuse cosmic neutrino flux. Future IceCube observations will test the LS 5039 hypothesis, providing the final verdict for the ideas discussed in this paper. Of course, a complete picture which accommodates all the shower events outside the galactic plane may well require an extragalactic component. Indeed most of the istropic background is dominated by muon tracks. Explaining the possible isotropy of shower events may eventually prove only to be possible by considering extragalactic sources, and we shall consider such kind of sources in the next section.

9.2 Astrophysical sources: Starbursts

Both the neutrino energy spectrum and directional measurements provide clues about which astrophysical sources may be responsible for extraterrestrial neutrinos. We will begin with a discussion of characteristics of the energy spectrum as it pertains to potential source candidates, and then move on to the issue of directional correlations with astrophysical objects. First, however, we should remind the reader that the three neutrino species ν_e, ν_μ and ν_τ induce different characteristic signal morphologies when they interact in ice producing the Cherenkov light detected by the IceCube optical modules. The charged current (CC) interaction of ν_e produces an electromagnetic shower which ranges out quickly. Such a shower produces a rather symmetric signal, and hence exhibits a poor angular resolution of about $15^\circ - 20^\circ$ [248]. On the other hand, a fully or mostly contained shower event allows one to infer a relatively precise measurement of the ν_e energy, with a resolution of $\Delta(\log_{10} E_\nu) \approx 0.26$ [251]. The situation is reversed for ν_μ events. In this case, CC interaction in the ice generates a muon which travels relatively unhindered leaving behind a track. Tracks point nearly in the direction of the original

ν_μ and thus provide good angular resolution of about 0.7°, while the "electromagnetic equivalent energy" deposited represents only a lower bound of the true ν_μ energy. The true energy may be up to a factor 10 larger than the observed electromagnetic equivalent energy. Finally, ν_τ CC interactions may, depending on the neutrino energy, produce "double bang" events [252], with one shower produced by the initial ν_τ collision in the ice, and the second shower resulting from most subsequent τ decays. Separation of the two bangs is feasible for ν_τ energies above about 3 PeV, while at lower energies the showers tend to overlap one another [253].

With these points in mind, we now move to the current state of the neutrino energy measurements. One striking feature of the IceCube spectrum is that, assuming an unbroken $E_\nu^{-\gamma}$, $\gamma = 2$ flux expected from Fermi acceleration in strong shocks, there is either a cutoff or a spectral break evident around 2 PeV. Notably, there is no increase in observation rate near 6.3 PeV, as one would expect from the Glashow resonance [277]. This implies that either the acceleration process dies out at some energy, or that the spectrum is simply steeper than $\gamma = 2$. It has been shown elsewhere that an unbroken power law spectrum with $\gamma = 2.3$ is also reasonably consistent with the IceCube data [295].

In order to ascertain the physical processes which could underlie these spectral features, let us discuss briefly plausible neutrino production mechanisms. It is generally thought that extraterrestrial neutrinos are produced via proton interactions with either photons or gas near the proton acceleration sites, resulting in pions which in turn generate neutrinos as decay products. For the case of neutrino production via $p\gamma$ interactions, the center-of-momentum energy of the interaction must be sufficient to excite a Δ^+ resonance, the $\Delta^+(1232)$ having the largest cross-section. The threshold proton energy for neutrino production on a thermal photon background of average energy E_γ is

$$E_{\rm th} = m_\pi(m_p + m_\pi/2)/E_\gamma\,, \tag{613}$$

where m_π and m_p are the masses of the pion and proton, respectively. Since the proton energy must be about 16 times higher than the daughter neutrino energies, Eq. (613) implies photons with energies in the range ~ 6 eV should be abundant in the region of

proton acceleration in order to generate $\sim$ PeV neutrinos. Gamma-ray bursts (GRBs) may be the only astrophysical objects capable of generating a photon background of the required energy for this scenario [289]. Furthermore, production of neutrinos in the 100 TeV range requires photon energies about an order of magnitude higher. In contrast, if neutrinos are produced via interaction in gas near the acceleration site, the energy threshold requirement is lifted, as *pp* interactions generate pions over a broad range of energies.

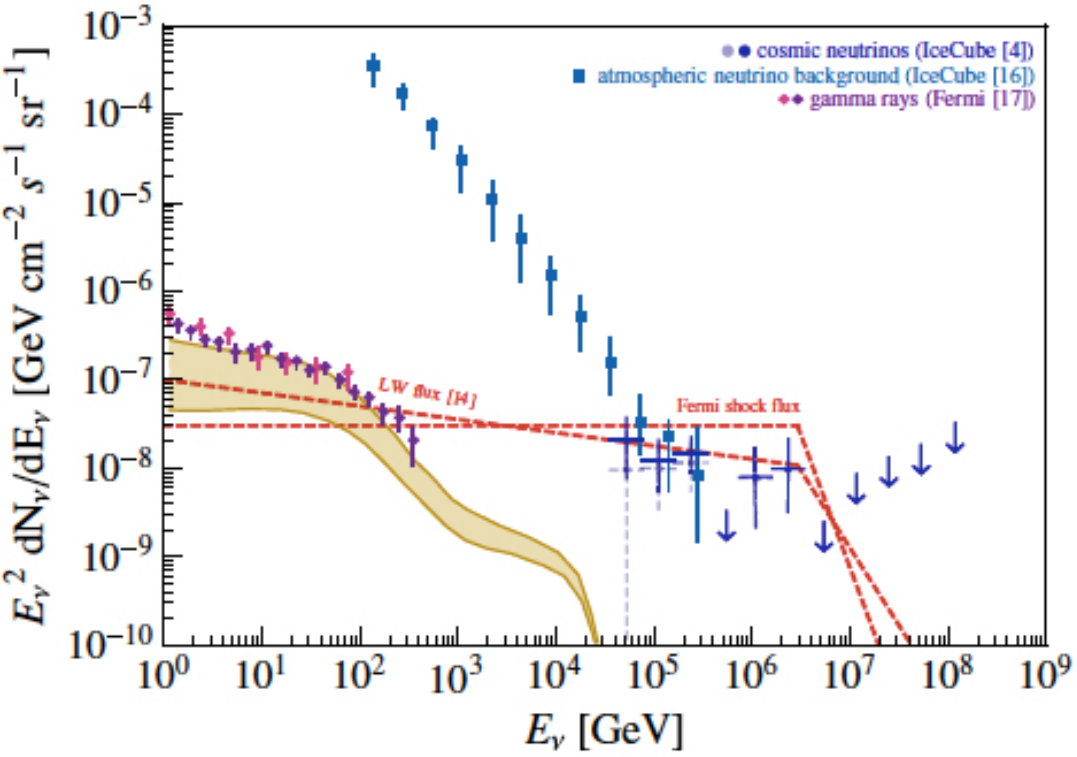

Figure 19: Neutrino and gamma ray spectra compared to two neutrino spectral indices. The squares show the background from atmospheric ν_μ events as observed by IceCube40 [261]. The circles and arrows show the recently reported IceCube flux (points with solid error bars do not include prompt background while those with dash error bars do) [249]. The The diamonds are gamma ray flux measurements from Fermi [262]. The two dashed lines correspond to $E_\nu^2 \mathrm{d}N_\nu/\mathrm{d}E_\nu = 10^{-7} E^{-0.15}$ GeV cm^{-2} s^{-1} sr^{-1} and $E_\nu^2 \mathrm{d}N_\nu/\mathrm{d}E_\nu = 3 \times 10^{-8}$ GeV cm^{-2} s^{-1} sr^{-1}, with the spectrum steepening above about 2 PeV to $\gamma = 3.75$ and $\gamma = 5.0$, respectively. For these two neutrino fluxes, the associated predictions for the gamma ray fluxes after propagation are displayed as the upper and lower bounds of the shaded region [284] . Note that the spectral index $\gamma = 2.15$ at injection agrees well with both the Fermi-LAT and IceCube measurements.

Extending previous multifrequency studies of individual galaxies [258], Loeb and Waxman (LW) [287] showed in 2006 that starburst galaxies constitute a compelling source for efficient neutrino production up to ~ 0.3 PeV, and possibly beyond, though for energies exceeding 1 PeV the predictions are quite uncertain. For energies up to ~ 1 PeV, the LW analysis predicts a spectral index $\gamma = 2.15 \pm 0.10$ which accurately fits the IceCube data, and indeed predicts an observation rate for E_ν of $10^{1.5\pm0.05}$ for a 1 km^3 detector, in line with the rate subsequently observed by IceCube. Neutrino production from $\pi^\pm$ decays must be accompanied by a corresponding flux of gamma rays from decays of π^0's produced in the pp interactions, providing a robust cross-check of the pion production rate and corresponding neutrino spectrum. A spectrum steeper than $\gamma \sim 2.2$ leads to an overproduction of gamma rays compared to measurements by Fermi-LAT [284], indicating that a soft unbroken $\gamma = 2.3$ spectrum is implausible for extragalactic sources. Thus, it seems that a cutoff or suppression must be at play. All in all, the starburst source hypothesis together with a steepening of the spectrum to at least $\gamma = 3.75$ above 3 PeV fits well to the IceCube data and satisfies the constraints from gamma ray observations, as shown in Fig. **??**.

We now discuss how double bang topologies may serve as a discriminator among possible astrophysical sources powered by highly relativistic winds. Extraterrestrial neutrino production proceeds via the decay chain

$$\begin{aligned} \pi^+ \to \quad & \mu^+ \quad \nu_\mu \qquad\qquad\qquad (\text{and the conjugate process})\,. \\ & \hookrightarrow \quad e^+\, \bar{\nu}_\mu\, \nu_e \end{aligned} \tag{614}$$

This decay chain may be complete in the sense that both decays indicated in Eq. (614) occur without significant change in the μ energy, or it may be incomplete, in which case the μ suffers possibly catastrophic energy loss before decay. For the case of a complete decay chain, each neutrino carries on average about 1/4 of the parent pion energy. If the μ radiates away energy before it decays, the ν_μ from the first decay will still carry on average 1/4 of the $\pi^\pm$ energy, while the other two neutrinos will emerge with less than

the nominal 1/4 of the parent pion energy. In such a scenario it is conceivable that the first ν_μ in the chain can be produced above 3 PeV, whereas $\bar{\nu}_e$ may not reach beyond 2 PeV, and in particular may not be able to reach the energy required to interact at the Glashow resonance.

We now discuss the muon energy loss quantitatively by exploiting the observation of gamma rays accompanying the neutrino flux. In the case of muons with energies in excess of 1 PeV, energy losses are dominated by synchrotron radiation. The synchrotron loss time is determined by the energy density of the magnetic field in the wind rest frame. Defining $\tau_{\mu,\rm syn}$ as the characteristic muon cooling time via synchrotron radiation and $\tau_{\mu,\rm decay}$ as the muon decay time, it is necessary that $\tau_{\mu,\rm syn} < \tau_{\mu,\rm decay}$ in order for the decay chain to be complete. $\tau_{\mu,\rm syn} \sim \tau_{\mu,\rm decay}$ determines a critical energy $E_\mu^{\rm syn}$ at which energy losses begin to affect the decay chain. For the characteristic parameters of a GRB wind, the maximum energy at which all neutrinos in the decay chain have on average 1/4 of the pion energy is

$$E_\nu^{\rm syn} \approx \frac{1}{3}\, E_\mu^{\rm syn} \sim \frac{1}{3} \frac{\Gamma_{2.5}^4\, \Delta t_{-3}}{L_{52}^{1/2}}\ {\rm PeV}, \tag{615}$$

where $\Gamma = 10^{2.5}\Gamma_{2.5}$ is the wind Lorentz factor, $L = 10^{52} L_{52}$ erg/s is the kinetic energy luminosity of the wind, and $\Delta t = 10^{-3}\Delta t_{-3}$ s is the observed variability time scale of the gamma-ray signal [263]. Equation 615 is also valid for neutrinos produced in blazars. In this case, $\Delta t \sim 10^4$ s, $\Gamma \sim 10$, and $L \sim 10^{47}$ erg/s, yielding $E_\nu^{\rm syn} \sim 1$ EeV. For starburts, the galactic wind is non-relativistic and the magnetic field is small enough to render synchrotron losses negligible in comparison. In summary, for GRBs, the muon cooling is sufficient to influence the decay chain in such a way as to affect the flavor ratios at PeV energies, whereas for blazar and starbursts the decay chain is only affected for muon energies $\gg 10$ PeV. Note that for GRBs, $\Delta t_{-3} \sim 1$ constitutes a lower bound, and hence the consequences discussed herein may require some fine-tuning of the parameters of Eq. (615).

It is nonetheless worth noting some potential consequences of the above hypotheses. As noted elsewhere $p\gamma$ interactions produce fewer $\bar{\nu}_e$ than pp ineractions [278]. Indeed,

most of the $\bar{\nu}_e$ flux originates via oscillations of $\bar{\nu}_\mu$ produced via μ^+ decay. For production of $E_\nu \gtrsim 1$ PeV in GRBs, the ν_μ in the chain of Eq. (614) is more energetic than the $\bar{\nu}_\mu$. This may suggest that the softening of the spectral index takes place at different energies for neutrino and antineutrino fluxes. If this were the case, at production the high energy end of the GRB flux would be dominated by ν_μ produced via π^+ decay. As described previously, however, IceCube can measure only lower bounds for the muon energies. As it turns out, IceCube has recently recorded a ν_μ with a minimum energy of 0.5 PeV [265], but which may have an energy as much as 10 times higher. If this is indeed the case, it could indicate a high energy muon from the first decay of Eq. (614). We can also speculate on more potentially convincing observations which may emerge in the future. Assuming maximal $\nu_\mu - \nu_\tau$ mixing, observation of a high energy ν_μ may imply eventual observation of a high energy ν_τ, which above about 3 PeV would exhibit the distinctive double bang topology discussed above. Note that some fine tuning of the model presented here may be required for such events to manifest. In particular, the $\mu^\pm$ cooling time of Eq. (615) must be smaller than the $\mu^\pm$ decay time in order to prevent the $\bar{\nu}_e$ from reaching the Glashow resonance (thus far not observed). Further, the $\pi^\pm$ cooling time must exceed its lifetime in order to produce a ν_τ above ~ 3 PeV. Further, as this is a phenomenological exercise, we have neglected possible experimental effects. As such, this study is not meant to make a concrete prediction, but rather to point out that *if* such double bang topologies are observed in the future while the Glashow resonance is not, it would provide a valuable piece to the puzzle of extraterrestrial neutrino origins, favoring the GRB hypothesis over the blazar or starburst ones, each of which would require implausible fine-tuning to be consistent with observation.

Now, since starburst galaxies are plausible source candidates, consistent with the neutrino energetics observed so far, the next obvious step is to check whether there are any correlations with the positions of starburst galaxies and the observed neutrino arrival directions. Before proceeding we note that hypernovae, which may well be responsible for sub-PeV to PeV neutrino emissions [266], are present in starburst galaxies as well as other star forming regions, though the rate of occurrence is higher in starburst galaxies.

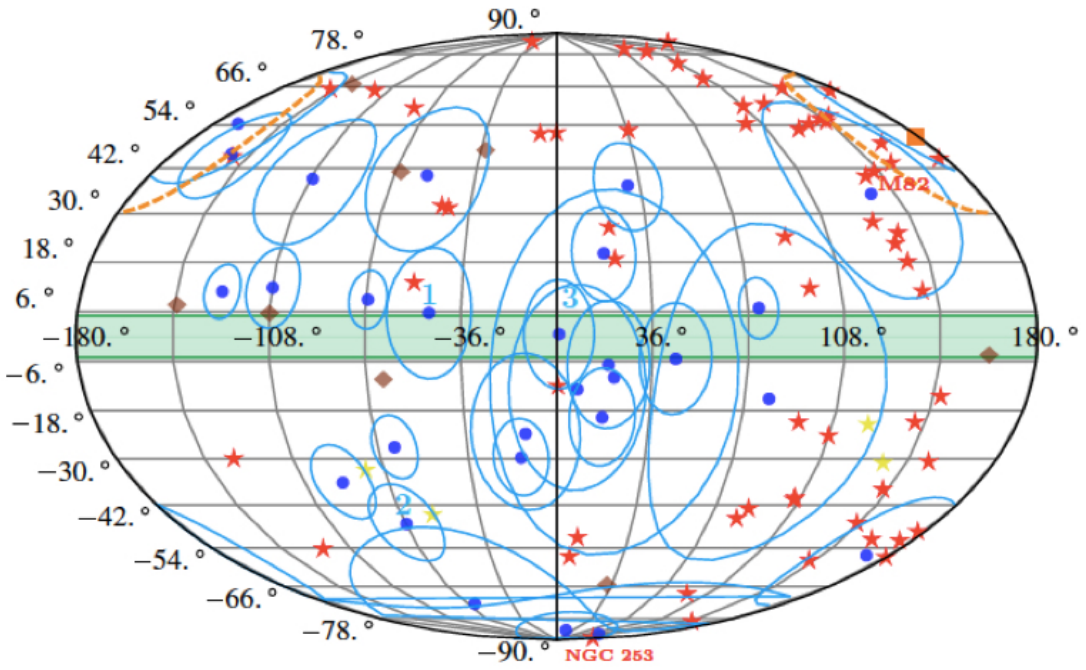

Figure 20: Comparison of IceCube event locations [249] with star-forming galaxies [267] and the ultrahigh energy cosmic ray hot-spot reported by the TA Collaboration [273] in a Mollweide projection. The 27 shower events (circles) and 8 track events (diamonds) reported by the IceCube Collaboration. The 3 highest energy events are labeled 1, 2, 3, from high to low, respectively. The red stars indicate the 64 star-forming galaxies beyond the Local Group. The 4 yellow stars indicate galaxies in the local group. NGC 253 and M82, our two closest starbursts, are labeled. The shaded band delimits the Galactic plane. The square in the upper right marks the center of the TA hot-spot, with the surrounding dashed line indicating its 20° extent..

To test the hypothesis that star forming regions correlate with the IceCube events, we have employed the list of star-forming regions compiled by the Fermi-LAT Collaboration [267], which includes 64 of the 65 sources of the HCN survey [268] as well as the local galaxies (SMC, LMC, M31, and M33). The HCN survey is, to date, the most complete study of galaxies with dense molecular gas content. It includes nearly all the IR-bright galaxies in the northern sky ($\delta \geq -35°$) with strong CO emission, as well as additional galaxies taken from other surveys. Objects within the Galactic latitudes $|b| < 10°$ are not included in the survey due to diffuse emission from the Galactic plane.

A comparison among all of the IceCube events and the star-forming galaxy survey is shown in Fig. **??**. Not surprisingly given the size of the localization error, there are a few coincidences, among them the two nearby starbursts M82 and NGC 253 (observed in

gamma-rays [270, 271] which are considered to be possible ultrahigh energy cosmic ray emitters [272]). The highest energy event correlates with NGC 4945, the second highest with the SMC, and the third highest correlates with IRAS 18293-3413. However, none of the track topologies correlates with an object in the survey.

To estimate the number of ν_μ required to make a statistically significant statement, we have run 10^6 simulations with 68 sources and computed the fraction correlating by chance with 1° circular regions of the sky. Of these, 90% of the simulations show 0 correlations. If future observations contain 5 or more ν_μ events which correlate with the 68 sources in the survey, an association by chance will be excluded at more than 99% CL [279].

For ν_μ events, the equivalent electromagnetic energy represents only a lower bound on the true neutrino energy. Consequently, escaping the background region requires setting a cut on the electromagnetic equivalent energy $\simeq 0.5$ PeV. This threshold is arrived at via the following argument. Figure 1 shows that at $E_\nu = 1$ PeV the background from prompt emission is negligible. Since the muon neutrino energy is at least 2 times the inferred electromagnetic equivalent energy, the proposed cut produces a virtually background-free sample. Since 1 such event has already been recorded, we might guess an observation rate of 1 event every ~ 2 years, indicating a long wait with the current 1 km^3 configuration. Next generation IceCube, which could increase the instrumented volume by up to an order of magnitude (but with larger string spacing), will therefore be greatly beneficial for this study, as well as other correlation analyses.

We conclude with one additional observation. It was recently noted [275] that the ultrahigh energy cosmic ray hot-spot reported by the TA Collaboration [273] correlates with 2 of the 28 events initially reported by the IceCube Collaboration [248], with a statistical significance of around 2σ. In the newer IceCube data (the 37 event sample [249]) there is one additional shower event which correlates with the TA hot-spot, as shown in Fig **??**. The hot-spot also contains an abundance of star-forming regions and is near M82.

9.3 Insufficiencies of astrophysical models

The neutrino flux in (1) is exceptionally high by astronomical standards, with a magnitude comparable to the Waxman-Bahcall bound [83]. A saturation of this bound can only be achieved within astrophysical environments where accelerator and target are essentially integrated. Potential candidate sources are discussed in [285]. These powerful sources produce roughly equal numbers of π^0, π^+ and π^- in the proton-proton beam dump. The π^0 accompanying the $\pi^\pm$ parents of IceCube neutrinos decay into γ-rays, which are only observed indirectly after propagation in the extragalactic radiation fields permeating the universe. These γ-rays initiate inverse Compton cascades that degrade their energy below 1 TeV. The relative magnitudes of the diffuse γ-ray flux detected by *Fermi* LAT [352] can then be used to constrain the spectral index, assuming the γ-rays produced by the π^0's accompanying the $\pi^\pm$ escape the source. Figure **??** shows that only a relatively hard injection spectrum is consistent with the data. Indeed, if IceCube neutrinos are produced through *pp* collisions in optically thin extragalactic sources, the γ-rays expected to accompany the neutrinos saturate the *Fermi* LAT flux for $\alpha \approx 2.2$ [284]. The overall isotropy of the observed arrival directions and the fact that a PeV event arrives from outside the Galactic plane disfavor a Galactic origin. Moreover, for the Galactic hypothesis one must consider another important caveat, namely that the expected photon flux in the PeV range [295] has been elusive [341].

10 Reconciling the Hubble constant measurements

10.1 Decaying dark matter and the Hubble parameter

The difficulties so far encountered in modeling the production of IceCube neutrinos in astrophysical sources fueled the interest in particle physics inspired models. By far the most popular model in this category is the decay of a heavy massive ($\sim$ few PeV) relic that constitute (part of) the cold dark matter (CDM) in the universe [89]. The lack of events in the vicinity of the Glashow resonance, implies the spectrum should decrease significantly at the energy of a few PeV. Spectra from dark matter decays always exhibit a sharp cutoff determined by the particle mass. Furthermore, the 3 highest energy events appear to have identical energies, up to experimental uncertainties. A line in the neutrino spectrum would be a smoking gun signature for dark matter. If the heavy relic also decays into quarks and charged leptons, the mono-energetic neutrino line may be accompanied by a continuous spectrum of lower-energy neutrinos, which can explain both the PeV events and some of the sub-PeV events. All of these considerations appear to be in agreement with the data [90]. Even much heavier relic particles, with masses well above a PeV, can generate the required neutrino spectrum from their decays if their lifetime is much shorter than the present age of the universe [91]. The spectrum of neutrinos is modified by a combination of redshift and interactions with the background neutrinos, and the observed spectrum can have a cutoff just above 1 PeV for a broad range of the relic particle masses. In this Letter we will reexamine the idea of a dark matter origin for IceCube events.

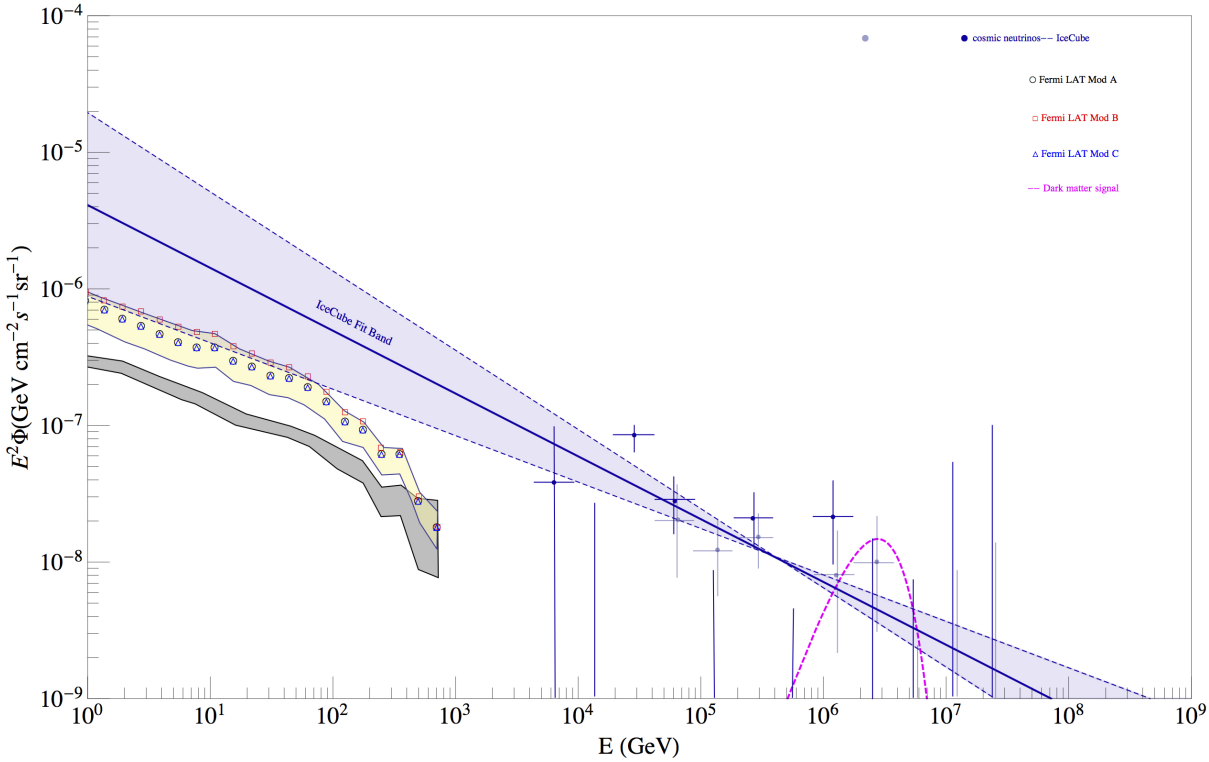

Figure 21: The open symbols represent the total extragalactic γ-ray background for different foreground (FG) models as reported by the Fermi LAT Collaboration [352]. For details on the modeling of the diffuse Galactic foreground emission in the benchmark FG models A, B and C, see [352]. The cumulative intensity from resolved *Fermi* LAT sources at latitudes $|b| > 20^\circ$ is indicated by a (grey) band. The solid symbols indicate the neutrino flux (per flavor) reported by the IceCube Collaboration. The blue points are from the data sample of the most recent IceCube analysis [351]. The light grey data points are from the 3-year data sample of [276], shifted slightly to the right for better visibility. The best fit to the data (extrapolated down to lower energies), is also shown for comparison [351]. The dashed line indicates the mono-energetic signal from dark matter decay. Note that a plotting of $E^2\Phi = EdF/(d\Omega\, dA\, dt\, d\ln E)$ versus $\ln E$ conserves the area under a spectrum even after processing the electromagnetic cascade. Thus, the area of the π^0 contribution to the diffuse γ-ray spectrum (total diffuse γ-ray flux provides an upper bound) implies the low energy cutoff (upper bound) to the $\pi^\pm$ origin of the neutrinos.

10.1.1 Connecting the dots

The tension between the CMB based determination of the Hubble constant and the h value inferred from direct low redshift measurements is intriguing and deserves further attention. On the one hand, the underlying source of discrepancy could be some systematic uncertainty in the calibration [96]. On the other hand, it could trace a deficiency of the concordance model of cosmology. In the spirit of [97], it has been recently conjec-

tured that *Planck*-inspired ΛCDM paradigm can be reconciled with HST measurements if a subdominant fraction f_X of CDM is unstable and decays rather quickly with respect to the present Hubble time [76]. The width of the unstable component Γ_X, normalized to H_0, is an independent parameter of the model. By forcing the X particles to decay after recombination Γ_X/H_0 is bounded from above. Moreover, the X is assumed to decay (dominantly) into invisible massless particles of the hidden sector and hence does not produce too many photons. A joint fit to *Planck*, supernova, and HST data reveals that the base ΛCDM model, with $\Gamma/H_0 = 0$, is outside the 2σ likelihood contours in the (Γ_X, f_X) plane [76]. The data instead favor $0.05 \lesssim f_X \lesssim 0.10$. The mean value and 1σ error derived from a maximum likelihood analysis are $h = 0.716 \pm 0.020$ [76]. Interestingly, within the same parameter range the model could also alleviate the emerging tension with the cluster data. (See, however, [98].) For example, for $f_X \simeq 0.10$ and $\Gamma_X/H_0 \simeq 2000$ the corresponding values of $\Omega_m \simeq 0.25$ and $\sigma_8 \simeq 0.80$ [76] are marginally consistent with the 2σ allowed contours by the *Planck* cluster mass scale [99] and the extended ROSAT-ESO Flux Limited X-ray Galaxy Cluster Survey (REFLEX II) [100]. For smaller values of f_X and or Γ_X/H_0 the values of Ω_m and σ_8 move closer to the base ΛCDM model [76]. Next, in line with our stated plan, we take $f_X \simeq 0.07$ and $\Gamma_X/H_0 \simeq 1500$ as benchmarks and investigate what would be the CDM fraction required to decay into the visible sector to accommodate IceCube observations.

10.1.2 Bump-Hunting

The two main parameters characterizing the X particle are its lifetime $\tau_X \simeq 3 \times 10^{14}$ s and its mass m_X, which is a free parameter. We assume the neutrino produced via X decay is mono-energetic, with energy $\varepsilon_\nu = m_X/2$. The neutrino energy distribution from X decay is given by $dN_\nu/dE_\nu = N_\nu\, \delta(E_\nu - \varepsilon_\nu)$, where N_ν is the neutrino multiplicity. We further assume the dominant decay mode into the visible sector, contributing to neutrino production, is $X \to \nu\bar{\nu}$ and so $N_\nu = 2$.

The evolution of the number density of neutrinos $n_\nu(E_\nu, z)$ produced at cosmological distances in the decay of X particles is governed by the Boltzmann continuity equation,

$$\frac{\partial[n_\nu/(1+z)^3]}{\partial t} = \frac{\partial[HE_\nu n_\nu/(1+z)^3]}{\partial E_\nu} + \mathcal{Q}_\nu\,, \tag{616}$$

together with the Friedman-Lemaître equations describing the cosmic expansion rate $H(z)$ as a function of the redshift z. This is given by $H^2(z) = H_0^2\,[\Omega_m(1+z)^3 + \Omega_\Lambda]$. The time-dependence of the red-shift can be expressed via $dz = -dt\,(1+z)H$. We have found that for the considerations in the present work neutrino interactions on the cosmic neutrino background can be safely neglected [101]. In (616),

$$\mathcal{Q}_\nu(E_\nu, t) = \frac{n_X(t)}{\tau_X}\,\mathcal{B}_{X\to\nu\bar{\nu}}\,\frac{dN_\nu}{dE_\nu}\,, \tag{617}$$

is the source term, $n_X(t) = Y_X\ s(t)\ e^{-t/\tau_X}$ is the number density of X, $\mathcal{B}_{X\to\nu\bar{\nu}}$ is the neutrino branching fraction, $s(t)$ is the entropy density, and

$$Y_X = 3.6\times 10^{-9}\frac{\Omega_X h^2}{m_X/\mathrm{GeV}} \tag{618}$$

is the comoving number density at the CMB epoch.

We solve for the number density at present time. The equation becomes:

$$\frac{\partial n_\nu}{\partial t} = -2Hn_\nu + HE\frac{\partial n_\nu}{\partial E} + Q_\nu, \tag{619}$$

which is a first order partial differential equation. Consider the general equation

$$au_x + bu_y = c, \tag{620}$$

where the subscript denotes partial derivative and a, b and c are functions of x, and y. The solutions of this equation are given by

$$\frac{dx}{ds} = a,\ \ \frac{dy}{ds} = b,\ \ \frac{du}{ds} = c. \tag{621}$$

Applying this to our problem, we get:

$$\frac{dt}{ds} = 1, \tag{622}$$

$$\frac{dE}{ds} = -HE, \tag{623}$$

$$\frac{dn}{ds} = -2Hn + Q_\nu. \tag{624}$$

From equation (622), we identify the parameter s as the variable t. The other important equation for us is (624), which has the solution:

$$n = e^{\int_{-\infty}^{t_0}(-2H)dt'}C + \int_{-\infty}^{t_0} e^{-\int_{t_0}^{t'}(-2H)dt''}Q_\nu(t', E)dt'. \tag{625}$$

We set the integration constant as zero. Now, take a closer look at the following integral:

$$\int 2Hdt = \int 2\frac{da/dt}{a}dt = \int 2\frac{da}{a} = ln(a/a_0)^2. \tag{626}$$

Using this result on (625), we get:

$$n_\nu = \int_{-\infty}^{t_0} e^{ln(a/a_0)^2}Q_\nu(t', E)dt' = \int_{-\infty}^{t_0} \left(\frac{a_0}{a}\right)^{-2} Q_\nu dt'. \tag{627}$$

If we assume that the decay process produces monochromatic neutrinos,

$$\frac{dN_\nu}{dE} = N_\nu\delta(E_\nu - \epsilon_\nu), \tag{628}$$

the source term, as defined in the paper, becomes

$$Q_\nu = \frac{n_X(t)}{\tau_X}B\frac{dN_\nu}{dE} = \frac{n_X(t)}{\tau_X}BN_\nu\delta(E - \epsilon_\nu). \tag{629}$$

The integral for n_ν can be solved,

$$n_\nu = \frac{N_\nu Y_X s(t_0)}{\tau_X E_\nu}\left[\frac{e^{-\bar{t}/\tau_X}}{H(\bar{t})}\right]_{1+z(\bar{t})=\epsilon_\nu/E_\nu} \tag{630}$$

We have an expression for n_ν. We can now define the flux Φ as:

$$\Phi = \frac{c}{4\pi} n_\nu. \tag{631}$$

By solving (616) we have obtained the (all flavor) neutrino flux at present epoch t_0,

$$\begin{aligned} \Phi(E_\nu) &= \frac{c}{4\pi} n_\nu(E_\nu, 0) \\ &= \frac{c}{4\pi} \frac{N_\nu Y_X s(t_0)}{\tau_X E_\nu} \mathcal{B}_{X\to\nu\bar{\nu}} \left. \frac{e^{-t_*/\tau_X}}{H(t_*)} \right|_{1+z(t_*)=\varepsilon_\nu/E_\nu}, \end{aligned} \tag{632}$$

with $s(t_0) \simeq 2.9 \times 10^3$ cm^{-3}. In order to obtain the curve for the dark matter signal, we need to rewrite the equation above in terms of energy. If we assume a Λ-CDM model, with the parameters

$$\Omega_{m_0} = 0.31566, \tag{633}$$

$$\Omega_{\Lambda_0} = 0.6844, \tag{634}$$

we need to express time (t) and the Hubble papameter ($H(\bar{t})$) as a function of energy. This can be accomplished by solving the following integral (from cosmology):

$$t = \frac{1}{H_0} \int_0^{(1+z)^{-1}} \frac{dx}{\sqrt{0.31566 x^{-1} + 0.6844 x^{-2}}}, \tag{635}$$

where the upper limit of integration can be obtained from

$$1 + z(t) = \frac{\epsilon_\nu}{E_\nu} \tag{636}$$

and the solution is (after using $\epsilon_\nu = 280$ PeV and 71.6 Km/ s / Mpc for the Hubble constant):

$$t = 3.4665 \times 10^{17} \text{ArcSinh}\left[3.14304 \times 10^{-13} E_\nu^{3/2}\right] \quad \text{s.} \tag{637}$$

Now, for the Hubble parameter:

$$H(z) = H_0(1+z)\sqrt{0.6844(1+z)^{-2} + 0.31566(1+z)}, \tag{638}$$

which gives

$$H(z) = 2.32468 \times 10^{-18}\sqrt{0.6844 + \frac{6.92805 \times 10^{24}}{E_\nu^3}} \quad \mathrm{s}^{-1}. \tag{639}$$

Putting all of this on the equation for Φ, as well as the values for the constants (yeld, entropy etc) we get:

$$\Phi = \frac{1.622 \times 10^{-11}}{\sqrt{0.6844 + \dfrac{6.92805 \times 10^{24}}{E_\nu^3}}E_\nu} \exp\left\{-1155.5 \text{ ArcSinh}\left[3.14304 \times 10^{-13} E_\nu^{3/2}\right]\right\} \tag{640}$$

Maximization of the flux yields the energy relation for the peak in the spectrum,

$$E_\nu^{\rm peak} \simeq \frac{1}{2}\,\frac{m_X/2}{1+z(\tau_X)}\,, \tag{641}$$

which sets the mass of the X. Since $z(\tau_X) \simeq 140$ to accommodate the PeV peak in IceCube's neutrino spectrum we take $m_X \simeq 560$ PeV. Now, from (618) we obtain $Y_X \approx 5.4 \times 10^{-20}$. Finally, we normalize the cosmic neutrino flux per flavor using (1). The intensity of the mono-energetic signal at the peak is taken as 60% of the flux reported by the IceCube Collaboration, yielding a neutrino branching fraction $\mathcal{B}_{X\to\nu\bar{\nu}} \sim 5\times10^{-8}$ into all three flavors. The width, an output of the Boltzmann equation, is shown in Fig. **??**. It is evident that the mono-energetic neutrino spectrum is in good agreement with the data. In particular, the flux suppression at the Glashow resonance, $\Phi(E_\nu^{\rm res})/\Phi(E_\nu^{\rm peak}) \simeq 0.011$, is consistent with data at 1σ.

The model is fully predictive and can also be confronted with *Fermi* LAT data. It is reasonable to assume that $\mathcal{B}_{X\to e^+e^-} \approx \mathcal{B}_{X\to\nu_e\bar{\nu}_e} \approx \mathcal{B}_{X\to u\bar{u}} \approx \mathcal{B}_{X\to d\bar{d}}$. About 1/3 of the energy deposited into either $u\bar{u}$ or $d\bar{d}$ is channeled into γ-rays via π^0 decay and about 1/6 of the energy is channeled into electrons and positrons. As previously noted, the γ-rays, electrons, and positrons trigger an electromagnetic cascade on the CMB, which develops

via repeated e^+e^- pair production and inverse Compton scattering. As a result of this cascade the energy gets recycled yielding a pile up of γ-rays at GeV $\lesssim E_\gamma \lesssim$ TeV, just below the threshold for further pair production on the diffuse optical backgrounds. We have seen that under very reasonable assumptions the energy deposited into neutrinos is comparable to the energy deposited into the electromagnetic cascade. Therefore, the neutrino energy density at the present epoch,

$$\omega_\nu = \int E_\nu \; n_\nu(E_\nu, 0) \; dE_\nu = 2.5 \times 10^{-11} \text{ eV cm}^{-3}, \tag{642}$$

provides reliable estimate of the cascade energy density ($\omega_{\rm cas} \sim \omega_\nu$), which is bounded by *Fermi* LAT data to not exceed $\omega_{\rm cas}^{\rm max} \sim 5.8 \times 10^{-7}$ eV cm^{-3} [102]. We conclude that the γ-ray flux associated with the neutrino line is found to be about 4 orders of magnitude smaller than the observed flux in the *Fermi* LAT region.

We now turn to discuss the possibility of distinguishing the neutrino line from an unbroken power-law spectrum without the neutrino line, with future IceCube data. The value of the spectral index is determined by the "low energy" events. Following the best IceCube fit we adopt a spectrum $\propto E_\nu^{-2.46}$. We assume that the IceCube events below 1 PeV have an astrophysical origin. Indeed, the steep spectrum $\propto E_\nu^{-2.46}$ may suggest we are witnessing the cutoff of TeV neutrino sources running out of power. Using the IceCube aperture for the high-energy starting event (HESE) analysis [276] we compute the event rate per year above 1 PeV for both the neutrino flux given in (1) and that of (632). The results are given in Table 8. As expected, the predictions from X decay are in good agreement with existing data. Because of the smeared energy-dependence of muon tracks, in what follows we will only consider cascades and double bang topologies initiated by charged current interactions of electron and tau neutrinos, as well as all neutral current interactions processes. We identify the events coming from the power law spectrum $\mathcal{N}_{\rm B}$ with background and adopt the standard bump-hunting method to establish the statistical significance of the mono-energetic signal. To remain conservative we define the noise $\equiv \sqrt{\mathcal{N}_{\rm B} + \mathcal{N}_{\rm S}}$, where $\mathcal{N}_{\rm S}$ is the number of signal events. In 10 years

Table 8: Event rates (yr^{-1}) at IceCube for $E_\nu^{\rm min} = 1$ PeV.

$E_\nu^{\rm max}$/PeV	spectrum $\propto E_\nu^{-2.46}$			X decay spectrum		
	ν_e	ν_μ	ν_τ	ν_e	ν_μ	ν_τ
2	0.20	0.18	0.20	0.25	0.23	0.25
3	0.27	0.24	0.27	0.46	0.41	0.46
4	0.31	0.27	0.30	0.58	0.51	0.56
5	0.34	0.29	0.32	0.66	0.56	0.62

of operation the total detection significance,

$$S_{\rm det} = \frac{\mathcal{N}_{\rm S}}{\sqrt{\mathcal{N}_{\rm B} + \mathcal{N}_{\rm S}}}\,, \tag{643}$$

would allow distinguishing the neutrino line from a statistical fluctuation of a power law spectrum $\propto E_\nu^{-2.46}$ at the 3σ level. Note that the shape of the distribution with energy conveys additional information allowing one to distinguish the line signal from fluctuations of a power-law background. The proposed *IceCube-Gen2* extension plans to increase the effective volume of IceCube by about a factor of 10 [103]. This facility will not only increase the HESE sensitivity but also improve the energy resolution for muon tracks. In a few years of operation *IceCube-Gen2* will collect enough statistics to elucidate the dark matter–neutrino connection with $S_{\rm det} > 5\sigma$.

We end with an observation: IceCube data can also be fitted by a neutrino line peaking at $E_\nu \sim 20$ TeV superimposed over a power law spectrum ($\propto E_\nu^{-2}$) of astrophysical neutrinos [104]. By duplicating our discussion for $m_X \sim 1$ PeV it is straightforward to see that the model can also accommodate this neutrino line.

Taking all of this into account, we have shown that the PeV flux of extraterrestrial neutrinos recently reported by the IceCube Collaboration can originate through the decay of heavy dark matter particles with a mass $\simeq 560$ PeV and a lifetime $\simeq 3 \times 10^{14}$ s. On a separate track, the tension between *Planck* data and low redshift astronomical measurements can be resolved if about 7% of the CDM component at CMB epoch is unstable. Assuming that such a fraction of quasi-stable relics is responsible for the IceCube flux we determined the neutrino branching fraction, $\mathcal{B}_{X\to\nu\bar{\nu}} \sim 5 \times 10^{-8}$. The model has no free parameters and will be tested by future IceCube data. Indeed 10 years of data taking

will be required to distinguish the neutrino line from an unbroken power-law spectrum at the 3σ level. The upgraded *IceCube-Gen2* will collect enough statistics to elucidate the dark matter-neutrino connection at the 5σ discovery level in a few years of operation.

References

[1] "IceCube neutrinos, decaying dark matter, and the Hubble constant" L. A. Anchordoqui, V. Barger, H. Goldberg, X. Huang, D. Marfatia, **L. H. M. da Silva** and T.J.Weiler; ***Physical Review D - Rapid Communication*** 92, 061301(R)

[2] "Majorana dark matter through the Higgs portal under the vacuum stability lamppost," L. A. Anchordoqui, V. Barger, H. Goldberg, X. Huang, D. Marfatia, **L. H. M. da Silva** and T.J.Weiler; ***Physical Review D*** 92, 063504

[3] "Estimating the Contribution of Galactic Sources to the Diffuse Neutrino Flux," L. A. Anchordoqui, H. Goldberg, T. C. Paul, **L. H. M. da Silva** and B. Vlcek; ***Physical Review D*** 90, 123010.

[4] "What IceCube Data Tell Us About Neutrino Emission from Star-Forming Galaxies," L. A. Anchordoqui, T. C. Paul, **L. H. M da Silva**, D. F. Torres and B. Vlcek; ***Physical Review D*** 89, 127304.

[5] "Weinberg's Higgs Portal Confronting Recent LUX and LHC Results Together with Upper Limits on B^+ and K^+ Decay Into Invisibles," L. A. Anchordoqui, P. B. Denton, H. Goldberg, T. C. Paul, **L. H. M. da Silva**, B. Vlcek and T. J. Weiler; ***Physical Review D*** 89, 083513.

[6] Luis Anchordoqui, Francis Halzen (2011),"Lessons in Particle Physics", [arXiv:0906.1271]

[7] Matthew Robinson, "Symmetry and the Standard Model" (2011), ISBN 978-1-4419-8266-7, DOI 10.1007/978-1-4419-8267-4, Springer New York Dordrecht Heidelberg London

[8] Carlo Giunti, Chung W. Kim, "Fundamentals of Neutrino Physics and Astrophysics" (2007), ISBN 978-0-19-850871-7, Oxford University Press 2007

[9] Robert Wald, "General relativity" (1984), ISBN 0-226-87033-2, The University of Chicago Press

[10] Michael E. Peskin, Daniel V.Schroeder, "Introduction to Quantum Field Theory" (1995), ISBN 0-201-50397-2, Addison-Wesley Publishing Company

[11] David Griffiths, "Introduction to elementary particles" (1987), ISBN 0-471-60386-4, John Wiley and Sons, Inc

[12] Edward W. Kolb, Michael S. Turner, "The Early Universe" (1994), ISBN-13: 978-0201626742, Westview Press

[13] Sadri Hassini, "Mathematical Physics", Second Edition (2013), ISBN 978-3-319-01194-3, Springer

[14] Scott Dodelson, "Modern Cosmology" (2003), ISBN-13: 978-0-12-219141-1, Academic Press

[15] Raymond F. Streater, Arthur S. Wightman, "PCT, Spin, Statistics and All That", (2010), ISBN-13: 978-0691070629, Princeton University Press.

[16] Nouredine Zettili, "Quantum Mechanics: Concepts and Applications", Second edition (2009), ISBN-13: 978-0470026793, Wiley.

[17] Thomas K. Gaisser, "Cosmic rays and particle physics", (1991), ISBN-13: 978-0521339315, Cambridge University Press.

[18] Raymond F. Streater, Arthur S. Wightman, "PCT, Spin, Statistics and All That", (2010), ISBN-13: 978-0691070629, Princeton University Press.

[19] Nouredine Zettili, "Quantum Mechanics: Concepts and Applications", Second edition (2009), ISBN-13: 978-0470026793, Wiley.

[20] Michio Kaku, "Quantum Field Theory", (1993), ISBN 0-19-507652-4, Oxford University Press.

[21] B. Delamotte, "A hint of renormalization", Am.J.Phys. 72 (2004) 170-184

[22] Michio Kaku, "Quantum Field Theory" (1993), ISBN 0-19-507652-4

[23] Jeffrey Goldstone, Abdus Salam, and Steven Weinberg, Phys. Rev. 127, 965

[24] Sheldon L. Glashow, "Resonant Scattering of Antineutrinos", Phys. Rev. 118, 316

[25] Luis A. Anchordoqui, Ignatios Antoniadis, Haim Goldberg, Xing Huang, Dieter Lust, Tomasz R. Taylor, 750 GeV diphotons from closed string states, arXiv:1512.08502.

[26] Luis A. Anchordoqui, Ignatios Antoniadis, Haim Goldberg, Xing Huang, Dieter Lust, Tomasz R. Taylor, Update on 750 GeV diphotons from closed string states, arXiv:1603.08294.

[27] M. G.Aartsen et al. (IceCubeCollaboration), arXiv:1405.5303

[28] IceCube Collaboration, Search for Astrophysical Tau Neutrinos in Three Years of IceCube Data, Phys. Rev. D 93, 022001 (2016)

[29] IceCube Collaboration, IceCube Preliminary Design Document (2011)

[30] D. F. Cowen for the IceCube Collaboration, Tau Neutrinos in IceCube

[31] IceCube Collaboration, Energy Reconstruction Methods in the IceCube Neutrino Telescope, INST 9 (2014), P03009

[32] K.A. Olive et al. (Particle Data Group), Chin. Phys. C, 38, 090001 (2014) and 2015 update

[33] H. L. Lai et al. Global QCD analysis of parton structure of the nucleon: CTEQ5 parton distributions. Eur. Phys. J., C12:375-392 (2000)

[34] CTEQ: The Coordinated Theoretical-Experimental Project on QCD. http://www.phys.psu.edu/ cteq/

[35] R. Gandhi, C. Quigg, M. H. Reno, and I. Sarcevic. Neutrino interactions at ultra-highenergies. Phys. Rev., D58:093009 (1998)

[36] F. Reines and C. L. Cowan. Detection of the free neutrino. Phys. Rev., 92:830-831, 1953. C. L. Cowan, F. Reines, F. B. Harrison, H. W. Kruse, and A. D. McGuire. Detection of the free neutrino: A Confirmation. Science, 124:103-104, 1956.

[37] Mead, C. A., "Quantum Theory of the Refractive Index". Physical Review 110 (2): 359 (1958)

[38] LIGO Scientific Collaboration and Virgo Collaboration, Observation of Gravitational Waves from a Binary Black Hole Merger, PRL 116, 061102 (2016)

[39] ANTARES Collaboration, IceCube Collaboration, LIGO Scientific Collaboration, Virgo Collaboration, High-energy Neutrino follow-up search of Gravitational Wave Event GW150914 with ANTARES and IceCube, arXiv:1602.05411v2.

[40] Planck 2015 results. XIII. Cosmological parameters, arXiv:1502.01589

[41] Eli Waxman and John Bahcall, "High Energy Neutrinos from Astrophysical Sources: An Upper Bound", Eli Waxman and John Bahcall, Phys.Rev.D59:023002 (1999)

[42] K. Greisen, Phys. Rev. Lett. 16, 748 (1966); G. T. Zatsepin and V. A. Kuzmin, Pis'ma ZhZhurnal Eksperimental noi i Teoreticheskoi Fiziki 4, 114 (1966), JETP Lett. 4, 78 (1966) (Engl. Transl.).

[43] H. Bethe, "The electromagnetic shift of energy levels", Phys. Rev. 72, 339-341 (1947)

[44] V. Barger, J. Learned and S. Pakvasa, arXiv:1207.4571 [astro-ph.HE]

[45] E. Roulet, G. Sigl, A. van Vliet and S. Mollerach, JCAP 1301, 028 (2013), arXiv:1209.4033

[46] F.J. Hasert; et al. (1973). "Search for elastic muon-neutrino electron scattering". Physics Letters B 46 (1): 121. F.J. Hasert; et al. (1973). "Observation of neutrino-like interactions without muon or electron in the Gargamelle neutrino experiment". Physics Letters B 46 (1): 138.

[47] S.L. Glashow (1961). Nuclear Physics 22 (4): 579-588.

[48] S. Weinberg (1967). "A Model of Leptons". Physical Review Letters 19 (21): 1264-1266. A. Salam (1968). N. Svartholm, ed. Elementary Particle Physics: Relativistic

Groups and Analyticity. Eighth Nobel Symposium. Stockholm: Almquvist and Wiksell. p. 367.

[49] Wu, C. S.; Ambler, E; Hayward, R. W.; Hoppes, D. D.; Hudson, R. P (1957). "Experimental Test of Parity Conservation in beta Decay". Physical Review 105 (4): 1413-1415.

[50] NA48 Collaboration, V. Fanti, A. Lai, D. Marras, L. Musa; et al. (1999). "A new measurement of direct CP violation in two pion decays of the neutral kaon". Physics Letters B 465 (1-4): 335-348.

[51] 3S. S. Gershtein and Y. B. Zel'dovich, Zh. Eksp. Teor. Fiz. 29, 698 (1955); R. P. Feynman and M. Gell-Mann, Phys. Rev. 109, 193 (1958); E. C. G. Sudarshan and R. E. Marshak, Phys. Rev. 109, 1860 (1958); J. J. Sakurai, Nuovo Cim. 7, 649 (1958).

[52] C. Amsler et al. Review of particle physics. Phys. Lett., B667:1, 2008

[53] F. J. Hasert et al. [Gargamelle Neutrino Collaboration], Phys. Lett. B 46, 138 (1973)

[54] 30M. Apollonio et al. [CHOOZ Collaboration], Phys. Lett. B 466, 415 (1999); S. M. Bilenky, D. Nicolo and S. T. Petcov, Phys. Lett. B 538, 77 (2002)

[55] M. C. Gonzalez-Garcia and M. Maltoni, Phys. Rept. 460, 1 (2008)

[56] Particle Physics (from lecture notes), Prof. M.A. Thomson, Cambridge University.

[57] V. Barger, J. Learned, S. Pakvasa, "IceCube PeV Cascade Events Initiated by Electron-Antineutrinos at Glashow Resonance", [arXiv:1207.4571v2]

[58] Tasi Lectures on inflation, arXiv:0907.5424 [hep-th]

[59] Consistency with Upper Limits on the Diffuse Gamma Ray Flux

[60] F. Zwicky, Helv. Phys. Acta 6, 110 (1933); V. C. Rubin, N. Thonnard and W. K. . Ford, Astrophys. J. 238, 471 (1980); K. G. Begeman, A. H. Broeils and R. H. Sanders, Mon. Not. Roy. Astron. Soc. 249, 523 (1991)

[61] Clemens (1985), Ap. J. 295, 422.

[62] A.G. Riess et al., "Observational evidence from supernovae for an accelerating universe and a cosmological constant", Astron. J., 116, 1009-1038, (1998)

[63] S. Perlmutter et al., "Measurement of Ω and Λ from 42 high-redshift supernovae", Astrophys. J., 517, 565-586, (1999)

[64] A.G. Riess et al., "Type Ia supernova discoveries at z ¿1 from the Hubble Space Telecope: Evidence for past deceleration and constraints on dark energy evolution", Astrophys. J., 607, 665-687, (2004)

[65] D. Larson et al. [WMAP Collaboration], Astrophys. J. Suppl. 192, 16 (2011)

[66] G. Bertone, D. Hooper and J. Silk, Phys. Rept. 405, 279 (2005); J. L. Feng, Annals Phys. 315, 2 (2005)

[67] Luis A. Anchordoqui, Vernon Barger, Ilias Cholis, Haim Goldberg, Dan Hooper, Alexander Kusenko, John G. Learned, Danny Marfatia, Sandip Pakvasa, Thomas C. Paul, Thomas J. Weiler, "Cosmic Neutrino Pevatrons: A Brand New Pathway to Astronomy, Astrophysics, and Particle Physics", [arXiv:1312.6587v3]

[68] A. M. Hillas, Ann. Rev. Astron. Astrophys. 22, 425 (1984)

[69] J. G. Learned and K. Mannheim. High-energy neutrino astrophysics. Ann. Rev. Nucl. Part. Sci., 50:679-749, 2000.

[70] Michelangelo Vincent D'Agostino, "First Evidence For Atmospheric Neutrino-Induced Cascades with the IceCube Detector", Ph.D. Dissertation, University of California, Berkeley

[71] Luis A. Anchordoqui, "Exploring the Universe beyond the Photon Window", Acta Phys.Polon. B36 (2005) 495-508

[72] Y. Fukuda *et al.* [Super-Kamiokande Collaboration], Phys. Lett. B **433**, 9 (1998); Phys. Rev. Lett. **81**, 1562 (1998); S. Fukuda *et al.* [Super-Kamiokande Collabora-

tion], Phys. Rev. Lett. **85**, 3999 (2000); Y. Ashie *et al.* [Super-Kamiokande Collaboration], Phys. Rev. D **71**, 112005 (2005).

[73] H. Bethe, "The electromagnetic shift of energy levels", Phys. Rev. 72, 339-341 (1947)

[74] K. G. Wilson and J. Kogut, "The renormalization group and the ϵ-expansion", Phys. Rep. C 12, 75-199 (1974)

[75] M. G. Aartsen *et al.* [IceCube Collaboration], Phys. Rev. Lett. **111**, 021103 (2013) [arXiv:1304.5356]; M. G. Aartsen *et al.* [IceCube Collaboration], Science **342**, 1242856 (2013) [arXiv:1311.5238]; M. G. Aartsen *et al.* [IceCube Collaboration], Phys. Rev. Lett. **113**, 101101 (2014) [arXiv:1405.5303 [astro-ph.HE]].

[76] Z. Berezhiani, A. D. Dolgov and I. I. Tkachev, arXiv:1505.03644 [astro-ph.CO].

[77] H. Goldberg and L. J. Hall, Phys. Lett. B **174**, 151 (1986).

[78] K. Petraki, L. Pearce and A. Kusenko, JCAP **1407**, 039 (2014) [arXiv:1403.1077 [hep-ph]]; R. Foot and S. Vagnozzi, Phys. Rev. D **91**, 023512 (2015) [arXiv:1409.7174 [hep-ph]]. See also, J. Fan, A. Katz, L. Randall and M. Reece, Phys. Dark Univ. **2**, 139 (2013) [arXiv:1303.1521 [astro-ph.CO]].

[79] E. J. Chun, J. C. Park and S. Scopel, JHEP **1102**, 100 (2011) [arXiv:1011.3300 [hep-ph]]; S. Cassel, D. M. Ghilencea and G. G. Ross, Nucl. Phys. B **827**, 256 (2010) [arXiv:0903.1118 [hep-ph]]; V. Barger, D. Marfatia and A. Peterson, Phys. Rev. D **87**, 015026 (2013) [arXiv:1206.6649 [hep-ph]]; A. Alves, S. Profumo and F. S. Queiroz, JHEP **1404**, 063 (2014) [arXiv:1312.5281 [hep-ph]].

[80] S. L. Glashow, Phys. Rev. **118**, 316 (1960).

[81] V. Barger, L. Fu, J. G. Learned, D. Marfatia, S. Pakvasa and T. J. Weiler, Phys. Rev. D **90**, 121301 (2014) [arXiv:1407.3255 [astro-ph.HE]]; L. A. Anchordoqui, H. Goldberg, T. C. Paul, L. H. M. da Silva and B. J. Vlcek, Phys. Rev. D **90**, 123010 (2014) [arXiv:1410.0348 [astro-ph.HE]].

[82] M. G. Aartsen *et al.* [IceCube Collaboration], Phys. Rev. D **91**, 022001 (2015) [arXiv:1410.1749 [astro-ph.HE]].

[83] E. Waxman and J. N. Bahcall, Phys. Rev. D **59**, 023002 (1999) [hep-ph/9807282].

[84] L. A. Anchordoqui, V. Barger, I. Cholis, H. Goldberg, D. Hooper, A. Kusenko, J. G. Learned, D. Marfatia, S. Pakvasa, T. C. Paul, and T. J. Weiler JHEAp **1-2**, 1 (2014) [arXiv:1312.6587 [astro-ph.HE]].

[85] M. Ackermann *et al.* [Fermi-LAT Collaboration], Astrophys. J. **799**, 86 (2015) [arXiv:1410.3696 [astro-ph.HE]].

[86] K. Murase, M. Ahlers and B. C. Lacki, Phys. Rev. D **88**, 121301 (2013) [arXiv:1306.3417 [astro-ph.HE]].

[87] L. A. Anchordoqui, H. Goldberg, M. H. Lynch, A. V. Olinto, T. C. Paul and T. J. Weiler, Phys. Rev. D **89**, 083003 (2014) [arXiv:1306.5021 [astro-ph.HE]].

[88] M. Ahlers and K. Murase, Phys. Rev. D **90**, 023010 (2014) [arXiv:1309.4077 [astro-ph.HE]].

[89] B. Feldstein, A. Kusenko, S. Matsumoto and T. T. Yanagida, Phys. Rev. D **88**, 015004 (2013) [arXiv:1303.7320 [hep-ph]].

[90] A. Esmaili and P. D. Serpico, JCAP **1311**, 054 (2013) [arXiv:1308.1105 [hep-ph]]; Y. Bai, R. Lu and J. Salvado, arXiv:1311.5864 [hep-ph]. A. Bhattacharya, M. H. Reno and I. Sarcevic, JHEP **1406**, 110 (2014) [arXiv:1403.1862 [hep-ph]]; C. Rott, K. Kohri and S. C. Park, arXiv:1408.4575 [hep-ph]; A. Esmaili, S. K. Kang and P. D. Serpico, JCAP **1412**, 054 (2014) [arXiv:1410.5979 [hep-ph]]; E. Dudas, Y. Mambrini and K. A. Olive, Phys. Rev. D **91**, 075001 (2015) [arXiv:1412.3459 [hep-ph]]; K. Murase, R. Laha, S. Ando and M. Ahlers, arXiv:1503.04663 [hep-ph]; M. Ahlers, Y. Bai, V. Barger and R. Lu, arXiv:1505.03156 [hep-ph]; A. Esmaili and P. D. Serpico, arXiv:1505.06486 [hep-ph].

[91] Y. Ema, R. Jinno and T. Moroi, Phys. Lett. B **733**, 120 (2014) [arXiv:1312.3501 [hep-ph]]; Y. Ema, R. Jinno and T. Moroi, JHEP **1410**, 150 (2014) [arXiv:1408.1745 [hep-ph]].

[92] P. A. R. Ade *et al.* [Planck Collaboration], arXiv:1502.01589 [astro-ph.CO].

[93] A. G. Riess *et al.*, Astrophys. J. **730**, 119 (2011) [Astrophys. J. **732**, 129 (2011)] [arXiv:1103.2976 [astro-ph.CO]].

[94] W. L. Freedman, B. F. Madore, V. Scowcroft, C. Burns, A. Monson, S. E. Persson, M. Seibert and J. Rigby, Astrophys. J. **758**, 24 (2012) [arXiv:1208.3281 [astro-ph.CO]].

[95] S. H. Suyu *et al.*, Astrophys. J. **766**, 70 (2013) [arXiv:1208.6010 [astro-ph.CO]].

[96] M. Rigault *et al.*, Astrophys. J. **802**, no. 1, 20 (2015) [arXiv:1412.6501 [astro-ph.CO]]. See, however, D. O. Jones, A. G. Riess and D. M. Scolnic, arXiv:1506.02637 [astro-ph.CO].

[97] K. R. Dienes and B. Thomas, Phys. Rev. D **85**, 083523 (2012) [arXiv:1106.4546 [hep-ph]].

[98] C. Angrick, F. Pace, M. Bartelmann and M. Roncarelli, arXiv:1504.03187 [astro-ph.CO].

[99] P. A. R. Ade *et al.* [Planck Collaboration], arXiv:1502.01597 [astro-ph.CO].

[100] H. Böhringer, G. Chon and C. A. Collins, Astron. Astrophys. **570**, A31 (2014) [arXiv:1403.2927 [astro-ph.CO]].

[101] T. J. Weiler, Phys. Rev. Lett. **49**, 234 (1982).

[102] V. Berezinsky, A. Gazizov, M. Kachelriess and S. Ostapchenko, Phys. Lett. B **695**, 13 (2011) [arXiv:1003.1496 [astro-ph.HE]].

[103] M. G. Aartsen *et al.* [IceCube Collaboration], arXiv:1412.5106 [astro-ph.HE].

[104] C. E. Aisati, M. Gustafsson and T. Hambye, arXiv:1506.02657 [hep-ph].

[105] G. Aad *et al.* [ATLAS Collaboration], Phys. Lett. B **716**, 1 (2012) [arXiv:1207.7214 [hep-ex]].

[106] S. Chatrchyan *et al.* [CMS Collaboration], Phys. Lett. B **716**, 30 (2012) [arXiv:1207.7235 [hep-ex]].

[107] G. Altarelli, arXiv:1308.0545 [hep-ph].

[108] J. L. Feng, Ann. Rev. Astron. Astrophys. **48**, 495 (2010) [arXiv:1003.0904 [astro-ph.CO]].

[109] G. Steigman and M. S. Turner, Nucl. Phys. B **253**, 375 (1985).

[110] R. Bernabei *et al.*, Phys. Lett. B **424** 195 (1998).

[111] R. Bernabei *et al.*, Eur. Phys. J. C **67** 39 (2010) [arXiv:1002.1028 [astro-ph.GA]].

[112] A. K. Drukier, K. Freese and D. N. Spergel, Phys. Rev. D **33** 3495 (1986).

[113] K. Freese, J. A. Frieman and A. Gould, Phys. Rev. D **37** 3388 (1988).

[114] G. Angloher *et al.*, Eur. Phys. J. C **72**, 1971 (2012) [arXiv:1109.0702 [astro-ph.CO]].

[115] C. E. Aalseth *et al.* [CoGeNT Collaboration], Phys. Rev. Lett. **106**, 131301 (2011) [arXiv:1002.4703 [astro-ph.CO]].

[116] C. E. Aalseth *et al.* [CoGeNT Collaboration], Phys. Rev. Lett. **107** 141301 (2011) [arXiv:1106.0650 [astro-ph.CO]].

[117] C. E. Aalseth *et al.* [CoGeNT Collaboration], Phys. Rev. D **88**, 012002 (2013) [arXiv:1208.5737 [astro-ph.CO]].

[118] R. Agnese *et al.* [CDMS Collaboration], Phys. Rev. Lett. **111**, 251301 (2013) [arXiv:1304.4279 [hep-ex]].

[119] J. Angle *et al.* [XENON10 Collaboration], Phys. Rev. Lett. **107**, 051301 (2011) [arXiv:1104.3088 [astro-ph.CO]].

[120] E. Aprile *et al.* [XENON100 Collaboration], Phys. Rev. Lett. **107**, 131302 (2011) [arXiv:1104.2549 [astro-ph.CO]].

[121] R. Agnese *et al.*, arXiv:1309.3259 [physics.ins-det].

[122] D. S. Akerib *et al.* [LUX Collaboration], arXiv:1310.8214 [astro-ph.CO].

[123] A. Kurylov and M. Kamionkowski, Phys. Rev. D **69**, 063503 (2004) [hep-ph/0307185].

[124] F. Giuliani, Phys. Rev. Lett. **95**, 101301 (2005) [hep-ph/0504157].

[125] J. L. Feng, J. Kumar, D. Marfatia and D. Sanford, Phys. Lett. B **703**, 124 (2011) [arXiv:1102.4331 [hep-ph]].

[126] M. T. Frandsen, F. Kahlhoefer, C. McCabe, S. Sarkar and K. Schmidt-Hoberg, JCAP **1307**, 023 (2013) [arXiv:1304.6066 [hep-ph]].

[127] J. L. Feng, J. Kumar and D. Sanford, Phys. Rev. D **88**, 015021 (2013) [arXiv:1306.2315 [hep-ph]].

[128] M. I. Gresham and K. M. Zurek, arXiv:1311.2082 [hep-ph].

[129] E. Del Nobile, G. B. Gelmini, P. Gondolo and J. -H. Huh, arXiv:1311.4247 [hep-ph].

[130] V. Cirigliano, M. L. Graesser, G. Ovanesyan and I. M. Shoemaker, arXiv:1311.5886 [hep-ph].

[131] G. Aad *et al.* [ATLAS Collaboration], Phys. Lett. B **710**, 49 (2012) [arXiv:1202.1408 [hep-ex]].

[132] S. Chatrchyan *et al.* [CMS Collaboration], Phys. Lett. B **710**, 26 (2012) [arXiv:1202.1488 [hep-ex]].

[133] G. Aad *et al.* [ATLAS Collaboration], Phys. Lett. B **726**, 88 (2013) [Phys. Lett. B **734**, 406 (2014)] [arXiv:1307.1427 [hep-ex]].

[134] S. Chatrchyan *et al.* [CMS Collaboration], Phys. Rev. D **89**, 092007 (2014) [arXiv:1312.5353 [hep-ex]].

[135] G. Aad *et al.* [ATLAS Collaboration], Phys. Rev. D **90**, 052004 (2014) [arXiv:1406.3827 [hep-ex]].

[136] V. Khachatryan *et al.* [CMS Collaboration], Eur. Phys. J. C **74**, 3076 (2014) [arXiv:1407.0558 [hep-ex]].

[137] M. Lindner, M. Sher and H. W. Zaglauer, Phys. Lett. B **228**, 139 (1989).

[138] M. Sher, Phys. Rept. **179**, 273 (1989).

[139] M. A. Diaz, T. A. ter Veldhuis and T. J. Weiler, Phys. Rev. Lett. **74**, 2876 (1995) [hep-ph/9408319].

[140] J. A. Casas, J. R. Espinosa and M. Quiros, Phys. Lett. B **342**, 171 (1995) [hep-ph/9409458].

[141] M. A. Diaz, T. A. ter Veldhuis and T. J. Weiler, Phys. Rev. D **54**, 5855 (1996) [hep-ph/9512229].

[142] J. A. Casas, J. R. Espinosa and M. Quiros, Phys. Lett. B **382**, 374 (1996) [hep-ph/9603227].

[143] G. Isidori, G. Ridolfi and A. Strumia, Nucl. Phys. B **609**, 387 (2001) [hep-ph/0104016].

[144] G. Isidori, V. S. Rychkov, A. Strumia and N. Tetradis, Phys. Rev. D **77**, 025034 (2008) [arXiv:0712.0242 [hep-ph]].

[145] L. J. Hall and Y. Nomura, JHEP **1003**, 076 (2010) [arXiv:0910.2235 [hep-ph]].

[146] J. Ellis, J. R. Espinosa, G. F. Giudice, A. Hoecker and A. Riotto, Phys. Lett. B **679**, 369 (2009) [arXiv:0906.0954 [hep-ph]].

[147] J. Elias-Miro, J. R. Espinosa, G. F. Giudice, G. Isidori, A. Riotto and A. Strumia, Phys. Lett. B **709**, 222 (2012) [arXiv:1112.3022 [hep-ph]].

[148] F. Bezrukov, M. Y. Kalmykov, B. A. Kniehl and M. Shaposhnikov, JHEP **1210**, 140 (2012) [arXiv:1205.2893 [hep-ph]].

[149] G. Degrassi, S. Di Vita, J. Elias-Miro, J. R. Espinosa, G. F. Giudice, G. Isidori and A. Strumia, JHEP **1208**, 098 (2012) [arXiv:1205.6497 [hep-ph]].

[150] D. Buttazzo, G. Degrassi, P. P. Giardino, G. F. Giudice, F. Sala, A. Salvio and A. Strumia, JHEP **1312**, 089 (2013) [arXiv:1307.3536 [hep-ph]].

[151] V. Branchina and E. Messina, Phys. Rev. Lett. **111**, 241801 (2013) [arXiv:1307.5193 [hep-ph]].

[152] V. Branchina, E. Messina and M. Sher, Phys. Rev. D **91**, 013003 (2015) [arXiv:1408.5302 [hep-ph]].

[153] Z. Lalak, M. Lewicki and P. Olszewski, JHEP **1405**, 119 (2014) [arXiv:1402.3826 [hep-ph]].

[154] L. Basso, S. Moretti and G. M. Pruna, Phys. Rev. D **82**, 055018 (2010) [arXiv:1004.3039 [hep-ph]].

[155] M. Kadastik, K. Kannike, A. Racioppi and M. Raidal, JHEP **1205**, 061 (2012) [arXiv:1112.3647 [hep-ph]].

[156] J. Elias-Miro, J. R. Espinosa, G. F. Giudice, H. M. Lee and A. Strumia, JHEP **1206**, 031 (2012) [arXiv:1203.0237 [hep-ph]].

[157] C. Cheung, M. Papucci and K. M. Zurek, JHEP **1207**, 105 (2012) [arXiv:1203.5106 [hep-ph]].

[158] L. A. Anchordoqui, I. Antoniadis, H. Goldberg, X. Huang, D. Lust, T. R. Taylor and B. Vlcek, JHEP **1302**, 074 (2013) [arXiv:1208.2821 [hep-ph]].

[159] S. Baek, P. Ko, W. I. Park and E. Senaha, JHEP **1211**, 116 (2012) [arXiv:1209.4163 [hep-ph]].

[160] W. Chao, M. Gonderinger and M. J. Ramsey-Musolf, Phys. Rev. D **86**, 113017 (2012) [arXiv:1210.0491 [hep-ph]].

[161] C. Coriano, L. Delle Rose and C. Marzo, Phys. Lett. B **738**, 13 (2014) [arXiv:1407.8539 [hep-ph]].

[162] W. Altmannshofer, W. A. Bardeen, M. Bauer, M. Carena and J. D. Lykken, JHEP **1501**, 032 (2015) [arXiv:1408.3429 [hep-ph]].

[163] A. Falkowski, C. Gross and O. Lebedev, JHEP **1505**, 057 (2015) [arXiv:1502.01361 [hep-ph]].

[164] J. Krog and C. T. Hill, arXiv:1506.02843 [hep-ph].

[165] L. D. Rose, C. Marzo and A. Urbano, arXiv:1506.03360 [hep-ph].

[166] B.W. Lee and S. Weinberg, Phys. Rev. Lett. 39, 165 (1977).

[167] D. A. Dicus, E.W. Kolb, and V. L. Teplitz, Phys. Rev. Lett. 39, 168 (1977); 39, 973(E) (1977).

[168] E.W. Kolb and K. A. Olive, Phys. Rev. D 33, 1202 (1986); 34, 2531(E) (1986).

[169] R. J. Scherrer and M. S. Turner, Phys. Rev. D 33, 1585 (1986); 34, 3263(E) (1986).

[170] G. Steigman, B. Dasgupta, and J. F. Beacom, Phys. Rev. D 86, 023506 (2012).

[171] J. Beringer et al. (Particle Data Group), PR D86, 010001 (2012) (URL: http://pdg.lbl.gov)

[172] J. L. Feng, Ann. Rev. Astron. Astrophys. **48**, 495 (2010) [arXiv:1003.0904 [astro-ph.CO]].

[173] R. Schabinger and J. D. Wells, Phys. Rev. D **72**, 093007 (2005) [hep-ph/0509209].

[174] B. Patt and F. Wilczek, hep-ph/0605188.

[175] V. Barger, P. Langacker, M. McCaskey, M. J. Ramsey-Musolf and G. Shaughnessy, Phys. Rev. D **77**, 035005 (2008) [arXiv:0706.4311 [hep-ph]].

[176] V. Barger, P. Langacker, M. McCaskey, M. Ramsey-Musolf and G. Shaughnessy, Phys. Rev. D **79**, 015018 (2009) [arXiv:0811.0393 [hep-ph]].

[177] L. M. Krauss and F. Wilczek, Phys. Rev. Lett. **62**, 1221 (1989).

[178] S. Weinberg, Phys. Rev. Lett. **110**, 241301 (2013) [arXiv:1305.1971 [astro-ph.CO]].

[179] P. Sikivie, Phys. Rev. Lett. **48**, 1156 (1982).

[180] A. Vilenkin and A. E. Everett, Phys. Rev. Lett. **48**, 1867 (1982).

[181] M. S. Turner and F. Wilczek, Phys. Rev. Lett. **66**, 5 (1991).

[182] G. R. Dvali, Phys. Lett. B **265**, 64 (1991).

[183] T. Hiramatsu, M. Kawasaki, K. 'i. Saikawa and T. Sekiguchi, JCAP **1301**, 001 (2013) [arXiv:1207.3166 [hep-ph]].

[184] J. R. Ellis, A. Ferstl and K. A. Olive, Phys. Lett. B **481**, 304 (2000) [hep-ph/0001005].

[185] M. Beltran, D. Hooper, E. W. Kolb and Z. C. Krusberg, Phys. Rev. D **80**, 043509 (2009) [arXiv:0808.3384 [hep-ph]].

[186] R. J. Hill and M. P. Solon, Phys. Rev. D **91**, 043505 (2015) [arXiv:1409.8290 [hep-ph]]. See, in particular, Table 10.

[187] P. Junnarkar and A. Walker-Loud, Phys. Rev. D **87**, 114510 (2013) [arXiv:1301.1114 [hep-lat]].

[188] L. A. Anchordoqui and B. J. Vlcek, Phys. Rev. D **88**, 043513 (2013) [arXiv:1305.4625 [hep-ph]].

[189] K. A. Olive *et al.* [Particle Data Group Collaboration], Chin. Phys. C **38**, 090001 (2014).

[190] C. Garcia-Cely, A. Ibarra and E. Molinaro, JCAP **1311**, 061 (2013) [arXiv:1310.6256 [hep-ph]].

[191] P. Gondolo and G. Gelmini, Nucl. Phys. B **360**, 145 (1991).

[192] K. Griest and M. Kamionkowski, Phys. Rev. Lett. **64**, 615 (1990).

[193] K. Blum, Y. Cui and M. Kamionkowski, arXiv:1412.3463 [hep-ph].

[194] D. S. Akerib *et al.* [LUX Collaboration], Phys. Rev. Lett. **112**, 091303 (2014) [arXiv:1310.8214 [astro-ph.CO]].

[195] R. Agnese *et al.* [SuperCDMS Collaboration], Phys. Rev. Lett. **112**, 241302 (2014) [arXiv:1402.7137 [hep-ex]].

[196] K. Choi *et al.* [Super-Kamiokande Collaboration], Phys. Rev. Lett. **114**, 141301 (2015) [arXiv:1503.04858 [hep-ex]].

[197] K. Schmidt-Hoberg, F. Staub and M. W. Winkler, Phys. Lett. B **727**, 506 (2013) [arXiv:1310.6752 [hep-ph]].

[198] J. D. Clarke, R. Foot and R. R. Volkas, JHEP **1402**, 123 (2014) [arXiv:1310.8042 [hep-ph]].

[199] L. A. Anchordoqui, P. B. Denton, H. Goldberg, T. C. Paul, L. H. M. Da Silva, B. J. Vlcek and T. J. Weiler, Phys. Rev. D **89**, 083513 (2014) [arXiv:1312.2547 [hep-ph]].

[200] P. del Amo Sanchez *et al.* [BaBar Collaboration], Phys. Rev. Lett. **107**, 021804 (2011) [arXiv:1007.4646 [hep-ex]].

[201] F. P. Huang, C. S. Li, D. Y. Shao and J. Wang, arXiv:1307.7458 [hep-ph].

[202] B. Aubert *et al.* [BaBar Collaboration], arXiv:0808.0017 [hep-ex].

[203] J. Insler *et al.* [CLEO Collaboration], Phys. Rev. D **81**, 091101 (2010) [arXiv:1003.0417 [hep-ex]].

[204] D. Buskulic *et al.* [ALEPH Collaboration], Phys. Lett. B **313**, 312 (1993).

[205] M. Acciarri *et al.* [L3 Collaboration], Phys. Lett. B **385**, 454 (1996).

[206] G. Alexander *et al.* [OPAL Collaboration], Phys. Lett. B **377**, 273 (1996).

[207] G. Abbiendi *et al.* [OPAL Collaboration], Eur. Phys. J. C **27**, 311 (2003) [hep-ex/0206022].

[208] G. Abbiendi *et al.* [OPAL Collaboration], Phys. Lett. B **682**, 381 (2010) [arXiv:0707.0373 [hep-ex]].

[209] K. Cheung, W. Y. Keung and T. C. Yuan, Phys. Rev. D **89**, 015007 (2014) [arXiv:1308.4235 [hep-ph]].

[210] B. Aubert *et al.* [BaBar Collaboration], Phys. Rev. Lett. **94**, 101801 (2005) [hep-ex/0411061].

[211] P. del Amo Sanchez *et al.* [BaBar Collaboration], Phys. Rev. D **82**, 112002 (2010) [arXiv:1009.1529 [hep-ex]].

[212] J. P. Lees *et al.* [BaBar Collaboration], Phys. Rev. D **87**, 112005 (2013) [arXiv:1303.7465 [hep-ex]].

[213] T. E. Browder *et al.* [CLEO Collaboration], Phys. Rev. Lett. **86**, 2950 (2001) [hep-ex/0007057].

[214] O. Lutz *et al.* [Belle Collaboration], Phys. Rev. D **87**, 111103 (2013) [arXiv:1303.3719 [hep-ex]].

[215] S. Adler *et al.* [E787 Collaboration], Phys. Rev. Lett. **88**, 041803 (2002) [hep-ex/0111091].

[216] V. V. Anisimovsky *et al.* [E949 Collaboration], Phys. Rev. Lett. **93**, 031801 (2004) [hep-ex/0403036].

[217] S. Adler *et al.* [E949 and E787 Collaborations], Phys. Rev. D **77**, 052003 (2008) [arXiv:0709.1000 [hep-ex]].

[218] A. V. Artamonov *et al.* [BNL-E949 Collaboration], Phys. Rev. D **79**, 092004 (2009) [arXiv:0903.0030 [hep-ex]].

[219] V. Barger, M. Ishida and W. Y. Keung, Phys. Rev. Lett. **108**, 261801 (2012) [arXiv:1203.3456 [hep-ph]].

[220] J. R. Espinosa, M. Muhlleitner, C. Grojean and M. Trott, JHEP **1209**, 126 (2012) [arXiv:1205.6790 [hep-ph]].

[221] K. Cheung, J. S. Lee and P. -Y. Tseng, JHEP **1305**, 134 (2013) [arXiv:1302.3794 [hep-ph]].

[222] P. P. Giardino, K. Kannike, I. Masina, M. Raidal and A. Strumia, JHEP **1405**, 046 (2014) [arXiv:1303.3570 [hep-ph]].

[223] J. Ellis and T. You, JHEP **1306**, 103 (2013) [arXiv:1303.3879 [hep-ph]].

[224] G. G. Raffelt, Phys. Rept. **198**, 1 (1990).

[225] W. Y. Keung, K. W. Ng, H. Tu and T. C. Yuan, Phys. Rev. D **90**, 075014 (2014) [arXiv:1312.3488 [hep-ph]].

[226] V. Khachatryan *et al.* [CMS Collaboration], Eur. Phys. J. C **75**, no. 5, 235 (2015) [arXiv:1408.3583 [hep-ex]].

[227] L. Lopez-Honorez, T. Schwetz and J. Zupan, Phys. Lett. B **716**, 179 (2012) [arXiv:1203.2064 [hep-ph]].

[228] L. Carpenter, A. DiFranzo, M. Mulhearn, C. Shimmin, S. Tulin and D. Whiteson, Phys. Rev. D **89**, 075017 (2014) [arXiv:1312.2592 [hep-ph]].

[229] J. Abdallah *et al.*, arXiv:1506.03116 [hep-ph].

[230] G. Steigman, D.N. Schramm and J.E. Gunn, Phys. Lett. B **66**, 202 (1977).

[231] P. A. R. Ade *et al.* [Planck Collaboration], arXiv:1502.01589 [astro-ph.CO].

[232] G. Mangano, G. Miele, S. Pastor, T. Pinto, O. Pisanti and P. D. Serpico, Nucl. Phys. B **729**, 221 (2005) [hep-ph/0506164].

[233] E. Aver, K. A. Olive, R. L. Porter and E. D. Skillman, JCAP **1311**, 017 (2013) [arXiv:1309.0047 [astro-ph.CO]].

[234] R. Cooke, M. Pettini, R. A. Jorgenson, M. T. Murphy and C. C. Steidel, arXiv:1308.3240 [astro-ph.CO].

[235] K. M. Nollett and G. Steigman, Phys. Rev. D **91**, 083505 (2015) [arXiv:1411.6005 [astro-ph.CO]].

[236] H. Arason, D. J. Castano, B. Keszthelyi, S. Mikaelian, E. J. Piard, P. Ramond and B. D. Wright, Phys. Rev. D **46**, 3945 (1992).

[237] S. Iso, N. Okada and Y. Orikasa, Phys. Lett. B **676**, 81 (2009) [arXiv:0902.4050 [hep-ph]].

[238] J. A. Casas, J. R. Espinosa, M. Quiros and A. Riotto, Nucl. Phys. B **436**, 3 (1995) [Erratum-ibid. B **439**, 466 (1995)] [hep-ph/9407389].

[239] S. Weinberg, Phys. Rev. Lett. **36**, 294 (1976).

[240] A. D. Linde, Phys. Lett. B **62**, 435 (1976).

[241] M. Sher, Phys. Lett. B **317**, 159 (1993) [Phys. Lett. B **331**, 448 (1994)] [hep-ph/9307342].

[242] G. Aad *et al.* [ATLAS Collaboration], Phys. Rev. Lett. **114**, 081802 (2015) [arXiv:1406.5053 [hep-ex]].

[243] V. Khachatryan *et al.* [CMS Collaboration], arXiv:1503.04114 [hep-ex].

[244] J. L. Feng *et al.*, arXiv:1401.6085 [hep-ex].

[245] L. Baudis, Phys. Dark Univ. **4**, 50 (2014) [arXiv:1408.4371 [astro-ph.IM]].

[246] M. G. Aartsen *et al.* [IceCube Collaboration], Phys. Rev. Lett. **111**, 021103 (2013) [arXiv:1304.5356]. Note, however, that a cosmogenic origin of these events is highly unlikely, M. G. Aartsen *et al.* [IceCube Collaboration], Phys. Rev. D **88**, 112008 (2013) [arXiv:1310.5477].

[247] S. Schonert, T. K. Gaisser, E. Resconi and O. Schulz, Phys. Rev. D **79**, 043009 (2009) [arXiv:0812.4308]; T. K. Gaisser, K. Jero, A. Karle and J. van Santen, arXiv:1405.0525.

[248] M. G. Aartsen *et al.* [IceCube Collaboration], Science **342**, 1242856 (2013) [arXiv:1311.5238].

[249] M. G. Aartsen *et al.* [IceCube Collaboration], arXiv:1405.5303.

[250] For a review of other possible origins of the IceCube events see, L. A. Anchordoqui, V. Barger, I. Cholis, H. Goldberg, D. Hooper, A. Kusenko, J. G. Learned and D. Marfatia, S. Pakvasa, T. C. Paul, and T J. Weiler, JHEAp **1-2**, 1 (2014) [arXiv:1312.6587].

[251] R. Abbasi *et al.* [IceCube Collaboration], Phys. Rev. D **84**, 072001 (2011) [arXiv:1101.1692].

[252] J. G. Learned and S. Pakvasa, Astropart. Phys. **3**, 267 (1995) [hep-ph/9405296, hep-ph/9408296].

[253] Neutral current interactions of all ν flavors also produce showers, but with a smaller rate than CC interactions.

[254] S. L. Glashow, Phys. Rev. **118**, 316 (1960).

[255] L. A. Anchordoqui, H. Goldberg, M. H. Lynch, A. V. Olinto, T. C. Paul and T. J. Weiler, Phys. Rev. D **89**, 083003 (2014) [arXiv:1306.5021].

[256] E. Waxman and J. N. Bahcall, Phys. Rev. Lett. **78**, 2292 (1997) [astro-ph/9701231].

[257] R. Abbasi *et al.* [IceCube Collaboration], Nature **484**, 351 (2012) [arXiv:1204.4219].

[258] T. A. D Paglione, A. P. Marscher, J. M. Jackson, and D. L. Bertsch, Astrophys. J. **460**, 295 (1996); V. Pavlidou and B. D. Fields, Astrophys. J. **58**, 63 (2001) [astro-ph/0105207]; D. F. Torres, Astrophys. J. **617**, 966 (2004) [astro-ph/0407240];

E. Domingo-Santamaria and D. F. Torres, Astron. Astrophys. **444**, 403 (2005) [astro-ph/0506240].

[259] A. Loeb and E. Waxman, JCAP **0605**, 003 (2006) [astro-ph/0601695].

[260] K. Murase, M. Ahlers and B. C. Lacki, Phys. Rev. D **88**, 121301 (2013) [arXiv:1306.3417]; I. Tamborra, S. 'i. Ando and K. Murase, arXiv:1404.1189.

[261] R. Abbasi *et al.* [IceCube Collaboration], Phys. Rev. D **83**, 012001 (2011) [arXiv:1010.3980].

[262] A. A. Abdo *et al.* [Fermi-LAT Collaboration], Phys. Rev. Lett. **104**, 101101 (2010) [arXiv:1002.3603]; M. Ackermann, in 4th Fermi Symposium, 2012.

[263] J. P. Rachen and P. Meszaros, Phys. Rev. D **58**, 123005 (1998) [astro-ph/9802280]; T. Kashti and E. Waxman, Phys. Rev. Lett. **95**, 181101 (2005) [astro-ph/0507599].

[264] L. A. Anchordoqui, H. Goldberg, F. Halzen and T. J. Weiler, Phys. Lett. B **621**, 18 (2005) [hep-ph/0410003].

[265] A. Karle, in Phenomenology 2014 Symposium.

[266] H. -N. He, T. Wang, Y. -Z. Fan, S. -M. Liu and D. -M. Wei, Phys. Rev. D **87**, 063011 (2013) [arXiv:1303.1253]; R. -Y. Liu, X. -Y. Wang, S. Inoue, R. Crocker and F. Aharonian, Phys. Rev. D **89**, 083004 (2014) [arXiv:1310.1263].

[267] M. Ackermann *et al.* [Fermi LAT Collaboration], Astrophys. J. **755**, 164 (2012) [arXiv:1206.1346].

[268] Y. Gao and P. M. Solomon, Astrophys. J. **606**, 271 (2004) [astro-ph/0310339]. The only galaxy from the HCN survey not included in the sample is NGC 6921.

[269] M. G. Aartsen, et al., IceCube-Gen2: A Vision for the Future of Neutrino Astronomy in Antarctica arXiv:1412.5106

[270] F. Acero *et al.* [H.E.S.S. Collaboration], Science **326**, 1080 (2009) [arXiv:0909.4651]; V. A. Acciari *et al.* [VERITAS Collaboration], Nature **462**, 770 (2009)

[arXiv:0911.0873]; A. A. Abdo [Fermi LAT Collaboration], Astrophys. J. **709**, L152 (2010) [arXiv:0911.5327].

[271] For detailed models of the gamma ray emission see *e.g.*, Y. Rephaeli, Y. Arieli and M. Persic, Mon. Not. Roy. Astron. Soc. **401**, 423 (2010) [arXiv:0906.1921]; E. d. C. del Pozo, D. F. Torres and A. Y. R. Marrero, Astrophys. J. **698**, 1054 (2009) [arXiv:0901.2688]; M. Persic, Y. Rephaeli and Y. Arieli, Astron. Astrophys. **486**, 143 (2008) [arXiv:0802.0818]; B. C. Lacki, S. Horiuchi and J. F. Beacom, Astrophys. J. **786**, 40 (2014) [arXiv:1206.0772].

[272] L. A. Anchordoqui, G. E. Romero and J. A. Combi, Phys. Rev. D **60**, 103001 (1999) [astro-ph/9903145].

[273] R. U. Abbasi *et al.* [TA Collaboration], arXiv:1404.5890.

[274] G. J. Feldman and R. D. Cousins, Phys. Rev. D **57**, 3873 (1998) [physics/9711021 [physics.data-an]].

[275] K. Fang, T. Fujii, T. Linden and A. V. Olinto, arXiv:1404.6237.

[276] M. G. Aartsen *et al.* [IceCube Collaboration], Phys. Rev. Lett. **111**, 021103 (2013) [arXiv:1304.5356]; M. G. Aartsen *et al.* [IceCube Collaboration], Science **342**, 1242856 (2013) [arXiv:1311.5238]; M. G. Aartsen *et al.* [IceCube Collaboration], arXiv:1405.5303.

[277] S. L. Glashow, Phys. Rev. **118**, 316 (1960).

[278] L. A. Anchordoqui, H. Goldberg, F. Halzen and T. J. Weiler, Phys. Lett. B **621**, 18 (2005) [hep-ph/0410003].

[279] G. J. Feldman and R. D. Cousins, Phys. Rev. D **57**, 3873 (1998) [physics/9711021 [physics.data-an]].

[280] V. Barger, L. Fu, J. G. Learned, D. Marfatia, S. Pakvasa and T. J. Weiler, arXiv:1407.3255 [astro-ph.HE].

[281] J. Abraham *et al.* [Pierre Auger Collaboration], Phys. Lett. B **685**, 239 (2010) [arXiv:1002.1975 [astro-ph.HE]].

[282] L. A. Anchordoqui, G. R. Farrar, J. F. Krizmanic, J. Matthews, J. W. Mitchell, D. Nitz, A. V. Olinto and T. C. Paul *et al.*, arXiv:1307.5312 [astro-ph.HE].

[283] For exotic explanations see e.g., L. A. Anchordoqui, V. Barger, H. Goldberg, J. G. Learned, D. Marfatia, S. Pakvasa, T. C. Paul and T. J. Weiler, Phys. Lett. B **739**, 99 (2014) [arXiv:1404.0622 [hep-ph]]; K. C. Y. Ng and J. F. Beacom, Phys. Rev. D **90**, 065035 (2014) [arXiv:1404.2288 [astro-ph.HE]]; F. W. Stecker and S. T. Scully, Phys. Rev. D **90**, 043012 (2014) [arXiv:1404.7025 [astro-ph.HE]]; J. G. Learned and T. J. Weiler, arXiv:1407.0739 [astro-ph.HE].

[284] K. Murase, M. Ahlers and B. C. Lacki, Phys. Rev. D **88**, 121301 (2013) [arXiv:1306.3417]; I. Tamborra, S. 'i. Ando and K. Murase, arXiv:1404.1189.

[285] L. A. Anchordoqui, V. Barger, I. Cholis, H. Goldberg, D. Hooper, A. Kusenko, J. G. Learned and D. Marfatia, S. Pakvasa, T. C. Paul, and T J. Weiler, JHEAp **1-2**, 1 (2014) [arXiv:1312.6587].

[286] L. A. Anchordoqui, H. Goldberg, F. Halzen and T. J. Weiler, Phys. Lett. B **600**, 202 (2004) [astro-ph/0404387].

[287] A. Loeb and E. Waxman, JCAP **0605**, 003 (2006) [astro-ph/0601695].

[288] L. A. Anchordoqui, T. C. Paul, L. H. M. da Silva, D. F. Torres and B. J. Vlcek, Phys. Rev. D **89**, 127304 (2014) [arXiv:1405.7648 [astro-ph.HE]]; J. B. Tjus, B. Eichmann, F. Halzen, A. Kheirandish and S. M. Saba, arXiv:1406.0506 [astro-ph.HE].

[289] E. Waxman and J. N. Bahcall, Phys. Rev. Lett. **78**, 2292 (1997) [astro-ph/9701231]; K. Murase, K. Ioka, S. Nagataki and T. Nakamura, Astrophys. J. **651**, L5 (2006) [astro-ph/0607104]; I. Cholis and D. Hooper, JCAP **1306**, 030 (2013) [arXiv:1211.1974 [astro-ph.HE]].

[290] K. Murase, S. Inoue and S. Nagataki, Astrophys. J. **689**, L105 (2008) [arXiv:0805.0104 [astro-ph]].

[291] F. Zandanel, I. Tamborra, S. Gabici and S. Ando, arXiv:1410.8697 [astro-ph.HE].

[292] O. E. Kalashev, A. Kusenko and W. Essey, Phys. Rev. Lett. **111**, no. 4, 041103 (2013) [arXiv:1303.0300 [astro-ph.HE]]; F. W. Stecker, Phys. Rev. D **88**, no. 4, 047301 (2013) [arXiv:1305.7404 [astro-ph.HE]]; P. Padovani and E. Resconi, Mon. Not. Roy. Astron. Soc. **443**, 474 (2014) [arXiv:1406.0376 [astro-ph.HE]]; O. Kalashev, D. Semikoz and I. Tkachev, arXiv:1410.8124 [astro-ph.HE]; S. S. Kimura, K. Murase and K. Toma, arXiv:1411.3588 [astro-ph.HE].

[293] M. Ahlers and F. Halzen, arXiv:1406.2160 [astro-ph.HE].

[294] D. B. Fox, K. Kashiyama and P. Mészarós, Astrophys. J. **774**, 74 (2013) [arXiv:1305.6606 [astro-ph.HE]]; A. Neronov, D. V. Semikoz and C. Tchernin, Phys. Rev. D **89**, 103002 (2014) [arXiv:1307.2158 [astro-ph.HE]].

[295] L. A. Anchordoqui, H. Goldberg, M. H. Lynch, A. V. Olinto, T. C. Paul and T. J. Weiler, Phys. Rev. D **89**, 083003 (2014) [arXiv:1306.5021].

[296] S. Razzaque, Phys. Rev. D **88**, 081302 (2013) [arXiv:1309.2756 [astro-ph.HE]].

[297] Y. Bai, A. J. Barger, V. Barger, R. Lu, A. D. Peterson and J. Salvado, arXiv:1407.2243 [astro-ph.HE].

[298] J. Braun, J. Dumm, F. De Palma, C. Finley, A. Karle and T. Montaruli, Astropart. Phys. **29**, 299 (2008) [arXiv:0801.1604 [astro-ph]].

[299] F. A. Aharonian, L. A. Anchordoqui, D. Khangulyan and T. Montaruli, J. Phys. Conf. Ser. **39**, 408 (2006) [astro-ph/0508658].

[300] I. F. Mirabel and L. F. Rodriguez, Nature **371**, 46 (1994).

[301] I. F. Mirabel and L. F. Rodriguez, Ann. Rev. Astron. Astrophys. **37**, 409 (1999) [astro-ph/9902062].

[302] A. A. Lutovinov, M. G. Revnivtsev, S. S. Tsygankov and R. A. Krivonos, arXiv:1302.0728 [astro-ph.HE].

[303] H. J. Grimm, M. Gilfanov and R. Sunyaev, Astron. Astrophys. **391**, 923 (2002) [astro-ph/0109239].

[304] J. S. Clark, P. Reig, S. P. Goodwin, L. M. Larionov, P. Blay, M. J. Coe, J. Fabregat, I. Negueruela, I. Papadakis, I. A. Sttele, Astron. Astrophys. **376**, 476 (2001).

[305] M. V. McSwain, D. R. Gies, W. Huang, P. J. Wiita, D. W. Wingert and L. Kaper, Astrophys. J. **600**, 927 (2004) [astro-ph/0307083].

[306] J. Casares, M. Ribo, I. Ribas, J. M. Paredes, J. Marti and A. Herrero, Mon. Not. Roy. Astron. Soc. **364**, 899 (2005) [astro-ph/0507549].

[307] C. Aragona, M. V. McSwain, E. D. Grundstrom, A. N. Marsh, R. M. Roettenbacher, K. M. Hessler, T. S. Boyajian and P. S. Ray, Astrophys. J. **698**, 514 (2009) [arXiv:0902.4015 [astro-ph.HE]].

[308] G. E. Sarty *et al.*, Mon. Not. Roy. Astron. Soc. **411**, 1293 (2011) [arXiv:1009.5150 [astro-ph.HE]].

[309] J. Moldon, M. Ribo, J. M. Paredes, W. Brisken, V. Dhawan, M. Kramer, A. G. Lyne and B. W. Stappers, arXiv:1205.2080 [astro-ph.HE].

[310] A. A. Abdo *et al.* [Fermi LAT Collaboration], Astrophys. J. **706**, L56 (2009) [arXiv:0910.5520 [astro-ph.HE]].

[311] F. Aharonian *et al.* [H.E.S.S. Collaboration], Science **309**, 746 (2005) [astro-ph/0508298].

[312] F. Aharonian *et al.* [H.E.S.S. Collaboration], Astron. Astrophys. **460**, 743 (2006) [astro-ph/0607192].

[313] J. M. Paredes, J. Marti, M. Ribo and M. Massi, Science **288**, 2340 (2000) [astro-ph/0102235].

[314] J. M. Paredes, M. Ribo, E. Ros, J. Marti and M. Massi, Astron. Astrophys. **393**, L99 (2002) [astro-ph/0210550].

[315] M. Ribo, J. M. Paredes, J. Moldon, J. Marti and M. Massi, Astron. Astrophys. **481**, 17 (2008) [arXiv:0801.2940 [astro-ph]].

[316] G. Dubus, Astron. Astrophys. **456**, 801 (2006) [astro-ph/0605287].

[317] A. Sierpowska-Bartosik and D. F. Torres, Astrophys. J. **674**, L89 (2008) [arXiv:0801.1487 [astro-ph]].

[318] A. Sierpowska-Bartosik and D. F. Torres, Astropart. Phys. **30**, 239 (2008) [arXiv:0801.3427 [astro-ph]].

[319] M. V. McSwain, P. S. Ray, S. M. Ransom, M. S. E. Roberts, S. M. Dougherty and G. G. Pooley, Astrophys. J. **738**, 105 (2011) [arXiv:1106.5550 [astro-ph.HE]].

[320] N. Rea, D. F. Torres, G. A. Caliandro, D. Hadasch, M. van der Klis, P. G. Jonker, M. Mendez and A. Sierpowska-Bartosik, Mon. Not. Roy. Astron. Soc. **416**, 1514 (2011) [arXiv:1105.5585 [astro-ph.GA]].

[321] A. Levinson and E. Waxman, Phys. Rev. Lett. **87**, 171101 (2001) [hep-ph/0106102].

[322] G. M. Frichter, T. K. Gaisser and T. Stanev, Phys. Rev. D **56**, 3135 (1997) [astro-ph/9704061].

[323] M. Bottcher and C. D. Dermer, Astrophys. J. **634**, L81 (2005) [astro-ph/0508359].

[324] F. A. Aharonian and A. V. Plyasheshnikov, Astropart. Phys. **19**, 525 (2003) [astro-ph/0208504].

[325] D. Khangulyan and F. Aharonian, AIP Conf. Proc. **745**, 359 (2005) [astro-ph/0503499].

[326] R. C. Hartman *et al.* [EGRET Collaboration], Astrophys. J. Suppl. **123**, 79 (1999).

[327] S. Adrian-Martinez *et al.* [ANTARES Collaboration], Astrophys. J. **786**, L5 (2014) [arXiv:1402.6182 [hep-ex]].

[328] C. Distefano, D. Guetta, E. Waxman and A. Levinson, Astrophys. J. **575**, 378 (2002) [astro-ph/0202200].

[329] Q. Z. Liu, J. van Paradijs and E. P. J. v. d. Heuvel, Astron. Astrophys. **455**, 1165 (2006) [arXiv:0707.0549 [astro-ph]].

[330] Q. Z. Liu, J. van Paradijs and E. P. J. v. d. Heuvel, Astron. Astrophys. **469**, 807 (2007) [arXiv:0707.0544 [astro-ph]].

[331] R. Krivonos, S. Tsygankov, A. Lutovinov, M. Revnivtsev, E. Churazov and R. Sunyaev, "INTEGRAL/IBIS 9-year Galactic Hard X-Ray Survey," Astron. Astrophys. **545**, A27 (2012) [arXiv:1205.3941 [astro-ph.IM]].

[332] J. M. Paredes and J. M. Marti, Contributions to Science **2**, 303 (2003); Institut d'Estudis Catalans, Barcelona.

[333] A. A. Zdziarski, M. Gierlinski, J. Mikolajewska, G. Wardzinski, B. A. Harmon and S. Kitamoto, Mon. Not. Roy. Astron. Soc. **351**, 791 (2004) [astro-ph/0402380].

[334] V. Bosch-Ramon, G. E. Romero, J. M. Paredes, A. Bazzano, M. Del Santo and L. Bassani, Astron. Astrophys. **457**, 1011 (2006) [astro-ph/0609150].

[335] R. Soria, J. W. Broderick, J. Hao, D. C. Hannikainen, M. Mehdipour, K. Pottschmidt and S. N. Zhang, arXiv:1103.3009 [astro-ph.HE].

[336] D. M. Russell, R. P. Fender, E. Gallo and C. R. Kaiser, Mon. Not. Roy. Astron. Soc. **376**, 1341 (2007) [astro-ph/0701645].

[337] M. Massi, M. Ribó, J. Paredes, M. Peracaula, and R. Estalella, Astron. Astrophys. **376**, 217 (2001).

[338] I. F. Mirabel, V. Dhawan, R. P. Mignani, I. Rodrigues and F. Guglielmetti, Nature **413**, 139 (2001) [astro-ph/0109098].

[339] I. F. Mirabel and I. Rodrigues, Astron. Astrophys. **398**, L25 (2003) [astro-ph/0301580].

[340] M. G. Aartsen *et al.* [IceCube Collaboration], Phys. Rev. D **87**, no. 6, 062002 (2013) [arXiv:1210.7992 [astro-ph.HE]].

[341] M. Ahlers and K. Murase, Phys. Rev. D **90**, 023010 (2014) [arXiv:1309.4077 [astro-ph.HE]].

[342] J. Albert *et al.* [MAGIC Collaboration], Science **312**, 1771 (2006) [astro-ph/0605549]; V. A. Acciari, M. Beilicke, G. Blaylock, S. M. Bradbury, J. H. Buckley, V. Bugaev, Y. Butt and K. L. Byrum *et al.*, arXiv:0802.2363 [astro-ph]; A. A. Abdo *et al.* [Fermi LAT Collaboration], Astrophys. J. **701**, L123 (2009) [arXiv:0907.4307 [astro-ph.HE]]; D. Hadasch, D. F. Torres, T. Tanaka, R. H. D. Corbet, A. B. Hill, R. Dubois, G. Dubus and T. Glanzman *et al.*, Astrophys. J. **749**, 54 (2012) [arXiv:1202.1866 [astro-ph.HE]].

[343] M. Massi, M. Ribo, J. M. Paredes, S. T. Garrington, M. Peracaula and J. Marti, Astron. Astrophys. **414**, L1 (2004) [astro-ph/0312091].

[344] W. Bednarek, Mon. Not. Roy. Astron. Soc. **397**, 1420 (2009) [arXiv:0901.0392 [astro-ph.HE]]. D. F. Torres, N. Rea, P. Esposito, J. Li, Y. Chen and S. Zhang, Astrophys. J. **744**, 106 (2012) [arXiv:1109.5008 [astro-ph.HE]].

[345] D. F. Torres and F. Halzen, Astropart. Phys. **27**, 500 (2007) [astro-ph/0607368].

[346] M. Ackermann *et al.* [AMANDA Collaboration], Phys. Rev. D **71**, 077102 (2005) [astro-ph/0412347]; A. Achterberg *et al.* [IceCube Collaboration], Phys. Rev. D **75**, 102001 (2007) [astro-ph/0611063]; R. Abbasi *et al.* [IceCube Collaboration], Phys. Rev. D **79**, 062001 (2009) [arXiv:0809.1646 [astro-ph]]; R. Abbasi *et al.* [IceCube Collaboration], Astrophys. J. **701**, L47 (2009) [arXiv:0905.2253 [astro-ph.HE]].

[347] M. G. Aartsen *et al.* [IceCube Collaboration], arXiv:1406.6757 [astro-ph.HE].

[348] S. Adrian-Martinez *et al.* [ANTARES Collaboration], JHEAp (2014) [arXiv:1402.1600 [astro-ph.HE]].

[349] T. K. Gaisser, F. Halzen and T. Stanev, Phys. Rept. **258**, 173 (1995) [Erratum-ibid. **271**, 355 (1996)] [hep-ph/9410384].

[350] W. Dehnen and J. Binney, Mon. Not. Roy. Astron. Soc. **294**, 429 (1998) [astro-ph/9612059].

[351] M. G. Aartsen *et al.* [IceCube Collaboration], arXiv:1410.1749 [astro-ph.HE].

[352] M. Ackermann *et al.* [The Fermi LAT Collaboration], arXiv:1410.3696 [astro-ph.HE].

[353] A. Borione, M. A. Catanese, M. C. Chantell, C. E. Covault, J. W. Cronin, B. E. Fick, L. F. Fortson and J. Fowler *et al.*, Astrophys. J. **493**, 175 (1998) [astro-ph/9703063]; M. C. Chantell *et al.* [CASA-MIA Collaboration], Phys. Rev. Lett. **79**, 1805 (1997) [astro-ph/9705246].

[354] Y. A. Fomin, N. N. Kalmykov, G. V. Kulikov, V. P. Sulakov and S. V. Troitsky, arXiv:1410.2599 [astro-ph.HE].

[355] L. A. Anchordoqui, H. Goldberg, A. V. Olinto, T. C. Paul, B. J. Vlcek and T. J. Weiler, J. Phys. Conf. Ser. **531**, 012009 (2014) [arXiv:1403.6628 [astro-ph.HE]].

[356] G. Giacinti, M. Kachelriess and D. V. Semikoz, Phys. Rev. D **90**, 041302 (2014) [arXiv:1403.3380 [astro-ph.HE]].

11 Appendix A - 4-momentum and Mandelstam variables

11.1 Special Relativity

Postulate 1: Principle of Relativity

The laws of physics are the same in all inertial frames.

Postulate 2: Invariance of the speed of light

The speed of light in vacuum, c, is the same in all inertial frames.

Now, we consider the following situation: suppose that an observer, at a certain position(x,y,z) and time t as seen in a reference frame S, decides to shine some light, in all directions; that's what we refer to as the event E. In a spacetime diagram 1+2 (we supress one spatial component), we would see something like this:

In the picture above, we also considered the "past portion" of what we call the light cone. The future corresponds to the portion of spacetime that can receive information about the event E; since nothing travels faster than the speed of light, the light cone defines the portion of the spacetime that is causally connected to the vent E. The "past" portion is analogous: corresponds to the portion of the spacetime that is able to reach E, i.e, that is causally connected to it. Note that the light cone obeys the following equation:

$$(c(t-t_0))^2 - (x-x_0)^2 - (y-y_0)^2 - (z-z_0)^2 = 0. \tag{644}$$

Now, suppose that in another inertial reference frame, S', somebody else decides to do the same thing. Since the speed of light is the same in both reference frames, the light cone passing through the same event (i.e. a point in the continuum of spacetime) would have the equation

$$(c(t'-t'_0))^2 - (x'-x'_0)^2 - (y'-y'_0)^2 - (z'-z'_0)^2 = 0. \tag{645}$$

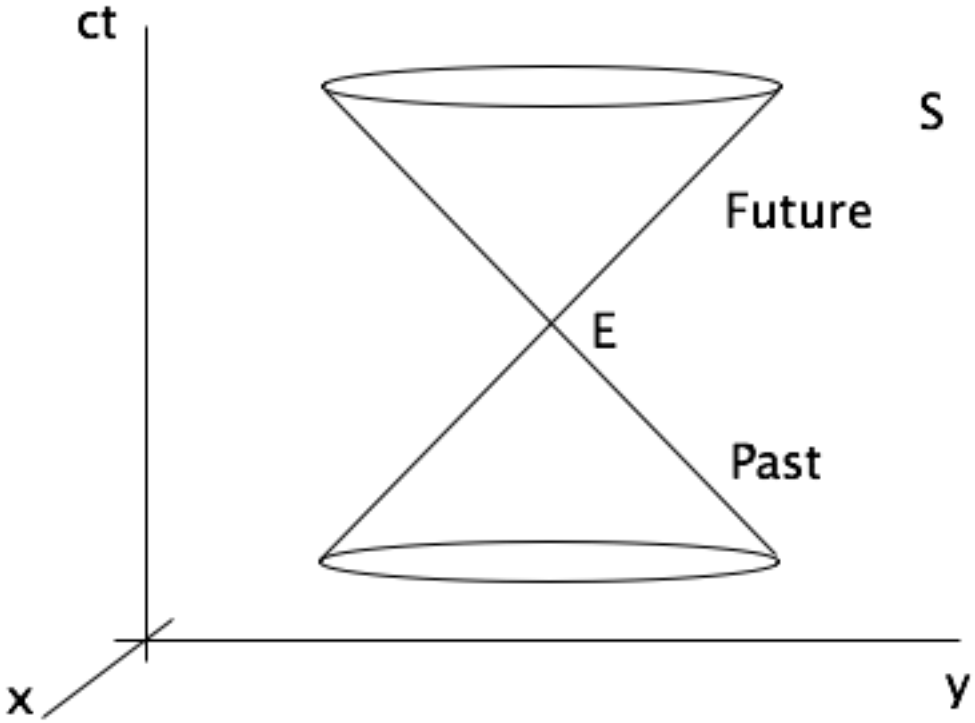

Figure 22: Light cone

After seeing this, it is therefore natural to ask: is there any sort of transformations, from S to S', that leaves the structure of the light cone unchanged? The answer is yes. First, using Einstein summation convention we write the equations above as

$$\eta_{\mu\nu}(x^\mu - x_0^\mu)(x^\nu - x_0^\nu) = 0 \tag{646}$$

$$\eta_{\mu\nu}(x'^\mu - x_0'^\mu)(x'^\nu - x_0'^\nu) = 0 \tag{647}$$

where

$$\eta = diag(1, -1, -1, -1). \tag{648}$$

Our first attemp is to search for linear transformations of the form:

$$x' = \Lambda_\nu^\mu x^\nu. \tag{649}$$

when applied to the light cone equation of the S' frame,

$$0 = \eta_{\mu\nu}(x'^{\mu} - x_0'^{\mu})(x'^{\nu} - x_0'^{\nu}) = \eta_{\alpha\beta}\Lambda^{\alpha}_{\mu}\Lambda^{\beta}_{\nu}(x^{\mu} - x_0^{\mu})(x^{\nu} - x_0^{\nu}), \tag{650}$$

comparison between the equations gives

$$\eta_{\alpha\beta}\Lambda^{\alpha}_{\mu}\Lambda^{\beta}_{\nu} = C\eta_{\mu\nu}, \tag{651}$$

where C is a constant. For simplicity, we look at the case C=1. So, we want transformations such that

$$\eta_{\alpha\beta}\Lambda^{\alpha}_{\mu}\Lambda^{\beta}_{\nu} = \eta_{\mu\nu}, \tag{652}$$

holds true.

Definition

The transformations that satisfy the condition above are called Lorentz transformations.

At this point, our problem reduced to the search of the transformations that leave the entity $\eta_{\mu\nu}$ unchanged. Before we proceed, it is important to take a closer look at this matrix.

Definition

$\eta_{\mu\nu}$, as defined above, is the metric of the Minkowski spacetime, the flat (zero curvature) spacetime of Special Relativity.

The metric carries a lot of information about the spacetime itself. Information about the geometry of the spacetime is contained on it, and it also tells us how to perform the scalar product in the spacetime it is defined (more details about this can be found in later chapters). In particular, in our case, the scalar product between two vectors, v and u, in the Minkowski spacetime is defined as:

$$\eta_{\alpha\beta}v^{\alpha}u^{\beta} = \eta_{00}v^0u^0 + \eta_{11}v^1u^1 + \eta_{22}v^2u^2 + \eta_{33}v^3u^3 = v^0u^0 - v^1u^1 - v^2u^2 - v^3u^3. \quad (653)$$

If one perform the reference frame transformations we have been talking about on the vectors v and u,

$$v'^{\mu} = \Lambda^{\mu}_{\nu}v^{\nu}, \quad (654)$$

$$u'^{\mu} = \Lambda^{\mu}_{\nu}u^{\nu}, \quad (655)$$

$$\eta_{\alpha\beta}v'^{\alpha}u'^{\beta} = \eta_{\alpha\beta}\Lambda^{\alpha}_{\mu}\Lambda^{\beta}_{\nu}v^{\mu}u^{\nu} = \eta_{\mu\nu}v^{\mu}u^{\nu}. \quad (656)$$

This means that the scalar product of two vectors in this spacetime remains unchanged by the transformations of reference frame. This is a very important result, and we will use it later.

The metric can also be used to "raise" and "lower" indices. From mathematics, we can recall the definition of dual vectors:

Definition

Let V be a vector space and Ω be the set of linear functionals that map V into the real numbers,

$$\omega \in \Omega, \;\; \omega : V \to \mathbb{R}, \quad (657)$$

the elements of Ω are called dual vectors.

Let v^{μ} be a vector defined in the Minkowski spacetime. The quantity

$$\eta_{\mu\nu}v^{\mu} \equiv v_{\nu} \quad (658)$$

satisfies the conditions stated in Def. 1.2; i.e, it is a dual vector (if we "insert" a vector u^ν on the equation above the result is a real number because we would be taking the scalar product between v^μ and u^ν). So, the metric naturally induces a mapping between the space of vectors and dual vectors. Those two spaces are isomorphic, and it can be shown that there is a one-to-one correspondence between its elements. This process, of starting with a vector and using the metric to obtain a dual vector is what we call lower an index; the inverse is called raise an index, and is done by using $\eta^{\mu\nu} = diag(1, -1, -1, -1)$ on a dual vector.

Let Λ and Θ be two Lorentz transformations. Look the product $\Theta\Lambda$

$$\eta_{\mu\nu} = \eta_{\alpha\beta}\Lambda^\alpha_\mu\Lambda^\beta_\nu = \eta_{\gamma\delta}\Theta^\gamma_\alpha\Theta^\delta_\beta\Lambda^\alpha_\mu\Lambda^\beta_\nu = \eta_{\gamma\delta}\Theta^\gamma_\alpha\Lambda^\alpha_\mu\Theta^\delta_\beta\Lambda^\beta_\nu, \tag{659}$$

but

$$\Theta^\gamma_\alpha\Lambda^\alpha_\mu = (\Theta\Lambda)^\gamma_\mu, \tag{660}$$

so $\Theta\Lambda$ is also a Lorentz transformation. Now, consider the inverse Λ^{-1}.

$$(\Lambda^{-1})^\mu_\nu\Lambda^\mu_\alpha = \delta^\alpha_\nu \tag{661}$$

where δ^α_ν is the Kronecker delta (the identity matrix). When we look at the definition of the Lorentz transformation,

$$\eta_{\alpha\beta}\Lambda^\alpha_\mu\Lambda^\beta_\nu = \eta_{\mu\nu} \Rightarrow (\Lambda^{-1})^\mu_\gamma(\Lambda^{-1})^\nu_\delta\eta_{\alpha\beta}\Lambda^\alpha_\mu\Lambda^\beta_\nu = (\Lambda^{-1})^\mu_\gamma(\Lambda^{-1})^\nu_\delta\eta_{\mu\nu} = \delta^\alpha_\gamma\delta^\beta_\delta\eta_{\alpha\beta} = \eta_{\gamma\delta}. \tag{662}$$

Hence,

$$(\Lambda^{-1})^\mu_\gamma(\Lambda^{-1})^\nu_\delta\eta_{\mu\nu} = \eta_{\gamma\delta}. \tag{663}$$

We see that $\Lambda\Theta$ and Λ^{-1} are Lorentz transformations. Clearly, the identity is also a Lorentz transformation. Thus, the set of all Λ that satisfy (9) form a group.

Definition

The set of Lorentz transformations form a group, the Lorentz group L.

Let's explore this idea a little bit. The matrix for a Lorentz transformation is a continous function of its components, which are real numbers. We therefore we can say that two Lorentz transformations can be connected by a continuous curve of Λ's. However, not all Lorentz transformations can be directly connected to each other, because a Lorentz transformation in one component can't be connected to a transformation in another component. To see this mathematically, consider (again) equation (9):

$$\eta_{\alpha\beta}\Lambda^{\alpha}_{\mu}\Lambda^{\beta}_{\nu} = \eta_{\mu\nu} \Rightarrow \Lambda^{T}\eta\Lambda = \eta. \tag{664}$$

Taking the determinant:

$$det(\eta) = det(\Lambda^{T}\eta\Lambda) \Rightarrow -1 = det(\Lambda^{T})det(\eta)det(\Lambda) = (-1)det(\Lambda^{T})det(\Lambda), \tag{665}$$

but $det(M) = det(M^{T})$:

$$det(\Lambda)^2 = 1 \Rightarrow det(\Lambda) = \pm 1. \tag{666}$$

In addition, look at the zeroth element in (9):

$$\eta_{00} = \Lambda^{\alpha}_{0}\Lambda^{\beta}_{0}\eta_{\alpha\beta} \Rightarrow 1 = (\Lambda^{0}_{0})^2 - \sum_{\mu=1}^{3}(\Lambda^{\mu}_{0})^2 \Rightarrow \mid \Lambda^{0}_{0} \mid \geq 1 \tag{667}$$

Therefore, the determinant and the sign of the zeroth element must be constant on any component. The whole thing breaks into four cases:

I) detΛ = 1, sgn $\Lambda^{0}_{0} = +1$, contains the identity

II) detΛ = -1, sgn $\Lambda^{0}_{0} = +1$, contains the space inversion

III) detΛ = 1, sgn $\Lambda^{0}_{0} = -1$, contains the space-time inversion

IV) $\det\Lambda$ = -1, sgn $\Lambda_0^0 = -1$, contains the time inversion

Definition

The space inversion I_s, time inversion I_t and space-time inversion I_{st} are defined by, respectively,

$$(I_s v)^0 = v^0, \;\; (I_s v)^j = -x^j, \;\; j \neq 0, \tag{668}$$

$$(I_t v)^0 = -v^0, \;\; (I_s v)^j = x^j, \;\; j \neq 0, \tag{669}$$

$$I_{st} v^\mu = -v^\mu. \tag{670}$$

It can be shown that the Lorentz group is connected Lie group (we won't do it here). In addition, it is important to introduce some extra terminology.

Definition

If $\Lambda_0^0 \geq 0$, it is said to be orthochronous; if $det\Lambda = 1$, it is called proper. If $det\Lambda = 1$ and $\Lambda_0^0 \geq 0$, the transformation is said to be orthochorous.

Now, our next task is to find an explicit form for the matrix Λ. The simplest non-trivial case for a transformation Λ is the one which mixes time and just one spatial component, namely:

$$\Lambda = \begin{pmatrix} a & b & 0 & 0 \\ c & d & 0 & 0 \\ 0 & 0 & 1 & 0 \\ 0 & 0 & 0 & 1 \end{pmatrix}$$

Inserting this on (9) ($\eta_{\alpha\beta}\Lambda^\alpha_\mu\Lambda^\beta_\nu = \eta_{\mu\nu}$), we get:

$$\begin{cases} a^2 - c^2 = 1 \\ ab - cd = 0 \\ b^2 - d^2 = 1 \end{cases}$$

with solutions

$$a = d = cosh\chi \tag{671}$$

$$b = c = -sinh\chi \tag{672}$$

Thus, our Λ looks like:

$$\Lambda = \begin{pmatrix} cosh\chi & -sinh\chi & 0 & 0 \\ -sinh\chi & cosh\chi & 0 & 0 \\ 0 & 0 & 1 & 0 \\ 0 & 0 & 0 & 1 \end{pmatrix}$$

All of this looks good, the only problem is that we have no idea of what χ and functions of it mean. In order to get a better understanding, let's see how this matrix acts on a vector.

$$x'^{\mu} = \lambda^{\mu}_{\nu} x^{\nu}, \tag{673}$$

y and z are left unchanged, and the x and t coordinates get mixed:

$$ct' = (cosh\chi)ct - (sinh\chi)x, \tag{674}$$

$$x' = -(sinh\chi)ct + (cosh\chi)x. \tag{675}$$

One thing that we could impose is that $dx' = dy' = dz' = 0$; physically this means that we are interested in how a static observer in S' would see the effect of the transfomation

on the event (t,x,y,z),

$$-c(sinh\chi)dt + (cosh\chi)dx = 0 \Rightarrow v_x = ctanh\chi \tag{676}$$

$$dy = dz = 0 \Longrightarrow v_y = v_z = 0. \tag{677}$$

Therefore, this coordinate change is equivalent to going from a frame S to a frame S' that is moving with velocity v (given above) with respect to the frame S. Using the equation for the hyperbolic tangent in terms of speed and the identity $cosh^2\chi - sinh^2\chi = 1$, one gets:

$$sinh(\chi) = \gamma\beta, \tag{678}$$

$$cosh(\chi) = \gamma, \tag{679}$$

where

$$\beta = \frac{v}{c}, \;\; \gamma = \frac{1}{\sqrt{1-\beta^2}}. \tag{680}$$

Our matrix for the transformation is given by:

$$\Lambda = \begin{pmatrix} \gamma & -\gamma\beta & 0 & 0 \\ -\gamma\beta & \gamma & 0 & 0 \\ 0 & 0 & 1 & 0 \\ 0 & 0 & 0 & 1 \end{pmatrix}$$

Definition

The matrices Λ, which mix time and spatial components, are called Lorentz boosts.

If we write the components separetely, from the matrix above we get

$$t' = \gamma\left(t - \frac{vx}{c^2}\right), \tag{681}$$

$$x' = \gamma\left(x - vt\right), \tag{682}$$

$$y' = y, \tag{683}$$

$$z' = z. \tag{684}$$

Geometrically, we can see the effect that a boost has on the inertial frames. Consider, for example, the event with coordinates

$$x' = 0 \Rightarrow ct = \beta^{-1}x, \;\; t' = 0 \Rightarrow ct = \beta x. \tag{685}$$

It is also possible to show that spatial rotations are also symmetry transformations. The process to do so is analogous, so we ommit it.

So, let's take a closer look on the structure of Special Relativity in a way that's more useful from the point of view of particle physics: the "group theory" approach. Consider the following (proper, orthocronous) matrices:

$$(B_1)^a_b = \begin{pmatrix} cosh(\phi_1) & -sinh(\phi_1) & 0 & 0 \\ -sinh(\phi_1) & cosh(\phi_1) & 0 & 0 \\ 0 & 0 & 1 & 0 \\ 0 & 0 & 0 & 1 \end{pmatrix}$$

$$(B_2)^a_b = \begin{pmatrix} cosh(\phi_2) & 0 & -sinh(\phi_2) & 0 \\ 0 & 1 & 0 & 0 \\ -sinh(\phi_2) & 0 & cosh(\phi_2) & 0 \\ 0 & 0 & 0 & 1 \end{pmatrix}$$

$$(B_3)^a_b = \begin{pmatrix} cosh(\phi_3) & 0 & 0 & -sinh(\phi_3) \\ 0 & 1 & 0 & 0 \\ 0 & 0 & 1 & 0 \\ -sinh(\phi_3) & 0 & 0 & cosh(\phi_3) \end{pmatrix}$$

$$(R_1)^a_b = \begin{pmatrix} 1 & 0 & 0 & 0 \\ 0 & 1 & 0 & 0 \\ 0 & 0 & cos(\theta_1) & sin(\theta_1) \\ 0 & 0 & -sin(\theta_1) & cos(\theta_1) \end{pmatrix}$$

$$(R_2)^a_b = \begin{pmatrix} 1 & 0 & 0 & 0 \\ 0 & cos(\theta_2) & 0 & sin(\theta_2) \\ 0 & 0 & 1 & 0 \\ 0 & -sin(\theta_2) & 0 & cos(\theta_2) \end{pmatrix}$$

$$(R_3)^a_b = \begin{pmatrix} 1 & 0 & 0 & 0 \\ 0 & cos(\theta_3) & sin(\theta_3) & 0 \\ 0 & -sin(\theta_3) & cos(\theta_3) & 0 \\ 0 & 0 & 0 & 1 \end{pmatrix}$$

The B's stand for the boosts, and the R's for spatial rotations. The generators are (K for boosts and J for rotations):

$$(K_1)^a_b = \begin{pmatrix} 0 & i & 0 & 0 \\ i & 0 & 0 & 0 \\ 0 & 0 & 0 & 0 \\ 0 & 0 & 0 & 0 \end{pmatrix}, \quad (K_2)^a_b = \begin{pmatrix} 0 & 0 & i & 0 \\ 0 & 0 & 0 & 0 \\ i & 0 & 0 & 0 \\ 0 & 0 & 0 & 0 \end{pmatrix}, \quad (K_3)^a_b = \begin{pmatrix} 0 & 0 & 0 & i \\ 0 & 0 & 0 & 0 \\ 0 & 0 & 0 & 0 \\ i & 0 & 0 & 0 \end{pmatrix}. \quad (686)$$

$$(J_1)^a_b = \begin{pmatrix} 0 & 0 & 0 & 0 \\ 0 & 0 & 0 & 0 \\ 0 & 0 & 0 & -i \\ 0 & 0 & i & 0 \end{pmatrix}, \quad (J_2)^a_b = \begin{pmatrix} 0 & 0 & 0 & 0 \\ 0 & 0 & 0 & i \\ 0 & 0 & 0 & 0 \\ 0 & -i & 0 & 0 \end{pmatrix}, \quad (J_3)^a_b = \begin{pmatrix} 0 & 0 & 0 & 0 \\ 0 & 0 & -i & 0 \\ 0 & i & 0 & 0 \\ 0 & 0 & 0 & 0 \end{pmatrix}. \quad (687)$$

They satisfy the following commutation relations:

$$\begin{aligned} [J_i, J_j] &= i\epsilon_{ijk} J_k, \\ [K_i, K_j] &= i\epsilon_{ijk} K_k, \\ [J_i, K_j] &= -i\epsilon_{ijk} J_k. \end{aligned} \quad (688)$$

One can also define the following linear combinations of the generators:

$$S_i^+ = \frac{1}{2}(J_i + iK_i), \quad (689)$$

$$S_i^- = \frac{1}{2}(J_i - iK_i), \quad (690)$$

which satisfy:

$$\begin{aligned} [S_i^+, S_j^+] &= i\epsilon_{ijk} S_k^+, \\ [S_i^-, S_j^-] &= i\epsilon_{ijk} S_k^-, \\ [S_i^+, S_j^-] &= 0 \end{aligned} \quad (691)$$

.

So the Lorentz group is locally equivalent to $SU(2) \oplus SU(2)$.

11.2 4-momentum

In our theory of Special Relativity, spacetime is a 4 dimensional manifolds without curvature, in which we define the Minkowski metric. Our next step is to study general tensor fields in this spacetime and their physical consequences.

The first question that arises here (and in any time that we want to develop a theory that is consistent with relativity) is why we need the tensor formalism. We saw how it naturally arises when we begin to add structure on our manifolds from a mathematical point of view, but we need a physical motivation. The main reason is because physics should not depend on coordinate system or choices of inertial frames, as stated in one of the postulates, and tensor fields are mathematical quantities that exist independently of them. A tensor equation will always hold true, no matter what coordinate system we choose to write it; thus, it makes perfect sense to try to do physics using the tensor formalism. We will now begin our study of physical quantities defined under those terms.

Definition

Let $\eta_{\mu\nu}$ represent the metric of our spacetime, and A and B denote two spacetime events (two spacetime points) with coordinates $x^\mu_A = (t_A, x_A, y_A, z_A)$, $x^\mu_B = (t_B, x_B, y_B, z_B)$ as seen by an observer in an arbitrary reference frame (note that the indices A and B are not spacetime indices, they are her only to label the events). The quantity

$$\Delta s^2 = \eta_{\mu\nu} x^\mu_A x^\mu_B = -c^2(t_B - t_A)^2 + (x_B - x_A)^2 + (y_B - y_A)^2 + (z_A - z_B)^2, \qquad (692)$$

is called invariant interval.

We have seen this before, when we were discussing the scalar product as we introduced the initial concepts of Special Relativity. There are many conclusions that we can draw from it. First, we notice that the result of this operation is a scalar, and its value is independent of the reference frame (we saw in the previous section that changes of coordinates leave this result unchanged); thus, it seems that scalars are a great way

to define observables in our theory, since all oberservers, independently of their inertial frame and coordinates will agree on the value.

Secondly, we take the fact that the quantity above is invariant under Lorentz transformations one step further. Geometrically, it is the equivalent of calculating a distance in spacetime, what means that we can use to classify the separation of events in spacetime.

I) $\Delta s^2 < 0 \Rightarrow$ Spacelike separation,

II) $\Delta s^2 = 0 \Rightarrow$ Null separation,

III) $\Delta s^2 > 0 \Rightarrow$ Timelike separation.

If we look at the light cone with vertex defined on the event A, if the event B lies outside of it, the separation is spacelike; if it lies of the surfaceit is null, and if it is inside it is timelike.

A set of connected points on the Minkowski spacetime can be used to define a curve on it.

Definition

A curve in Minkowski space $\mathbb{M}$ is a smooth function, $\Gamma : \mathbb{R} \to \mathbb{M}$,

$$\Gamma(\lambda) = (ct(\lambda), x(\lambda), y(\lambda), z(\lambda)) \in \mathbb{M}, \tag{693}$$

where λ parametrizes the curve.

For a given curve, we can define the tangent vector

$$v^\mu = \frac{d\Gamma(\lambda)}{d\lambda} = \left(c\frac{dt(\lambda)}{d\lambda}, \frac{dx(\lambda)}{d\lambda}, \frac{dy(\lambda)}{d\lambda}, \frac{dz(\lambda)}{d\lambda} \right). \tag{694}$$

The distance between two points infinitesimally close within the curve is given by

$$d\Gamma(\lambda) = \Gamma(\lambda + d\lambda) - \Gamma(\lambda), \tag{695}$$

which can be rewritten as

$$d\Gamma(\lambda) = (dt(\lambda), dx(\lambda), dy(\lambda), dz(\lambda)) = dx^{\mu}(\lambda). \tag{696}$$

On the other hand,

$$ds^2 = cdt^2 - dx^2 - dy^2 - dz^2 = \eta_{\mu\nu} dx^{\mu}(\lambda) dx^{\nu}(\lambda) \Rightarrow \eta_{\mu\nu} v^{\mu} v^{\nu} = \frac{ds^2}{d\lambda^2}. \tag{697}$$

We can extend the definition for the invariant inerval to the scalar product above, and classify it as timelike, spacelike or null. A curve is said to be timelike, spacelike or null if the vectors tangent to it are timelike, spcelike or null. In addition, we can see physically see that a partilcle that has mass can not travel faster than light; therefore, particles have timelike trajectories and light travels on null curves. Also, we can always find a reference frame in which P and Q occur in the same point of space (see the geometric interpretation of boost). In that frame, the invariant interval between those events is given by

$$\Delta s^2 = c\Delta t^2 \Rightarrow \Delta t' = \frac{1}{c}\sqrt{\Delta s^2}. \tag{698}$$

Suppose that we have a certain timelike curve. If we have two infinitesimally close events as seen from an oberver in a refenrence frame where they happen at the same point of space, the invariant interval between them is given by

$$d\tau = \frac{\sqrt{dt^2}}{c}, \tag{699}$$

and since the events are arbitrarily close, we can think of $d\tau$ as the time interval between the events as measured by an observer which follows the spacetime trajectory of the particle in question. In other words, it is the time interval as measured from the rest frame of the timelike curve, and we can write

$$\Delta\tau = \int_{\Gamma} d\tau = \frac{1}{c}\int_{\Gamma} \sqrt{\eta_{\mu\nu} v^{\mu} v^{\nu}} d\lambda. \tag{700}$$

Note that since τ is given in terms of λ, we can reparametrize a timelike curve in terms of τ. This motivates the following definition:

Definition

Let Γ be a timelike curve parametrized by τ. We call τ the proper time, and the tangent vector parametrized by it

$$u^\mu = \frac{dx^\mu}{d\tau}, \tag{701}$$

the 4-velocity. It satisfies

$$\eta_{\mu\nu} u^\mu u^\nu = \frac{ds^2}{d\tau^2} = c^2. \tag{702}$$

There is good physical reason to introduce quantities such as the proper time, which are viewed from the point of view of the rest frame of the particle (or whatever is moving) through spacetime. Suppose that we have two obervers in two different frame, and they want to know, let's say, what is the time interval between two events P and Q. They might disagree on the value when each of them measures it on their own frames, but they will always agree if they calculate the time interval as seen by the moving particle, on its rest frame. In other words, all observers agree on the quantities measured from the rest frame, as it provides a natural connection between them all. It is interesting to write a few extra definitions at this point.

Definition

Scalars are quantities characterized by a numerical value that remains unchanged upon changes of reference frames. Therefore, they are ideal to define observables in our theory. Examples would be the invariant interval and the proper time.

Definition

We define the 4-momentum of a particle of rest mass m and 4-velocity v^μ as

$$p^\mu = m\gamma(c, \vec{v}) = (E/c, \vec{p}). \tag{703}$$

Note that the energy that appears on the equation above is the energy measured by the observers at rest on a lab frame, and the energy if the particle as measured by these observers is given by

$$u^\mu = (c, 0) \Rightarrow E = p^\mu u_\mu = \eta_{\mu\nu} p^\mu u^\nu. \tag{704}$$

If we take an observer moving with the particle (on its rest frame $u^\mu = v^\mu$) we obtain the rest energy,

$$E_0 = p^\mu u_\mu = m v^\mu v_\mu = mc^2. \tag{705}$$

Now that we have defined 4-momentum, we are now ready to study collisions and particle reactions. Note that this is a simplified approach on particle reactions, where we only take momentum and energy into account. Other features will be approached later, when we discuss quantum electrodynamics.

11.3 Mandelstam variables

In this section, we will expose the typical definition of Mandelstam variables, as presented in [6].For high energy physics, it is convenient to define some variables to describe particle reactions of the form

$$A + B \to C + D, \tag{706}$$

instead of directly working with the (relativistic invariant) scalar product of the 4-momentum of the particles (the reason for this will become more clear when we study

QED and unpolarized cross sections). We define

$$s = (p_A + p_B)^2 = (p_C + p_D)^2, \tag{707}$$

$$t = (p_A - p_C)^2 = (p_B - p_D)^2, \tag{708}$$

$$u = (p_A - p_D)^2 = (p_B - p_C)^2. \tag{709}$$

Recall that

$$p_n^2 = m_n^2, \tag{710}$$

$$p_A + p_B = p_C + p_D, \tag{711}$$

and we have

$$s + t + u = \sum_i m_i^2. \tag{712}$$

If we go the center-of-mass frame we are able to explicitly evaluate the Mandelstam variables (we will make $\vec{p} = \hbar\vec{k} = \vec{k},\ \hbar = 1$),

$$p_A = (E, \vec{k}_i),\ \ p_B = (E, -\vec{k}_i),\ \ p_C = (E, \vec{k}_f),\ \ p_D = (E, -\vec{k}_f), \tag{713}$$

with $E^2 = k^2 + m^2$. For $\vec{k}_i.\vec{k}_f = k^2 cos(\theta)$, the variables become

$$s = 4(k^2 + m^2), \tag{714}$$

$$t = -(\vec{k}_i - \vec{k}_f)^2 = -2k^2(1 - cos(\theta)), \tag{715}$$

$$u = -(\vec{k}_i + \vec{k}_f)^2 = -2k^2(1 + cos(\theta)). \tag{716}$$

From the results above, we can see that s is a positive quantity, while t and u are negative ($cos(\theta) \in [-1, 1] \subset \mathbb{R}$). If we have t or u equal to zero, we have forward or backward scattering respectively.

We can consider other reactions, when we have antiparticles involved, for example. Consider the following reaction:

$$A + \bar{C} \to \bar{B} + D. \tag{717}$$

The antiparticles will have 4-momenta oppositeto the ones presented in the first equation, namely

$$p_B \to -p_B, \;\; p_C \to -p_C, \tag{718}$$

and we have the Mandelstam variables

$$s = (p_A - p_B)^2, \tag{719}$$

$$t = (p_A + P_C)^2), \tag{720}$$

$$u = (p_A - P_D)^2). \tag{721}$$

In this situation, t is positive (the squared energy) and the other variables are zero or negative. Finally, we present one more example:

$$A + \bar{D} \to \bar{B} + C, \tag{722}$$

$$s = (p_A - p_B)^2, \tag{723}$$

$$t = (p_A + p_C)^2, \tag{724}$$

$$u = (p_A - p_D)^2, \tag{725}$$

which is the case in which u is the positive variable.

As we can see, in all of those cases we have a variable that was positive and equal to the nergy of the center of mass frame, while the other two could be zero or negative numbers. We can see that they represent the square of the moemntum transfer between particles (in the first example t is the transfer between A and C while u is the transfer between A and D). This allows us to classify those reactions into three channels:

I) $s > 0,\ \ t \leq 0,\ \ u \leq 0$: s channel,

II) $t > 0,\ \ s \leq 0,\ \ u \leq 0$: t channel,

III) $u > 0,\ \ s \leq 0,\ \ t \leq 0$: u channel.

12 Appendix B - Gauge Theories

12.1 Gauging the symmetry

Consider the Dirac Lagrangian for a free particle,

$$\mathcal{L}_D = \bar{\psi}(i\gamma^\mu \partial_\mu - m)\psi, \tag{726}$$

and one can easily verify that the transformation

$$\psi \to e^{i\alpha}\psi, \tag{727}$$

leaves the Lagrangian invariant. At this point, we want to implement interactions in our theory, but we want to do it in a somehow more systematic way. Our first attemp is to try to improve the Lagrangian we obtained, by studying its symmetries a bit more. The free Lagrangian was obtained mainly by the use of the Clifford algebra, which is closely related to the Poincaré group.

Well, as mentioned above, the Lagrangian is invariant under a certain transformation, which happes to be a global U(1) gauge transformation. The lesson we learned in the derivation of the free Lagrangian was that by imposing symmetry, some structure arise (in that case, we started with the Lorentz invariance). Since imposing totally new symmetries seems unnatural, we will try to work and improve what we have: the U(1) symmetry.

A first step towards generalization is to make the global symmetry a local one; this process is called gauging the symmetry. Now, suppose that the phase is now a function of spacetime points,

$$\alpha \to \alpha(x^\mu). \tag{728}$$

If we apply this transformation on the Lagrangian,

$$\mathcal{L}_D = \bar{\psi}(i\gamma^\mu \partial_\mu - m)\psi \to \mathcal{L}_D = \bar{\psi}e^{-i\alpha(x^\mu)}(i\gamma^\mu \partial_\mu - m)e^{i\alpha(x^\mu)}\psi, \tag{729}$$

we realize that the diferential operators now act on the phases,

$$\mathcal{L}_D = \bar{\psi} e^{-i\alpha(x^\mu)} (i\gamma^\mu \partial_\mu - m) e^{i\alpha(x^\mu)} \psi = \mathcal{L}_D = \bar{\psi}(i\gamma^\mu \partial_\mu - m)\psi - (\gamma^\mu \partial_\mu \alpha(x^\mu))\psi. \quad (730)$$

We see that the Lagragian is not invariant, we have an extra term, and to have invariance it must be eliminated. To find the answer to this problem, we need to have a better understanding of what we just did, i.e., a better understanding of the consequences of the local gauge transformation.

A bit more though gives a hint: the problem lies within the derivative. In a field with a global symmetry, the phase convention is universal, the field is affected in the same way, everywhere by the gauge transformation. Well, a derivative can be thought as a difference, and since the same phase was applied everywhere, we can still study how the field changes from point A to point B. To illustrate this a bit, consider the complex plane, and two complex numbers, z_1 and z_2. Suppose that we are interested in calculating $d =\mid z_2 - z_1 \mid$, before and after a U(1) global gauge transformation, $e^{i\alpha}$.

We see that $d =\mid z_2 - z_1 \mid$ was not affected at all. But if we apply a local transformation, the phase that z_1 gets can be different from the phase z_2 gets, and $\mid z_2 - z_1 \mid \neq \mid z_2 e^{i\alpha_2} - z_1 e^{i\alpha_1} \mid$; we see that the usual notion of derivative becomes meaningless. The conclusion is that we need to be able to compare the field at different points, so that we can define a proper derivative operator.

It is necessary to define a new field, the Wilson line.

Definition

Let x^μ and x^ν correspond to two spacetime points. The Wilson line is a field which depends on those spacetime points, and transforms as

$$\Phi(x^\mu, x^\nu) \to e^{i\alpha(x^\mu)} \Phi(x^\mu, x^\nu) e^{-i\alpha(x^\nu)}, \;\; \Phi(x^\mu, x^\mu) = 1. \quad (731)$$

The job of the Wilson line is to "transport" the gauge from a point A to a point B.

Now, consider the quantity $\Phi(x^\mu, x^\nu)\psi(x^\mu) - \psi(x^\nu)$. Under the local gauge transformation,

$$\begin{aligned}\Phi(x^\mu, x^\nu)\psi(x^\mu) - \psi(x^\nu) &\to e^{i\alpha(x^\mu)}\Phi(x^\mu, x^\nu)e^{-i\alpha(x^\nu)}e^{i\alpha(x^\nu)}\psi(x^\mu) - e^{i\alpha(x^\nu)}\psi(x^\nu) \\ &= e^{i\alpha(x^\mu)}(\Phi(x^\mu, x^\nu)\psi(x^\mu) - \psi(x^\nu)),\end{aligned} \tag{732}$$

and this is well defined. We can use this to define a covariant derivative,

$$D_\mu\psi(x^\mu) = \lim_{\epsilon(x^\mu)\to 0} \frac{\psi(x^\mu + \epsilon(x^\mu)) - \Phi(x^\mu, x^\mu + \epsilon(x^\mu))\psi(x^\mu)}{\epsilon(x^\mu)}, \tag{733}$$

which trasforms as

$$\begin{aligned}&D_\mu\psi(x^\mu) \to \\ &\lim_{\epsilon(x^\mu)\to 0} \frac{e^{i\alpha(x^\mu)}\Phi(x^\mu, x^\mu + \epsilon(x^\mu))e^{-i\alpha(x^\mu+\epsilon(x^\mu))}e^{i\alpha(x^\mu+\epsilon(x^\mu))}\psi(x^\mu + \epsilon(x^\mu)) - e^{i\alpha(x^\mu)}\psi(x^\mu)}{\epsilon(x^\mu)} \\ &\lim_{\epsilon(x^\mu)\to 0} e^{i\alpha(x^\mu)}\frac{\Phi(x^\mu, x^\mu + \epsilon(x^\mu))\psi(x^\mu + \epsilon(x^\mu)) - \psi(x^\mu)}{\epsilon(x^\mu)} = e^{i\alpha(x^\mu)}D_\mu\psi(x^\mu).\end{aligned} \tag{734}$$

We will use this new derivative operator, D_μ, to replace our usual partial derivative. However, we need a more explicit form of it, since we don't want to be calculating it by its limit definition all the time. In order to do so, we recall the definition of the Wilson line,

$$\Phi(x^\mu, x^\mu) = 1 \Rightarrow \Phi(x^\mu + \epsilon^\mu(x), x^\mu) \approx 1 - ie\,\epsilon(x^\mu)A_\mu(x^\mu) + \mathcal{O}(\epsilon)^2. \tag{735}$$

The equation above is accurate up to first order, with respect to an infinitesimal displacement. We introduced two parameters, for the sake of generality: a constant of proportionality, e, and a field A_μ, which accounts for the fact that the first order term

may be a function of the point x^μ. Going back to the definition of the covariant derivative,

$$\begin{aligned} D_\mu\psi(x^\mu) &= \lim_{\epsilon(x^\mu)\to 0} \frac{[\psi(x^\mu+\epsilon(x^\mu))] - [1 - ie\ \epsilon(x^\mu)A_\mu(x^\mu)]\psi(x^\mu)}{\epsilon(x^\mu)} \\ &= \lim_{\epsilon(x^\mu)\to 0} \frac{\psi(x^\mu+\epsilon(x^\mu)) - \psi(x^\mu) + ie\ \epsilon(x^\mu)A_\mu(x^\mu)\psi(x^\mu)}{\epsilon(x^\mu)} \\ &= \lim_{\epsilon(x^\mu)\to 0} \frac{(\partial_\mu\psi(x^\mu))\epsilon(x^\mu) + ie\ \epsilon(x^\mu)A_\mu(x^\mu)\psi(x^\mu)}{\epsilon(x^\mu)} \\ &= [\partial_\mu + ieA_\mu(x^\mu)]\psi(x^\mu). \end{aligned} \tag{736}$$

We are interested in finding out how the field A_μ transforms. Thus, look again at how the Wilson line transforms,

$$\begin{aligned} \Phi(x^\mu+\epsilon^\mu(x), x^\mu) &\to e^{i\alpha(x^\mu, x^\mu+\epsilon^\mu(x))}\Phi(x^\mu+\epsilon^\mu(x), x^\mu)e^{-i\alpha(x^\mu)} \\ &= e^{i\alpha(x^\mu, x^\mu+\epsilon^\mu(x))}[1 - ie\ \epsilon(x^\mu)A_\mu(x^\mu)]e^{-i\alpha(x^\mu)}, \end{aligned} \tag{737}$$

which implies:

$$\begin{aligned} 1 - ie\ \epsilon(x^\mu)A_\mu(x^\mu) &\to e^{i\alpha(x^\mu+\epsilon^\mu(x))}[1 - ie\ \epsilon(x^\mu)A_\mu(x^\mu)]e^{-i\alpha(x^\mu)} \\ &= [e^{i\alpha(x^\mu)} + (\partial_\mu e^{i\alpha(x^\mu)})\epsilon^\mu(x)][1 - ie\ \epsilon(x^\mu)A_\mu(x^\mu)]e^{-i\alpha(x^\mu)} \\ &= [e^{i\alpha(x^\mu)} + (\partial_\mu e^{i\alpha(x^\mu)})\epsilon^\mu(x) - e^{i\alpha(x^\mu)}ie\ \epsilon(x^\mu)A_\mu(x^\mu) + \mathcal{O}(\epsilon)^2]e^{-i\alpha(x^\mu)} \\ &= e^{i\alpha(x^\mu)}\left(1 - ie\left[A_\mu(x^\mu) - \frac{1}{e}(\partial_\mu\alpha(x^\mu))\right]\epsilon^\mu(x)\right)e^{-i\alpha(x^\mu)}, \end{aligned} \tag{738}$$

and we obtain the transformation rule,

$$A_\mu \to A_\mu - \frac{1}{e}\partial_\mu\alpha(x^\mu). \tag{739}$$

In the context of differential geometry, the field A_μ is a connection, just like the Christoffel symbol in General Relativity. It also contains a very deep geometrical meaning, but we will not discuss it here; we will leave it to a later moment. In our context, we refer to A_μ

as the gauge field.

The final missing element here is a closed form for the Wilson line. We will proceed just as we do in Group Theory with the generators and the exponential map. We have:

$$1 + ie\,\epsilon(x^\mu)A_\mu(x^\mu) \Rightarrow \Phi_{x^\mu \to x^\nu} = exp\left(-ie\int_{x^\mu}^{x^\nu} A_\mu(x^\sigma)dx^\mu\right), \tag{740}$$

where the integral above is a line integral from the initial point to the final. We can parametrize the path, and changing the notation sligthly, we write:

$$\Phi_{A\to B} = exp\left(-ie\int_A^B A_\mu dx^\mu\right). \tag{741}$$

One may verify this actually satisfies the transformation law that defines the Wilson line under the local gauge transformation we have been working with (recall that in our notation, the point A is a label for x^μ and B for x^ν.

$$\begin{aligned}\Phi_{A\to B} = exp\left(-ie\int_A^B A_\mu dx^\mu\right) &\to exp\left(-ie\int_A^B (A_\mu - \frac{1}{e}\partial_\mu\alpha)dx^\mu\right)\\ &= exp\left(-ie\int_A^B A_\mu dx^\mu + i\int_A^B \partial_\mu\alpha\, dx^\mu\right)\\ &= exp\left(-ie\int_A^B A_\mu dx^\mu + i(\alpha(x^\mu) - \alpha(x^\nu))\right)\\ &= e^{i\alpha(x^\mu)}\Phi_{A\to B}e^{-i\alpha(x^\nu)}.\end{aligned} \tag{742}$$

The endpoints may form a closed path;

$$\Phi_C = exp\left(-ie\oint A_\mu dx^\mu\right), \tag{743}$$

and this is called a Wilson loop. From the check we just performed, we see that when the loop is closed, the integral is locally gauge invariant (its result do not change if we perform a gauge transformation because the phase difference $\alpha(x^\mu) - \alpha(x^\nu)$ vanishes).

It is important to getter a bettter understanding of the Wilson loop, and so we use Stoke's Theorem,

$$\Phi_C = exp\left(-ie \oint A_\mu dx^\mu\right) = exp\left(-ie \int F_{\mu\nu} d\sigma^{\mu\nu}\right), \tag{744}$$

where $d\sigma^{\mu\nu}$ is the area element. Let's explore the newly defined quantity $F_{\mu\nu}$, the field strength.

Our main task is to find an expression for $F_{\mu\nu}$. It is not really very helpful to start with the right-hand side of the equation above, so we will begin with the left-hand side, since we are more familiar with the Wilson loop. The derivation will not be rigorous uo to a mathematician's standards, but we hope to provide some more insight on the nature of these quantities and the Stokes Theorem.

Consider a usual derivative, and a certain real function f,

$$\frac{df}{dx} = \lim_{\epsilon \to 0} \frac{f(x+\epsilon) - f(x)}{\epsilon} \Rightarrow f(x+\epsilon) = f(x) + \epsilon \frac{df}{dx}. \tag{745}$$

We can think of the derivative as generating the transport of the function, from being evaluated at x and then at $x + \epsilon$. In our case, the same idea still applies, but we use a generalized derivative operator, the covariant D_μ, which tells us how to "walk" in our more complicated space, where the local gauge transformations are allowed. The key for this is the gauge field, A_μ; in differential geometry, A_μ is reffered to as a connection, and the motivation comes from this idea.

Suppose now that we have a field ϕ (scalar, spinor, an arbitrary field), and we want to "transport" it around a loop, a very small one. Following the ideas of the last paragraph, we can argue that since the covariant derivative is related to "transporting" the field, whichever phase that the ϕ acquires by going around the loop will be directly related to the derivatives. Since our loop is very small and the field is arbitrary, we can focus our attention on the derivatives, and forget about the rest.

Going around the loop above can be thought as applying the derivatives on the field, but in a different order. The total change around the loop is related to:

$$D_\mu D_\nu - (D_\nu D_\mu) = [D_\mu, D_\nu], \tag{746}$$

where the first term (of the left hand side) accounts for the path $O \to A \to B$, and the second term accounts for $B \to A' \to O$. We can calculate this quantity explictly,

$$D_\mu D_\nu \phi = (\partial_\mu + ieA_\mu)(\partial_\nu + ieA_\nu)\phi = \partial_\mu(\partial_\nu\phi) + ie(\partial_\mu A_\nu)\phi + ieA_{mu}(\partial_\nu\phi) - e^2 A_\mu A_\nu \phi, \tag{747}$$

now, $D_\nu D_\mu \phi$:

$$D_\nu D_\mu \phi = (\partial_\nu + ieA_\nu)(\partial_\mu + ieA_\mu)\phi = \partial_\nu(\partial_\mu\phi) + ie(\partial_\nu A_\mu)\phi + ieA_\nu(\partial_\mu\phi) - e^2 A_\nu A_\mu \phi, \tag{748}$$

subtracting,

$$(D_\mu D_\nu - D_\nu D_\mu)\phi = ie(\partial_\mu A_\nu - \partial_\nu A_\mu + ie[A_\mu, A_\nu])\phi. \tag{749}$$

The U(1) group is Abelian, which implies $[A_\mu, A_\nu]$ in this specific case. Now, this motivates us to define:

$$[D_\mu, D_\nu] = \frac{i}{e} F_{\mu\nu}, \tag{750}$$

because of the way it transforms. Now we go back to the integral of the Wilson loop. According to Stokes Theorem, we need to take the curl of A_μ,

$$-ie \oint A_\mu dx^\mu = -ie \int d\sigma^{\mu\nu}(\nabla_\mu A_\nu - \nabla_\nu A_\mu), \tag{751}$$

but

$$\nabla_\mu A_\nu - \nabla_\nu A_\mu = (\partial_\mu + ieA_\mu)A_\nu - (\partial_\nu + ieA_\nu)A_\mu = \partial_\mu A_\nu - \partial_\nu A_\mu + ie[A_\mu, A_\nu], \tag{752}$$

which is precisely the definition of the field strength. We are led to make the identification

$$-ie \oint A_\mu dx^\mu = -ie \int d\sigma^{\mu\nu}[D_\mu, D_\nu] = \int d\sigma^{\mu\nu} F_{\mu\nu}. \tag{753}$$

In differential geometry the commutator of two covariant derivatives is related to the curvature of the space in which the connections (and therefere the covariant derivatives) are defined, a concept that is one of the key elements in General Relativity. In that theory, the curvature is governed by Einstein's equations, which dictate the dynamics of matter, energy and the spacetime curvature itself.

Now we know what the field strength is and how it relates to the Wilson loop, which is a locally gauge invariant quantity and therefore an observable (we will explore this concept in further detail on the next section), we are interested in include the dynamics of the gauge field A_μ in our theory. In order to do so, we need a kinetic term on the Lagrangian. That term needs to be a scalar, and invariant under Lorentz and the local gauge transformation. Consider a collection of field strength tensors, which transforms as

$$F_{\alpha\beta}F_{\gamma\delta}...F_{\mu\nu} \to e^{i\theta(x)}F_{\alpha\beta}F_{\gamma\delta}...F_{\mu\nu}e^{-i\theta(x)}. \tag{754}$$

Taking the trace of the equation above and using its cyclicity,

$$\begin{aligned} Tr(F_{\alpha\beta}F_{\gamma\delta}...F_{\mu\nu}) &\to Tr(e^{i\theta(x)}F_{\alpha\beta}F_{\gamma\delta}...F_{\mu\nu}e^{-i\theta(x)}) \\ &= Tr(e^{-i\theta(x)}e^{i\theta(x)}F_{\alpha\beta}F_{\gamma\delta}...F_{\mu\nu}) = Tr(F_{\alpha\beta}F_{\gamma\delta}...F_{\mu\nu}), \end{aligned} \tag{755}$$

and we see that the trace is gauge invariant. The simplest combinatton we can think of is something proportional to

$$\mathcal{L}_{kin} \; \alpha \; F_{\mu\nu}F^{\mu\nu}. \tag{756}$$

We set the constant as -1/4 for convenience (in the end we are trying to derive electromagnetism). Finally, we need to include a source term for A_μ,

$$\mathcal{L}_{source} = -J^\mu A_\mu. \tag{757}$$

Our full Lagrangian is

$$\mathcal{L}_D = \bar{\psi}(i\gamma^\mu D_\mu - m)\psi - \frac{1}{4}F_{\mu\nu}F^{\mu\nu} - J^\mu A_\mu, \tag{758}$$

which turns out to be the correct one. The focus of this section was more mathematical, and even though we paid attention to the motivation to include and construct the terms in the Lagrangian, we did not dicusses the physical meaning of them in detail. We leave this to the next sections.

12.2 Yang- Mills Theory

12.2.1 The non-Abelian case

As we saw before in the spin-half case, gauging a symmetry allows us to express an interaction in QFT. In this section, we will generalize the procedure, which will allow us to use more complicated groups, even non-Abelian ones. Our discussion will be more straightfoward, since the motivation and the ideas are essentially the same for the U(1) case.

Assume a certain group, SU(N). Let $\mathcal{L}$ denote a Lagrangian density, composed, as usual, by N scalar or spinor fields, which we denote as ϕ_i. Suppose that the symmetry

$$\phi_i \to U_i^j \phi_j, \tag{759}$$

leaves the Lagrangian unchanged (U is an operator induced by the Lie group, a N x N matrix). In order to mimic the procedure used in obtaining the interacting Dirac Lagrangain, we need to define a gauge field and a covariant derivative, which also contains the charge of the field. Kinetic terms and sources for the gauge field are defined as well, and we can implement interactions in a perturbative fashion, up to as amny orders as considered necessary.

In general, our group element U can be written as

$$U(x) = e^{-ig\theta_a(x)T^a}, \;\; [T^a, T^b] = if_{abc}T^c. \tag{760}$$

Note that the $N^2 - 1$ parameters θ_a are local, and g is a constant.

The next step is to give a prescription of how our gauge field transforms. Now, let's denote the gauge field by A_μ. Note that since the gauge field is generated by infinitesimal transformations, it can be decomposed in terms of the generators t^a of the Lie group. Let's write the covariant derivative as

$$D_\mu = \mathbb{I}^{N\times N}\partial_\mu - CA_\mu \Rightarrow D_\mu\phi_i = \partial_\mu\phi_i - CA_\mu\phi_i, \tag{761}$$

where C is to be determined. Since each component of A_μ is an $N \times N$ matrix, we need to multiply the partial derivative by the unit matrix of the correponding dimension. The action of such an operator in a scalar field is given by

$$(D_\mu\phi)_i = \partial_\mu\phi_j(x) - C[A_\mu]_{ij}\phi_j(x), \tag{762}$$

making it clear that we are working with matrices in general. For the sake of simplicity, we will ommit uneccessary indices in the following derivation. Back to our problem, after the transformation U, the covariant derivative becomes

$$D_\mu \rightarrow D'_\mu = UD_\mu, \tag{763}$$

and can be written as:

$$(D_\mu\phi_i)' = \partial_\mu\phi'_i - C(A_\mu\phi_i)'. \tag{764}$$

We are interested in the gauge field, so we will try to work with A'_μ.

$$C(A_\mu\phi_i)' = \partial_\mu\phi'_i - (D_\mu\phi_i)'. \tag{765}$$

Now, we need to express our transformed scalar field (and its partial derivatives) in a

more convinient way. Our field ϕ_i and its partial derivatives transforms as:

$$\phi_i \to \phi_i' = U\phi_i, \;\; \partial_\mu \phi_i' = \partial_\mu (U\phi_i) = (\partial_\mu U)\phi_i + U\partial\phi_i, \tag{766}$$

and the covariant derivative, by definition,

$$D_\mu \phi_i \to (D_\mu \phi_i)' = U D_\mu \phi_i. \tag{767}$$

Therefore, we have:

$$C(A_\mu \phi_i)' = \partial_\mu \phi_i' - (D_\mu \phi_i)' = (\partial_\mu U)\phi_i + U\partial\phi_i - UD_\mu\phi_i = (\partial_\mu U)\phi_i + U(\partial\phi_i - D_\mu)\phi_i. \tag{768}$$

Finally, note that one may write

$$\phi_i = U^{-1}\phi_i', \tag{769}$$

which implies

$$C(A_\mu \phi_i)' = ((\partial_\mu U)U^{-1} + UCA_\mu U^{-1})\phi_i'. \tag{770}$$

Since we imposed no restriction over the field ϕ_i, it remais arbitrary. This implies the following transformation law:

$$A_\mu \to A_\mu' = \frac{1}{C}(\partial_\mu U)U^{-1} + UA_\mu U^{-1}. \tag{771}$$

$$A_\mu \to A_\mu' = \frac{1}{C}(\partial_\mu U)U^{-1} + UA_\mu U^{-1}, \tag{772}$$

For the case of an unitary operator, $U^{-1} = U^\dagger$. One may also be interested in raising an index with the metric.

$$A^\mu \to A^{\mu\prime} = \frac{1}{C}(\partial^\mu U)U^\dagger + UA^\mu U^\dagger \tag{773}$$

Geometrically, this result resembles a rotation in a complex scenario, except for the fact that it also has the extra term with the operator's derivative.

It is important to perform a consistency check of the results obtained so far; if we redefine C = ig and consider a U(1) transformation,

$$U = e^{ig\theta(x)} \Rightarrow A^\mu \rightarrow A^\mu + \partial^\mu \theta(x), \tag{774}$$

we are able to recover the result of the spin half field.

Listing our results, we have:

$$(D_\mu \phi)_i = \partial_\mu \phi_j(x) - ig[A_\mu]_{ij}\phi_j(x), \tag{775}$$

$$A^\mu \rightarrow A^{\mu\prime} = -\frac{i}{g}(\partial^\mu U)U^\dagger + UA^\mu U^\dagger \tag{776}$$

$$F_{\mu\nu}(x) = \frac{i}{g}[D_\mu, D_\nu] = \partial_\mu A_\nu - \partial_\nu A_\mu - ig[A_\mu, A_\nu], \tag{777}$$

where $F_{\mu\nu}$ is our field strength. Note that the commutator $[A_\mu, A_\nu]$ vanishes for Abelian groups. We will not explore the geometrical meaning of these quantities so much here, so we keep focused on our goal. More detail will be found when we start looking at General Relativity in the next chapter.

Now, we consider the Wilson line. In the context of non-Abelian groups, the integral contains now $A_\mu(x)$, which does not necessarily commute at different points. Therefore, we introduce a path-ordering:

$$\Phi_{A\rightarrow B} = P\left\{exp\left(ig\int_0^1 ds \frac{dx^\mu}{ds}A_\mu(x)\right)\right\}. \tag{778}$$

$\Phi_{A\rightarrow B}$ needs to be unitary if we want changes in phase to conserve probability.

We need to find a way of introducing the field strength in a kinetic term if the Lagrangian. We pick:

$$\mathcal{L}_{kin} = -\frac{1}{2} F_{\mu\nu} F^{\mu\nu}. \tag{779}$$

The conclusion is that by following the procedure above, every Lie group defines a gauge field, and therefore, describes an interaction. It is important to mention that the representations that will be useful for us are the adjoint, the Fundamental and anti-Fundamental (see Appendix A).

12.3 Gravity

In the gravitational physics context, it is not possible to define observers that are totally isolated from the interactions of the system, because everything is coupled to the gravitational field. One can not simply define an isolated background (what we normally refer to as the "lab frame" as in non gravitational physics); the solution for this is just to accept that spacetime is not flat, and that all the bodies fall into geodesics defined in a curved spacetime.

The consequences of this treatment is that gravity is no longer treated as a force, but implemented as the very structure of spacetime: the geodesics (observers) are now consistent with the equivalence principle. As an additional constraint, all equations must be reduced to the ones obtained in Special Relativity when the limit for a flat metric is taken.

Postulate - The Equivalence Principle

There is no difference in the outcome of a physical experiment performed in a suffciently small freely falling laboratory over a sufficiently small amount of time and the same experiment in an inertial frame in free space.

This last version makes essentially states that at least locally, there is no difference between following a geodesic or being in free space. Thus, following our geodesics is the

equivalent of "being in a inertial frame at rest" in a curved spacetime; locally, a general spacetime "looks like" flat spacetime.

When dealing with non-gravitational physics, a certain approach is commonly used to describe phenomena. First, one defines observers that are not affected by the interactions that take part in the physical system studied, so that they can be used to define an inertial frame. Then, by the use of test bodies and the way they interact, one extracts information about the system.

The problem with this approach when studying gravitational physics is that there is no way of constructing inertial observers in the sense of non-relativistic physics, since everything is coupled to the gravitational field; there is no way of defining a "background". General relativity then accepts the fact that we can't construct inertial observes in the usual sense; it postulates that spacetime is not flat, and free falling bodies in a gravitational field are the geodesics in a curved spacetime. The geodesics (observers) agree with the equivalence principle, and gravity is no longer a force, but the very structure of the spacetime. In addition, when working with General relativity we also require that our equations reduce to the ones in special relativity when the metric is flat.

12.3.1 Gravity as a Gauge Theory

Well, we can, in a very loose way, think of General Relativity as Special Relativity together with a new postulate, the Principle of Equivalence. From that perspective, we can draw interesting conclusions.

The first thing we notice is the result of enforcing the Principle of Equivalence in our theory; it defines a local equivalence between a spacetime with gravity (freely falling laboratory) and an inertial frame in free space, i.e., in the absence of gravity, as studied in Special Relativity. As defined previously spacetime is a 4-dimensional manifold, and a spacetime with gravity needs to be, according to the Principle of Equivalence, locally flat. Note that we have no contraints over the global nature of spacetime, and in fact the most general solution to our problem is to have a spacetime that is curved but locally "looks like" Minkowski spacetime. This idea is actually familiar to us; for example: we know

that Earth's surface is curved, but locally it looks flat (this actually mislead mankind for centuries).

In order to see this mathematically, consider the next proposition.

Proposition

Given a metric in a certain component system, it is always possible to find, for a given point p, new coordinates such that

$$g_{\alpha\beta}\Big|_p = \eta_{\alpha\beta}. \tag{780}$$

Proof. Given a certain coordinate system, the metric can be written as a 4x4 real symmetric matrix at point p. However, from linear algebra, any real symmetric matrix can be diagonalized by a linear transformation. When written in diagonal form, we can rescale the coordinates by constant factors such that all entries of the metric are ± 1.

□

Another property our spacetime must have is that the physics should not depend on the coordinate system adopted, as in Special Relativity; the Principle of Equivalence does not affect this. If General Relativity does not depend on the coordinate system, i.e, the physics is left unchanged under the change of the coordinate system, this is a symmetry of our theory.

If we have two manifolds M and N related by a diffeomorphism, they have the same manifold structure. With this in mind, suppose that we have a collection of tensor fields defined on M. We may write:

$$(M, \{T\}) \to (N, \{\phi^\star T\}), \tag{781}$$

via ϕ. As far as physics is concerned, we can't distinguish between the manifolds and their tensor fields; any physical statement regading one of the manifolds will be satisfied by other. Note that this is not the case if the manifolds are not diffeomorphic. We can say that diffeomorphisms are the "gauge freedom" of any theory that is based on tensors on spacetime manifolds. In particular, General Relativity.

Let (U_1, ψ_1) and (U_2, ψ_2) be two charts, which overlap on the region $U_1 \cap U_2 = O$. For smooth and invertible (with smooth inverse) mappings, the coordinate transformation

$$\psi_2 \circ \psi_1^{-1} : \mathbb{R}^n \to \mathbb{R}^n, \tag{782}$$

is a diffeomorphism. Physics is independent of the coordinate choice, so coordinate transformations can be though as a "gauge symmetry" of the theory. Under a general change of coordinates,

$$\partial_\mu \to \partial'_\mu = \frac{\partial x^\nu}{\partial x'^\mu} \partial_\nu, \tag{783}$$

$$dx^\mu \to dx^{\mu'} = \frac{\partial x'^\mu}{\partial x^\nu} dx^\nu. \tag{784}$$

In order to follow the notation used in previous sections, we define:

$$U^\mu_\nu(x) = \frac{\partial x'^\mu}{\partial x^\nu}, \tag{785}$$

$$[U^{-1}]^\mu_\nu(x) = \frac{\partial x^\nu}{\partial x'^\mu}, \tag{786}$$

and those can be viewed as local transformations. Since the transformation is local, we have

$$\partial_\mu U^\mu_\nu \neq 0, \tag{787}$$

and the partial derivatives of vectors, dual vectors and tensor fields do not transform properly under our symmetry transformation, the change of coordinates. Furthermore, we would like to enforce some constraints in our derivative operator. Let R and S be two arbitrary tensor fields and f a scalar function,

I) Linearity: $\nabla_a(\alpha R + \beta S) = \alpha \nabla_a(R) + \beta \nabla_a(S), \ \ \forall R, S \in \tau(m, s), \ \ \alpha, \beta \in \mathbb{R},$

II) Leibnitz rule: $\nabla_a(RS) = (\nabla_a R)S + R(\nabla_a S), \ \ \forall R, S \in \tau(m, s),$

III) Commutativity with contraction: $\nabla_d(R^{a_1,\ldots,c,\ldots,a_m}_{b_1,\ldots,c,\ldots,b_s}) = (\nabla_d R^{a_1,\ldots,c,\ldots,a_m}_{b_1,\ldots,c,\ldots,b_s})$, $\forall R, S \in \tau(m,s)$,

IV) Consistency with diretional derivatives on scalar fields as tangent vectors: $v(f) = v^a \nabla_a(f)$

V) Torsion free: $\nabla_a \nabla_b f = \nabla_b \nabla_a f$.

It is interesting to mention that the last condition is sometimes dropped in alternative theories of gravity (but not in General Relativity).

Following the procedure on the Yang-Mills section, we now write

$$\partial_a \to \nabla_a, \tag{788}$$

which acts on dual vectors as

$$\nabla_a \omega_b = \partial_a \omega_b - \Gamma^c_{ab} \omega_c. \tag{789}$$

Γ^c_{ab} is a symmetric tensor field, and is called the Christoffel symbol.Note that by writing the derivative operator in this way our constraints are satisfied. However, our derivation is still not complete; in order to find out how this derivative operator acts on vectors. From property (4), by considering the result of the contraction $\omega_b v^b$ (a scalar), one obtains

$$\nabla_a v^b = \partial_a v^b + \Gamma^b_{ac} v^c, \tag{790}$$

which implies for a general tensor field,

$$\nabla_a T^{b_1\ldots b_n}_{c_1\ldots c_m} = \partial_a T^{b_1\ldots b_n}_{c_1\ldots c_m} - \sum_i \Gamma^{b_i}_{ad} T^{b_1\ldots d\ldots b_n}_{c_1\ldots c_m} + \sum_j \Gamma^d_{ac_j} T^{b_1\ldots b_n}_{c_1\ldots d\ldots c_m}. \tag{791}$$

12.3.2 The metric and the Levi-Civita connection

In order to better understand the covariant derivative, we will list now a few results. For details on the proofs, see [9].

Proposition

Any two derivative operators defined in a manifold are related by a symmetric tensor field S^c_{ab}. In the context of General Relativity, we denote this field by Γ^c_{ab}.

Theorem

Let M be a manifold, which possesses the metric g_{ab}. Then

$$\nabla_c \, g_{ab} = 0, \;\; \forall p \in M, \tag{792}$$

holds true for a unique derivative operator.

Proof. The proof will follow through construction. We will find a way of expressing the Christoffel symbol in terms of the metric. We know how a derivative operator acts on a $(0, 2)$ tensor,

$$0 = \nabla_a g_{bc} = \partial_a g_{bc} - \Gamma^d_{ab} g_{dc} - \Gamma^d_{ac} g_{bd}. \tag{793}$$

Now, the condition $\nabla_c g_{ab} = 0$ holds true if and only if

$$\partial_a g_{bc} = \Gamma_{cab} + \Gamma_{bac}. \tag{794}$$

If we started the derivation with indices chosen as $\nabla_c g_{ab}$, we would have a different appearence on the equation above. With that in mind, we consider permutations of the indices,

$$\partial_c g_{ab} = \Gamma_{bca} + \Gamma_{acb}, \tag{795}$$

$$\partial_b g_{ac} = \Gamma_{cba} + \Gamma_{abc}, \tag{796}$$

We will add eq. (?) and (?) and subtract (?) (add the first, the third and subtract the second), and use the symmetry of Γ^a_{bc} to write

$$2\,\Gamma_{cab} = \partial_a g_{bc} + \partial_b g_{ac} - \partial_c g_{ab} \Rightarrow \Gamma^c_{ab} = \frac{1}{2} g^{cd} \left(\partial_a g_{bd} + \partial_b g_{ad} - \partial_d g_{ab}\right). \tag{797}$$

This expression for Γ^c_{ab} is unique and satisfies $\nabla_c g_{ab} = 0$. In diffferential geometry, the tensor field that appears in the covariant is called a connection, and the field Γ^a_{bc} is known as the Levi Civita connection.

□

12.3.3 Killing vector fields and Lie algebras

At this point, one might be thinking about the relation between the derivative operator and the Lie derivative we defined a while ago, when we were introducing the concept of manifolds, specially after all the work done related to diffeomorphisms.

The Lie derivative induces a translation of the tensor field (in which we are operating) by the use of a certain diffeormorphism, and then calculates the difference of the induced tensor field and the usual tensor at a point p. However, if a tensor does not change under the diffeormorphism, for example,

$$\phi_t^\star g_{ab} = g_{ab}, \tag{798}$$

then we expect its Lie derivative to be zero. The next definition explores this idea.

Definition

A diffeomeorphism is an isometry if and only if

$$\pounds_\xi \; g_{ab} = 0. \tag{799}$$

Definition

Let $\{\phi_t\}$ be a set of one-parameter diffeomorphisms, $\phi_t : M \to M$ which are also isometries,

$$\phi_t^\star g_{ab} = g_{ab}. \tag{800}$$

The vector field which generates ϕ_t is called a Killing vector field.

From the definitions and ideas discussed, we see that a diffeomeorphism is an isometry if and only if

$$\pounds_\xi \, g_{ab} = 0. \tag{801}$$

Thus, if we apply the definition of the Lie derivative for a general tensor field:

$$\pounds_\xi \, g_{ab} = \xi^c \nabla_c g_{ab} + g_{cb} \nabla_a \xi^c + g_{ac} \nabla_b \xi^c, \tag{802}$$

and use the property $\nabla_c g_{ab} = 0$, we have

$$\pounds_\xi \, g_{ab} = \xi^c \nabla_c g_{ab} + g_{cb} \nabla_a \xi^c + g_{ac} \nabla_b \xi^c = 0, \tag{803}$$

$$0 = g_{cb} \nabla_a \xi^c + g_{ac} \nabla_b \xi^c = \nabla_a (g_{cb} \xi^c) + \nabla_b (g_{ac} \xi^c), \tag{804}$$

and finally,

$$\nabla_a \xi_b + \nabla_b \xi_a = 0. \tag{805}$$

This is called the Killing's equation.

As we can see, the Killing vectors carry information about the symmetries in the metric, and they actually help in making the study of symmetries of the metric more "concrete". It is useful now to consider an example.

Consider the following metric (the Schwarschild metric, in Schwarschild coordinates)

$$ds^2 = -\left(1 - \frac{2M}{r}\right) dt^2 + \left(1 - \frac{2M}{r}\right)^{-1} dr^2 + r^2 (d\theta^2 + sin^2\theta d\phi^2). \tag{806}$$

One way of finding the Killing vectors is by attacking the Killing equation directly. In other words, obtaining all the Christoffel symbols for this metric, writing the expression for the covariant derivative and solving the differential equation. Another way is by directly inspecting the metric and checking the dependence on the coordinates.

The coordinates we are using here are (t, r, θ, ϕ). Note that, for instance, the metric does not have a functional dependence on the time; thus, we have a Killing vector

$$\xi^{\mu} = (1, 0, 0, 0). \tag{807}$$

It can also be shown that the commutator of two Killing vector fields is also a Killing vector field,what implies that the set of Killing vectors fields of a manifold forms a Lie algebra.

We conclude this discussion by considering a very intersting example, in the spirit of [13]: the metric of the unit S^2 sphere. Note that this metric is part of many metrics of General Relativity, such as the Schwarzchild metric (which is actually a spherically symmetric solution).

$$ds^2 = d\theta^2 + sin^2(\theta)d\phi^2, \tag{808}$$

which yelds the following equations for the Killing vectors:

$$2\partial_{\theta}\xi^{\theta} = 0, \tag{809}$$

$$2\partial_{\phi}\xi^{\phi} + 2sin(\theta)cos(\theta)\xi^{\theta} = 0, \tag{810}$$

$$\partial_{\phi}\xi^{\theta} + \partial_{\theta}\xi^{\phi} - 2cot(\theta)\xi_{\phi} = 0. \tag{811}$$

From the first equation, there is no explicit dependence on θ as the partial derivative indicates. Thus, ξ^{θ} is a function of ϕ only; using this result on the second equation,

$$\partial_\phi \xi^\phi = -sin(\theta)cos(\theta)\xi^\theta = -\frac{1}{2}2sin(\theta)cos(\theta)\xi^\theta = -\frac{1}{2}sin(2\theta)\xi^\theta, \tag{812}$$

Since this equation involves a partial derivative, if we solve it by integration we need to introduce a function $f(\theta)$,

$$\xi^\phi = -\frac{1}{2}Fsin(2\theta) + f(\theta), \;\; \xi^\theta = \frac{dF}{d\phi}. \tag{813}$$

From the last equation,

$$\begin{aligned} -Fcos(2\theta) + \frac{df}{d\theta}c + \frac{d\xi^\theta}{d\phi} + 2cot(\theta)\left(\frac{1}{2}Fsin(2\theta) - f(\theta)\right) = 0 \\ \Rightarrow \frac{df}{d\theta} - 2cot\theta f(\theta) = -\left(\frac{d\xi^\theta}{d\phi} + F\right), \end{aligned} \tag{814}$$

which are differential equations on independet variables. Thus, we can introduce a constant C such that

$$\frac{df}{d\theta} - 2cot\theta f(\theta) = -\left(\frac{d\xi^\theta}{d\phi} + F\right) = C. \tag{815}$$

Solving each of the equations:

$$f(\theta) = (C' - Ccot\theta)sin^2\theta, \tag{816}$$

$$\xi^\theta = Asin(\phi) + Bcos(\phi), \tag{817}$$

and all of this implies

$$\xi^\phi = (Acos\phi - Bsin\phi)sin\theta cos\theta + C'sin^2\theta. \tag{818}$$

We can write a Killing vector field as

$$\xi^\theta\partial_\theta + \xi^\phi\partial_\phi = AL_y + BL_x + C'L_z, \tag{819}$$

with the generators of $SO(3)$:

$$L_x = -cos\phi\ \partial_\theta + cot\theta sin\phi\ \partial_\phi, \tag{820}$$

$$L_y = sin\phi\partial_\phi + cot\theta cos\phi\partial_\phi, \tag{821}$$

$$L_z = \partial_\phi. \tag{822}$$

13 Appendix C - Gamma matrices

Here, we list some identities involving Gamma matrices and slashed quantities.

13.1 Dirac representation

$$\gamma^0 = \begin{pmatrix} 1 & 0 & 0 & 0 \\ 0 & 1 & 0 & 0 \\ 0 & 0 & -1 & 0 \\ 0 & 0 & 0 & -1 \end{pmatrix}, \quad \gamma^1 = \begin{pmatrix} 0 & 0 & 0 & 1 \\ 0 & 0 & 1 & 0 \\ 0 & -1 & 0 & 0 \\ -1 & 0 & 0 & 0 \end{pmatrix}, \tag{823}$$

$$\gamma^2 = \begin{pmatrix} 0 & 0 & 0 & -i \\ 0 & 0 & i & 0 \\ 0 & 0 & i & 0 \\ -i & 0 & 0 & 0 \end{pmatrix}, \quad \gamma^3 = \begin{pmatrix} 0 & 0 & 1 & 0 \\ 0 & 0 & 0 & -1 \\ -1 & 0 & 0 & 0 \\ 0 & -1 & 0 & 0 \end{pmatrix}, \tag{824}$$

$$\gamma^5 = \gamma^0\gamma^1\gamma^2\gamma^3 = \begin{pmatrix} 0 & 0 & 1 & 0 \\ 0 & 0 & 0 & 1 \\ 1 & 0 & 0 & 0 \\ 0 & 1 & 0 & 0 \end{pmatrix}, \tag{825}$$

but also,

$$\gamma^5 = \epsilon_{\mu\nu\alpha\beta}\gamma^\mu\gamma^\nu\gamma^\alpha\gamma^\beta. \tag{826}$$

where ϵ is the Levi-Civita symbol.

For the metric signatute (+ - - -),

$$\{\gamma^\mu, \gamma^\nu = 2\eta^{\mu\nu}\}, \tag{827}$$

$$\gamma_\mu = \eta_{\mu\nu}\gamma^\mu \Rightarrow \gamma_\mu = \{\gamma^0, -\gamma^1, -\gamma^2, -\gamma^3\}. \tag{828}$$

13.2 Identities

$$\gamma^\mu \gamma_\mu = 4\mathbb{I}, \tag{829}$$

$$\gamma^\mu \gamma^\nu \gamma_\mu = -2\gamma^\nu, \tag{830}$$

$$\gamma^\mu \gamma^\nu \gamma^\rho \gamma_\mu = 4\eta^{\nu\rho}\mathbb{I}, \tag{831}$$

$$\gamma^\mu \gamma^\nu \gamma^\alpha \gamma^\beta \gamma_\mu = -2\gamma^\beta \gamma^\alpha \gamma^\nu \tag{832}$$

$$\gamma^\mu \gamma^\nu \gamma^\alpha = \eta^{\mu\nu}\gamma^\alpha + \eta^{\nu\alpha}\gamma^\mu - \eta^{\mu\alpha}\gamma^\nu - i\epsilon^{\beta\mu\nu\alpha}\gamma_\beta \gamma^5. \tag{833}$$

13.3 Traces

The trace operator Tr satisfies

$$\mathrm{Tr(A + B) = Tr(A) + Tr(B)}, \tag{834}$$

$$\mathrm{Tr(cA) = cTr(A)}, \tag{835}$$

$$\mathrm{Tr(ABC) = Tr(CAB) = Tr(BCA)}. \tag{836}$$

Denoting $\not{a} = \gamma_\mu a^\mu$,

I) $\mathrm{Tr}(\gamma^\mu) - \mathrm{Tr}(\gamma^\mu)$

II) $\mathrm{Tr}\mathbb{I} = 4$ (we are working with 4x4 matrices)

III) Trace of an odd number of γ_μ's vanishes.

IV) $\mathrm{Tr}(\not{a}\not{b}) = 4\,\mathrm{a}\,.\,\mathrm{b}$

V) $\mathrm{Tr}(\not{a}\not{b}\not{c}\not{d}) = 4[(\mathrm{a}\,.\,\mathrm{b})(\mathrm{c}\,.\,\mathrm{d}) - (\mathrm{a}\,.\,\mathrm{c})(\mathrm{b}\,.\,\mathrm{d}) + (\mathrm{a}\,.\,\mathrm{d})(\mathrm{b}\,.\,\mathrm{c})]$

VI) $\mathrm{Tr}(\gamma_5) = 0$

VII) $\mathrm{Tr}(\gamma_5) = -\mathrm{Tr}(\gamma^5)$.

VIII) $\mathrm{Tr}(\gamma_5\not{a}\not{b}) = 0$.

IX) $\mathrm{Tr}(\gamma_5\not{a}\not{b}\not{c}\not{d}) = 4\mathrm{i}\,\epsilon_{\mu\nu\lambda\sigma}\ \mathrm{a}^\mu\ \mathrm{b}^\nu\ \mathrm{c}^\lambda\ \mathrm{d}^\sigma$

X) $\gamma_\mu\gamma^\mu = 4$

XI) $\gamma_\mu\not{a}\gamma^\mu = -2\not{a}$

XII) $\gamma_\mu\not{a}\not{b}\gamma^\mu = 4a\,.\,b$

XIII) $\gamma_\mu\not{a}\not{b}\not{c}\gamma^\mu = -2\not{c}\not{b}\not{a}$.

XIV) $\mathrm{Tr}(\gamma^\mu\not{p}_1\gamma^\nu\not{p}_2) = 4\,[\mathrm{p}_1^\mu\mathrm{p}_2^\nu + \mathrm{p}_2^\mu\mathrm{p}_1^\nu - \mathrm{g}^{\mu\nu}(\mathrm{p}_1\,.\,\mathrm{p}_2)]$

XV) $\mathrm{Tr}[\gamma^\mu(\mathrm{mathbbI} - \gamma^5)\not{p}_1\gamma^\nu(\mathbb{I} - \gamma^5)\not{p}_2] = 2\mathrm{Tr}(\gamma^\mu\not{p}_1\gamma^\nu\not{p}_2) + 8\mathrm{i}\epsilon^{\mu\alpha\nu\beta}\mathrm{p}_{1\alpha}\mathrm{p}_{2\beta}$

XVI) $\mathrm{Tr}(\gamma^\mu\not{p}_1\gamma^\nu\not{p}_2)\mathrm{Tr}(\gamma_\mu\not{p}_3\gamma_\nu\not{p}_4) = 32[(\mathrm{p}_1\,.\,\mathrm{p}_3)(\mathrm{p}_2\,.\,\mathrm{p}_4) + (\mathrm{p}_1\,.\,\mathrm{p}_4)(\mathrm{p}_2\,.\,\mathrm{p}_3)]$

XVII) $\mathrm{Tr}(\gamma^\mu\not{p}_1\gamma^\nu\gamma^5\not{p}_2)\mathrm{Tr}(\gamma_\mu\not{p}_3\gamma_\nu\gamma^5\not{p}_4) = 32[(\mathrm{p}_1\,\mathrm{p}_3)(\mathrm{p}_2\,.\,\mathrm{p}_4) - (\mathrm{p}_1\,.\,\mathrm{p}_4)(\mathrm{p}_2\,.\,\mathrm{p}_3)$

14 Appendix D - Effective coupling

To determine the value of G_q/m_q we look back at (499) along with the SM Yukawa interaction term, which involves the mixing of both scalar fields, h_1 and h_2. For interactions of WIMPs with SM quarks, the relevant terms are

$$\mathscr{L} = \frac{m_q \cos\theta}{\langle\phi\rangle} h_{1,2}\bar{\psi}_q\psi_q - \frac{m_q sin\theta}{\langle\phi\rangle} h_{2,1}\bar{\psi}_q\psi_q + \cdots + \frac{f sin\theta}{2} h_{1,2}\bar{\psi}_-\psi_- + \frac{f\cos\theta}{2} h_{2,1}\bar{\psi}_-\psi_-. \quad (837)$$

The scattering of a w particle off a quark then gives

$$\begin{aligned} \mathfrak{M} &= i\frac{f m_q sin\theta\cos\theta}{\langle\phi\rangle}\ \bar{u}_q(p')\ u_q(p)\left(\frac{1}{t-m_{h_{1,2}}^2} - \frac{1}{t-m_{h_{2,1}}^2}\right)\ \bar{u}(k')\ u(k) \\ &\approx i\frac{f m_q \lambda_3\langle r\rangle}{m_{h_1}^2 m_{h_2}^2}\bar{u}_q(p')u_q(p)\bar{u}(k')u(k). \end{aligned} \quad (838)$$

This leads to the identification of the effective coupling

$$\frac{2G_q}{\sqrt{2}} = \frac{m_q f\lambda_3\langle r\rangle}{m_{h_1}^2 m_{h_2}^2} \Rightarrow \frac{G_q}{m_q} = \frac{\sqrt{2} f\lambda_3\langle r\rangle}{2\ m_{h_1}^2 m_{h_2}^2}. \quad (839)$$

15 Appendix E - Obtaining RG equations

To establish the one-loop RG equations for the parameters of the scalar potential, we first compute the one-loop effective potential and then impose its independence from the renormalisation scale. To one-loop level, the scalar potential is given by $V = V^{(0)} + \Delta V^{(1)}$, where $V^{(0)}$ is the tree-level potential and $\Delta V^{(1)}$ indicates the one-loop correction to it. To compute the latter it is useful to re-write the tree-level potential (479) in terms of the real scalar fields:

$$\Phi = \frac{1}{\sqrt{2}} \begin{pmatrix} \varphi_1 + i\varphi_2 \\ \varphi_3 + i\varphi_4 \end{pmatrix} \qquad \text{and} \qquad S = \frac{1}{\sqrt{2}} \left(\varkappa_1 + i\varkappa_2\right) . \tag{840}$$

The particular combination of fields relevant for the calculation are $\varphi^2 = \varphi_1^2 + \varphi_2^2 + \varphi_3^2 + \varphi_4^2$ and $\varkappa^2 = \varkappa_1^2 + \varkappa_2^2$; hence (479) can be rewritten as

$$V^{(0)}(\varphi, r) = \frac{1}{2}\mu_1^2\varphi^2 + \frac{1}{2}\mu_2^2\varkappa^2 + \frac{1}{4}\lambda_1\varphi^4 + \frac{1}{4}\lambda_2\varkappa^4 + \frac{1}{4}\lambda_3\varphi^2\varkappa^2 . \tag{841}$$

In the Landau gauge the one-loop correction to the tree-level potential (841) reads:

$$\Delta V^{(1)}(\varphi, \varkappa) = \frac{1}{64\pi^2} \sum_i (-1)^{2s_i}(2s_i + 1) M_i^4(\varphi^2, \varkappa^2) \left[\ln \frac{M_i^2(\varphi^2, \varkappa^2)}{Q^2} - c_i \right] , \tag{842}$$

where c_i are constants that depend on the renormalisation scheme. For the $\overline{\text{MS}}$ scheme, we have $c_i = 5/6$ for vectors, and $c_i = 3/2$ for scalars and fermions. Next, we expand (842) and we just keep the contributions from the scalar fields, the top-quark, the gauge bosons, and the Majorana fermions,

$$\begin{aligned} \Delta V^{(1)} = & \frac{1}{64\pi^2} \left\{ \mathcal{G}_1^2 \left[\ln \frac{\mathcal{G}_1}{Q^2} - \frac{3}{2} \right] + \mathcal{G}_2^2 \left[\ln \frac{\mathcal{G}_2}{Q^2} - \frac{3}{2} \right] \right\} \\ & + \frac{1}{64\pi^2} \left\{ \text{Tr} \left(\mathcal{H}^2 \left[\ln \frac{\mathcal{H}}{Q^2} - \frac{3}{2} \right] \right) - 12\, T_\varphi^2 \left[\ln \frac{T_\varphi}{Q^2} - \frac{3}{2} \right] \right\} \\ & + \frac{1}{64\pi^2} \left\{ 3\text{Tr} \left(M_\varphi^2 \left[\ln \frac{M_\varphi}{Q^2} - \frac{5}{6} \right] \right) - 4 W_\varkappa^2 \left[\ln \frac{W_\varkappa}{Q^2} - \frac{3}{2} \right] \right\} \end{aligned} \tag{843}$$

where (in a self-explanatory notation) the field-dependent squared masses are,

$$\mathcal{G}_1(\varphi,\varkappa) = \mu_1^2 + \lambda_1\varphi^2 + \frac{\lambda_3}{2}\varkappa^2\,, \tag{844}$$

$$\mathcal{G}_2(\varphi,\varkappa) = \mu_2^2 + \lambda_2\varkappa^2 + \frac{\lambda_3}{2}\varphi^2\,, \tag{845}$$

$$\mathcal{H}(\varphi,\varkappa) = \begin{pmatrix} \mu_1^2 + 3\lambda_1\varphi^2 + \frac{\lambda_3}{2}\varkappa^2 & \lambda_3\varphi\varkappa \\ \lambda_3\varphi\varkappa & \mu_2^2 + 3\lambda_2\varkappa^2 + \frac{\lambda_3}{2}\varphi^2 \end{pmatrix}, \tag{846}$$

$$T_\varphi(\varphi) = \frac{1}{2}\left(Y_t\varphi\right)^2\,, \tag{847}$$

$$M_\varphi(\varphi) = \frac{1}{4}\begin{pmatrix} {g_Y}^2\varphi^2 & -g_2 g_Y\varphi^2 \\ -g_2 g_Y\varphi^2 & g_2^2\varphi^2 \end{pmatrix}, \tag{848}$$

$$W_\varkappa(\varkappa) = \frac{1}{4}\left(f\varkappa\right)^2\,. \tag{849}$$

We define the beta functions β_i ($i = 1\ldots3$) for the quartic couplings, the gamma functions γ_{μ_1,μ_2} for the scalar masses, and the scalar anomalous dimensions $\gamma_{\varphi,\varkappa}$ according to: $d\lambda_i/dt = \beta_i$, $d\mu_1^2/dt = \gamma_{\mu_1}\mu_1^2$, $d\mu_2^2/dt = \gamma_{\mu_2}\mu_2^2$, $d\varphi^2/dt = 2\gamma_\varphi\varphi^2$, and $d\varkappa^2/dt = 2\gamma_\varkappa\varkappa^2$. We then extract the RG equations for the parameters of the scalar potential by forcing the first derivative of the effective potential with respect to the scale t to vanish

$$\frac{d}{dt}V^{(1)} \equiv \frac{d}{dt}(V^{(0)} + \Delta V^{(1)}) \equiv 0\,, \tag{850}$$

keeping only the one-loop terms. After a bit of algebra (850) leads to the following equations:

$$
\begin{aligned}
\frac{\mu_1^2\varphi^2}{2}\left[\gamma_{\mu_1}+2\gamma_\varphi-\frac{1}{16\pi^2}\left(12\lambda_1+2\frac{\mu_2^2}{\mu_1^2}\lambda_3\right)\right] &= 0\,,\\
\frac{\mu_2^2\varkappa^2}{2}\left[\gamma_{\mu_2}+2\gamma_\varkappa-\frac{1}{16\pi^2}\left(8\lambda_2+4\frac{\mu_1^2}{\mu_2^2}\lambda_3\right)\right] &= 0\,,\\
\frac{\varphi^4}{4}\left[\beta_1+4\lambda_1\gamma_\varphi-\frac{1}{16\pi^2}\left(24\lambda_1^2+\lambda_3^2-6Y_t^4+\frac{9}{8}g_2^4+\frac{3}{8}g_Y^4+\frac{3}{4}g_2^2g_Y^2\right)\right] &= 0\,,\\
\frac{\varkappa^4}{4}\left[\beta_2+4\lambda_2\gamma_\varkappa-\frac{1}{8\pi^2}\left(10\lambda_2^2+\lambda_3^2-\frac{1}{4}f^4\right)\right] &= 0\,,\\
\frac{\varphi^2\varkappa^2}{4}\left[\beta_3+2\lambda_3(\gamma_\varphi+\gamma_\varkappa)-\frac{1}{8\pi^2}\left(6\lambda_1\lambda_3+4\lambda_2\lambda_3+2\lambda_3^2\right)\right] &= 0\,.
\end{aligned}
\tag{851}
$$

Requiring that each term between squared brackets vanishes, we arrive at the RG equations for the parameters of the scalar potential. Namely, substituting the explicit expression of the scalar anomalous dimensions [138]

$$
\gamma_\varphi=-\frac{1}{16\pi^2}\left(3Y_t^2-\frac{9}{4}g_2^2-\frac{3}{4}g_Y^2\right)\qquad\text{and}\qquad\gamma_\varkappa=-\frac{1}{8\pi^2}\,f^2\,,
\tag{852}
$$

into (851) we obtain (522).

16 Appendix F - Stability

To explore the impact of the complex singlet scalar on the stability of the Higgs sector we follow [156] and consider a tree level scalar potential of the form

$$V\left(\Phi,S\right)=\lambda_1\left(\Phi^\dagger\Phi-\frac{\langle\phi\rangle^2}{2}\right)^2+\lambda_2\left(S^\dagger S-\frac{\langle r\rangle^2}{2}\right)^2+\lambda_3\left(\Phi^\dagger\Phi-\frac{\langle\phi\rangle^2}{2}\right)\left(S^\dagger S-\frac{\langle r\rangle^2}{2}\right). \tag{853}$$

For $\lambda_3>0$, the third term can only be negative when either one of the factors is negative. The parameter space for $\Phi^\dagger\Phi<\langle\phi\rangle^2/2$ is, in principle, described by the effective potential of the SM (with one Higgs). So herein we only consider $S^\dagger S<\langle r\rangle^2/2$. As argued in [156], the most dangerous region of the field configuration is given by $S=0$.[11] In this region, we have

$$V\left(\Phi,0\right)=\lambda_1(Q)\left(|\Phi|^2-\frac{\langle\phi\rangle^2}{2}\right)^2+\lambda_2(Q)\left(\frac{\langle r\rangle^2}{2}\right)^2-\frac{\langle r\rangle^2}{2}\lambda_3(Q)\left(|\Phi|^2-\frac{\langle\phi\rangle^2}{2}\right). \tag{854}$$

The couplings are now replaced by their values at some scale Q. We take $\langle\phi\rangle$ and $\langle r\rangle$ to be the physical VEV and only the couplings λ_i run. This is possible in some renormalization scheme (like taking vacuum expectation $|\Phi|=\langle\phi\rangle, |S|=\langle r\rangle$ as one of the renormalization conditions, which is satisfied trivially for this particular form of potential). Keeping only terms with $\langle r\rangle$ (since $\langle r\rangle\gg\langle\phi\rangle$), the condition $V=0$ can be rewritten as,

$$\lambda_1(Q)\mid\Phi\mid^4+\frac{\lambda_2(Q)\langle r\rangle^4}{4}-\frac{\lambda_3(Q)\langle r\rangle^2}{2}|\Phi|^2=0. \tag{855}$$

Next, we assume that $\lambda_2(Q)\langle r\rangle^2\sim-\mu_2(Q)^2$ is almost unchanged under the RG flow and remains $\frac{1}{2}m_{h_2}^2$ (*i.e.* we assume that λ_i does not run by much). Under this assumption (855) becomes

[11] The instability region is defined by both relations $Q_-<\Phi<Q_+$ and $\lambda_1\lambda_2<(2\lambda_3)^{-2}$, with the couplings evaluated at the scale Φ. The second relation is more likely to be satisfied at a high energy scale, and therefore $|\Phi|=Q_+$ is the most dangerous region of the field configuration to reach the instability region, *i.e.* $V(\Phi,S)=0$.

$$\lambda_1(Q)|\Phi|^4 - \frac{\lambda_3(Q)m_{h_2}^2}{4\lambda_2(Q)}|\Phi|^2 + \frac{m_{h_2}^4}{16\lambda_2(Q)} = 0. \tag{856}$$

The solution to this equation gives Eq. (535); the first condition comes from $|S|^2 < \langle r\rangle^2/2 \sim \frac{1}{2}m_{h_2}^2$, with $\langle\phi\rangle = \sqrt{2}|\Phi|$ [156].

For $\lambda_3 < 0$, we can consider a field configuration with both $|\Phi| \sim Q$, $|S| \sim Q$ much larger than $\langle r\rangle$. The point is that we only need to find a configuration in which the stability is violated. In this case, we must keep only the quartic term and the potential becomes

$$V(\Phi, S) = \lambda_1|\Phi|^4 + \lambda_2|S|^4 + \lambda_3|\Phi|^2|S|^2 . \tag{857}$$

On the one hand, following [156] we can duplicate the procedure to obtain (537). These conditions can be satisfied and therefore the vacuum becomes unstable. On the other hand, we can just consider the eigenvalues of the matrix

$$\begin{pmatrix} \lambda_1 & \frac{1}{2}\lambda_3 \\ \frac{1}{2}\lambda_3 & \lambda_2 \end{pmatrix}. \tag{858}$$

In fact, the second approach also tells us why in the case of $\lambda_3 > 0$, a potential with the form of (857) is in fact stable. The eigenvector with the negative eigenvalue is given by

$$\left(-\frac{-\lambda_1 + \lambda_2 + \sqrt{\lambda_1^2 - 2\lambda_1\lambda_2 + \lambda_2^2 + \lambda_3^2}}{\lambda_3}, 1\right)$$

When $\lambda_3^2 \geq 4\lambda_1\lambda_2$, the first component is negative. So it requires either $|\Phi|^2$ or $|S|^2$ to be negative, which is impossible. As a result, for $\lambda_3 > 0$ we need to consider a particular field configuration to study the instability.

We now relate the two functional forms of the Higgs potential. At the classical level (479) differs from (853) by a constant; that is the vacuum energy is shifted. In fact (479) has a negative vacuum energy $\sim -\frac{1}{4}\lambda_2(\langle r\rangle)\langle r\rangle^4$ (again neglecting all $\langle\phi\rangle$ corrections) and the instability requires the potential to be smaller than this negative vacuum energy.

At a particular scale Q, all the couplings λ_i in (479) can be replaced by $\lambda_i(Q)$ and

$\mu_{1,2}(Q)$, so that (479) can be rewritten in the form of (853) with some $\langle\phi(Q)\rangle, \langle r(Q)\rangle$ as a combination of $\lambda_i(Q)$ and $\mu_i(Q)$. Note that we can still adopt our previous arguments to consider only the configuration $|S| = 0$. In this case,

$$V(\Phi, 0) = \mu_1^2(Q)\,|\Phi|^2 + \lambda_1(Q)\,|\Phi|^4 \tag{859}$$

The condition for stability is saturated when

$$\mu_1^2(Q)\,|\Phi|^2 + \lambda_1(Q)\,|\Phi|^4 + \frac{1}{4}\lambda_2(\langle r\rangle)\ \langle r\rangle^4 = 0\,. \tag{860}$$

Solving (485) we have $-\mu_1^2(\langle r\rangle) = \frac{1}{2}\lambda_3(\langle r\rangle)\,\langle r\rangle^2$. Now, assuming that all the λ_i do not run too much along the RG flow we obtain (856).

When $\lambda_{1,2}$ remains relative away from zero, (535) remains a reasonable approximation for the scale $Q_\pm$ between which (*i.e.*, $Q_- < \sqrt{2}|\Phi| < Q_+$) the potential can become negative. Note that a naïve argument for instability using only the quartic potential (which is usually how we get to $\lambda_3^2 \geq 4\lambda_1\lambda_2$) is only valid for $\lambda_3 < 0$. As a result, the potential can only become unstable in a some very particular field configuration. In this region, however, the effective potential is not valid since the field values are far away from the scale Q.

17 Curriculum Vitae

17.1 Research Experience

High Energy Physics: Phenomenology, Elementary Particle Theory, Physics Beyond the Standard Model, Dark Matter, Cosmology, Particle Phenomenology, High Energy Neutrinos, Neutrino Astrophysics and Cosmology

17.2 Education

I) Ph.D., Physics, September 2013 - May 2016, **The University of Wisconsin - Milwaukee, Milwaukee, WI, USA**

II) B.S., Physics, December 2012, **The University of São Paulo, São Carlos, SP, Brazil**

17.3 Refereed Journal Publications

I) "IceCube neutrinos, decaying dark matter, and the Hubble constant" L. A. Anchordoqui, V. Barger, H. Goldberg, X. Huang, D. Marfatia, **L. H. M. da Silva** and T.J.Weiler; ***Physical Review D - Rapid Communication*** 92, 061301(R)

II) "Majorana dark matter through the Higgs portal under the vacuum stability lamppost," L. A. Anchordoqui, V. Barger, H. Goldberg, X. Huang, D. Marfatia, **L. H. M. da Silva** and T.J.Weiler; ***Physical Review D*** 92, 063504

III) "Estimating the Contribution of Galactic Sources to the Diffuse Neutrino Flux," L. A. Anchordoqui, H. Goldberg, T. C. Paul, **L. H. M. da Silva** and B. Vlcek; ***Physical Review D*** 90, 123010.

IV) "What IceCube Data Tell Us About Neutrino Emission from Star-Forming Galaxies," L. A. Anchordoqui, T. C. Paul, **L. H. M da Silva**, D. F. Torres and B. Vlcek; ***Physical Review D*** 89, 127304.

V) "Weinberg's Higgs Portal Confronting Recent LUX and LHC Results Together with Upper Limits on B^+ and K^+ Decay Into Invisibles," L. A. Anchordoqui, P. B. Denton, H. Goldberg, T. C. Paul, **L. H. M. da Silva**, B. Vlcek and T. J. Weiler; ***Physical Review D*** 89, 083513.

17.4 Conference Talks

I) L.H.M da Silva: Neutrinos from Galactic Microquasars

In: *The IceCube Particle Astrophysics Symposium - IPA 2015*, Madison, WI, USA, May 4 – 6 , 2015.

17.5 Awards

I) **Papastamatiou Scholarship**

from UWM Physics Dept. for outstanding performance in Theoretical Physics, AY 2014/2015

II) **Research Excellence Award**

from UWM Physics Dept., Fall 2014

III) **Litchman Award**

from UWM Physics Dept., Fall 2014

IV) **Graduate Student Award**

from UWM Foundation, Fall 2014

V) **Summer Research Scholarship**

from UWM Physics Dept. for excellent performance in passing the written qualifying exam on first attempt, Summer 2014

VI) **Chancellor's Graduate Student Award**

from UWM Graduate School, Fall 2013

VII) **Exceptional Applicant Award**

from UWM Physics Dept., AY 2013/2014